AD-A127 969 SPECTROMETER SENSITIVITY INVESTIGATIONS ON THE SPECTROMETRIC OIL ANALYSIS PROGRAM(U) DAYTON UNIV OH RESEARCH INST W E RHINE ET AL. 22 APR 83 NAEC-92-169 1/2

UNCLASSIFIED N68335-81-C-4587 F/G 1/3 NL

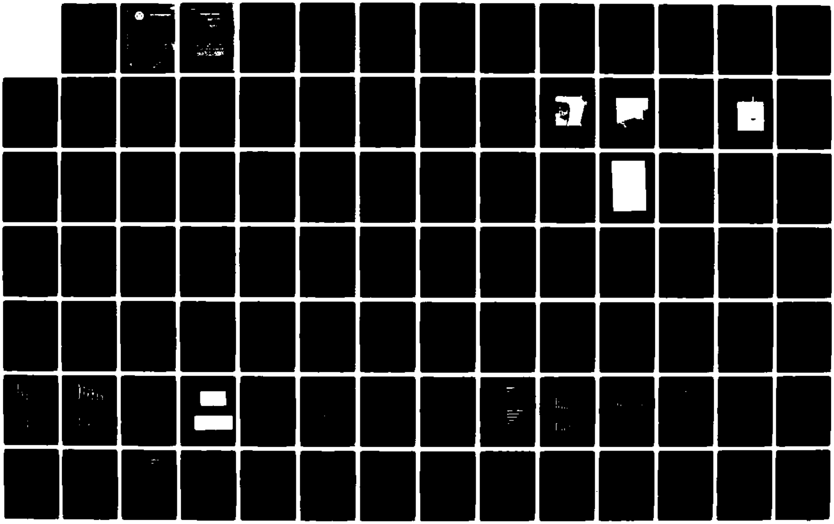

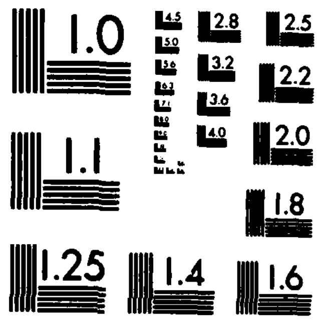

MICROCOPY RESOLUTION TEST CHART
NATIONAL BUREAU OF STANDARDS-1963-A

UNCLASSIFIED

SECURITY CLASSIFICATION OF THIS PAGE (When Data Entered)

REPORT DOCUMENTATION PAGE

READ INSTRUCTIONS BEFORE COMPLETING FORM

1. REPORT NUMBER NAEC-92-169	2. GOVT ACCESSION NO. AD A127 959	3. RECIPIENT'S CATALOG NUMBER
4. TITLE (and Subtitle) SPECTROMETER SENSITIVITY INVESTIGATIONS ON THE SPECTROMETRIC OIL ANALYSIS PROGRAM		5. TYPE OF REPORT & PERIOD COVERED Final Technical 28 Aug 81 - 28 Aug 82
		6. PERFORMING ORG. REPORT NUMBER NAEC-92-169
7. AUTHOR(s) Wendell E. Rhine Costandy S. Saba Robert E. Kauffman		8. CONTRACT OR GRANT NUMBER(s) N68335-81-C-4587
9. PERFORMING ORGANIZATION NAME AND ADDRESS University of Dayton Research Institute 300 College Park Dayton, Ohio 45469		10. PROGRAM ELEMENT, PROJECT, TASK AREA & WORK UNIT NUMBERS W A03V3400/051B/2F41-460-000
11. CONTROLLING OFFICE NAME AND ADDRESS Naval Air Systems Command Code Air-313A Washington, DC 20361		12. REPORT DATE 22 APRIL 1983
		13. NUMBER OF PAGES 180
14. MONITORING AGENCY NAME & ADDRESS (if different from Controlling Office) Naval Air Engineering Center Support Equipment Engineering Department Code 92A3 Lakehurst, New Jersey 08733		15. SECURITY CLASS. (of this report) Unclassified
		15a. DECLASSIFICATION/DOWNGRADING SCHEDULE

16. DISTRIBUTION STATEMENT (of this Report)

APPROVED FOR PUBLIC RELEASE: DISTRIBUTION UNLIMITED

17. DISTRIBUTION STATEMENT (of the abstract entered in Block 20, if different from Report)

18. SUPPLEMENTARY NOTES

19. KEY WORDS (Continue on reverse side if necessary and identify by block number)

Lubricant Contaminants
Wear Metal Analysis
Atomic Emission Spectroscopy
Particle Analysis
Rotating Disk Electrode
Arc/Spark Emission
Engine Condition Monitoring

20. ABSTRACT (Continue on reverse side if necessary and identify by block number)

An investigation was conducted in order to determine the particle detection capabilities of the A/E35U-3 rotating disk electrode arc/spark emission spectrometer used by the Joint Oil Analysis Program. It was found that the analyses determined with the rotating disk electrode (RDE) spectrometer were particle-size dependent and that the RDE spectrometer cannot quantitatively analyze particles larger than 5-10 μm. micrometers

(continued)

DD FORM 1 JAN 73 1473 EDITION OF 1 NOV 65 IS OBSOLETE

UNCLASSIFIED

SECURITY CLASSIFICATION OF THIS PAGE (When Data Entered)

20. (Continued)

The reasons for the low particle detection capabilities were examined and found to be related to particle settling rates which limit the rotating disk's capability to transport particles to the source. Particle transport is improved by using viscous matrices, but the source does not possess the energy required to simultaneously vaporize the oil and excite the metal particles present. Therefore, the particle detection capability of the RDE spectrometer is limited by the low particle transport efficiency of its rotating disk and the low energy of its source.

In order to improve the particle detection capabilities of the RDE spectrometer, several alternative sample introduction methods were investigated. Of the methods investigated, the ashing techniques offer the most promise for improving the particle detection capabilities of the RDE spectrometer.

PREFACE

This report describes the research conducted by personnel of the University of Dayton Research Institute on Contract No. N68335-81-C-4587. The work reported herein was performed during the period of 28 August 1981 to 28 August 1982, and was supported by the Naval Air Engineering Center, Support Equipment Engineering Department (92A3), Lakehurst, New Jersey. The effort was monitored by 92A3 personnel of the Naval Air Engineering Center whose advice and direction were significant in the successful completion of this effort.

The authors wish to acknowledge the use of figures copyrighted by Baird Corporation. The figures appear in Section II and are appropriately referenced.

The authors also wish to thank Dr. Kent J. Eisentraut for the use of his facilities, including the A/E35U-1. We also wish to thank Tom O'Shaughnessy, Ken Blackburn, and Bill Crawford for permission to use the A/E35U-3 and the personnel from the 4950th Test Wing, Wright-Patterson Air Force Base, Ohio, who calibrated and maintained the spectrometer.

THIS PAGE LEFT BLANK
INTENTIONALLY

TABLE OF CONTENTS

TABLE OF CONTENTS (CONT'D)

TABLE OF CONTENTS (CONCLUDED)

LIST OF TABLES

LIST OF TABLES (CONCLUDED)

LIST OF ILLUSTRATIONS

LIST OF ILLUSTRATIONS (CONT'D)

LIST OF ILLUSTRATIONS (CONT'D)

LIST OF ILLUSTRATIONS (CONCLUDED)

LIST OF ABBREVIATIONS

AA	Atomic Absorption
AAS	Atomic Absorption Spectrometry
ADM	Acid Dissolution Method
AE	Atomic Emission
AEE	Atlantic Equipment Engineers
A/E35U-1	Rotating Disk Electrode Arc/Spark Emission Spectrometer used prior to the A/E35U-3
A/E35U-3	Rotating Disk Electrode Arc/Spark Emission Spectrometer Currently used for Oil Analysis
ARD	Arizona Road Dust
JOAP	Joint Oil Analysis Program
NAEC	Naval Air Engineering Center
NAS	Naval Air Station
OAP	Oil Analysis Program
PE305B	Perkin-Elmer's Atomic Absorption Spectrometer, Model No. 305B
RDE	Rotating Disk Electrode
ROC/RIC	Research Organic/Inorganic Chemical Corp.
RPE	Rotating Platform Electrode
TSC	Technical Support Center
VMC	Vacuum Metallurgical Co.
Ag	Silver
Al	Aluminum

LIST OF ABBREVIATIONS (CONT'D)

B	Boron
Ba	Barium
Be	Beryllium
C	Carbon
Cd	Cadmium
Co	Cobalt
Cr	Chromium
Cu	Copper
Fe	Iron
Mg	Magnesium
Mn	Manganese
Mo	Molybdenum
Na	Sodium
Ni	Nickel
O	Oxygen
Pb	Lead
Si	Silicon
Sn	Tin
Ti	Titanium
V	Vanadium
W	Tungsten
Zn	Zinc
HCl	Hydrochloric Acid
HF	Hydrofluoric Acid

LIST OF ABBREVIATIONS (CONCLUDED)

HNO_3	Nitric Acid
MIBK	Methyl Isobutyl Ketone
TiC	Titanium Carbide
Si_3N_4	Silicon Nitride
105	Phillips Condor 105
7808	MIL-L-7808
2369	MIL-L-23699
245	Conostan 245 Base Oil
ppm	Parts per Million
cs	Centistoke
AZE	Di-2-Ethylhexyl Azelate
MOB	Mobil
HUM	Humble
Ball	Ball Milled
Vent	Ventron
Neodol 91-6	$RO(CH_2CH_2O)_6H$ where $R = C_9H_{19}, C_{10}H_{21}, C_{11}H_{23}$ (Shell Oil Co.)
Neodol 91-8	$RO(CH_2CH_2O)_8H$ where $R = C_9H_{19}, C_{10}H_{21}, C_{11}H_{23}$ (Shell Oil Co.)
µl	Microliter
µm	Micrometer
ml	Milliliter
mm	Millimeter
g	gram

I. INTRODUCTION

A. The Joint Oil Analysis Program (JOAP) uses rotating disk electrode arc/spark emission spectrometers to determine the presence of wear metal in used oil samples taken from operational aircraft. The presence of metallic debris, which is usually referred to as wear metal, in used oil samples is indicative of oil-wetted component wear. By detecting component wear before equipment failure occurs, JOAP has been successful in increasing fleet reliability and in reducing maintenance costs.

B. However, every year JOAP experiences equipment failures without prior detection of severe wear. One possible reason for these unpredicted failures is the inability of JOAP spectrometers to detect large wear metal particles. Several cases have been reported where metallic wear particles produced by severe component wear were not detected by spectrometric methods [references (a)-(d)]. In two of these cases [references (c) and (d)] the inability of the spectrometers to detect the large wear metal particles led to aircraft, oil-wetted component failures where no abnormal wear was indicated by spectrometric oil analysis. Research conducted by the University of Dayton Research Institute (UDRI) also demonstrated that the rotating disk electrode arc/spark emission spectrometer could not quantitatively determine the concentration of wear metal particles larger than 5-10 μm [reference (e)].

C. Although the particle size dependence of the JOAP spectrometers is well established, very little is known about the factors which *limit their* capability to analyze wear metal particles. Therefore, a thorough investigation was carried out to determine the factors which limit the

---

Ref: (a) Beerbower, A. "Spectrometry and Other Analysis Tools for Failure Prognosis". J. American Soc. of Lub. Engineers, V. 32, No. 6, P. 285-293, 1975.

(b) Seifert, W.W. and Wescott, V.C. "Investigation of Iron Content of Lubricating Oils Using a Ferrograph and an Emission Spectrometer". Wear, V. 23, No. 2, P. 239, 1973.

(c) Naval Aviation Integrated Logistic Support Center Report No. 03-41 of 27 May 1976: An Investigation of the Navy Oil Analysis Program (NOAP).

(d) Lee, R., Technical Support Center, Naval Air Station, Pensacola, FL, Private Communication, 1979.

(e) AFWAL Report No. TR-82-4017 of February 1982: Evaluation of Plasma Source Spectrometers for the Air Force Oil Analysis Program.

particle detection capability of the A/E35U-3 emission spectrometer so that possible solutions or alternatives could be recommended to improve the effectiveness of the Joint Oil Analysis Program.

D. In order for particles to be analyzed, first they must be transported to the source and then they must be vaporized and forced into excited states by the thermal energy of the source. The emission spectrometer used by the JOAP, the A/E35U-3, employs a rotating disk electrode to transport the oil sample to the source and employs an arc/spark source to vaporize and excite any metal particles present.

E. To determine the factors limiting the capability of the A/E35U-3 to transport, vaporize, and excite particles, suspensions of Ag, Al, Cr, Cu, Fe, Mg, Mo, Ni and Ti metal powders, ceramic powders, and road dust were prepared in various fluids. The fluids used included Mobil MIL-L-7808, Humble MIL-L-7808, Exxon MIL-L-23699, Phillips Condor 105, Conostan 245, di-2-ethylhexyl azelate, mineral oil and MIL-H-83282A hydraulic fluid. Each suspension was filtered through a 1, 3, 5, 8, 10, or 12 μm Nuclepore filter to obtain six separate filtrates with known maximum particle sizes. These suspensions were used to determine the effect of matrix, particle morphology, particle composition, oil viscosity, oil additives, particle settling rates, particle transport efficiency of the rotating disk electrode, electrode configuration and source energy on the A/E35U-3's capability to analyze metallic particles. The effects of calibration standards on the A/E35U-3's analytical results were also determined.

F. Work was also initiated on several alternatives or solutions designed to improve the particle detection capability of the A/E35U-3. Alternative methods of sample introduction, ashing techniques, and an acid dissolution method for the A/E35U-3 were investigated.

II. EQUIPMENT AND PROCEDURES

A. INTRODUCTION.

1. The spectrometric analysis of wear metals in lubricating oils requires procedures for the preparation of standards and samples and for calibration of the instrument. The accuracy of the analytical results depends primarily on the requirement that the standards and samples be as similar as possible.

2. This section describes the emission and atomic absorption spectrometers used, the procedures followed to prepare and analyze the standards and samples, and the techniques used to evaluate the atomic emission spectrometers.

B. INSTRUMENTATION.

1. EMISSION SPECTROMETERS.

a. Introduction. The two instruments studied during this investigation are the A/E35U-1 (Figure 1) and A/E35U-3 (Figure 2) rotating disk electrode arc emission spectrometers manufactured by Baird Corporation, Bedford, Massachusetts. The A/E35U-1 is capable of simultaneously analyzing for Ag, Al, Cr, Cu, Fe, Mg, Ni, Pb, Si and Sn, while the A/E35U-3 is equipped with 20 channels for the simultaneous analysis of Ag, Al, B, Ba, Be, Cd, Cr, Cu, Fe, Mg, Mn, Mo, Na, Ni, Pb, Si, Sn, Ti, V and Zn. The A/E35U-1 is located in the AFWAL/MLBT, Wright-Patterson Air Force Base, Ohio, and was used with the permission of Dr. Kent J. Eisentraut. The A/E35U-3 is located in the San Antonio Oil Testing Laboratory, Wright-Patterson Air Force Base, Ohio, and was used with permission of Tom O'Shaughnessy, Bill Crawford, and Ken Blackburn. The A/E35U-3, located in the San Antonio Testing Laboratory, is routinely used for the Air Force JOAP. Standard JOAP analysis procedures were followed for operating the A/E35U-1 and the A/E35U-3 spectrometers [reference (f)].

b. Theory of Operation.

(1) Atomic emission (AE) spectrometry refers to analytical methods based on the measurement of atomic emission spectra. Emission spectrometry is based on a principle of atomic physics. An atom in its ground state consists of a nucleus and orbiting electrons in discrete energy levels. When the atom is subjected to high temperatures, it

---

Ref: (f) Naval Air Systems Command Report No. NA17-15-50 of 1 May 1977; Joint Oil Analysis Program Laboratory Manual.

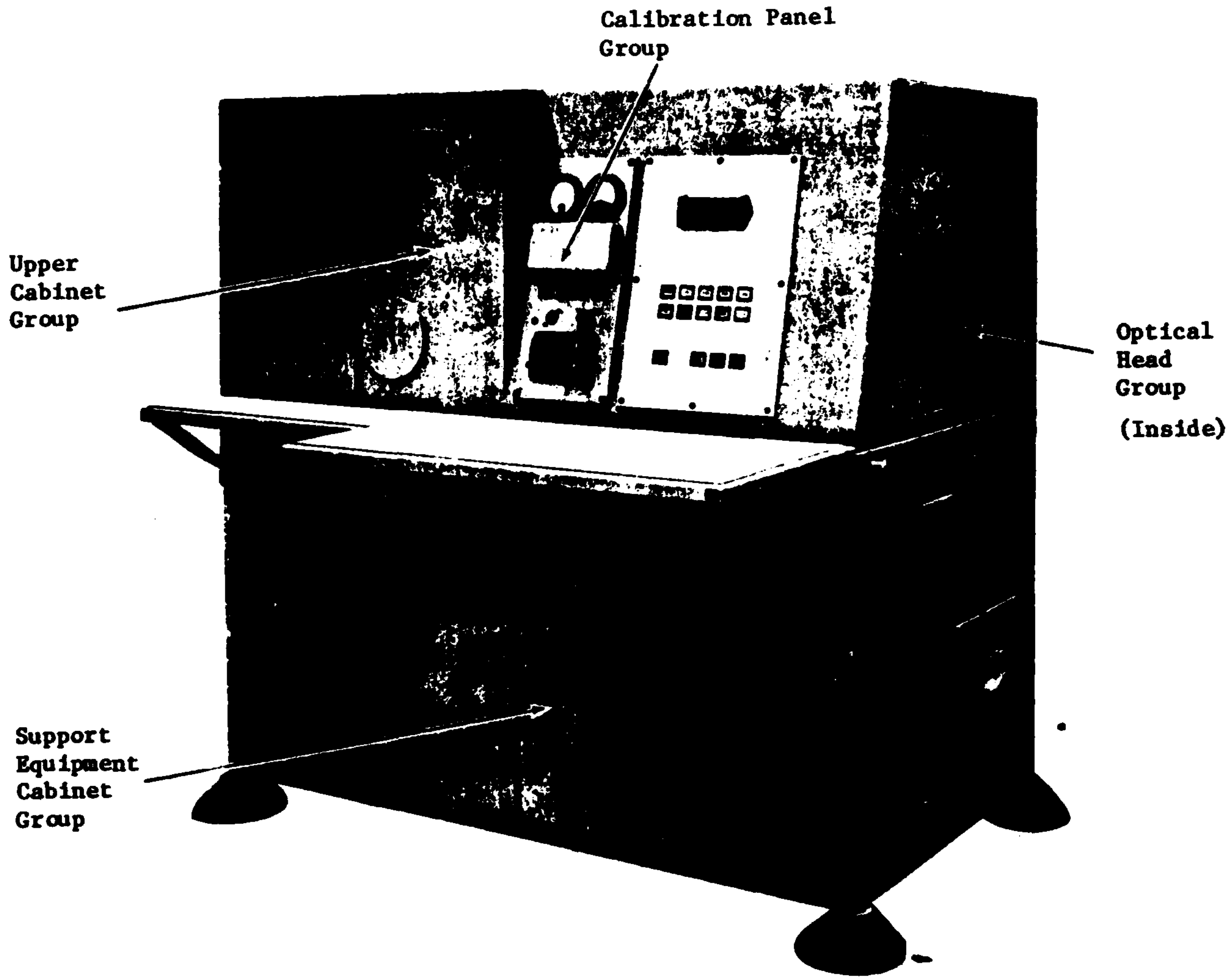

Figure 1. The A/E35U-1 Rotating Disk Electrode Arc/Spark Emission Spectrometer. [Reproduced from reference (g)].

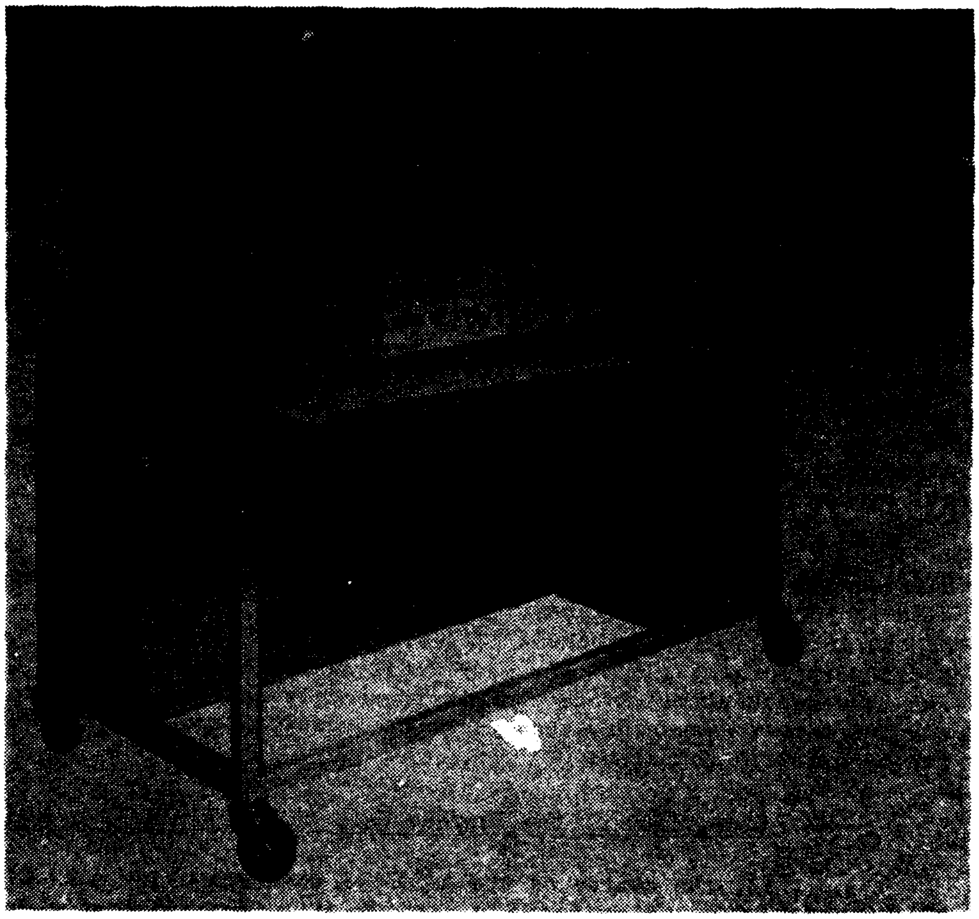

Figure 2. The A/E35U-3 Rotating Disk Electrode Arc/Spark Emission Spectrometer. [Reproduced from reference (h)].

absorbs energy in specific quantities (Quanta), which forces the atom's electrons into higher energy levels, leaving the atom in an unstable excited state. Atoms in excited states spontaneously revert to their ground state by releasing the absorbed energy in the form of light in one or more characteristic wavelengths. To determine the concentration of metal in oil, the intensity of a suitable emission line for each element of interest is measured and compared with the emission intensities observed for standards.

(2) Inherently, atomic emission spectrometry has some distinct advantages when compared to atomic absorption spectrometry which make it a desirable method for wear metal analyses. Since all the elements present in the sample are excited simultaneously, emission spectrometers have been designed to simultaneously detect the light emitted from all the elements of interest. Since emission spectrometers can analyze all the potential wear metals simultaneously, the determination of wear metals in used oil samples by emission spectrometry saves tremendous amounts of analysis time when compared to atomic absorption spectrometry where the elements must be sequentially analyzed.

(3) The A/E35U-3 and the A/E35U-1 spectrometers are equipped with a rotating disk electrode (RDE) (Figure 3) to transport the oil sample to the arc/spark excitation source. The oil sample is placed in the sample vessel beneath the rotating electrode (Figure 3) on a moveable platform. The platform is raised so that the rotating disk is partially immersed (1-2 mm) in the oil sample. The rotating disk electrode transports the sample to the arc/spark source where the elements in the oil can be vaporized and excited.

(4) The A/E35U-3 and A/E35U-1 spectrometers employ a diffraction grating to disperse the emitted light which is detected by side-on photomultiplier tubes. Figure 4 depicts the schematic diagram of the optical system of the A/E35U-3. The spectral lines used by the A/E35U-3 and the A/E35U-1 for wear metal analysis are listed in Tables 1 and 2, respectfully. Since each instrument is calibrated with the same single element standards, the analytical results from both instruments can be directly compared.

c. Comparison of the Sources Used on the A/E35U-1 and the A/E35U-3.

(1) The source on the A/E35U-1 operates using a 12 KV alternating RF current at 3.4-3.6 amperes [reference (g)]. The inductance is 360 millihenries and the capacitance is 0.0025 microfarads. A high voltage transformer charges a bank of capacitors through a current limiting resistor to furnish the high voltage ac spark necessary to analyze an oil sample. When the voltage across the capacitors reaches a certain level, an auxiliary gap breaks down and provides a short circuit path to the analytical

---

Ref: (g) Baird Corp. Report No. FSN6650-937-4401 of 15 May 1972: Spectrometer, Engine Oil Analysis, A/E35U-1 Technical Manual.

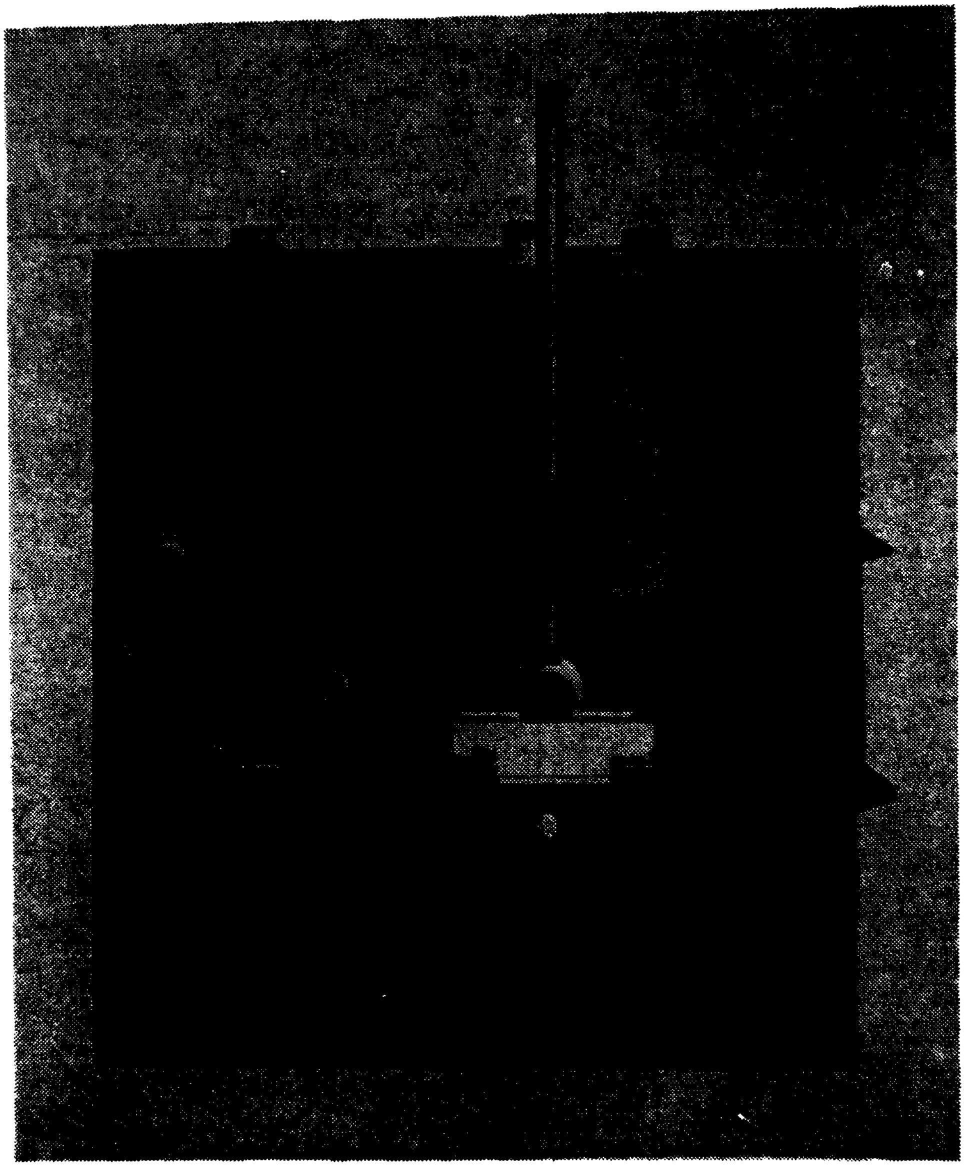

Figure 3. Analytical Source Assembly for the A/E35U-3. [Reproduced from reference (h)].

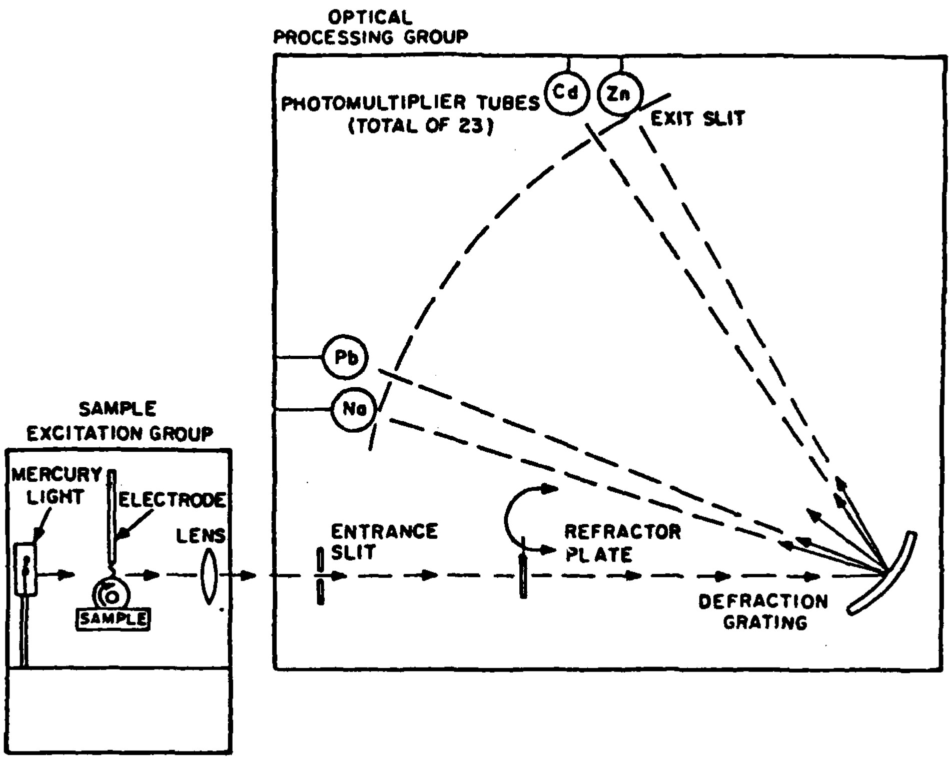

Figure 4. Schematic Diagram of the Optical System Used by the A/E35U-3. [Reproduced from reference (h)].

TABLE 1. WAVELENGTHS USED BY THE A/E35U-3 FOR WEAR METAL ANALYSES

ELEMENT	TYPE*	WAVELENGTH(Å)	ELEMENT	TYPE	WAVELENGTH(Å)
Ag	I	3281	Mn	II	2576
Al	I	3082	Mo	II	2816
B	I	2497	Na	I	5896
Ba	II	4554	Ni	I	3415
Be	I	2651	Pb	I	2833
Cd	II	2265	Si	I	2516
Cr	I	4254	Sn	I	3175
Cu	I	3274	Ti	II	3349
Fe	II	2599	V	I	4379
Mg	II	2803	Zn	I	2139

*I Emission from Neutral Atom

II Emission from Ionized Atom

TABLE 2. WAVELENGTHS USED BY THE A/E35U-1 FOR WEAR METAL ANALYSES

ELEMENT	TYPE*	WAVELENGTH(Å)
Al	I	3082
Fe	II	2598
Cr	I	4254
Ag	I	3280
Cu	I	3248
Sn	-	2859
Mg	II	2803
Pb	II	2203
Ni	I	3414
Si	I	2881

*I Emission from Neutral Atom

II Emission from Ionized Atom

gap. The discharge current can run as high as 40,000 peak amperes which provides sufficient power to volatilize the oil sample in the gap. The intense electrical field produced by such high power excites the atoms of the metals present, and they emit their characteristic radiation which is detected by photomultiplier tubes.

(2) In comparison, the excitation source on the A/E35U-3 is of relatively low power [reference (h)]. The power supply is divided into an igniter circuit and a low voltage power circuit. The igniter circuit provides energy (22KV) for the auxiliary gap to initially strike the arc while the low-voltage power circuit provides the energy to maintain the analytical arc with an average of five to six pulses per half cycle.

(3) The igniter is a high voltage circuit which provides approximately 14,000 volt pulses across the auxiliary gap. As soon as the auxiliary gap breaks down, the analytical gap ignites. After the analytical gap has been ionized, the low-voltage (175 volt peaks) power circuit is able to discharge and provides the required excitation energy to raise the energy of the atoms above the ground state.

d. Calibration. The A/E35U-3 was calibrated by Air Force personnel using D18-100 standards supplied by JOAP-TSC, NAS, Pensacola, FL. The A/E35U-3 was used with the understanding that we not adjust the calibration or alter the instrument in any manner. The concentration of metal in each sample was determined from working curves produced by analyzing single element standards and plotting the instrument readout vs the known concentration of each standard. The working curves for the determinations of Ag, Al, Cr, Cu, Fe, Mg, Mo, Ni, Si and Ti are shown in Figures A1-A7 (Appendix A).

2. ATOMIC ABSORPTION SPECTROMETER.

a. Introduction. A Perkin-Elmer Model 305B flame atomic absorption spectrometer was used to analyze samples treated by the acid dissolution method.

b. Theory of Operation.

(1) Atomic absorption (AA) spectrometry can be described as the absorption of external radiation by ground state atoms. For absorption to occur, the wavelength of the radiation must correspond to the exact amount of energy required to force a ground state atom into an excited state. The magnitude of light absorbed is directly proportional to the concentration

---

Ref: (h) Baird Corporation Report No. FSN6650-251-0712 of 1 February 1973: Operation Instructions, Maintenance Instructions, Fluid Analysis Spectrometer (FAS-2).

of free atoms in the path of the light beam. Since light emitted by an iron hollow cathode lamp can be absorbed only by iron atoms, the chance of interference by other elements is almost nil.

(2) The main advantages of AA spectrometers over the emission spectrometers are that the sample solutions can easily be analyzed by the AA spectrometer, and AA analyses are more accurate and precise than the AE analyses.

(3) The PE305B is a double beam instrument, and a nitrous oxide-acetylene flame was used as an atomizing source. For analysis by atomic absorption, the samples were diluted with 8 parts of a Neodol 91-6/methyl isobutyl ketone solution (Neodol 91-6/MIBK) and nebulized into a spray chamber where the sample is mixed with fuel and oxidant and transported to the flame as an aerosol.

(4) The wavelengths selected for the determination of wear metals are those recommended by the Perkin-Elmer Corp. [reference (i)].

c. Calibration. All light absorbing methods, including atomic absorption spectrometry, are based on the Beer-Lambert Law which states that the intensity of a light beam passing through an absorbing medium decreases exponentially with the number of absorbing atoms. In the concentration region where the law holds, a plot of absorbance vs concentration is linear. Such plots are referred to as working curves and were prepared for the metals analyzed in this work by analyzing Neodol 91-6/MIBK solutions of Conostan (D20's) standards and plotting the absorbances vs concentrations for D20-0, D20-25, D20-50, D20-75 and D20-100 standards.

C. SUPPLIES.

1. CONOSTAN CONCENTRATES.

a. Single element metal alkyl aryl sulfonate concentrates were obtained from the Continental Oil Company, Conostan Standard Division, Ponca City, Oklahoma. These concentrates are viscous liquids which are miscible with each other and other lubricants.

b. Table 3 lists the metal concentrations in each concentrate as determined by the National Bureau of Standards. Each concentrate contains Na and Fe as contaminants. When multielement standards are prepared, the concentrations of Na and Fe in each concentrate must be taken into account to obtain a multielement standard with the correct final concentrations of Na and Fe.

Ref: (i) Perkin-Elmer Corp. Report No. PC-1 of March 1973: Analytical Methods for Atomic Absorption Spectrophotometry.

TABLE 3. CONCENTRATION OF METAL IN CONOSTAN CONCENTRATES

ELEMENT	%METAL	FE (PPM)	NA (PPM)
Ag	5.07	8	120
Al	2.29	25	8
B	1.10	14	11
Ba	7.56	14	11
Be	0.526	20	46
Cd	8.32	17	14
Cr	1.89	59	29
Cu	4.61	37	170
Fe	2.55		59
Mg	2.10	11	248
Mn	2.93	49	6
Mo	2.10	77	45
Na	3.79	10	
Ni	3.43	19	110
Pb	9.92	13	32
Si	13.11	9	1
Sn	5.91	19	23
Ti	6.13	16	7
V	2.02	25	19
Zn	4.41	16	102

2. METAL POWDERS. The metal powders used during this study were obtained from Research Organic/Inorganic Chemical Company (ROC/RIC), Sun Valley, CA; Vacuum Metallurgical Company (VMC), Tokyo, Japan; Atlantic Equipment Engineers (AEE), Bergenfield, NJ; and Alfa Inorganics (Ventron), Danvers, MA. A portion of the ROC/RIC -325 mesh Fe powder was ground on a planetary ball mill (Microjet 6PM4) by Micro Material Corp., Westbury, NY, and is referred to as the ball-milled Fe powder. The particle size distributions are different for each powder; therefore, the powders were passed through a 20 μm sieve so that each powder had similar, maximum-sized particles.

3. CERAMIC POWDERS. The TiC and Si_3N_4 ceramic powders used for this investigation were produced by Herman C. Starck and GTE-Sylvania, respectively, and were obtained through the courtesy of Dr. Alan Katz and K. Mazdiyasni (AFWAL/MLL, Wright-Patterson Air Force Base, Ohio). The metallic impurities and the Ti concentration in the TiC powder are shown in Table 4.

4. ARIZONA ROAD DUST. The fine and coarse grades of Arizona Road Dust were obtained through the courtesy of C.E. Snyder, Jr. (AFWAL/MLBT). The particle size and chemical composition of the fine and coarse grades of Arizona Road Dust are listed in Table 5.

D. PREPARATION OF SINGLE ELEMENT STANDARDS. Single element standards were prepared by diluting the appropriate single element concentrates with the fluids used to prepare the suspensions (Table 6).

E. PREPARATION OF MULTIELEMENT STANDARDS.

1. The multielement standards were prepared by diluting D20-900 (20-element) standards in the appropriate fluid. The standards are referred to as DX-Y where X indicates the number of elements present and Y refers to the concentration of each element. Multielement standards were used to determine the effect of concomitant elements on Ti emission. Six standards were used in this study. Three were prepared by this laboratory in 245 base oil and three were prepared by the JOAP-TSC in 1100 base oil. The standards prepared by the JOAP-TSC are referred to as D20-100 (R-6), D20-100 (R-5) and D14-100. The standards prepared in this laboratory are referred to as D'20-100, D'18-100 and D'14-100. The D14-100 standards did not contain B, Ba, Be, Cd, Mn and V, while the D'18-100 standard did not contain B and Be.

2. These standards were diluted 1:5 with MIBK for AA analysis. Standards prepared by diluting a D20-300 (Batch M4) were used to prepare the Ti working curve. The concentrations of Ti as determined by AA analysis are listed in Table 7.

TABLE 4. ELEMENTAL ANALYSIS OF TiC CERAMIC POWDER

ELEMENT	% BY WEIGHT
Ti	79.3
Cr	0.05
Co	0.12
Fe	0.05
W	0.65
O	0.25
C	~19.58

TABLE 5. ARIZONA ROAD DUST CHARACTERISTICS

CHEMICAL ANALYSIS

ELEMENT	% BY WEIGHT[a]
Si	32.0
Fe	2.8
Al	8.5
Cu	2.1
Mg	0.6

PARTICLE SIZE DISTRIBUTION BY WEIGHT PERCENT

SIZE(μm)	FINE GRADE	COARSE GRADE
0-5	39±2	12±2
5-10	18±3	12±3
10-20	16±3	14±3
20-40	18±3	23±3
40-80	9±3	30±3
80-200	0	9±3

[a]Other 54% is oxygen plus traces of other elements.

TABLE 6. SUSPENSIONS PREPARED

ELEMENT	MOBIL MIL-L-7808	HUMBLE MIL-L-7808	MIL-L-23699	PHILLIPS CONDOR 105	CONOSTAN 245	LIGHT MINERAL OIL	HYDRAULIC FLUID MIL-H-83282A	DI-2-ETHYLHEXYL AZELATE
Ag	X							
Al	X	X	X	X	X			X
Cr	X							
Cu	X	X	X	X	X		X	X
Fe	X	X	X	X	X		X	
Mg	X	X	X	X	X			X
Mo	X		X					
Ni	X							
Ti	X		X					
TiC			X					
Si_3N_4			X					
ARD-Coarse[a]			X					
ARD-Fine[a]			X				X	
Fe AEE					X	X		
Fe Ball Milled					X	X		
Fe ROC/RIC					X	X		
Fe Ventron					X	X		
Fe VMC					X	X		

[a]Arizona Road Dust

TABLE 7. FLAME AA ANALYSES OF MULTIELEMENT STANDARDS

STANDARD	MATRIX	PREPARATION	TI (PPM)
D14-100	1100	JOAP-TSC	123 ± 1.4
D20-100(R-6)	1100	JOAP-TSC	99 ± 1.4
D20-100(R-5)	1100	JOAP-TSC	89 ± 1.4
D'14-100	245	UDRI	116 ± 1.4
D'18-100	245	UDRI	101 ± 1.4
D'20-100	245	UDRI	98 ± 1.4

F. PREPARATION OF SUSPENSIONS. The metal powder, ceramic powder, and Arizona Road Dust suspensions were prepared by suspending 40 to 60 mg of the powder or dust in 500 g of lubricating oil or hydraulic fluid. The suspensions prepared for this research are listed in Table 6.

G. FILTRATION PROCEDURE. The suspension was agitated ultrasonically for 15 minutes at 65°C and then shaken using a paint shaker until the particles were uniformly suspended in the oil. An aliquot of the well-agitated suspension was then taken and filtered through either a 12, 10, 8, 5, 3 or 1 μm filter. The aliquots filtered ranged in size from 20 ml (12 μm filter) to 5 ml (1 μm filter). The filter was then washed twice with an equal amount of pentane, i.e., 20 ml of pentane for the 12 μm filtration. This procedure was repeated with a new aliquot of the suspension and a fresh filter until 30-40 ml of the suspension had been filtered. The filtrates and pentane washings were combined and the pentane allowed to evaporate overnight. The filtrates were then placed in a vacuum oven at 40°C for 4 hours to remove any remaining pentane. In this manner six filtrates with maximum particle sizes of 12, 10, 8, 5, 3 and 1 μm were prepared from each suspension. The concentration of metal in each filtrate was then determined by the acid dissolution method (ADM).

H. ACID DISSOLUTION METHOD (ADM). To 2 g of filtrate, 0.4 g of acid was added. The mixture was shaken by hand for 10 sec, and then ultrasonically agitated for 5 minutes at 65°C. The acid used for the Al, Cr, Cu, Fe, Mg, Mo, Ni and Ti metal powder suspensions was made by combining 8 parts HCl with 1 part HF and 1 part HNO_3 and is referred to as the 1:8:1 ($HF/HCl/HNO_3$) acid mixture. The 1:8:1 acid mixture was found to give incomplete recoveries of Ag metal powder, of Ti from TiC, and of Si from Arizona Road Dust or Si_3N_4. Concentrated HNO_3 was found to give quantitative recoveries of Ag metal powder. An acid mixture containing 3 parts HF and 1 part HNO_3 was found to give quantitative recoveries of Ti from TiC. Quantitative recoveries of Si from Arizona Road Dust were achieved with an acid mixture prepared by combining 2 parts HCl with 1 part HF and 1 part HNO_3 and is referred to as the 1:2:1 ($HF/HCl/HNO_3$) acid mixture. No acid mixture was discovered that would dissolve Si_3N_4. To make the acid/oil mixture homogeneous for analysis, 1.9 g of Neodol 91-6 (Shell Surfactant) and 5.7g of methyl isobutyl ketone were added to the sample. The diluted samples were shaken by hand until homogeneous and then analyzed by atomic absorption spectrometry to determine the metal content of each filtrate.

I. ANALYSIS OF SAMPLES. Each suspension was agitated ultrasonically to resuspend any particles which had settled out and to reduce the number of agglomerated particles in suspension. Immediately before analysis, the samples were vigorously hand shaken until the suspension was uniform. The samples were analyzed in duplicate on the A/E35U-1 and for 3-5 replicates on the A/E35U-3.

J. PARTICLE TRANSPORT EFFICIENCY OF THE ROTATING DISK.

1. To determine the capability of the rotating disk electrode to transport metal particles, a rotating disk test rig was constructed. The test rig was set up so that a disk was rotated at 30 rpm and the oil sample was heated to 40°C (avg. temperature for the A/E35U-1 and A/E35U-3). The oil sample was hand shaken until uniform, poured into a glass vessel, and allowed to stand undisturbed for 25 $\pm$ 3 seconds (avg. time for A/E35U-1 and A/E35U-3). A preweighed disk was allowed to rotate 1-2 times while dipped in the oil and then reweighed to determine the amount of oil picked up by the disk. The concentration of particles picked up by the disk was determined by the ADM. Both dry disks and disks dipped in blank oil were tested with the same procedure to insure that the metal concentration, as determined by the ADM, was due to the particles picked up by the disk and not to trace metals extracted from the disk.

2. To determine the capabilities of the rotating disk electrodes to transport metal particles to the sources of the A/E35U-1 and A/E35U-3, the above procedure was altered so that the test conditions matched the operating conditions of the A/E35U-1 and A/E35U-3 spectrometers. The oil sample was heated so that its temperature increased at 1.1°C/second (A/E35U-1 and A/E35U-3 conditions), and the particle transport efficiency of the disk was determined at 10 second intervals between 5-55 seconds. The particle transport efficiencies of the A/E35U-1 and A/E35U-3 were calculated as described in Section III.

K. A/E35U-3 ACID DISSOLUTION METHOD. An acid dissolution method was developed for the A/E35U-3 which uses the 1:8:1 acid mixture (used in the ADM-AA method). In this case, 0.1 g of acid and 0.9 g of Neodol 91-8 surfactant were added to each gram of oil. Since no solvent is used in this method, a larger amount of the surfactant is needed to obtain a homogeneous solution. The resulting mixture was agitated for two minutes on a vortex mixer providing a homogeneous solution suitable for analysis on the A/E35U-3.

L. BURN TIME. The A/E35U-1 has a hood (Figure 5) to block stray light from entering the instrument. Removing the hood, which allows more light to enter the instrument, had the effect of substantially reducing the burn time from 41 seconds to 18 seconds.

M. ASHING TECHNIQUE. The ashing technique was performed in the same manner for each electrode type: rotating disk electrode, rotating platform electrode, and crater tip electrode. Twenty microliters of blank oil was deposited onto the electrode, and the electrode was placed inside a 500°C muffle furnace for 5 minutes. The same procedure was followed for both the standards and metal powder suspensions. The electrodes prepared in this manner were analyzed on the A/E35U-1. All analyses reported were conducted with the hood removed. The absence of oil on the surface of the ashed electrode increased the burn time from 18 seconds (oil on surface) to 36 seconds (ashed surface).

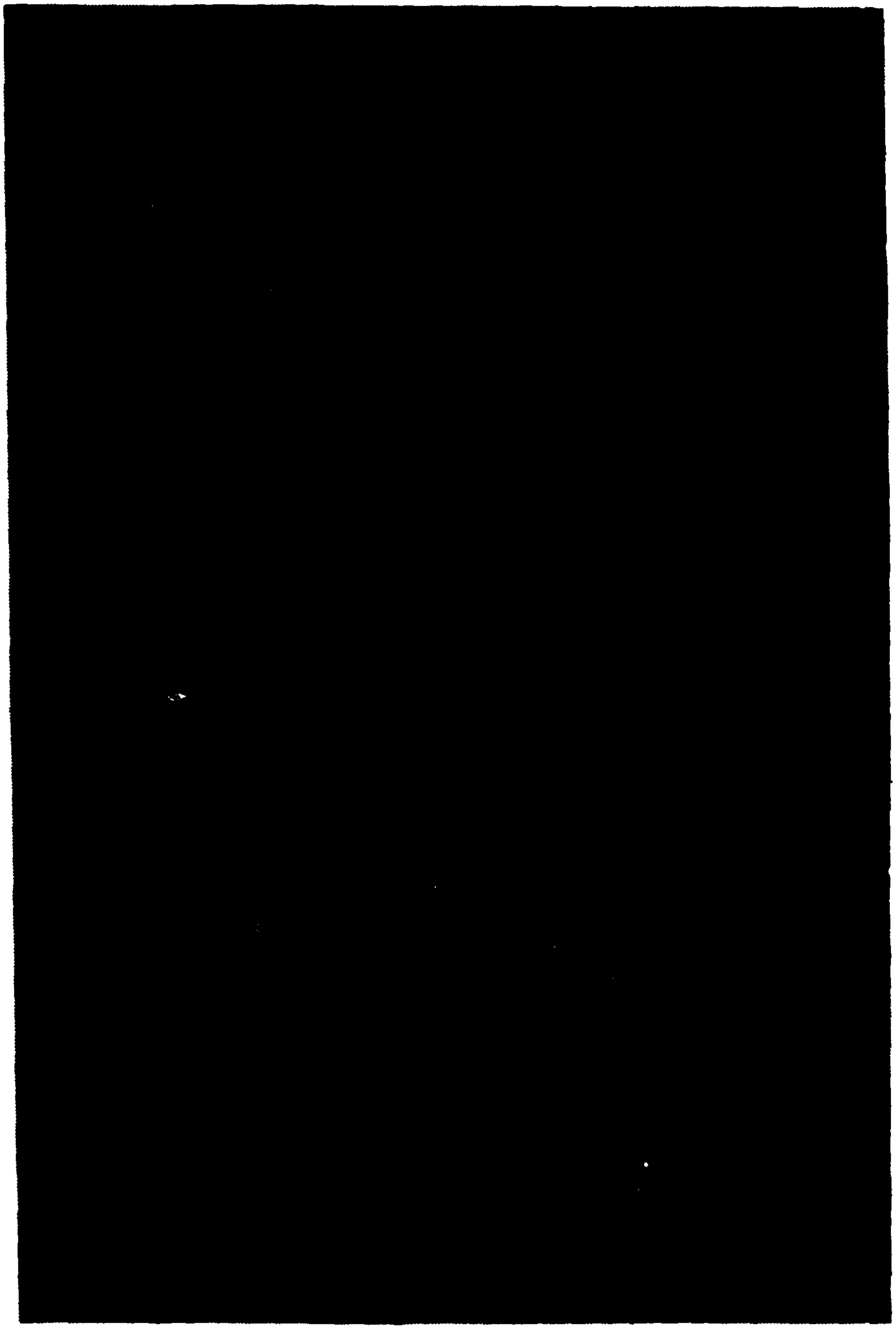

Figure 5. Analytical Source Assembly for the A/E35U-1. [Reproduced from reference (g)].

N. ROTATING DISK ELECTRODE. The 3 mm and 5 mm rotating disk electrodes used in this study were obtained from Bay Carbon, Inc., Bay City, Michigan. Except where specified, the 5 mm wide electrode was used for all the analyses on the A/E35U-1 and A/E35U-3 spectrometers. The installation of the disk electrode for analysis on the A/E35U-1 and A/E35U-3 spectrometers is given in [references (g) and (h)].

O. CRATER TIP ELECTRODE. Crater electrodes were prepared by using a 11/64" drill bit to produce a hole 1/8" deep in the rim of the 5-mm rotating disk electrode. The motor which rotates the disk was disconnected so that the disk would remain stationary during analysis. The ashed crater tip electrodes were placed on the stationary spindle of the A/E35U-1 for analysis.

P. ROTATING PLATFORM ELECTRODE. The rotating platform electrodes used in this study were obtained from Zeebac Inc., Berea, Ohio. The rotating platform is shown in Figure 6. During analyses it is rotated at a preset speed of 10 rpm. For the analyses on the A/E35U-1 the upper electrode was positioned at the point halfway between the center and the edge of the electrode.

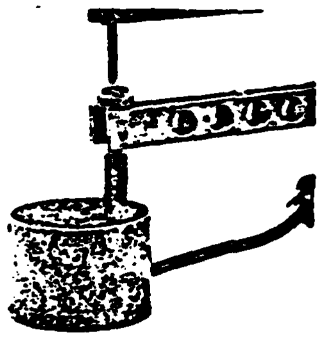

Figure 6. Rotating Platform Electrode.

Q. ROD ELECTRODE. The 160° and 15° tip angles were formed on the rod electrodes using the A/E35U-3 and A/E35U-1 Baird-Atomic Electrode sharpeners, respectively. The 17° tip was formed on the upper electrode using a pencil sharpener. The installation and gapping procedures for the upper electrode for the A/E35U-1 and A/E35U-3 spectrometers are given in [references (g) and (h)].

III. ANALYSIS

A. DETERMINATION OF THE PARTICLE DETECTION CAPABILITIES OF EMISSION SPECTROMETERS.

1. The particle detection capabilities of the rotating disk electrode emission spectrometers were determined by analyzing the filtrates obtained by filtering the metal particle suspensions through Nuclepore polycarbonate membrane filters. The particle size distribution of the suspension was determined by plotting the concentration of metal (M_n) (determined by the acid dissolution method) versus the maximum sized particle in each filtrate (Figures A8A-A52A). The filtrates were assumed to contain maximum sized particles as defined by the pore size of the Nuclepore filter. Since the concentrations of metal determined by the acid dissolution method were obtained using an AA spectrometer, the error in these metal concentrations is low ($\pm$ 3%) and the percent metal analyzed for each filtrate was calculated using the actual data points.

2. On the other hand, the concentrations of wear metal determined by the emission instruments (X_n) are accurate to only $\pm$ 10%. Also the errors are directly proportional to the size of the particles being analyzed. For this reason we determined the percent metal analyzed (% A) for each filtrate from points (T_n) on the "best curve". The "best curve" was drawn with the assumption that the percent metal analyzed should be inversely proportional to metal particle size, i.e., a 20 μm particle is less analyzable than a 10 μm. If the "best curve" was drawn through the data points (X_n) in the example shown in Figure 7, the percent metal analyzed for the 10-, 12- and 20-μm particles would at best be confusing and a 20-μm particle would have a higher % A than a 12 μm particle.

3. To calculate the percent metal analyzed by the spectrometers the following calculations were carried out for each suspension.

n = Filtrate number

M_n = Concentration of metal as determined by the acid dissolution method in filtrate n.

$D_n = M_n - M_{n-1}$ Concentration of metal with particle sizes between those in filtrates n and n-1.

T_n = Total metal analyzed by spectrometer as determined from "best curve" in filtrate n.

$C_n = T_n - T_{n-1}$ Concentration of metal determined by spectrometer with particle sizes between those in filtrates n and n-1.

$\% A = (C_n/D_n) \cdot 100$ Percent metal analyzed by spectrometer.

X_n = Concentration of metal in filtrate n as determined by spectrometer.

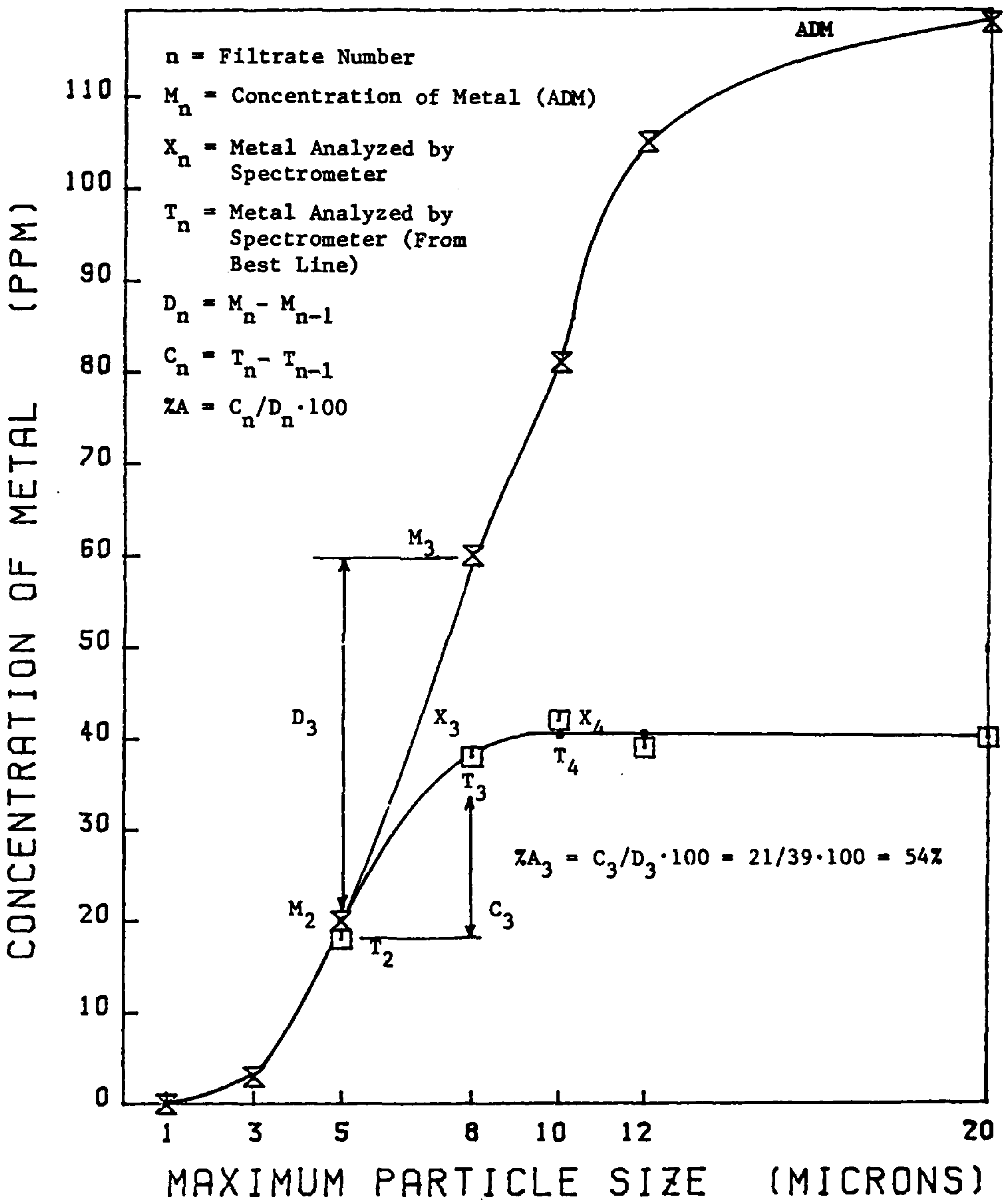

Figure 7. Typical Calculation for Percent Metal Analyzed.

An example of the data collected for the analysis of metal particles will be used to illustrate the above equations. The data are plotted in Figure 7.

Filter Size (μm)	Filtrate n	M_n	D_n	% A	C_n	T_n	X_n
	0	0					
3	1	3	3	100	3	3	3
5	2	21	18	83	15	18	18
8	3	60	39	54	21	39	39
10	4	81	21	14	3	42	43
12	5	105	24	0	0	42	41
unfiltered	6	119	14	0	0	42	42

4. Calculations for particles between 5 and 8 μm are:

$D_3 = M_3 - M_2 = 60-21 = 39$ ppm

D_3 equals the concentration of metal (ADM) which passes through an 8 μm Nuclepore filter but is retained by a 5-μm filter.

$C_3 = T_3 - T_2 = 39 - 18 = 21$ ppm

C_3 equals the concentration of metal analyzed by the spectrometer for particles which passes through an 8-μm Nuclepore filter but is retained by a 5-μm Nuclepore filter.

$\% A = (C_3/D_3) \cdot 100 = 54\%$

% A equals the percent of metal analyzed by the spectrometer with particle sizes between 8 and 5 μm.

The percent metal analyzed for the different suspensions is plotted in Appendix A (Figures A8B-A52B).

B. CALCULATION OF AVERAGE PERCENT METAL TRANSPORTED BY THE DISK ELECTRODE. To compare the transport efficiency of the rotating disk electrode as used in the A/E35U-1 and the A/E35U-3 spectrometers, the concentration of metal transported by the rotating disk electrode was determined versus time using the procedure described in Section II. The A/E35U-1 spectrometer used in this work had a 12-second preburn and a 33-second emission integration time while the A/E35U-3 used in this work had a 6 second preburn and a 30 second emission integration time. The transport efficiencies for the A/E35U-1 and the A/E35U-3 were determined by plotting the percent metal transported versus time. The metal particles detected by the spectrometers are those transported between 6 and 36 seconds for the A/E35U-3 and between 12 and 45 seconds for the A/E35U-1. The percent metal transported during the integration time was used to calculate the "average percent metal transported" by the rotating disk electrode according to the equation:

$$\text{Avg Percent Metal Transported} = \left[\int_0^{T_2} (\text{Percent Metal Transported})\, dt \right] \div T_2$$

where T_2 is the integration time. The average percent of metal transported was calculated and plotted versus particle size for each suspension. The results are discussed in Section IV.

C. <u>CALCULATION OF CONCOMITANT ELEMENT EFFECT</u>.

1. The presence of concomitant elements in the standard can cause interferences, i.e., systematic errors in the measure of the emission signal. An interference will cause an error in the analytical results only if the interference is not adequately accounted for in the procedure. The analyte concentration determined when the interference is not accounted for is called the "apparent concentration".

2. To determine the effect of concomitant elements on the analytical results from the A/E35U-3, multielement and single element standards were analyzed. For each element studied, the "apparent concentration" was calculated according to the equation:

$$\text{Apparent Conc.} = \frac{\text{Readout from Single Element Std.}}{\text{Readout from Multielement Std.}} \times \begin{array}{l}\text{Actual Metal}\\ \text{Concentration}\end{array}$$

where the actual metal concentration is the concentration of analyte in both standards. Any difference between the "apparent concentration" and the actual metal concentration is due to the combined effect of the other nineteen elements on the emission signal of the analyte.

3. The apparent concentration was plotted versus the metal concentration to illustrate the effect of concomitant elements. The resulting plots are presented in Section IV.

IV. RESULTS AND DISCUSSION

A. COMPARISON OF AE AND AA ANALYSES.

1. INTRODUCTION.

a. When wear metal analyses from A/E35U-3 emission and atomic absorption (AA) spectrometers are compared, the concentrations determined by the A/E35U-3 are enhanced relative to the concentrations determined by the AA spectrometer. These differences are advantageous to the oil analysis program and are used to increase the sensitivity of the A/E35U-3 spectrometer.

b. For this work, the factors which affect the concentrations determined by the A/E35U-3 had to be nullified so that an accurate assessment of the A/E35U-3's capability to analyze particles in the various lubricating oils could be made. There are essentially two factors which affect the A/E35U-3's results. These two factors are matrix and concomitant element effects. When these two factors are compensated for, the results from AE and AA spectrometers can be directly compared.

2. EFFECT OF OIL MATRIX.

a. When synthetic ester oils are analyzed for metals using the A/E35U-3, a large error results if the A/E35U-3 is calibrated using the standards supplied by the JOAP-TSC. The error stems from the fact that oil matrices affect the results from the A/E35U-3. The standards supplied by the JOAP-TSC are prepared in a heavy hydrocarbon oil (1100 base oil), and an error results because the synthetic ester and the hydrocarbon oils affect the intensity of the emission lines differently.

b. To determine the effect of the oil matrix, multielement standards were prepared in each oil of interest. Figures 8, 9, 10 and 11 are plots of the instrument readout versus standard concentration for Al, Cu, Fe and Mg and show the enhancement of the emission from metals in an ester oil matrix relative to metals in a hydrocarbon oil matrix. The results indicate that, when the A/E35U-3 is calibrated with D20-100 standards prepared in hydrocarbon oil and a sample prepared in MIL-L-7808 oil is analyzed, superficially high metal concentrations will be observed. Therefore, to accurately analyze oil samples it is imperative that the matrix used to prepare the standard matches the matrix of the samples. Therefore, the concentration of metal analyzed in each suspension was calculated from working curves prepared by analyzing standards dissolved in the same oil as the suspension.

3. EFFECT OF CONCOMITANT ELEMENTS.

a. Another source of error occurs if the instrument is calibrated using multielement standards prepared in a synthetic ester oil matrix. The presence of concomitant elements in the standard can cause a systematic

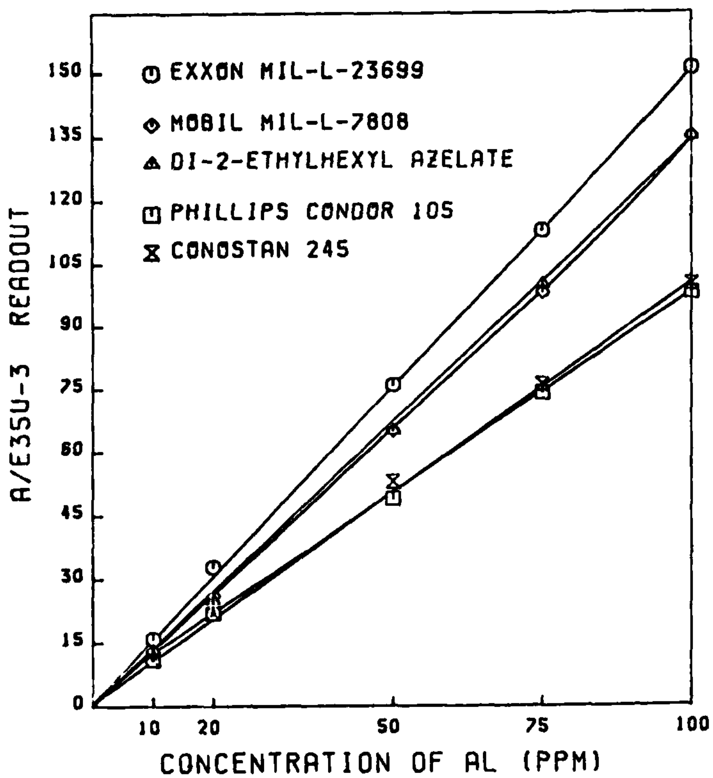

Figure 8. Plot of Instrument Readout versus Concentration of Al in Multielement Standards.

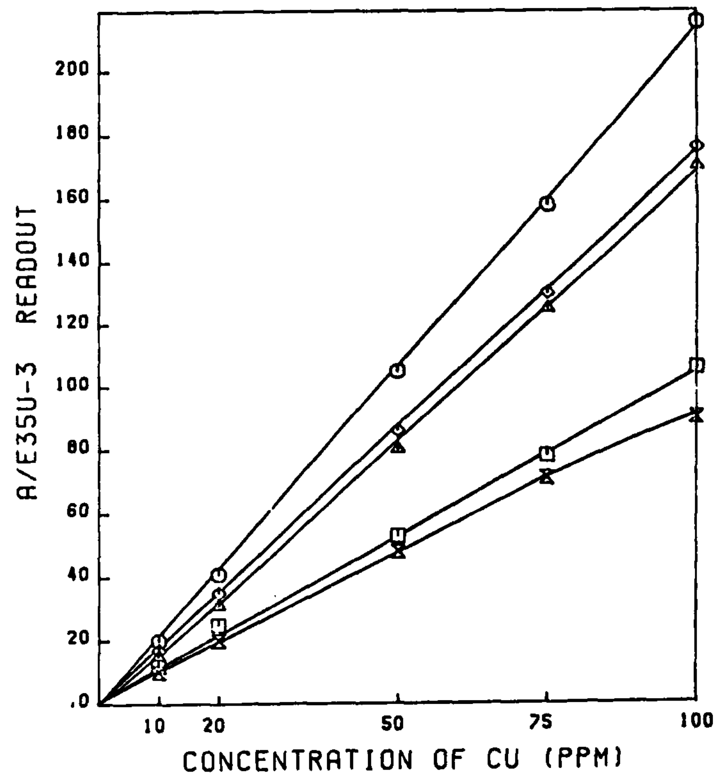

Figure 9. Plot of Instrument Readout versus Concentration of Cu in Multielement Standards.

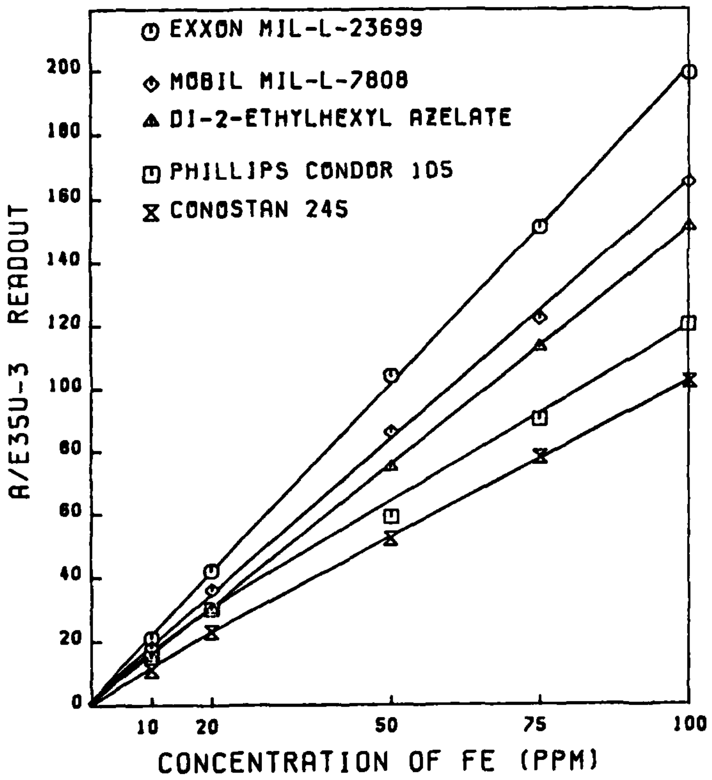

Figure 10. Plot of Instrument Readout versus Concentration of Fe in Multielement Standards.

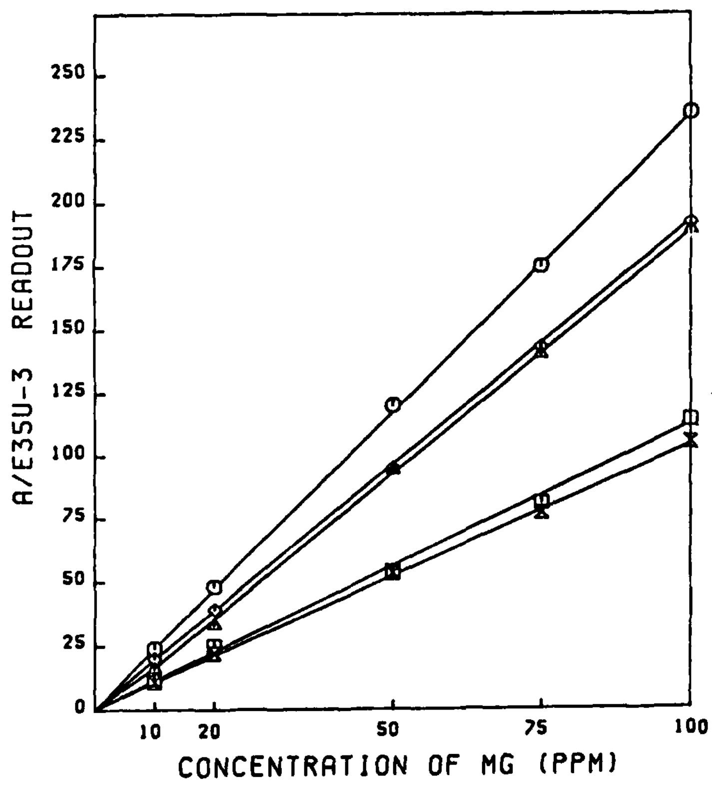

Figure 11. Plot of Instrument Readout versus Concentration of Mg in Multielement Standards.

error in the emission signal which must be accounted for to obtain the correct analytical result. The analyte concentration determined without accounting for the interference is called the "apparent concentration" and was calculated according to the following equation:

$$\text{Apparent Concentration} = \frac{\text{Readout from Single Element Std.}}{\text{Readout from Multielement Std.}} \times \begin{matrix}\text{Actual Metal}\\ \text{Concentration}\end{matrix}$$

b. To determine the effect of using multielement standards to calibrate the A/E35U-3, single element and multielement standards were analyzed. The "apparent concentration" of the analyte in the single element standard was plotted versus the analyte's actual concentration. When the interferences are negligible, the "apparent concentration" and the actual concentration will be equal, and the plotted results will coincide with the line of perfect correlation (broken line). If the results fall above the line of perfect correlation, the "apparent concentration" of the analyte in the single element standard is larger than the actual concentration, and the concomitant elements present in the multielement standard depressed the analyte's emission signal. On the other hand, if the results fall below the line of perfect correlation, the "apparent concentration" was less than the actual concentration, and the concomitant elements present in the multielement standard enhanced the analyte's emission signal.

c. The data plotted in Figures 12-15 illustrates that errors occur if multielement standards are used to calibrate the A/E35U-3. However, the "apparent concentrations" can be corrected mathematically or by calibrating the A/E35U-3 with single element standards. The latter approach was used in this work, and metal concentrations were determined from working curves prepared by analyzing single element standards dissolved in each oil of interest.

4. EFFECT OF ADDITIVES ON A/E35U-3 ANALYSES. Oil additives also affect the emission intensity observed for standards prepared in ester oils. The effects of additives on the emission signals of Al, Cu, Fe and Mg were determined by comparing the analytical results observed for single element standards prepared in Mobil MIL-L-7808 and di-2-ethylhexyl azelate (Figures A1-A4 of Appendix A). The additives present in Mobil MIL-L-7808 enhance the emission signal for Fe but depress the emission signal for Al, Cu and Mg. The effects of additives on the emission of Fe are shown in Figure 10.

B. COMPARISON OF 14 and 20 ELEMENT CALIBRATION STANDARDS.

1. Although the enhanced metal concentrations obtained for metals in ester oils are of no concern to the Joint Oil Analysis Program, there is some concern regarding any errors that may result by changing the number of elements in calibration standards. The standards currently being used will no

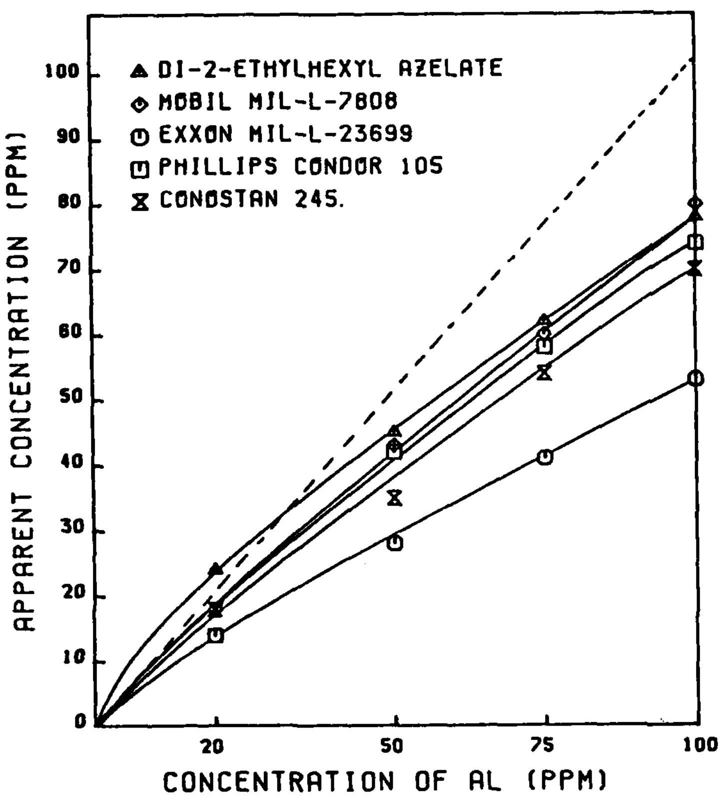

Figure 12. Plot of Apparent Concentration versus Actual Concentration for Al.

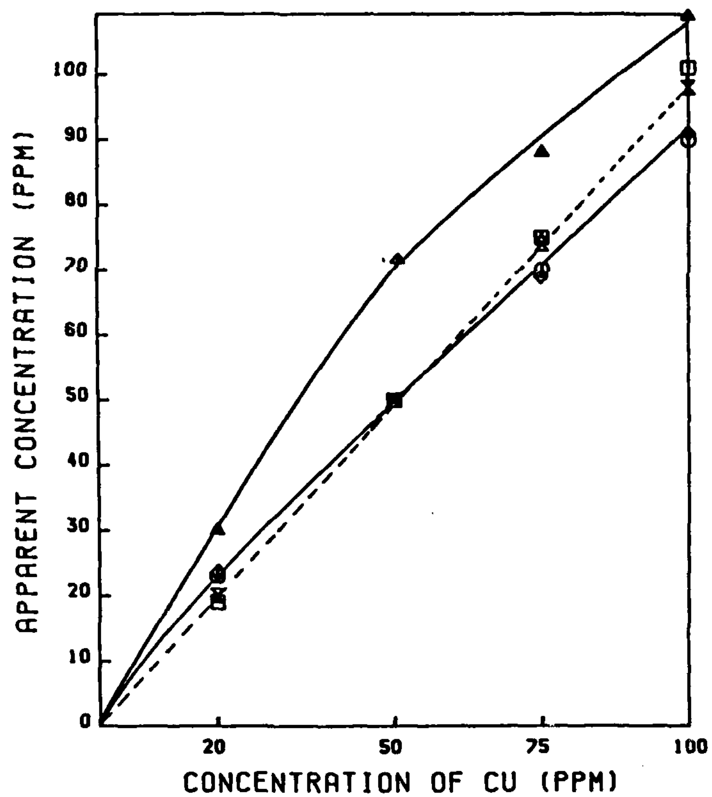

Figure 13. Plot of Apparent Concentration versus Actual Concentration for Cu.

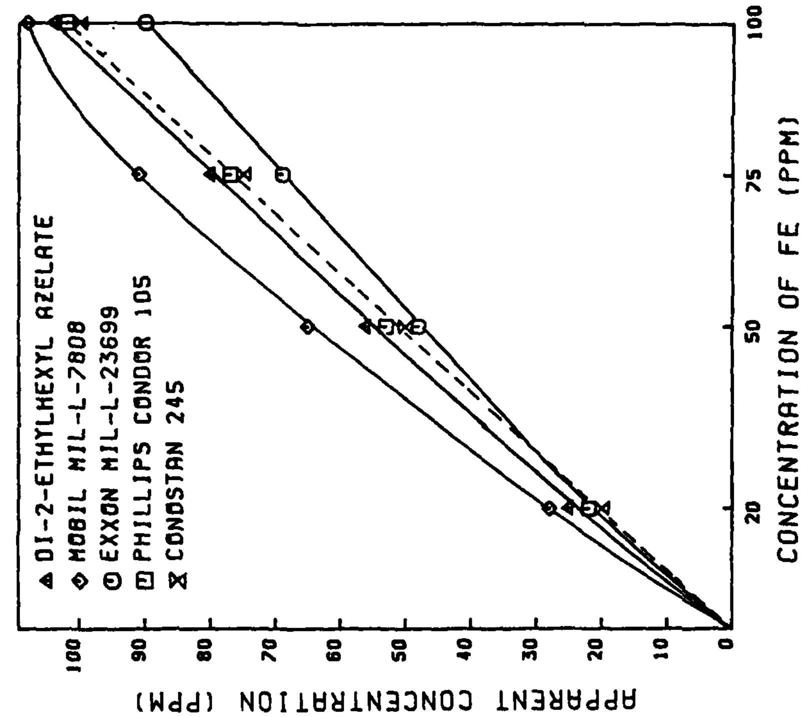

Figure 14. Plot of Apparent Concentration versus Actual Concentration for Fe.

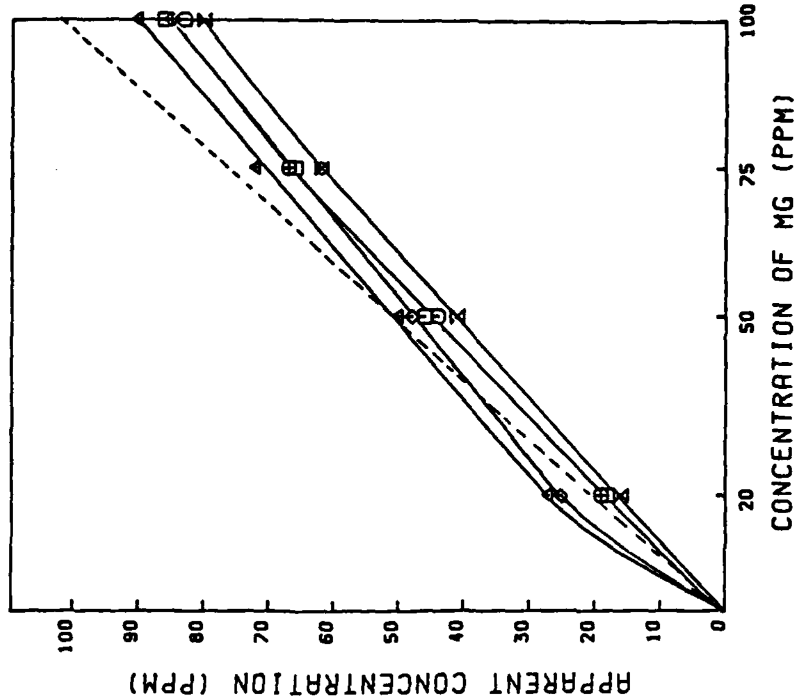

Figure 15. Plot of Apparent Concentration versus Actual Concentration for Mg.

longer be produced, and D14-Y standards (D20 minus B, Ba, Be, Cd, Mn and V) will be provided by the JOAP-TSC as calibration standards. There was also some concern that slight variations in the 1100 base oil might affect the results. Therefore, an investigation into the effects the new standards might have on the analytical results from the A/E35U-3 was carried out.

2. To examine the differences between 14 and 20 element standards, 6 standards were analyzed on the A/E35U-3. Three standards were prepared in this laboratory and contained 14, 18 (D20 minus B and Be) and 20 elements at 100 ppm in Conostan 245 oil. The other three standards were prepared by the JOAP-TSC in 1100 base oil. The average concentration and the standard deviation obtained from 10 replicates are listed in Table 8.

3. As can be seen from the data listed in Table 8, eliminating six of the elements from the 20 element standard has an effect on the Ti emission. In both 1100 and 245 base oils, emission from Ti in the fourteen element (D14-100 and D'14-100) standards was enhanced by 9-10 ppm relative to the D20-100 standards. To check on the accuracy of the Ti emission, the JOAP-TSC purposely reduced the concentration of Ti in sample D20-100(R-5). The enhanced Ti emission was also observed for the D'18-100 standard which indicates that the absence of B or Be is probably responsible for the change in the Ti emission.

4. The analytical results were similar for all other metals in both 1100 and 245 base oil except for Na which gave higher results in Conostan 245. Since Na is not a critical wear metal, the results indicate that slight variations in the hydrocarbon base oil will not affect the results in a serious manner.

C. PARTICLE DETECTION CAPABILITIES OF THE A/E35U-3 AND THE A/E35U-1 EMISSION SPECTROMETERS.

1. Table 9 lists the percent metal analyzed (% A) for the suspensions prepared in Mobil MIL-L-7808. The results indicate that the capabilities of the A/E35U-1 and the A/E35U-3 for analyzing particles depend upon the size of the particles as well as the metal being analyzed. The data illustrates that the A/E35U-1 can analyze Al, Cr, Fe and Mg particles better than the A/E35U-3. On the other hand, the A/E35U-3 analyzes Ag, Cu and Ni particles in MIL-L-7808 better than the A/E35U-1.

2. Table 10 lists the data for the analysis of the suspensions prepared in Exxon MIL-L-23699. The MIL-L-23699 suspensions gave results similar to the MIL-L-7808 suspensions. Again Al, Fe and Mg particles were analyzed better on the A/E35U-1, while the suspension of Cu particles gave similar results on both instruments.

TABLE 8. ANALYSIS OF MULTIELEMENT STANDARDS IN CONOSTAN 245 BASE OIL AND 1100 BASE OIL USING THE A/E35U-3 SPECTROMETER

Standard	Spectrometric Analysis[a]																			
	Fe	Ag	Al	Be[b]	Cr	Cu	Mg	Na	Ni	Pb	Si	Sn	Ti	B[b]	Ba	Cd	Mn	Mo	V	Zn
D'20-100	104.4	102.9	109.2		108.1	103.2	107.6	124.6	106.8	118.0	109.1	111.3	116.5		111.1	114.0	107.0	105.4	109.9	105.1
σ	3.1	5.0	3.7		2.7	4.3	8.0	8.0	2.5	3.1	2.4	3.5	4.3		2.9	4.5	4.3	3.1	2.6	7.1
D'18-100	108.2	109.2	110.1		109.9	105.9	111.2	125.1	109.9	119.7	110.2	112.7	125.2		118.1	117.4	110.6	107.8	112.6	117.2
σ	2.9	5.2	2.2		3.4	4.1	5.1	6.9	2.7	3.1	2.0	3.3	5.0		9.7	2.1	5.2	2.0	3.4	8.6
D'14-100	105.7	99.9	106.2		107.3	101.2	104.7	113.2	106.3	115.8	108.2	109.3	125.6					108.2		104.2
σ	2.8	3.2	2.7		2.2	3.7	5.2	6.0	2.0	2.7	2.5	2.6	5.3					3.6		6.6
D20-100 (R-6)	105.0	101.0	110.5		107.0	103.6	108.4	109.3	109.1	112.2	107.7	109.7	118.2		116.6	111.2	108.8	101.0	110.3	101.0
σ	3.0	2.7	3.9		1.3	3.1	3.3	7.6	2.4	2.3	3.4	2.3	3.3		2.2	3.2	3.3	3.3	2.4	2.1
D20-100 (R-5)	99.5	98.8	104.1		101.9	97.8	101.3	105.6	103.4	106.4	103.1	105.2	102.2		108.3	105.4	103.1	97.9	105.0	94.7
σ	2.8	2.4	2.7		1.6	3.4	2.8	6.4	2.5	1.8	3.3	2.5	4.3		2.5	3.7	4.9	6.1	2.0	5.4
D14-100	106.0	100.4	106.0		105.9	100.9	103.3	108.7	107.7	110.8	107.6	105.1	128.2					107.8		101.1
σ	1.5	1.3	2.3		1.2	2.4	2.7	5.1	1.8	0.9	2.0	1.6	2.2					3.0		4.0

[a] Avg. of ten replicates

[b] A/E35U-3 was not calibrated for Be and B

TABLE 9. PERCENT METAL ANALYZED (%A) BY THE A/E35U-1 AND A/E35U-3 FOR PARTICLES SUSPENDED IN MIL-L-7808

PARTICLE SIZE (µm)	AG		AL		CR		CU		FE		MG		MO		NI		TI	
	-1[a]	-3[b]	-1	-3	-1	-3	-1	-3	-1	-3	-1	-3	-1[d]	-3	-1	-3	-1[d]	-3
0-1	86	82	-[c]	-	-	-	89	94	-	-	100	100	-	96	-	-	-	100
1-3	69	64	-	-	100	100	64	71	100	100	100	100	-	90	40	75	-	100
3-5	10	36	100	75	88	43	15	18	67	50	100	100	-	70	16	26	-	75
5-8	5	16	63	46	50	28	7	12	29	13	91	81	-	27	3	14	-	29
8-10	0	0	58	41	19	8	3	8	13	8	80	40	-	13	0	6	-	28
10-12	0	0	34	5	8	8	0	3	7	3	44	21	-	8	0	0	-	18
12-UNF[e]	0	0	27	4	5	4	0	0	3	0	37	17	-	3	0	0	-	11

[a] Results for the A/E35U-1

[b] Results for the A/E35U-3

[c] - = Not Analyzed

[d] A/E35U-1 does not Analyze for Mo and Ti

[e] UNF = Unfiltered

TABLE 10. PERCENT METAL ANALYZED (%A) BY THE A/E35U-1 AND A/E35U-3 FOR PARTICLES SUSPENDED IN MIL-L-23699

PARTICLE SIZE (microns)	AL		CU		FE		MG		MO		TI	
	-1[a]	-3[b]	-1	-3	-1	-3	-1	-3	-1[d]	-3	-1[d]	-3
0-1	-[c]	-	100	100	-	-	100	100	-	-	-	-
1-3	100	80	74	63	100	98	100	100	-	65	-	88
3-5	90	50	60	50	75	50	100	100	-	40	-	50
5-8	52	28	37	38	53	20	95	80	-	13	-	22
8-10	38	24	25	28	36	10	88	48	-	7	-	12
10-12	25	18	7	14	12	6	66	39	-	5	-	6
12-UNF[e]	9	8	1	10	6	3	42	33	-	3	-	2

[a]Results for the A/E35U-1

[b]Results for the A/E35U-3

[c]- = Not Analyzed

[d]A/E35U-1 does not Analyze for Mo or Ti

[e]UNF = Unfiltered

3. Data was also collected for metal powder suspensions prepared in Humble MIL-L-7808, Conostan 245, Phillips Condor 105, light mineral oil, MIL-H-83282A and 2-ethylhexyl azelate in order to investigate the effects of matrix, particle settling rates, transport efficiency, and source energy on the particle detection capability of the A/E35U-3.

4. In addition to metal powders, suspensions of Arizona Road Dust and ceramic powders were prepared and analyzed. The Arizona Road Dust was used to simulate lubricants and hydraulic fluids containing an ingested contaminant. Silicon is the major element present in Arizona Road Dust and is the element which was analyzed to determine the capability of the rotating disk electrode spectrometers to detect dust contaminants.

5. Since dust is ingested by the engine, the particle size distribution found in used oil samples should be similar to the Arizona Road Dust's with the maximum particle size found in the oil being determined by the engine's filters. The 200 ppm suspensions of fine and coarse grade Arizona Road Dust (64 ppm Si, 17 ppm Al, 6 ppm Fe) prepared in MIL-L-23699 oil and MIL-H-83282A hydraulic fluid were analyzed on the A/E35U-3 and the A/E35U-1 spectrometers. The results listed in Table 11 indicate that the capabilities of the A/E35U-1 and A/E35U-3 for analyzing Road Dust are similar. As expected, the fine grade is analyzed better than the coarse grade, and the concentrations of Si determined in MIL-L-23699 and MIL-H-83282A were similar.

6. To determine the particle size detection limitations of the A/E35U-1 and A/E35U-3 spectrometers for analyzing dust particles, the MIL-H-83282A hydraulic fluid suspension of the fine grade Arizona Road Dust was filtered and analyzed. As shown in Figure 16, both instruments are incapable of quantitatively determining the Si content of the particles which passed through the 1 μm filter.

7. Suspensions of silicon nitride and titanium carbide in MIL-L-23699 were also analyzed. Both of these refractory materials proved to be difficult to analyze. As can be seen in Figure 17 and Table 12, the A/E35U-3 is incapable of quantitatively analyzing for Ti in TiC or Si in Si_3N_4 particles, respectively.

TABLE 11. ANALYSIS OF ARIZONA ROAD DUST SUSPENDED IN EXXON MIL-L-23699 OIL AND MIL-H-83282A HYDRAULIC FLUID

ARIZONA ROAD DUST[a]	MATRIX	CONCENTRATION METAL (PPM) AL -1[b]	AL -3[c]	FE -1	FE -3	SI -1	SI -3	SI TRANSPORTED BY DISK
Coarse	MIL-L-23699	0	0.1	1	1	4	4.5	24.1
	MIL-H-83282A	1	0.3	2	1.5	9	8.0	10.8
Fine	MIL-L-23699	1	0.5	2	1.7	12	13.1	44.1
	MIL-H-83282A	1	0.7	4	3.0	13	14.0	24.5

[a]Concentration of Al, Fe and Si in suspension was 17, 5.6 and 64 ppm, respectively.

[b]Analyzed by A/E35U-1

[c]Analyzed by A/E35U-3

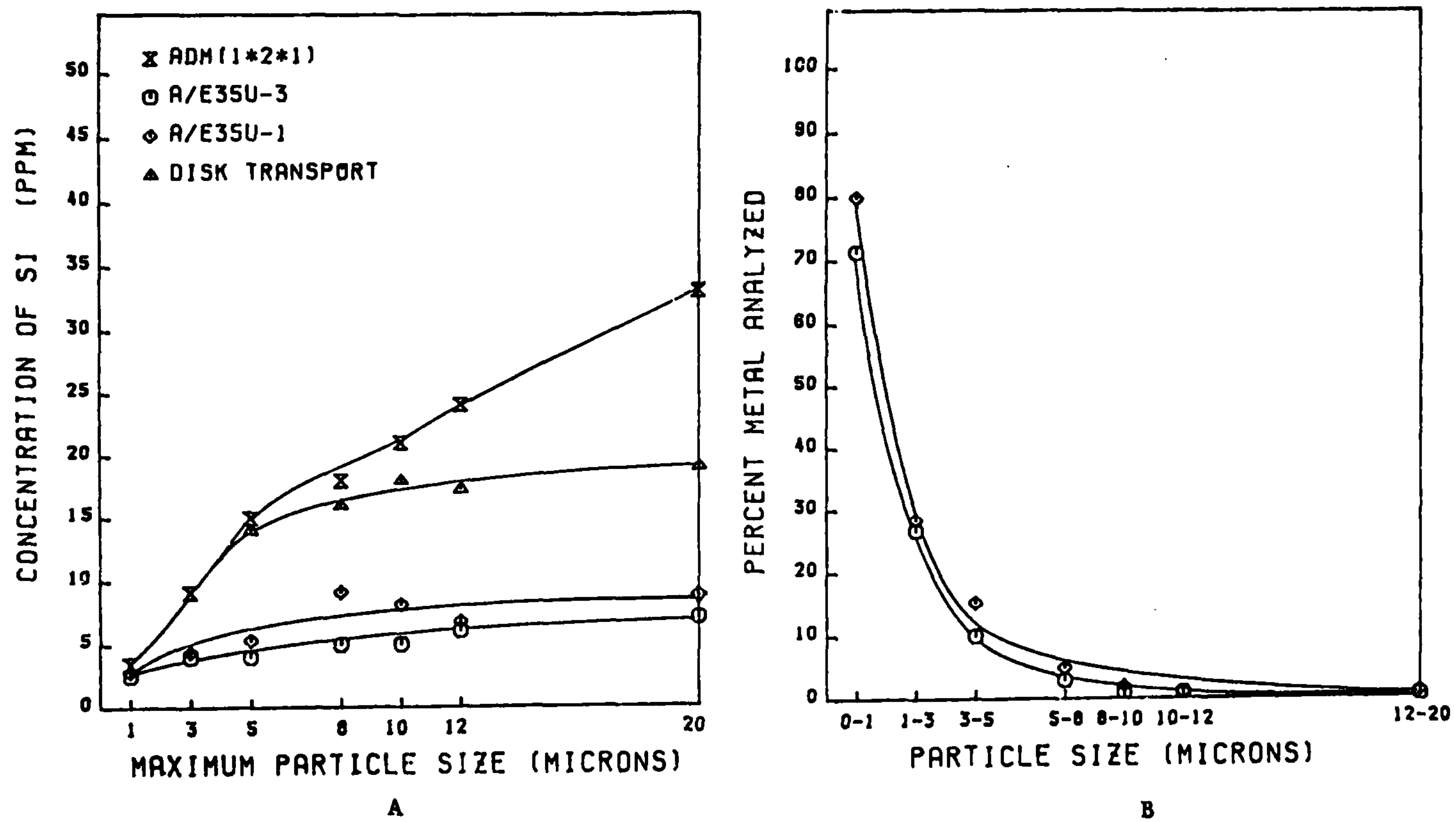

Figure 16. Spectrometric Analysis (A) and Percent Metal Analyzed (B) for Si in Fine Arizona Road Dust Suspended in MIL-H-83282A Hydraulic Fluid.

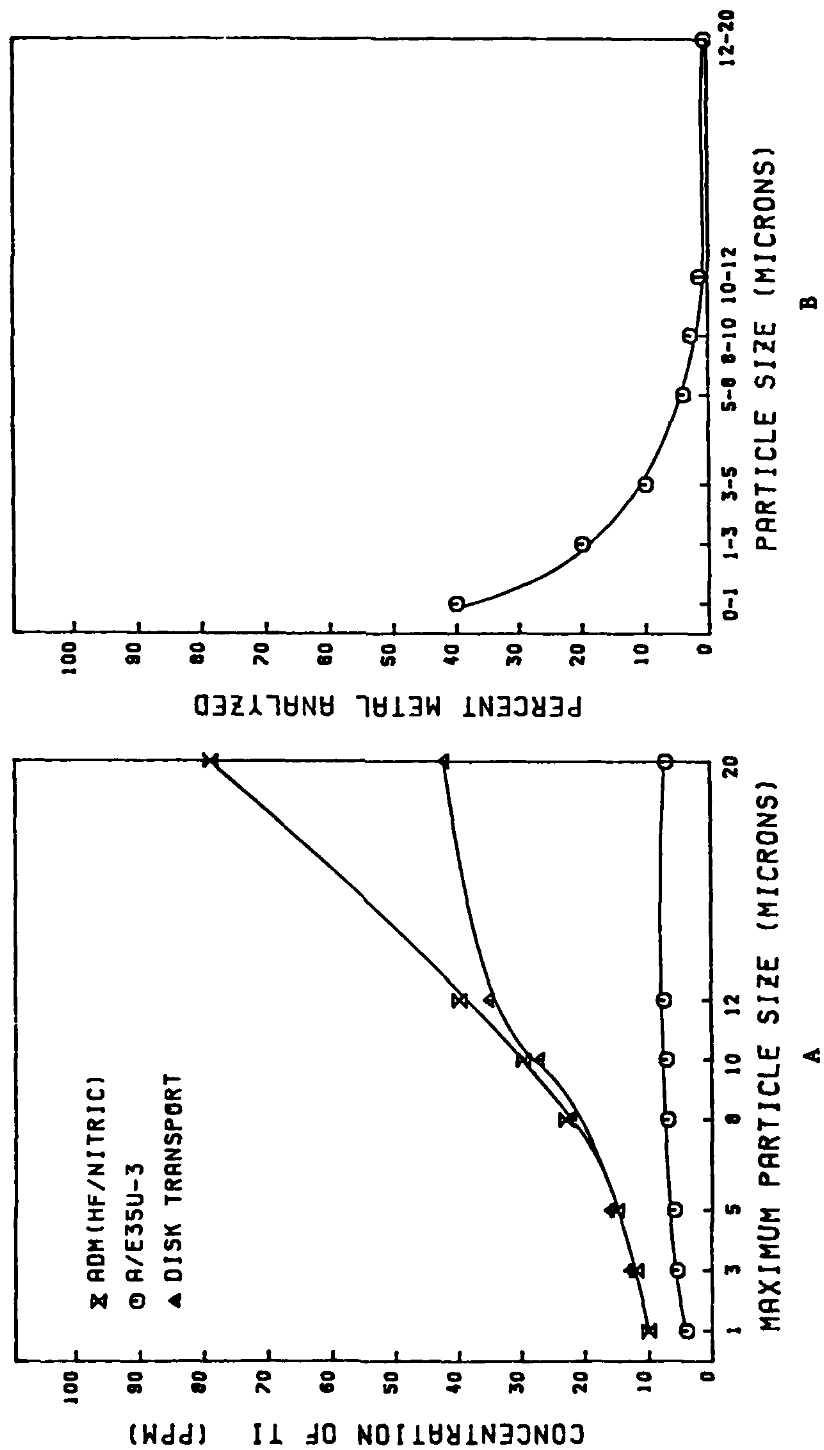

Figure 17. Spectrometric Analysis (A) and Percent Metal Analyzed (B) for Ti in TiC Ceramic Powder Suspended in Exxon MIL-L-23699.

TABLE 12. ANALYSIS OF SILICON NITRIDE SUSPENDED IN EXXON MIL-L-23699

Concentration of Si (ppm)	A/E35U-1 (ppm)	A/E35U-3 (ppm)
60	18	14.4
120	35	30.1

D. FACTORS WHICH AFFECT THE PARTICLE SIZE DETECTION CAPABILITIES OF THE A/E35U-3 AND THE A/E35U-1 EMISSION SPECTROMETERS.

1. INTRODUCTION. The particle size detection capabilities of the A/E35U-1 and A/E35U-3 spectrometers are controlled by the efficiency with which the rotating disk electrode transports particles to the source (particle transport efficiency) and the efficiency with which the arc/spark source vaporizes and excites the transported particles (source efficiency). In Appendix A, the figures produced by plotting the percent metal analyzed vs the particle size, show that the particle size detection capabilities of the A/E35U-3 and A/E35U-1 differ and are dependent on the metal as well as the oil in which the metal is suspended. Therefore, the effects of matrix and particle characteristics on the particle transport and source efficiencies, and consequently on the particle size detection capability of the A/E35U-3, were thoroughly investigated.

2. EFFECT OF PARTICLE TRANSPORT EFFICIENCY.

a. Introduction. In order for the A/E35U-3 to analyze particles, the particles must first be transported to the arc/spark source. Therefore, the transport efficiency of the rotating disk was investigated. The transport efficiency of the rotating disk was defined as

$$\text{Percent Metal Transported} = \frac{\text{Conc of Metal on Disk}}{\text{Conc of Metal in Sample}} \times 100$$

and, in general, was found to be inversely proportional to particle size.

b. Comparison of Transport Efficiencies for the A/E35U-1 and the A/E35U-3 Spectrometers.

(1) We also observed that the transport efficiencies of the A/E35U-1 and the A/E35U-3 were slightly different.

(2) In order to evaluate the transport efficiencies of the A/E35U-1 and A/E35U-3 spectrometers, Ag, Fe and Mg metal powder suspensions in Mobil MIL-L-7808 and Exxon MIL-L-23699 were prepared and studied under the appropriate conditions. The A/E35U-1 employs a 12-second preburn and a 33-second emission integration time for a total burn time of 45 seconds. During this burn time, the temperature of the oil sample rises from 25°C to 75°C or at a rate of 1.1°C/second. The A/E35U-3 employs a 6-second preburn and a 30-second emission integration time for a total burn time of 36 seconds. During this time the sample temperature rises from 25°C to

$65^{o}C$, or at a rate of $1.1^{o}C$/second. Therefore, the length of the burn time, not the rate of the temperature rise, is the reason that a sample analyzed on the A/E35U-1 reaches a temperature $10^{o}C$ higher than a sample analyzed on the A/E35U-3. Therefore, the transport efficiencies of the A/E35U-1 and the A/E35U-3 were determined under identical experimental conditions but for different integration times.

(3) Suspensions of magnesium, iron and silver particles were used to determine the efficiency of particle transport for the A/E35U-1 and the A/E35U-3 spectrometers. Mg, Fe and Ag were chosen because of their low (1.74 g/ml), intermediate (7.86 g/ml) and high (10.5 g/ml) densities, respectively. The percent of metal transported was plotted versus time for Ag, Fe and Mg particles suspended in Mobil MIL-L-7808 and Exxon MIL-L-23699. The plotted results are shown in Figure 18 and illustrate that particle transport efficiency decreases with an increase in the metal's density.

(4) To determine the transport efficiencies for the two instruments, the percent metal transported was plotted versus the integration time for each instrument. The integration time is the interval that each instrument spends integrating the emission signal. The integrated emission intensity is used to determine the element's concentration. The metal particles detected by the A/E35U-3 are those transported between 6 and 36 seconds, and the particles detected by the A/E35U-1 are those transported between 12 and 45 seconds. The plot of percent metal transported versus integration time is shown in Figure 19. The data illustrates that the transport efficiencies for the A/E35U-3 are higher than those for the A/E35U-1 because of the shorter preburn time employed by the A/E35U-3.

(5) To compare the transport efficiencies of the two instruments, the average percent metal transported during the integration time was calculated according to the equation:

$$\text{Avg \% Metal Transported} = \left[\int_{0}^{T_2} (\text{\% Metal Transported})\, dt\right] \div T_2$$

where T_2 is the integration time.

(6) The calculated average percent metal transported for each metal suspension and the respective metal density are listed in Table 13. For Ag and Fe the particle transport efficiency of the A/E35U-3 is higher than that for the A/E35U-1. The transport efficiency for Mg particles is approximately 100% for both instruments.

(7) The difference in the transport efficiencies between the A/E35U-1 and the A/E35U-3 increases with increasing particle density so that the differences between the instruments are very small for Mg but are large for Ag. This helps explain why the A/E35U-3 spectrometer produces higher percent metal analyzed than the A/E35U-1 for the denser metals such as Ag, Cu and Ni in MIL-L-7808 oils.

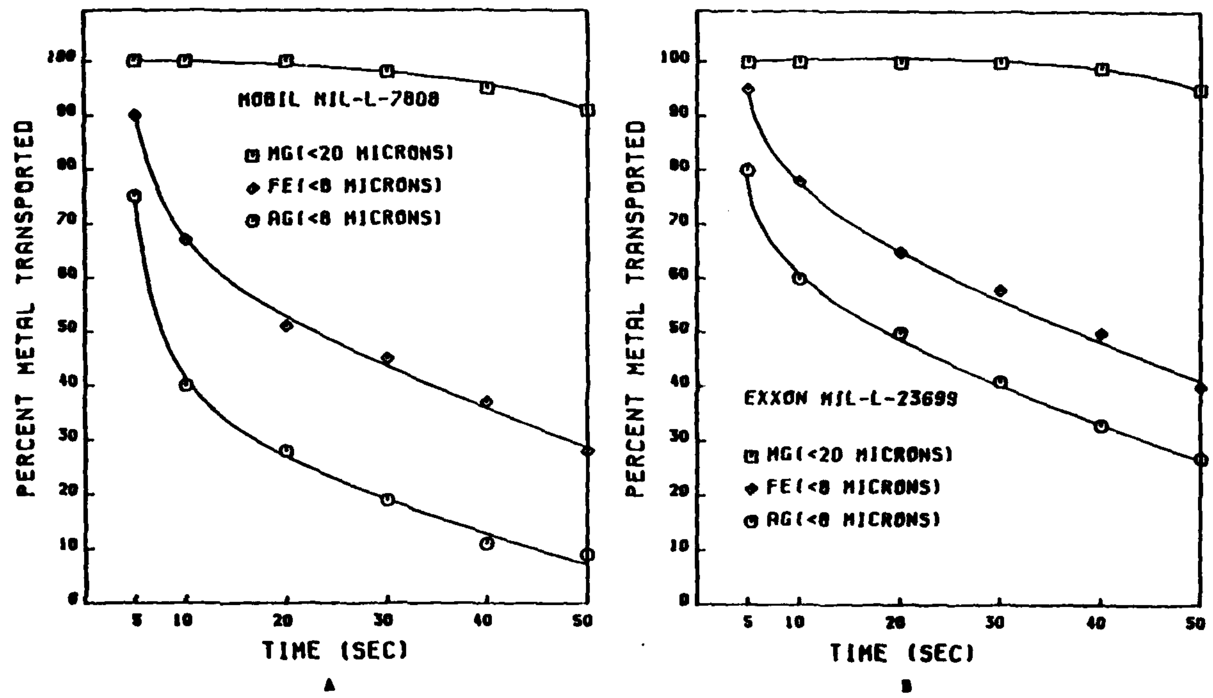

Figure 18. Percent Metal Transported by the Rotating Disk Electrode versus Time for Ag, Fe and Mg Powders Suspended in Mobil MIL-L-7808 (A) and Exxon MIL-L-23699 (B).

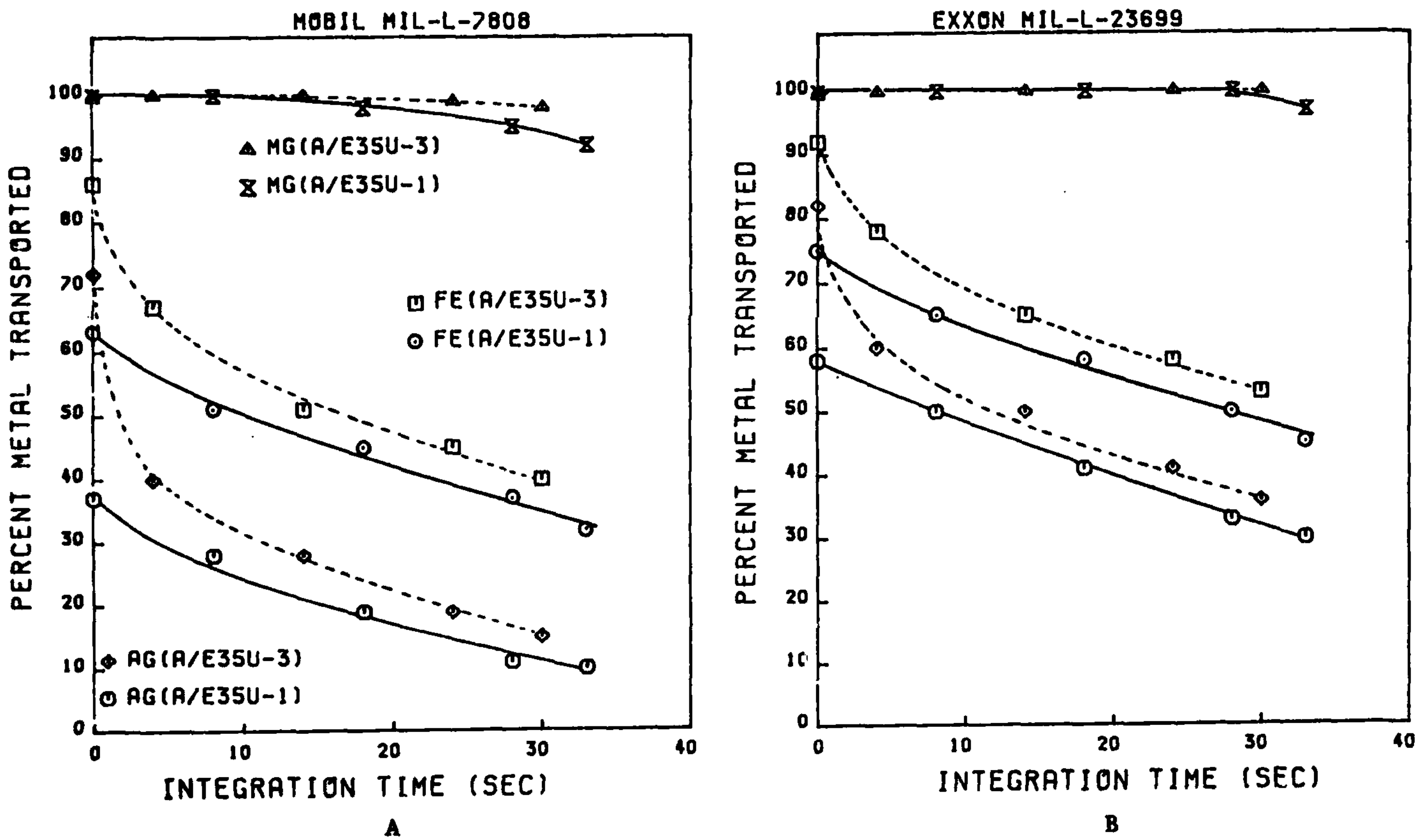

Figure 19. Percent Metal Transported by the Rotating Disk Electrode versus Integration Time for Ag, Fe and Mg Powders Suspended in Mobil MIL-L-7808 (A) and Exxon MIL-L-23699 (B).

TABLE 13. AVERAGE PERCENT METAL TRANSPORTED IN TWO DIFFERENT ESTER OILS FOR THE A/E35U-1 AND A/E35U-3 SPECTROMETERS

			% METAL TRANSPORTED	
ELEMENT	DENSITY	OIL	A/E35U-1	A/E35U-3
Ag (< 8 μm)	10.5	Mobil MIL-L-7808	21.3	30.2
		Exxon MIL-L-23699	42.8	50.6
Fe (< 8 μm)	7.9	Mobil MIL-L-7808	46.0	53.0
		Exxon MIL-L-23699	59.0	66.7
Mg (< 20 μm)	1.7	Mobil MIL-L-7808	97.7	99.0
		Exxon MIL-L-23699	99.5	100.0

(8) The filtrates obtained for the suspensions of Al, Cu, Fe and Mg particles in MIL-L-23699 were analyzed in a similar manner and the results are plotted in Figures 20-23. These results again illustrate that the transport efficiencies are higher for the A/E35U-3, especially for the denser metals.

c. Transport Efficiency of the Rotating Disk Electrode.

(1) To conduct a thorough investigation of the type discussed in the previous paragraph would be very time consuming and was not deemed necessary to identify the particle transport efficiency of the rotating disk as one factor which limits the particle detection capability of the A/E35U-3. Therefore, the particle transport efficiencies for the remaining suspensions were determined at times of 24 ± 4 seconds which is the average time for transporting one-half the total metal transported for the A/E35U-3 and the A/E35U-1. The actual times chosen depended upon the density of the metal. Shorter times were used for the denser metals, while longer times used for the lighter metals.

(2) The concentrations of metal transported by the disk were plotted versus particle size, and the results are included in Appendix A (Figures A8A-A52A). Although the particle transport data was intended to give a qualitative comparison rather than a quantitative one, there is a good correlation between the metal transport data and the spectrometric determinations which are plotted in Figures A8A-A52A. The low particle transport data obtained for Ag and Mo (Figures A14 and A20) is probably due to a combination of the metals high density and the low viscosity of Mobil MIL-L-7808 which enhances the inherent differences between the experimental and spectrometric conditions. The plots in Appendix A as well as in Figures 20-23 do illustrate that the larger particles are not being transported to the source. The low disk transport efficiency for the large particles is one factor which limits the particle detection capability of the A/E35U-3.

d. Effect of Particle Settling Rates.

(1) Initially, we expected the rotating disk to be an efficient method for transporting particles to an emission source. In light of the transport efficiency results, we concluded that there must be a factor operating which limits the rotating disk's efficiency. The factor most likely responsible is the particle settling rate. The effect of particle settling rates was examined by determining the particle transport efficiency versus time and temperature. If settling rates are significant, the particle transport efficiencies will decrease with time and temperature increase.

(2) The particle transport efficiency of the rotating disk electrode was first evaluated for a suspension of Fe (< 8 μm) particles in Conostan 245 at temperatures of 25°C and 75°C and at times between 5 and 50 seconds. The efficiency of particle transport was 100% in all cases. Therefore, the particle settling rate is not an important factor for the analysis of Fe particles in the most viscous oils. However, when the same experiment was carried out for Fe (< 8 μm) particles suspended in Mobil MIL-L-7808, the particle transport efficiency decreased with time and temperature increase (Figure 24).

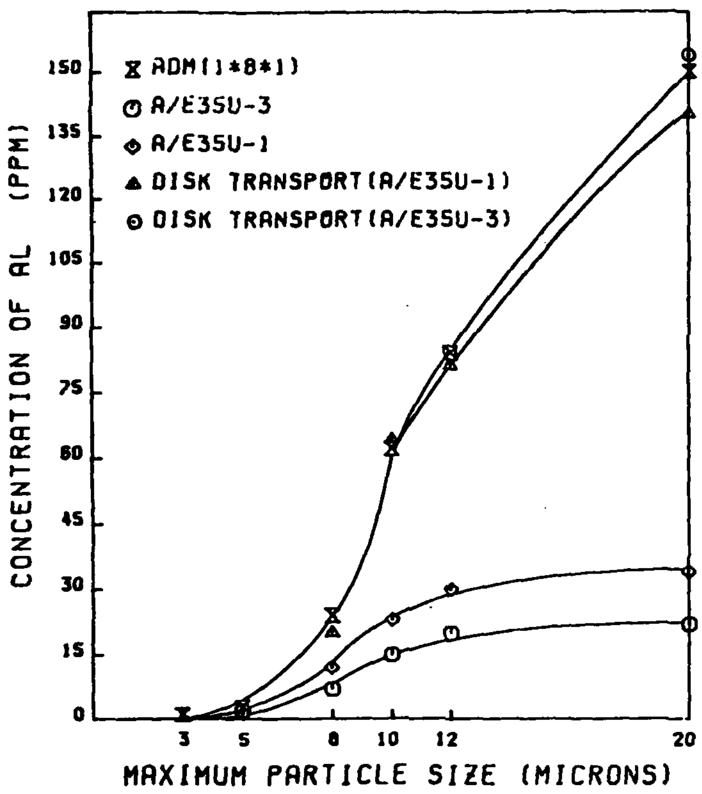

Figure 20. Concentration of Metal Transported by the Rotating Disk Electrodes of the A/E35U-1 and A/E35U-3 for Al Powder Suspended in Exxon MIL-L-23699.

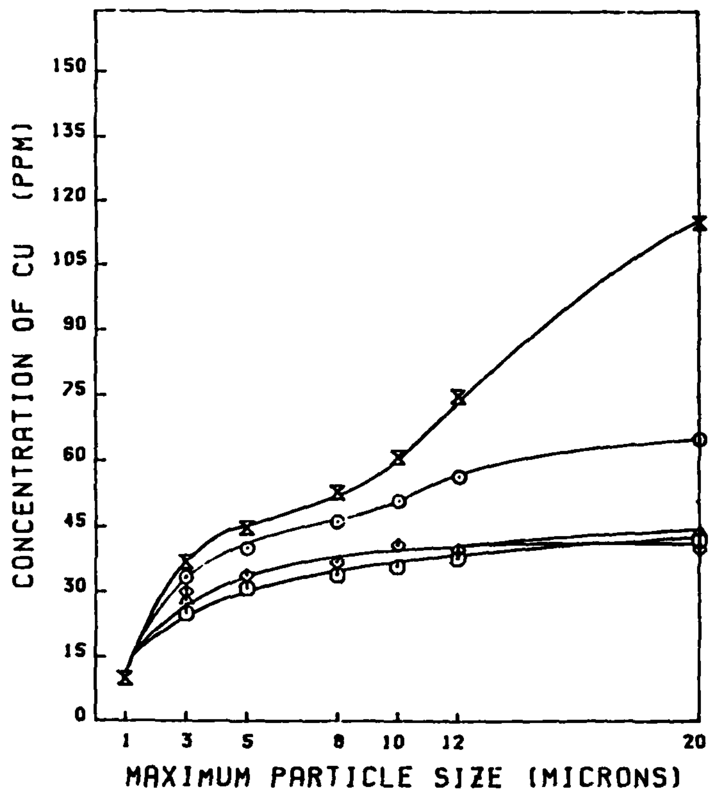

Figure 21. Concentration of Metal Transported by the Rotating Disk Electrodes of the A/E35U-1 and A/E35U-3 for Cu Powder Suspended in Exxon MIL-L-23699.

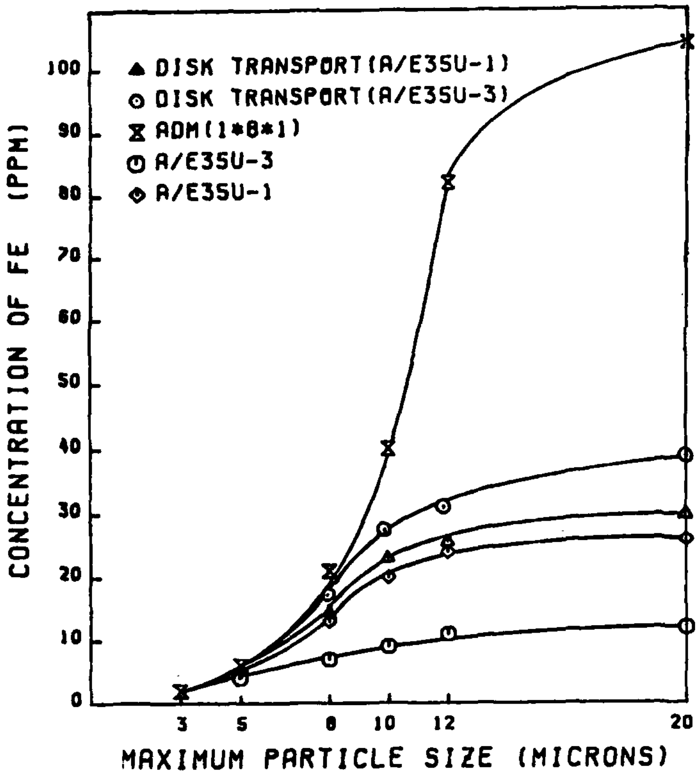

Figure 22. Concentration of Metal Transported by the Rotating Disk Electrodes of the A/E35U-1 and A/E35U-3 for Fe Powder Suspended in Exxon MIL-L-23699.

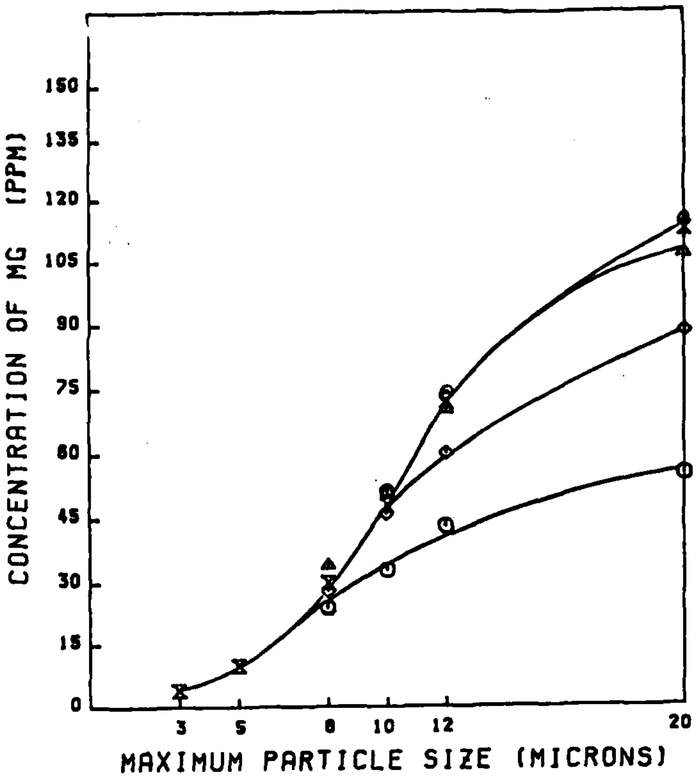

Figure 23. Concentration of Metal Transported by the Rotating Disk Electrodes of the A/E35U-1 and A/E35U-3 for Mg Powder Suspended in Exxon MIL-L-23699.

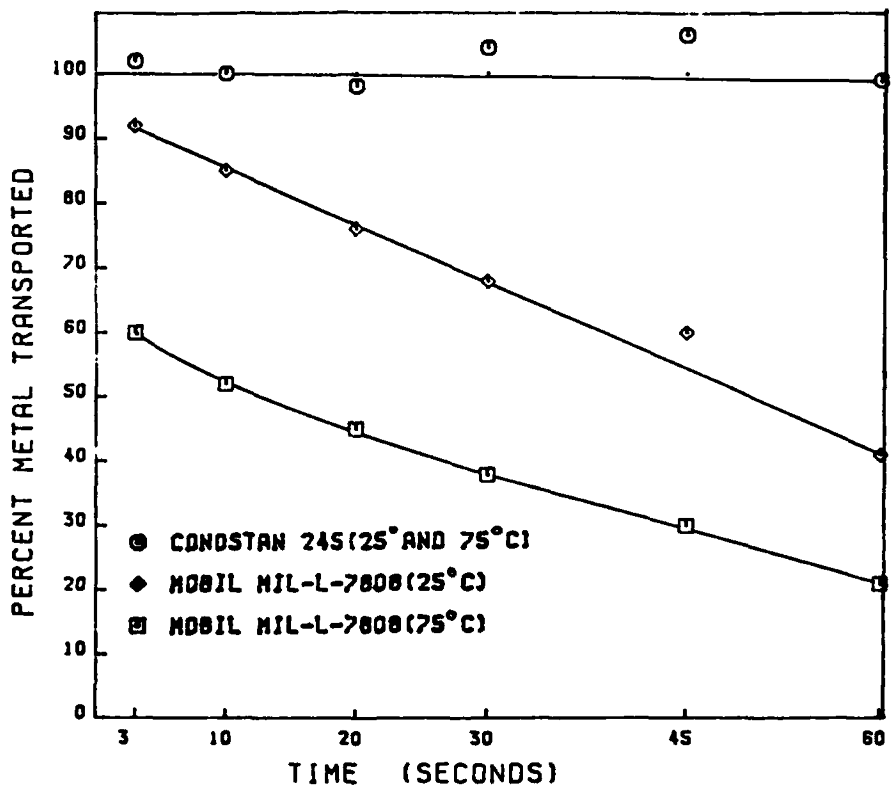

Figure 24. Plot of Percent Metal Transported versus Time at 25°C and 75°C for Fe Powder Suspended in Mobil MIL-L-7808 and Conostan 245.

(3) The efficiency results determined in Mobil MIL-L-7808 indicate that the particle detection capability of the A/E35U-3 is limited by the particle settling rates. This limiting factor is especially important during the analyses, since the sample temperature increases during the burn cycle. The temperature increase has the ultimate effect of increasing the particle settling rates and decreasing the particle transport efficiency.

e. Effect of Particle Density on Disk Transport Efficiency. As just stated, the particle settling rate is an important factor which limits the capability of the A/E35U-3. Since the particle settling rate is directly proportional to the density of the metals, the efficiency of particle transport should be inversely proportional to the density of the particles. The particle transport efficiencies determined for the metal particles suspended in Mobil MIL-L-7808 were plotted vs particle density, and the expected inverse relationship was verified as shown in Figure 25.

f. Effect of Metal Concentration. To determine the effect of the concentration of metal on the disk transport efficiency of the A/E35U-1 and A/E35U-3 spectrometers, an Fe metal powder (< 20 micron) suspension was prepared in light mineral oil. This suspension was diluted to produce metal powder suspensions which contain identical particle size distributions but have metal concentrations ranging from 10 to 100 ppm. The particle transport efficiency was found to be constant for these diluted suspensions, indicating that transport efficiency is not affected by the concentration of particles in the suspension.

g. Effect of Matrix Viscosity.

(1) Since the particle settling rates have been shown to be a limiting factor, the viscosity of the matrix should have an effect on particle transport. Two lubricating oils with similar compositions but widely different viscosities were used to determine the effect of viscosity on particle transport. Phillips Condor 105 and Conostan 245 lubricating oils are both hydrocarbon-based with viscosities of 19 cs and 215 cs, respectively (Table 14).

(2) The viscosity of the oil affects both the amount of oil and the size of particles transported to the source (Table 14 and Figure 26). The disk transports over twice as much Conostan 245 as Condor 105, and the efficiency of particle transport in Conostan 245 is 100% for Al, Fe and Mg particles less than 20 μm in size and for Cu particles less than 5 μm in size. The efficiency of particle transport is much less in Condor 105.

h. Effect of Particle Morphology.

(1) To determine the effect of particle morphology on the particle transport efficiency of the disk, suspensions of the five Fe metal powders (< 20 μm) prepared in light mineral oil were used.

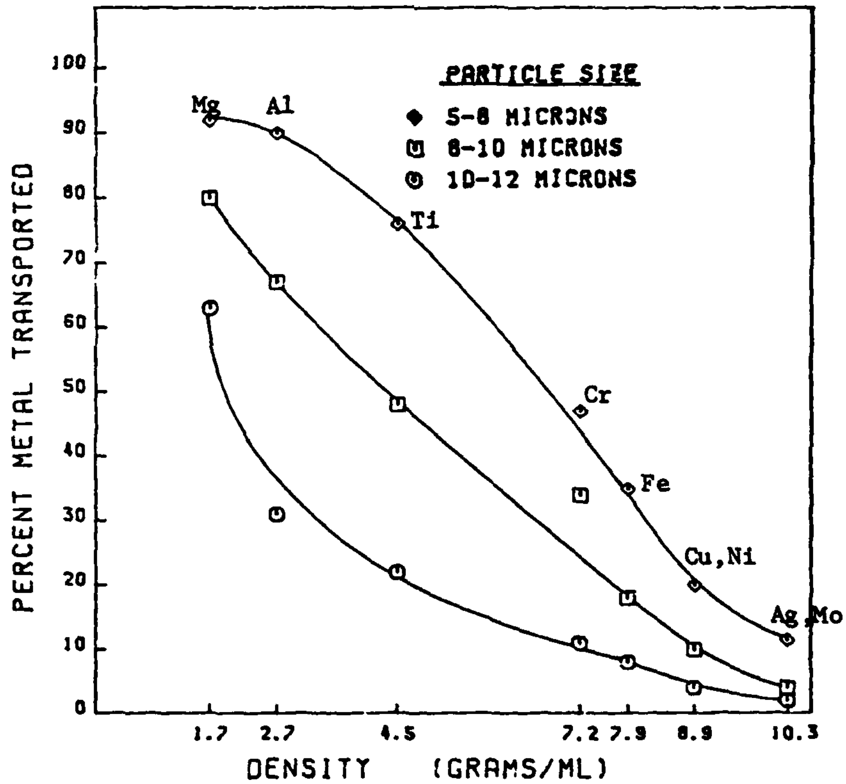

Figure 25. Plot of Percent Metal Transported versus Density for Different Particle Sizes.

TABLE 14. COMPOSITION AND PHYSICAL PROPERTIES OF THE FLUIDS USED TO PREPARE THE SUSPENSIONS

MATRIX	COMPOSITION	VISCOSITY[a] (cs)	OIL TRANSPORTED BY DISK (g)
Di-2-Ethylhexyl Azelate	Dibasic Ester	11	0.036 ± 0.006
Mobil MIL-L-7808	Dibasic Ester	13	0.039 ± 0.003
Humble MIL-L-7808	Polyol Ester	14	0.040 ± 0.004
Light Mineral Oil	Hydrocarbon	16	0.034 ± 0.004
MIL-H-83282A	Synthetic Hydrocarbon (Fire Resistant Hydraulic Fluid)	16	0.040 ± 0.005
Phillips Condor Grade 105	Hydrocarbon	19	0.038 ± 0.002
Exxon MIL-L-23699	Pentaerythritol Ester	24	0.047 ± 0.002
Conostan 245	Hydrocarbon	215	0.096 ± 0.003

[a] $100^{\circ}F$

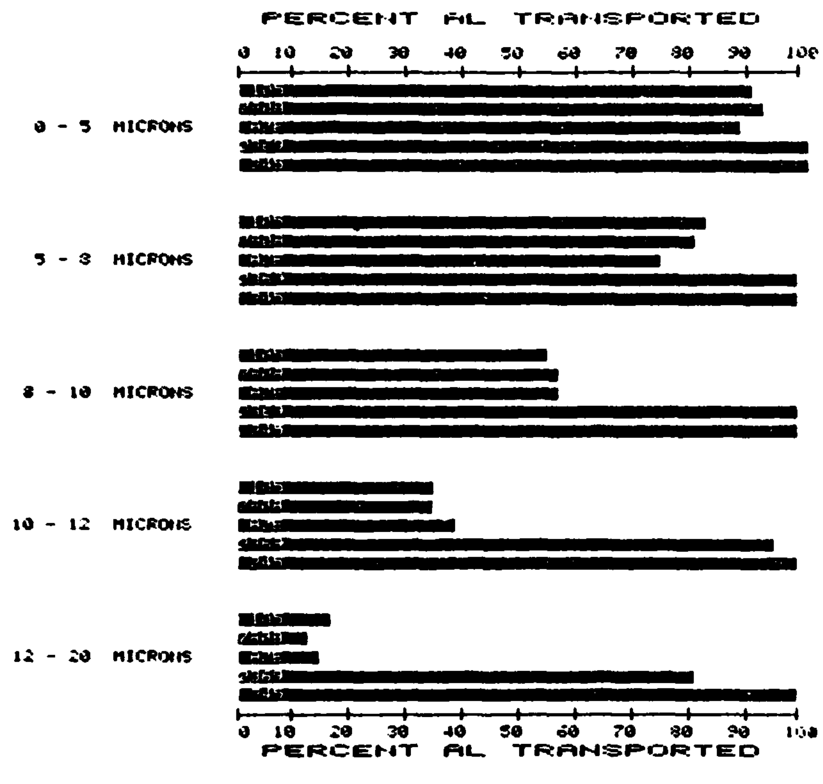

A

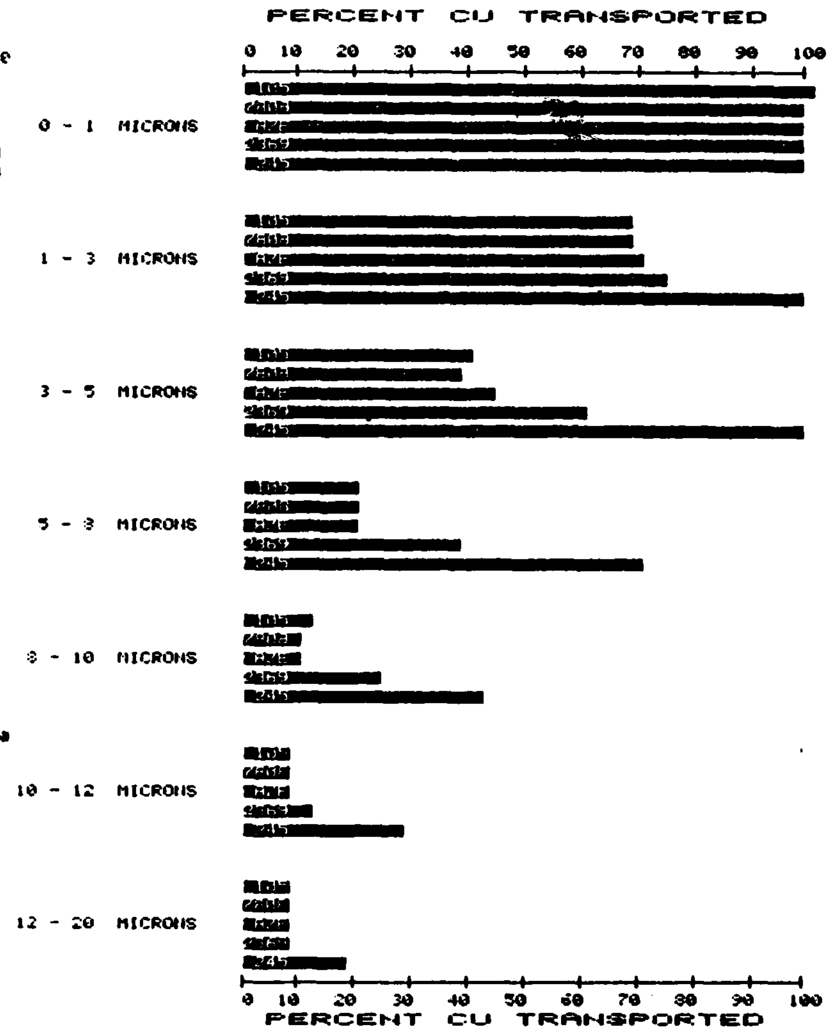

B

Figure 26. Matrix Effects on the Particle Transport Efficiency of the Rotating Disk Electrode for Al (A), Cu (B), Fe (C) and Mg (D) Powders Suspended in Phillips Condor 105, Mobil MIL-L-7808, Di-2-Ethylhexyl Azelate, Exxon MIL-L-23699, and Conostan 245.

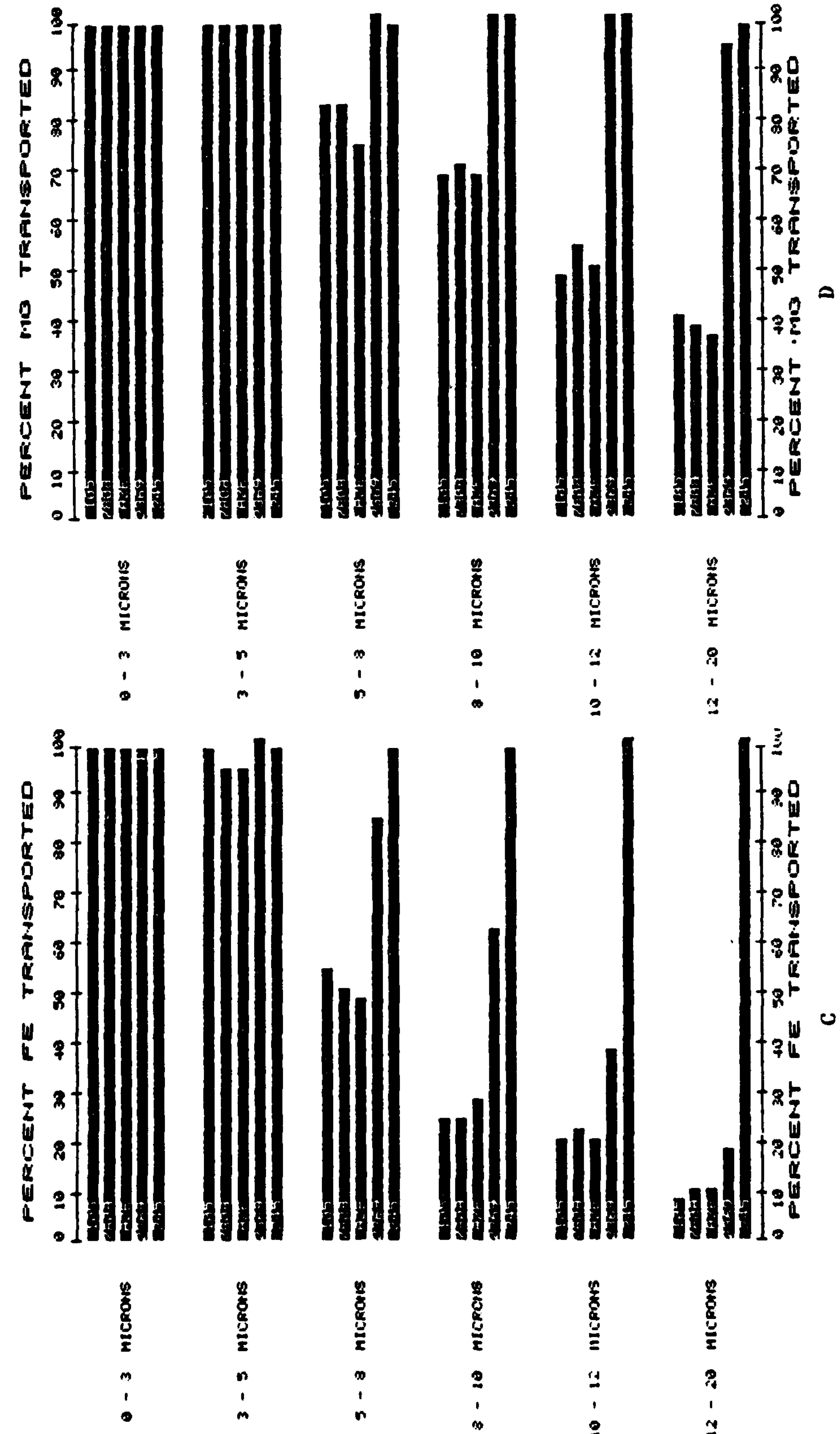

Figure 26. Concluded.

(2) The shapes of the metal particles were determined by a scanning electron microscope (SEM), and the photomicrographs are shown in Figure 27. The Ventron Fe powder consists of agglomerated, spherical particles (Figure 27A) and the VMC Fe powder is made up of very small, spherical particles with a reported average size of 0.3 micron (Figure 27B). The small particles in the VMC Fe powder form agglomerates which greatly reduce the filtering efficiency and the particles do not readily pass through the 3 micron filter. The AEE and ROC/RIC Fe powders contain slightly larger particles than the ball-milled metal powder but the three powders are similar in shape containing nonspherical particles (Figures 27C, D, E).

(3) The data listed in Table 15 shows that the suspensions of the Ventron and Ball Milled Fe powders in light mineral oil have similar particle size distributions as determined by the filtration method. Therefore, any difference between the percent metal transported for the Ball Milled and Ventron Fe powders can be attributed directly to particle shape. As seen in Figure 28 the transport efficiency of the Ball Milled Fe powder is higher than that for the Ventron Fe powder.

3. EFFICIENCY OF THE ARC/SPARK SOURCE.

a. Introduction.

(1) The figures in Appendix A (A8-A52) and Figures 20-23 show that the particle detection capabilities and the transport efficiencies of the rotating disk electrode are different for the A/E35U-1 and A/E35U-3 spectrometers, respectively. In order to compare the source efficiencies for the two instruments, differences in transport efficiencies had to be reduced or eliminated so that any difference between metal analyses on the A/E35U-1 and the A/E35U-3 could be directly related to the differences in source efficiency for the two spectrometers.

(2) Since the transport efficiencies for suspensions of Al, Cu, Fe and Mg in Conostan 245 are the same for both instruments, these suspensions were used to compare the effectiveness of the spark sources. The A/E35U-1 gives higher metal particle recoveries for Al, Cu, Fe and Mg suspensions prepared in Conostan 245 (Table 16) and most other oils (Figures A8B-A52B). Therefore, we must conclude that the source employed by the A/E35U-1 is more appropriate for metal particle analyses.

b. Matrix Effects.

(1) Introduction.

(a) To determine the effects of the matrix on the particle detection capability of the A/E35U-3 spectrometer, Al, Cu, Fe, Mg, Mo and Ti powders were suspended in Mobil MIL-L-7808, Exxon MIL-L-23699 and

A. VENTRON (1000X)

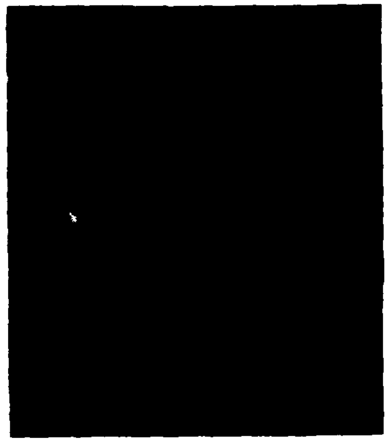

B. VMC (1000X)

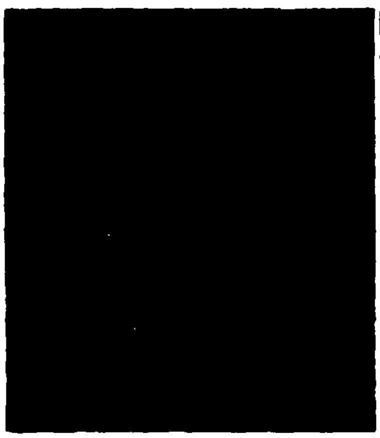

C. AEE (300X)

D. ROC/RIC (300X)

E. BALL MILLED (300X)

Figure 27. Photomicrographs of Ventron (A), VMC (B), AEE (C), ROC/RIC (D), and Ball-Milled (E) Fe Powders.

TABLE 15. PARTICLE SIZE DISTRIBUTION AS DETERMINED BY FILTRATION FOR FE POWDERS SUSPENDED IN LIGHT MINERAL OIL

MAXIMUM PARTICLE SIZE (μm)	CONCENTRATION OF FE (PPM)[a]				
	VMC	VENTRON	BALL MILLED	AEE	ROC/RIC
20 (unfiltered)	110	140	140	140	140
12	50	85	87	70	35
10	30	64	67	36	15
8	17	35	43	21	3
5	15	19	20	8	0
3	13	4	5	4	0

[a]Concentration of Fe determined by the ADM and is the ppm of metal which passed through filter.

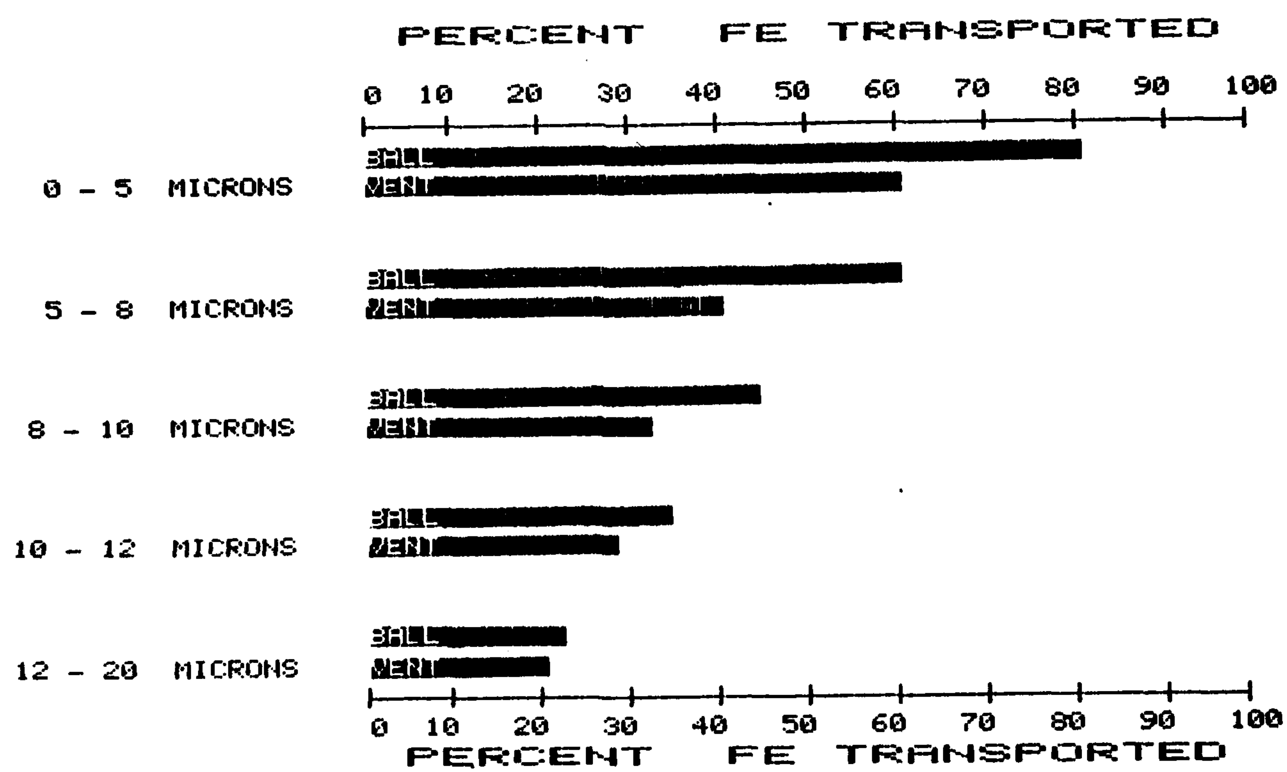

Figure 28. Percent Fe Transported by the Rotating Disk Electrode for Ball-Milled and Ventron Fe Powders Suspended in Light Mineral Oil.

TABLE 16. PERCENT METAL ANALYZED (%A) BY THE A/E35U-1 AND A/E35U-3 FOR PARTICLES SUSPENDED IN CONOSTAN 245

PARTICLE SIZE (μm)	AL		CU		FE		MG	
	-1[a]	-3[b]	-1	-3	-1	-3	-1	-3
0-1	-[c]	-	100	100	-	-	-	-
1-3	100	100	101	93	100	100	100	102
3-5	100	67	66	50	76	50	100	103
5-8	100	38	22	24	50	33	100	100
8-10	93	28	12	14	32	18	101	100
10-12	33	17	8	12	15	10	94	66
12-UNF[d]	12	8	5	5	6	4	72	53

[a] Results for the A/E35U-1

[b] Results for the A/E35U-3

[c] - = Not Analyzed

[d] UNF = Unfiltered

Conostan 245. These three lubricants were chosen because of their different physical properties and chemical compositions (Table 14).

(b) The data listed in Table 14 shows that the amount of oil transported by the disk increases with the oil's viscosity. Figures 26 and 29 show that the efficiency of particle transport is also directly related to the oil's viscosity. In fact, in the most viscous oil studied (Conostan 245), 100% of the Al, Fe, Mg and Ti particles less than 20 μm were transported by the disk.

(c) The particle transport efficiencies suggest that the spectrometer's particle detection capabilities should be the greatest for suspensions prepared in Conostan 245 and lowest for suspensions prepared in Mobil MIL-L-7808. This result was the case for Al, Fe and Mg particles suspended in Mobil MIL-L-7808, Exxon MIL-L-23699 and Conostan 245 oils (Figure 30A, C and D). However, emission from Cu, Ti and Mo particles did not follow the expected pattern (Figures 30B and 31). The highest Ti and Mo concentrations were obtained in Mobil MIL-L-7808 and the highest Cu concentrations (>3 μm) were obtained in MIL-L-23699. It appears, factors other than particle transport efficiency must be affecting the A/E35U-3's particle detection capabilities. Therefore, a thorough investigation of the factors affecting the source efficiency of the A/E35U-3 was conducted.

(2) Effect of Oil Viscosity

(a) To determine the effect of lubricant viscosity on the particle detection capability of the A/E35U-3, two hydrocarbon oils with widely different viscosities were used. The viscosity of Conostan 245 is 215 cs (100^{o}F) and that of Condor 105 is 19 cs (100^{o}F) as shown in Table 14.

(b) The viscosity affects both the amount of oil transported and the efficiency of the disk for transporting particles to the source (Table 14 and Figure 26). The disk transports over twice as much Conostan 245 as Condor 105, and the efficiency of particle transport is 100% for Al, Fe and Mg particles less than 20 μm suspended in Conostan 245. The efficiency of particle transport is much less in Condor 105. Therefore, recoveries of metal particles are expected to be the highest in Conostan 245. However, the highest Cu concentrations were obtained in Condor 105. Apparently, the increased quantity of Conostan 245 transported by the disk decreases the efficiency of the source resulting in decreased recoveries of Cu particles.

(c) Since 100% of the particles of Al, Fe and Mg are transported to the source in Conostan 245, we anticipated obtaining quantitative recoveries for these metals. However, the results are much lower than expected (Figures 30A, C and D). In fact, less than 50% of the Fe and Al particles larger than 5 μm were analyzed by the A/E35U-3. Magnesium particles were easier to analyze, and those smaller than 10 μm were quantitatively analyzed by the A/E35U-3.

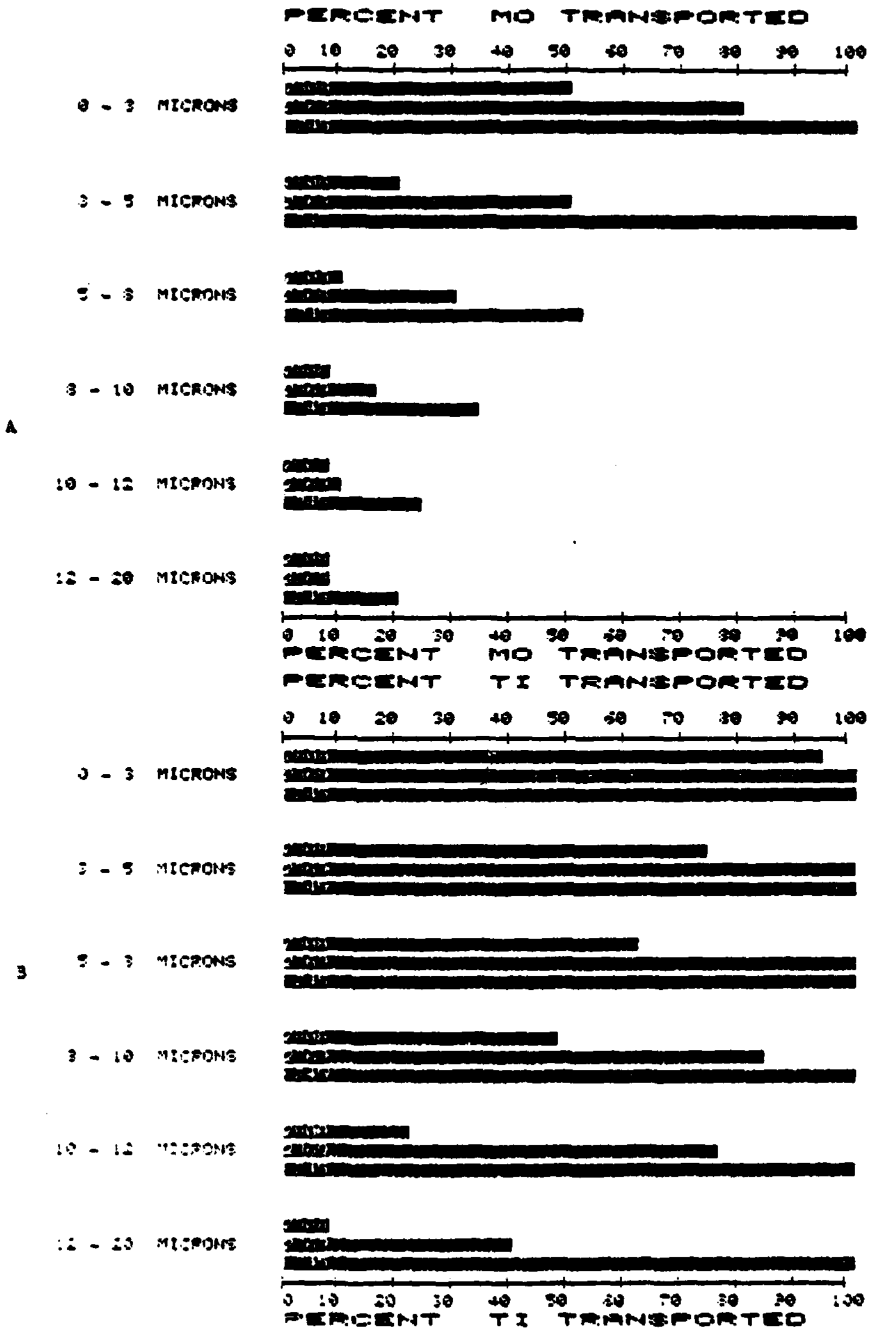

Figure 29. Matrix Effects on the Particle Transport Efficiency of the Rotating Disk Electrode for Mo (A) and Ti (B) Powders Suspended in Mobil MIL-L-7808, Exxon MIL-L-23699, and Conostan 245.

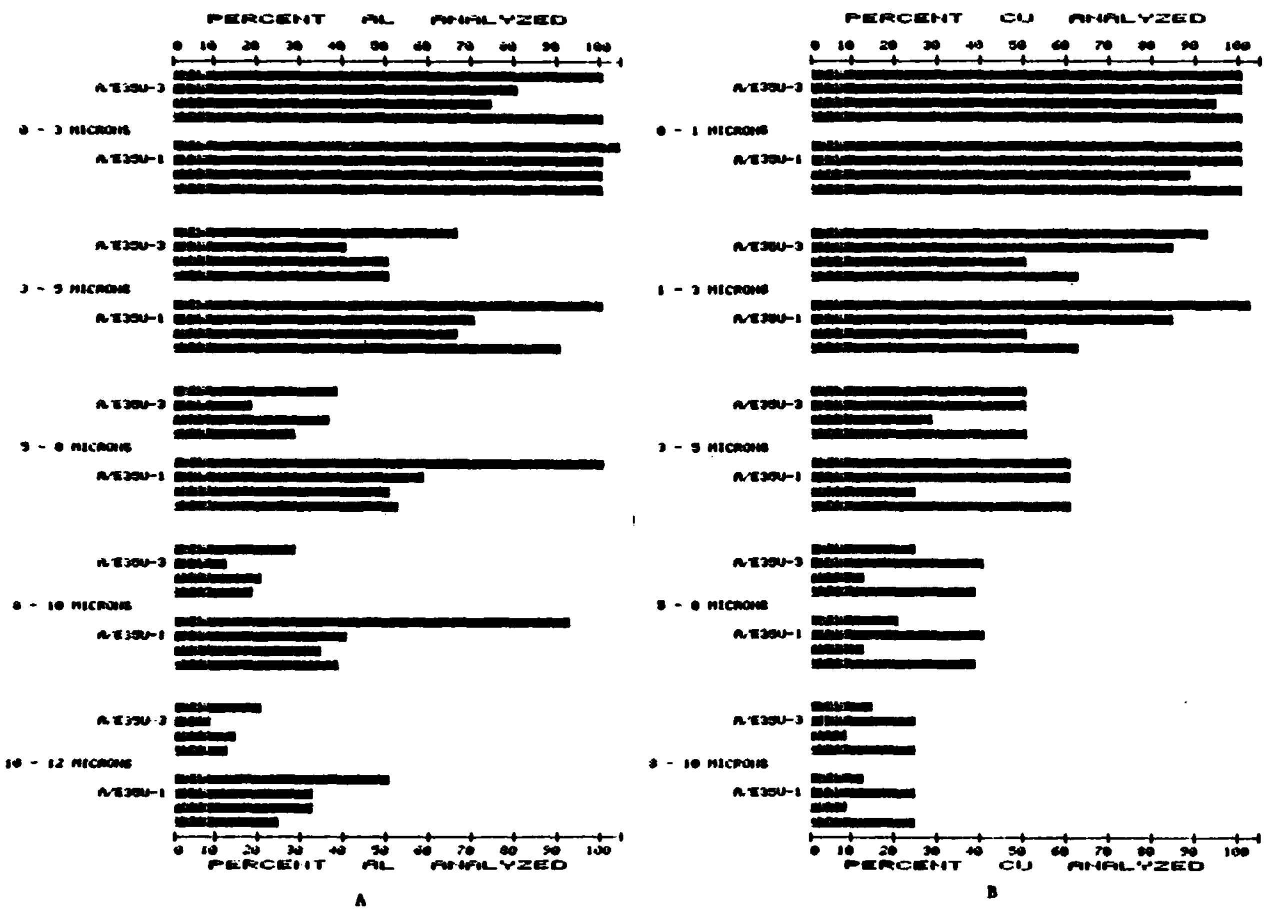

Figure 30. Matrix Effects on the Percent Metal Analyzed by the A/E35U-3 and A/E35U-1 for Al (A), Cu (B), Fe (C), and Mg (D) Powders Suspended in Conostan 245, Phillips Condor 105, Mobil MIL-L-7808 and Exxon MIL-L-23699.

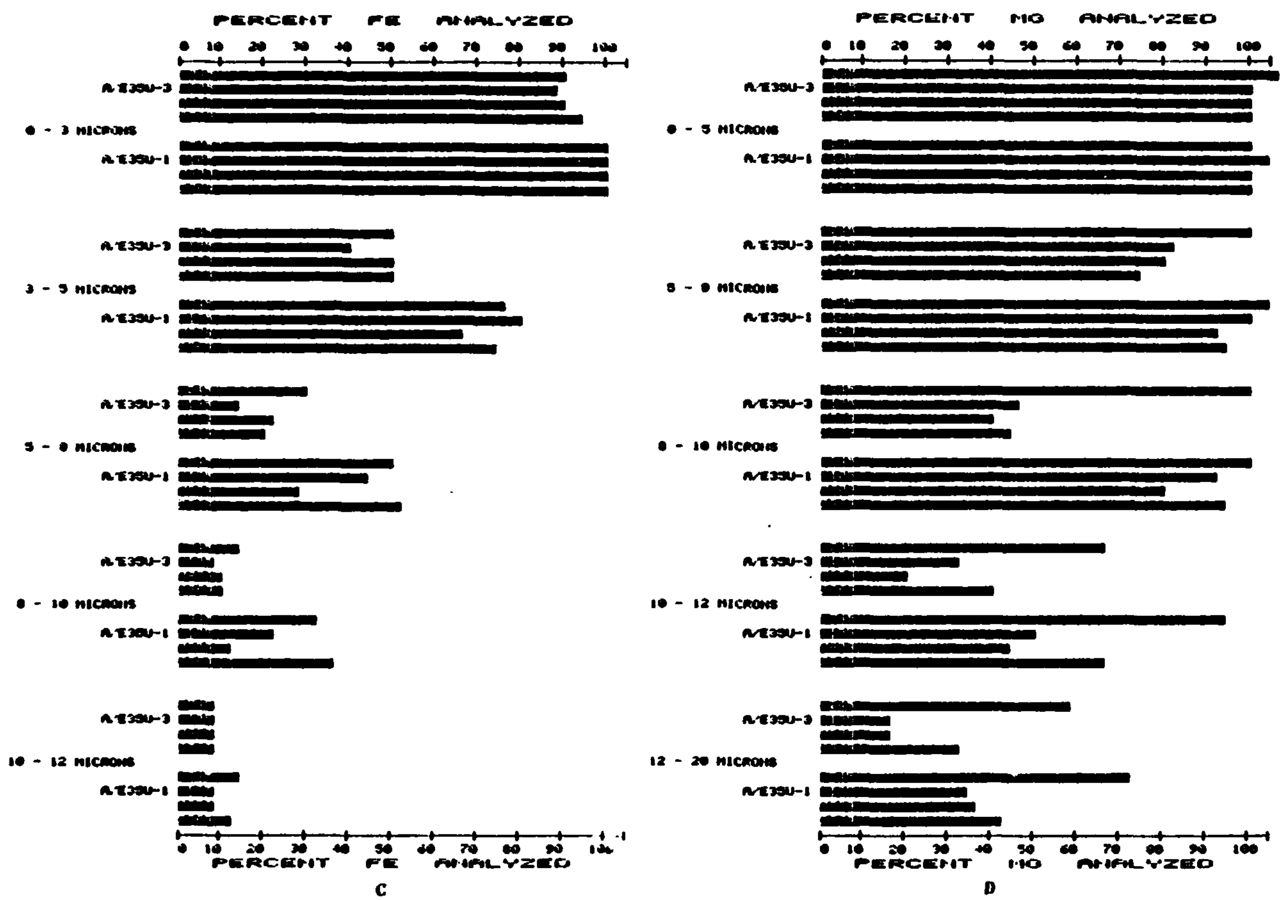

Figure 30. Concluded.

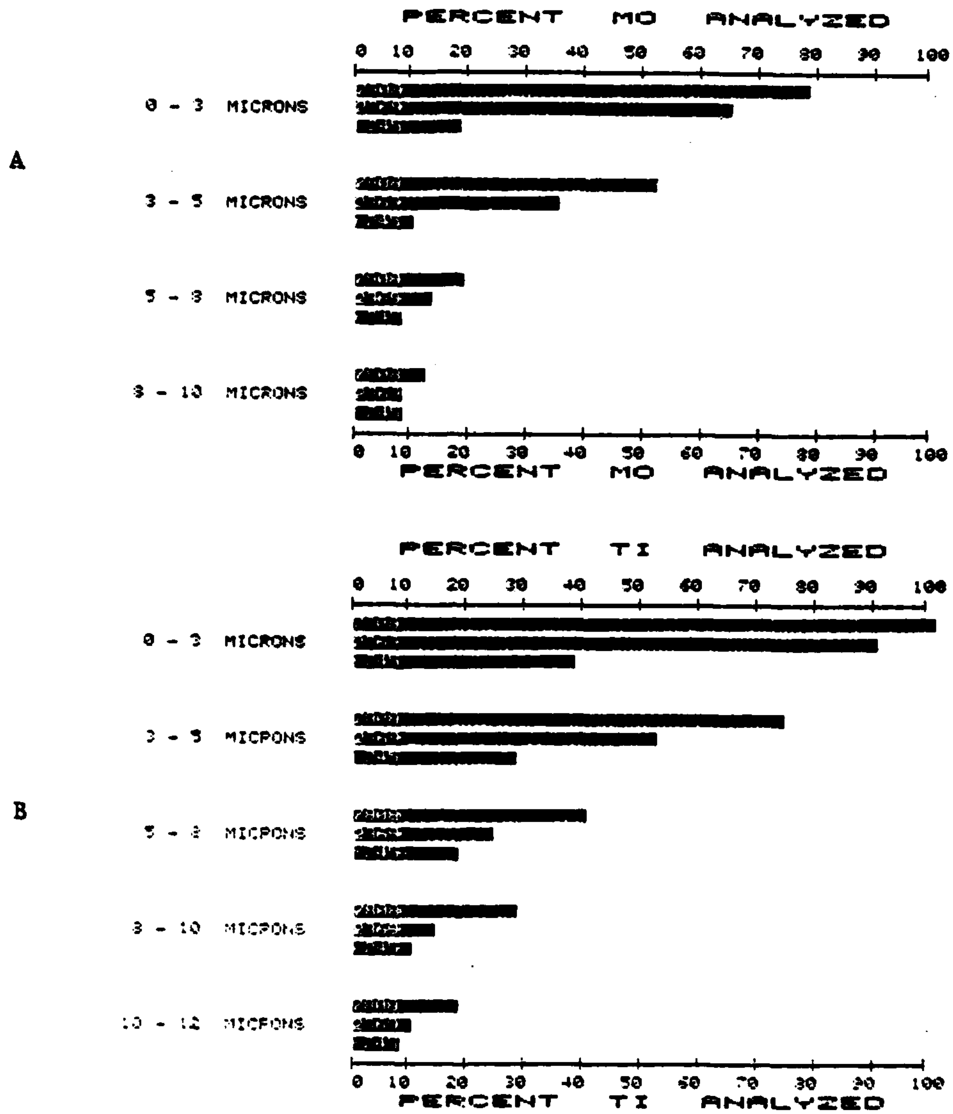

Figure 31. Matrix Effects on the Percent Metal Analyzed by the A/E35U-3 for Mo (A) and Ti (B) Powders Suspended in Mobil MIL-L-7808, Exxon MIL-L-23699 and Conostan 245.

(d) Again, there were exceptions to the rule, and Cu particles suspended in Phillips Condor 105 were analyzed better than particles suspended in Conostan 245 (Figure 30B). These results were obtained even though the transport efficiency for Cu particles suspended in Conostan 245 is about twice that for Cu particles suspended in Phillips Condor 105 (Figure 26B). Therefore, once again the increased quantity of Conostan 245 transported by the disk decreased the efficiency of the source.

(e) The suspensions prepared in Conostan 245 and Phillips Condor 105 were also analyzed on the A/E35U-1. The A/E35U-1 analyzed the suspensions of Al, Fe and Mg better than did the A/E35U-3 (Figure 30A, C and D). Furthermore, the differences in percent metal analyzed for particles suspended in the two oils were more pronounced, and, as expected, the percent metal analyzed was higher in the more viscous Conostan 245 than in the less viscous Phillips 105 except for Cu particles greater than 5 μm in size. Therefore, it appears that the source efficiency of the A/E35U-1 is affected less by increased amounts of oil on the disk than is the source efficiency of the A/E35U-3.

(3) Effect of Matrix Composition.

(a) The effect of oil composition on the source efficiency of the A/E35U-3 was investigated by analyzing the metallic particles suspended in a hydrocarbon oil (Phillips Condor 105) and in an ester oil (Mobil MIL-L-7808). Although the viscosities of Phillips Condor 105 and the Mobil MIL-L-7808 were not identical, the quantity of oil transported and the efficiency of particles transported to the source were similar for these oils (Table 14 and Figure 26). Therefore, any large differences in the A/E35U-3 analytical results for metal particles suspended in the different oils can be attributed directly to the effect of oil composition on the emission signal produced by the A/E35U-3.

(b) The A/E35U-3 analytical results shown in Figure 30 indicate that the detection of Mg particles is unaffected by the chemical differences between Mobil MIL-L-7808 and Phillips Condor 105. However, there is an effect due to differences in oil composition on the analysis of Al, Cu and Fe particles (Figures 30A, B and C). Copper is analyzed more efficiently in the hydrocarbon oil while aluminum and iron are analyzed more efficiently in the ester oil. If viscosity differences were influencing the analyses; one would expect Al, Cu, and Fe analyses to be affected in a similar manner.

(c) The suspensions were also analyzed on the A/E35U-1. The bar graphs in Figure 30B and C show that the A/E35U-1 analyzed the Cu and Fe particles in the Phillips Condor 105 oil more efficiently than the particles suspended in the MIL-L-7808 ester oil. Therefore, the oil composition has an effect on the source efficiencies of both the A/E35U-3 and A/E35U-1 spectrometers.

(d) Since each manufacturer of MIL-L-7808 or MIL-L-23699 uses a different base stock and their own additive package in formulating their lubricant, we decided to determine if the differences between MIL-L-7808 lubricants supplied by Humble and Mobil have any effect on the capability of the A/E35U-3 to detect metallic particles. The exact differences between these two lubricants are not known but they are formulated using different base stocks as shown by their gas chromatograms (Figure 32). We have saponified the Mobil MIL-L-7808 and determined that the lubricant is predominantly di-2-ethylhexyl azelate.

(e) The amount of oil and percent of particles transported by the rotating disk electrode are equal for suspensions of Al, Cu, Fe and Mg particles in Humble and Mobil MIL-L-7808 oils. The A/E35U-3 analytical results are also equal for the two MIL-L-7808 oil suspensions (Figure 33). Therefore, the two tested lubricant formulations for Humble and Mobil MIL-L-7808 oils do not affect the particle size detection capabilities of the A/E35U-3.

(f) To determine the effect of other matrices on A/E35U-3 analyses, Fe and Cu powder suspensions were prepared in MIL-H-83282A hydraulic fluid. MIL-H-83282A hydraulic fluid has a synthetic hydrocarbon base and a viscosity of 16 cs at 100°F. Because of its viscosity, it was compared to Mobil MIL-L-7808 oil (ester base, 13 cs at 100°F) and Phillips Condor 105 (hydrocarbon oil, 19 cs at 100°F). Although the viscosities of the oils and hydraulic fluid were not identical, the quantity of liquid transported and the efficiency of the particle transported to the source were similar.

(g) Within the experimental error associated with the analyses of Fe and Cu particles, these two matrices gave similar results and no differences were noted which could be attributed to differences in matrix composition (Figure 34).

(4) Effect of Additives. The effect of the additives present in Mobil MIL-L-7808 can be seen by comparing the bars labeled AZE (di-2-ethylhexyl azelate) and MOB (Mobil MIL-L-7808) in Figure 33. Although the additives have no effect on the particle transport efficiency of the rotating disc electrode, the data depicted in Figure 33 show that the additives improve the capability of the A/E35U-3 to analyze particles less than 5 μm for Mg and Al, less than 8 μm for Fe, and less than 3 μm for Cu. Apparently the additives have little effect on the larger particles.

c. Effect of Particle Composition. The composition of the particles greatly influences the particle detection capability of the A/E35U-3 spectrometer. For instance, the A/E35U-3 was capable of quantitatively analyzing Mg particles less than 5 μm suspended in MIL-L-23699 (Table 10) but was not capable of quantitatively analyzing Al particles less than 3 μm in size, although both were quantitatively transported to the source. For the

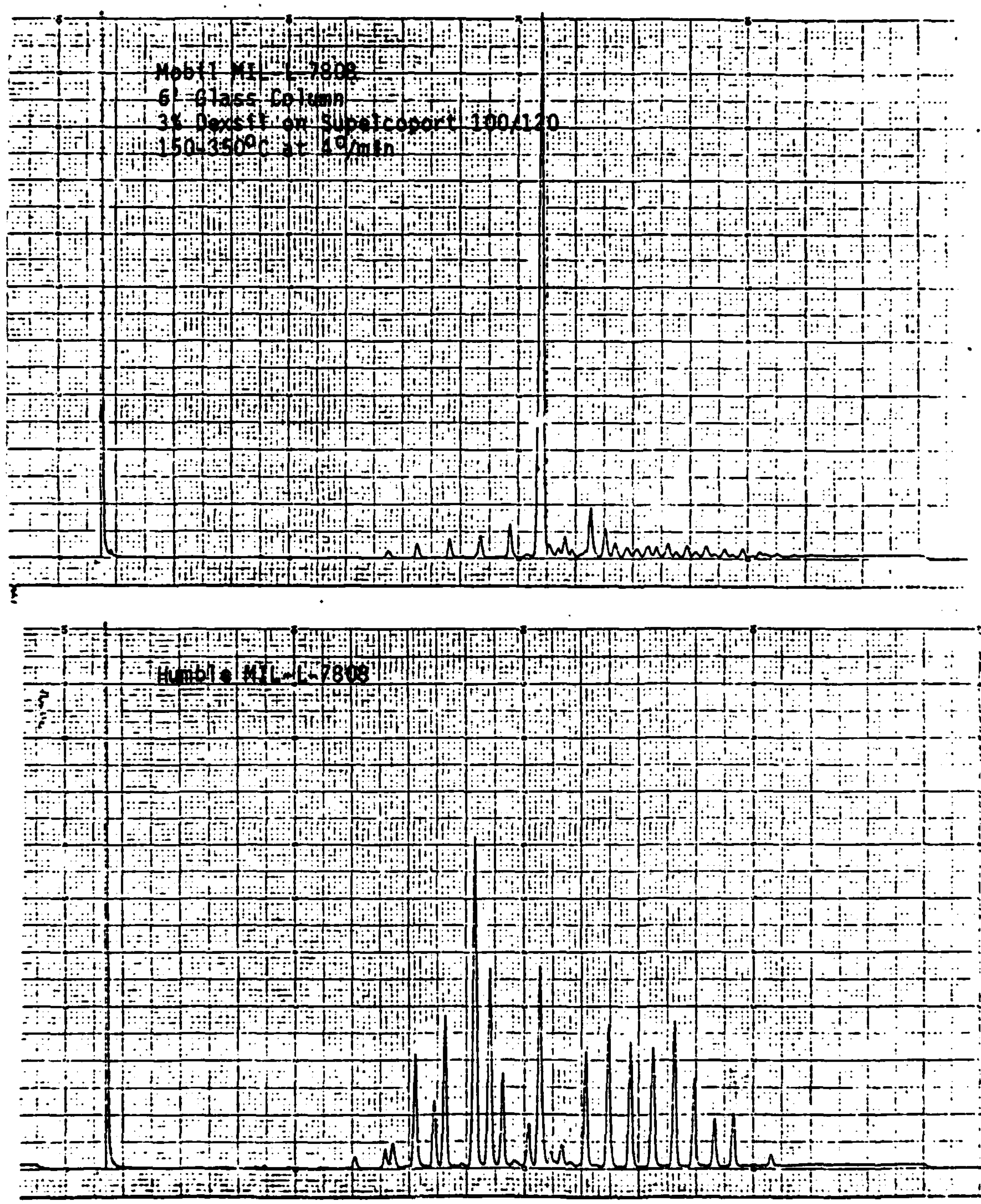

Figure 32. Gas Chromatograms of Mobil MIL-L-7808 and Humble MIL-L-7808.

A

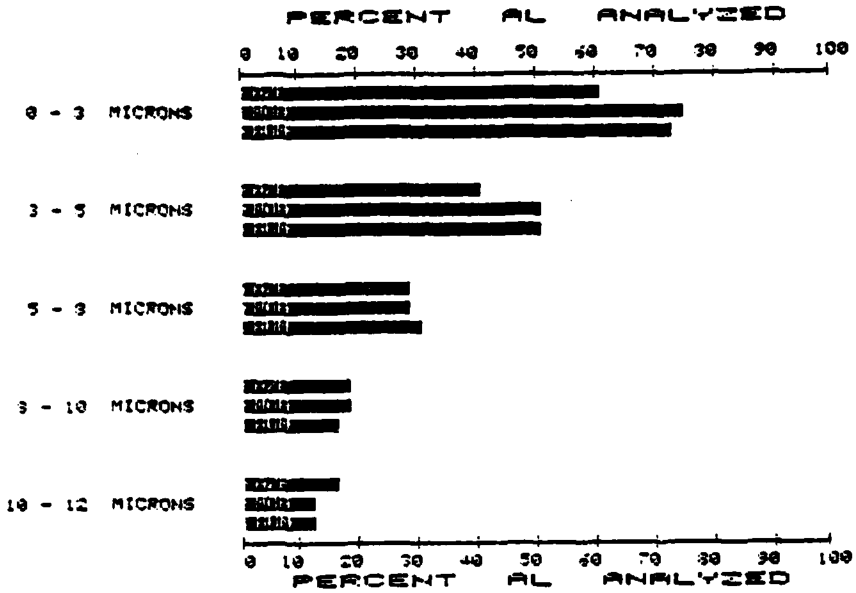

B

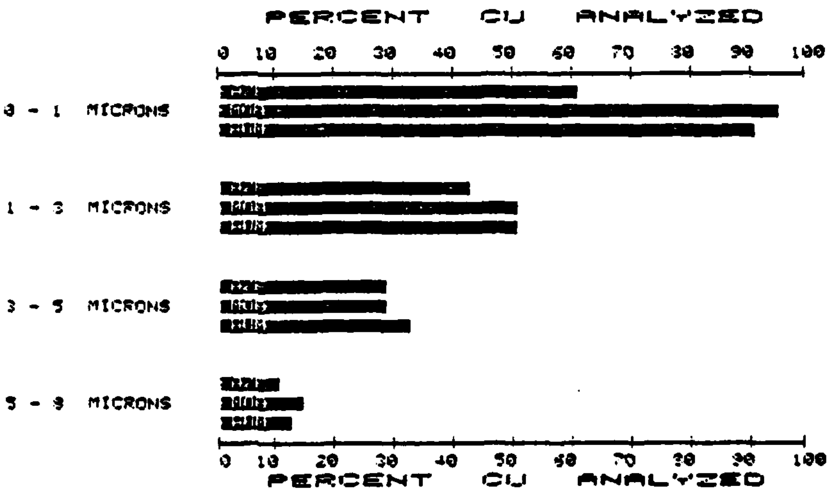

Figure 33. Effect of Oil Composition on the Perceut Metal Analyzed by the A/E35U-3 for Al (A), Cu (B), Fe (C), and Mg (D) Powders Suspended in Di-2-Ethylhexyl Azelate, Mobil MIL-L-7808 and Humble MIL-L-7808.

C

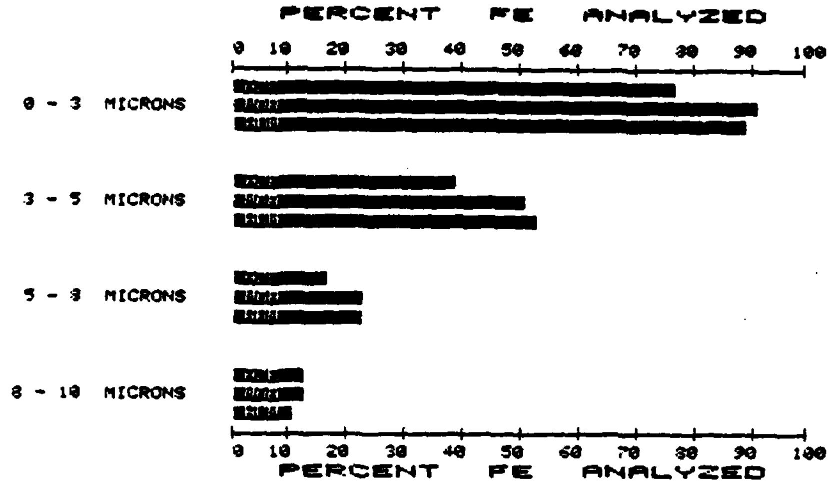

D

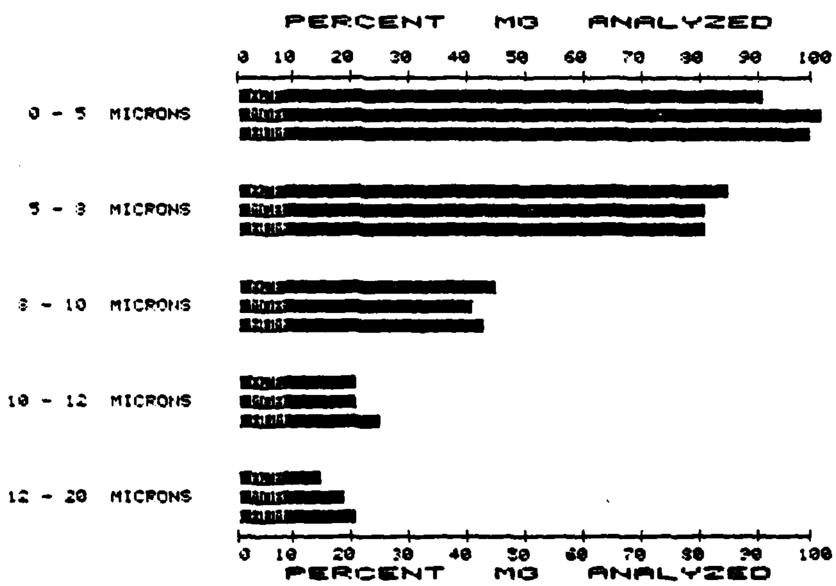

Figure 33. Concluded.

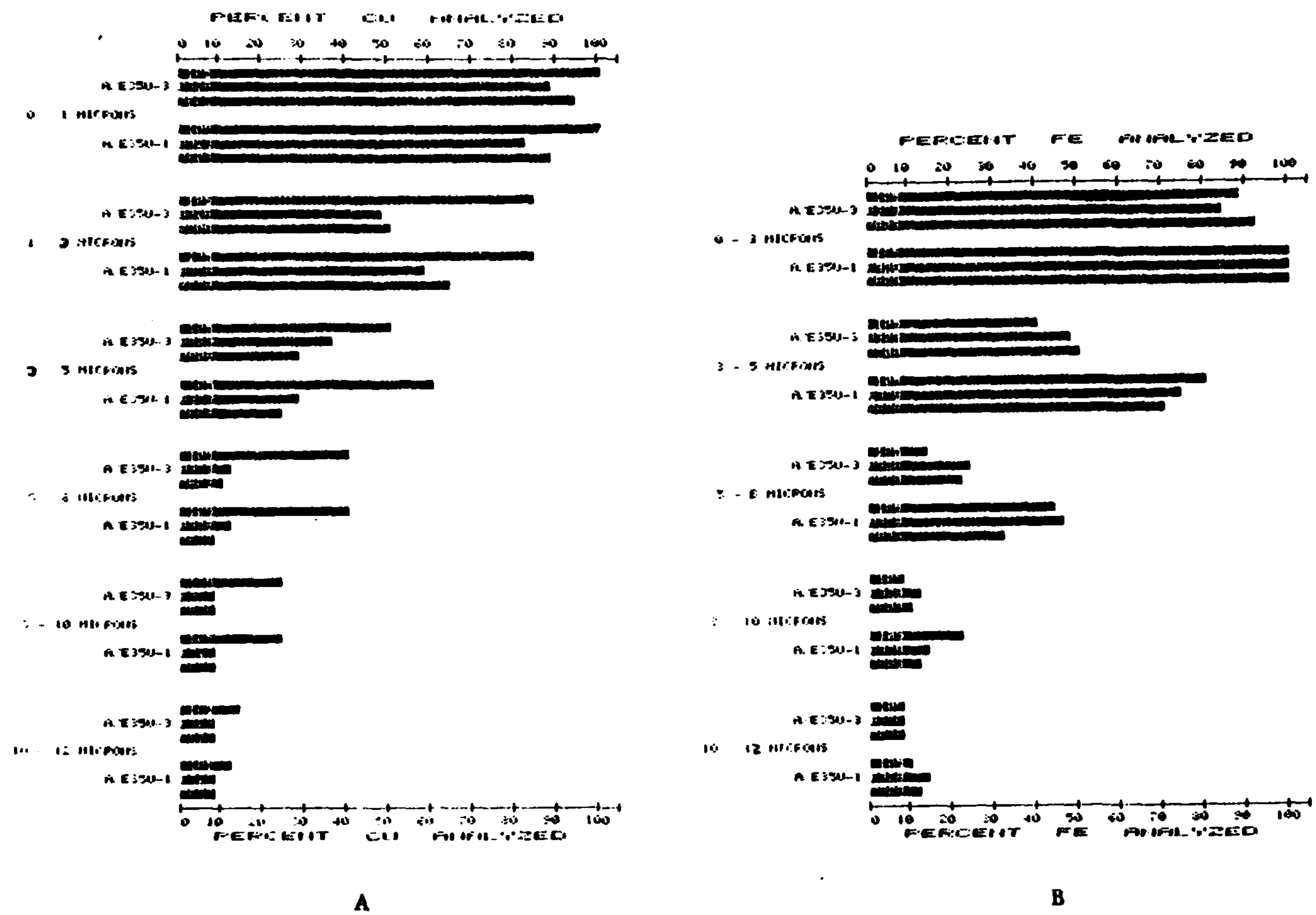

Figure 34. **Effect of Matrix Composition on the Percent Metal Analyzed by the A/E35U-3 and A/E35U-1 for Cu (A) and Fe (B) Powders Suspended in Phillips Condor 105 MIL-H-83282A and Mobil MIL-L-7808.**

nonmetallic particles tested so far (silicon nitride, titanium carbide and road dust), the A/E35U-3 was unable to quantitatively analyze (100%) particles of these materials which passed through a 1 μm filter, although particles of these materials less than 5-8 μm were quantitatively transported to the source (Table 12 and Figures 16 and 17).

d. Effect of Metal Concentration.

(1) To determine the effects of the concentration of particles on the detection capabilities of the A/E35U-3, a Fe powder suspension was prepared in Conostan 245. This suspension was diluted with Conostan 245 to prepare suspensions with identical particle size distributions but varying concentrations of metal (10-100 ppm).

(2) The instrument readout for each suspension was plotted versus the particle concentration. If the ratio of instrument readout to suspension concentration remains constant regardless of concentration, the plot of instrument readout versus suspension concentration would be linear and there would be no effect due to the concentration of metal in suspension.

(3) As seen in Figure 35, the plot of A/E35U-3 readout vs concentration of Fe is linear for the Conostan 245 oil suspensions. Therefore, the concentration of particles present in each suspension does not have an effect on the efficiency of the source, and consequently has no effect on the particle detection capabilities of the A/E35U-1 and A/E35U-3 spectrometers.

e. Effect of Particle Morphology.

(1) To determine the effect of particle shape on the detection capabilities of the A/E35U-1 and A/E35U-3 instruments, suspensions of the Ball Milled and Ventron Fe powders (< 20 μm) prepared in Conostan 245 oils were analyzed, since the Fe particles suspended in Conostan 245 are transported with 100% efficiency to the source regardless of particle morphology.

(2) The Ventron powder consists of agglomerated, spherical particles (Figure 27A) while the ball-milled Fe powder contains nonspherical particles (Figure 27E). The data listed in Table 17 shows that the Conostan 245 suspensions of the Ventron and ball-milled Fe powders have similar particle size distributions as determined by filtration. Therefore, any difference between the percent recoveries of the two Fe powders on the A/E35U-1 and A/E35U-3 can be attributed directly to particle shape.

(3) As seen in Figure 36 the percent Fe analyzed for the ball-milled Fe powder is higher than for the Ventron Fe powder for both spectrometers. Since the particle transport for both powders is 100% in Conostan 245, the difference in percent Fe analyzed is due to morphology differences between the ball-milled Fe powder and the Ventron Fe powder.

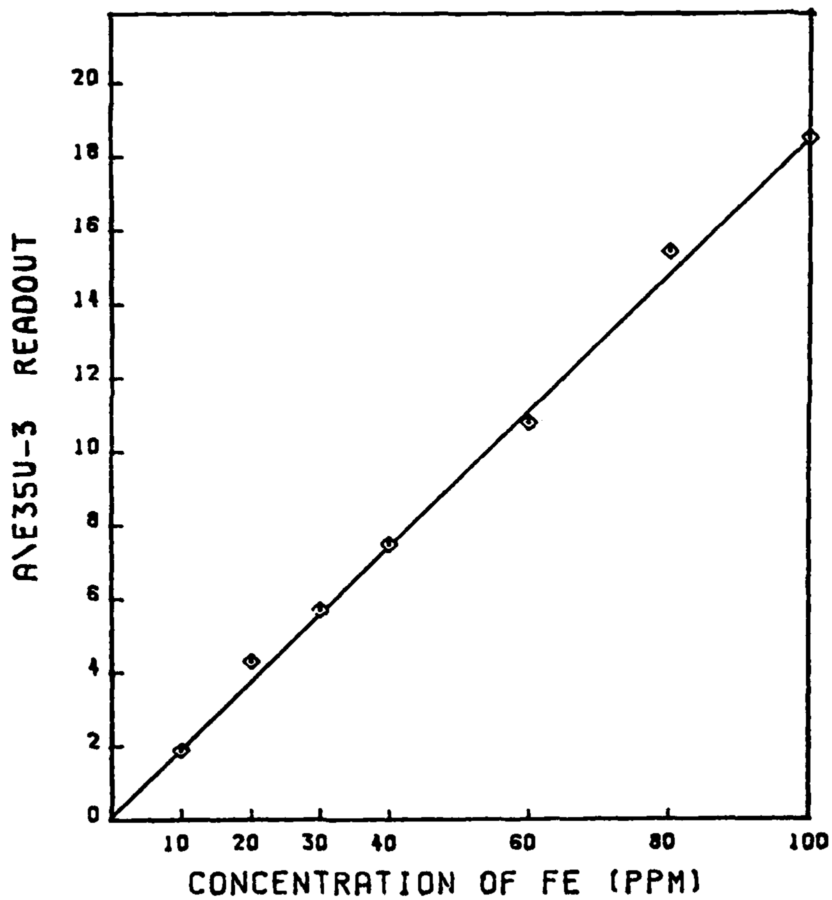

Figure 35. Plot of A/E35U-3 Emission Readout versus Concentration for Fe Powder Suspended in Conostan 245.

TABLE 17. PARTICLE SIZE DISTRIBUTION AS DETERMINED BY FILTRATION FOR THE FE POWDERS SUSPENDED IN CONOSTAN 245

MAXIMUM PARTICLE SIZE (μm)	CONCENTRATION OF FE (PPM)[a]				
	VMC	VENTRON	BALL MILLED	AEE	ROC/RIC
20 (unfiltered)	100	140	140	140	140
12	50	78	80	78	45
10	27	57	60	36	21
8	19	40	43	23	8
5	14	20	20	9	4
3	10	5	7	5	1

[a]Concentration of Fe determined by the ADM and is the ppm of Fe which passed through the filter.

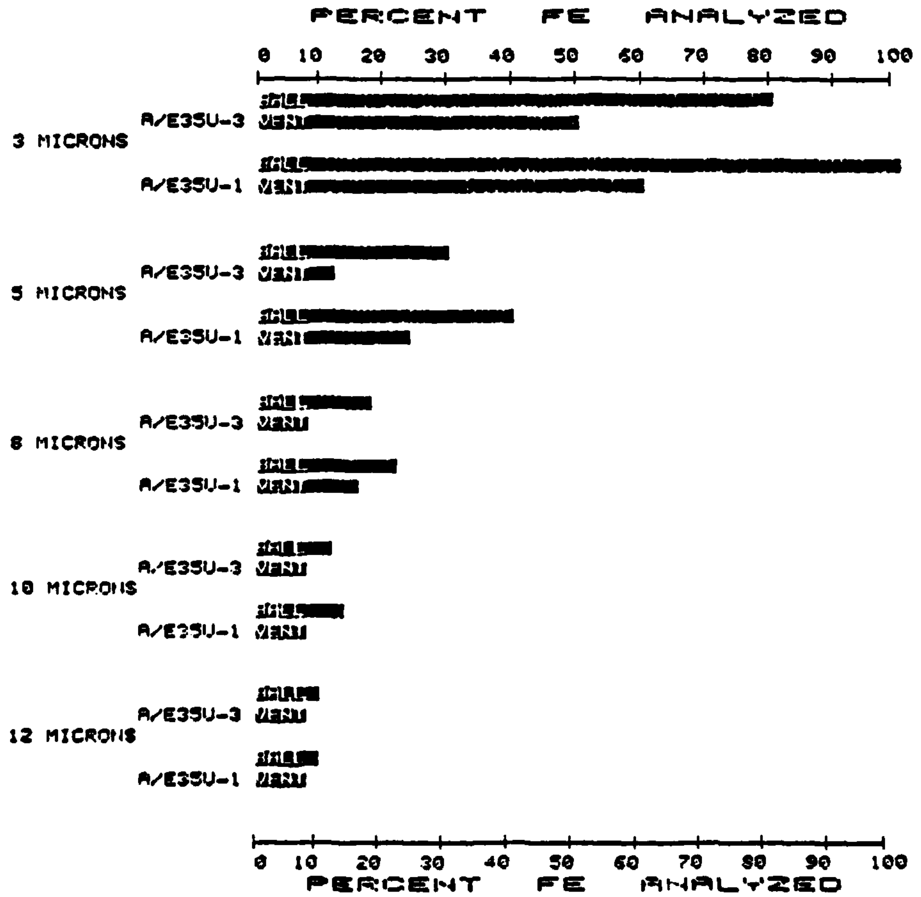

Figure 36. Percent Fe Analyzed by the A/E35U-3 and A/E35U-1 for Ball-Milled and Ventron Fe Powders Suspended in Conostan 245.

f. Effect of Electrode Configuration.

(1) Three different configurations (tip angle) of the upper electrode were studied. The configurations will be referred to as the 160°, 17° and 15° electrodes (Figure 37), where the angles refer to the tip angle of the electrodes. The 160° electrode is the one recommended by the instrument manufacturer for the A/E35U-3, and the 15° taper electrode is the one recommended for the A/E35U-1.

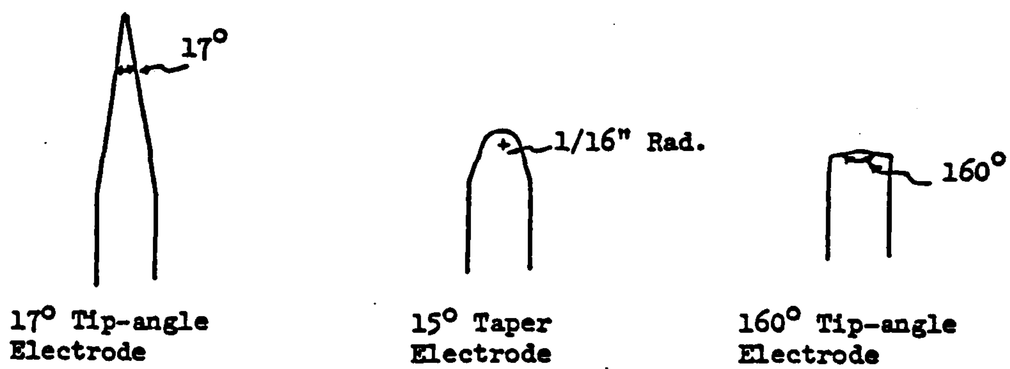

Figure 37. Emission Electrode Configuration.

(2) To determine the effect of the upper electrode's tip angle on metal particle analyses, suspensions of Al, Cu, Fe and Mg particles in Conostan 245 were analyzed. Conostan standards prepared in Conostan 245 were also analyzed.

(3) Figure 38 shows that the 160° electrode gives the largest emission signals for Conostan Al, Fe, and Mg standards on both instruments. Copper is the exception where the 160° electrode gives the highest emission signal on the A/E35U-3 and the 15° taper electrode gives the highest emission signal on the A/E35U-1.

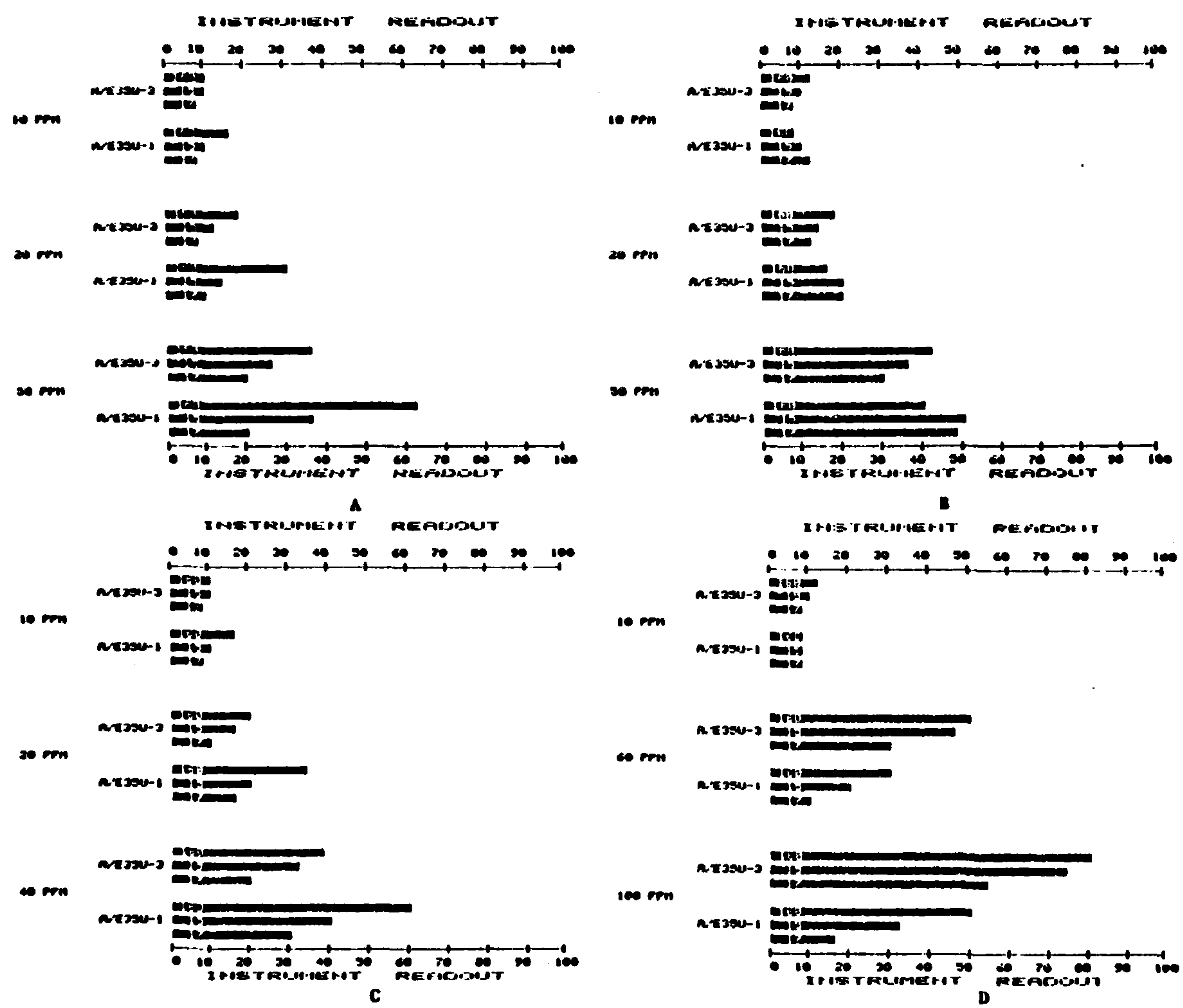

Figure 38. Effect of Electrode Configuration on the Emission Readout of the A/E35U-3 and A/E35U-1 for Al (A), Cu (B), Fe (C) and Mg (D) Conostan Standards Prepared in Conostan 245.

(4) As expected, the 160° electrode gives the highest metal recoveries for the A/E35U-3. Although the 160° electrode produces the largest emission signals for the Conostan standards, the 15° taper electrode gives the highest metal particle recoveries on the A/E35U-1. However, Cu is again the exception and is analyzed best on the A/E35U-1 using the 160° electrode (Figure 39). The A/E35U-1 always gave the highest recoveries of metal particles regardless of the electrode used which indicates that the source electronics used by the A/E35U-1 are responsible for its higher efficiency.

(5) To determine the differences between configurations of the upper electrodes, disks were coated with silver paint and subjected to 20 second burns in the two instruments. The area of paint vaporized is different for each type of upper electrode configuration and follows a logical pattern. The 17° tip angle electrode gives the narrowest burn track, and the 160° electrode gives the widest burn track. However, none of the electrodes vaporized the paint over the entire width of the disk.

(6) The above observations led to determining the effect of the disk's width on the detection of metal particles. Rotating disk electrodes with widths of 3.0 mm and 5.0 mm were compared.

(7) Samples of Cu in Exxon MIL-L-23699 and Fe in Conostan 245 were used for this study. The standard solutions were analyzed on the A/E35U-3 and the A/E35U-1. The width of the disk electrode did not affect the A/E35U-3 analyses. On the A/E35U-1, identical results were obtained using the 160° upper electrode with either the 3 mm or the 5-mm disk. However, the 15° taper electrode gave better results with the 5-mm disk. The emission results obtained on the A/E35U-1 are shown in Figures 40 and 41.

(8) The Cu and Fe particle suspensions were analyzed on each instrument using both the 3 and 5 mm disks. The disk width did not affect the metal particle analyses on the A/E35U-3. On the A/E35U-1, the better Cu and Fe particle detection capability was obtained by using the 3 mm disk with the 160° electrode (Figures 42 and 43). The 15° taper electrode gave the best particle recoveries with the 3 mm disk also.

E. METHODS STUDIED TO IMPROVE THE PARTICLE DETECTION CAPABILITIES OF THE ROTATING DISK EMISSION SPECTROMETERS.

1. INTRODUCTION. During the course of this work, various solutions/alternatives were investigated in order to improve the particle detection capabilities of the A/E35U-3 and the A/E35U-1 spectrometers. The preliminary results on an acid dissolution method, alternative methods of sample introduction and an ashing technique are presented herein. These investigations were conducted using the A/E35U-1 spectrometer.

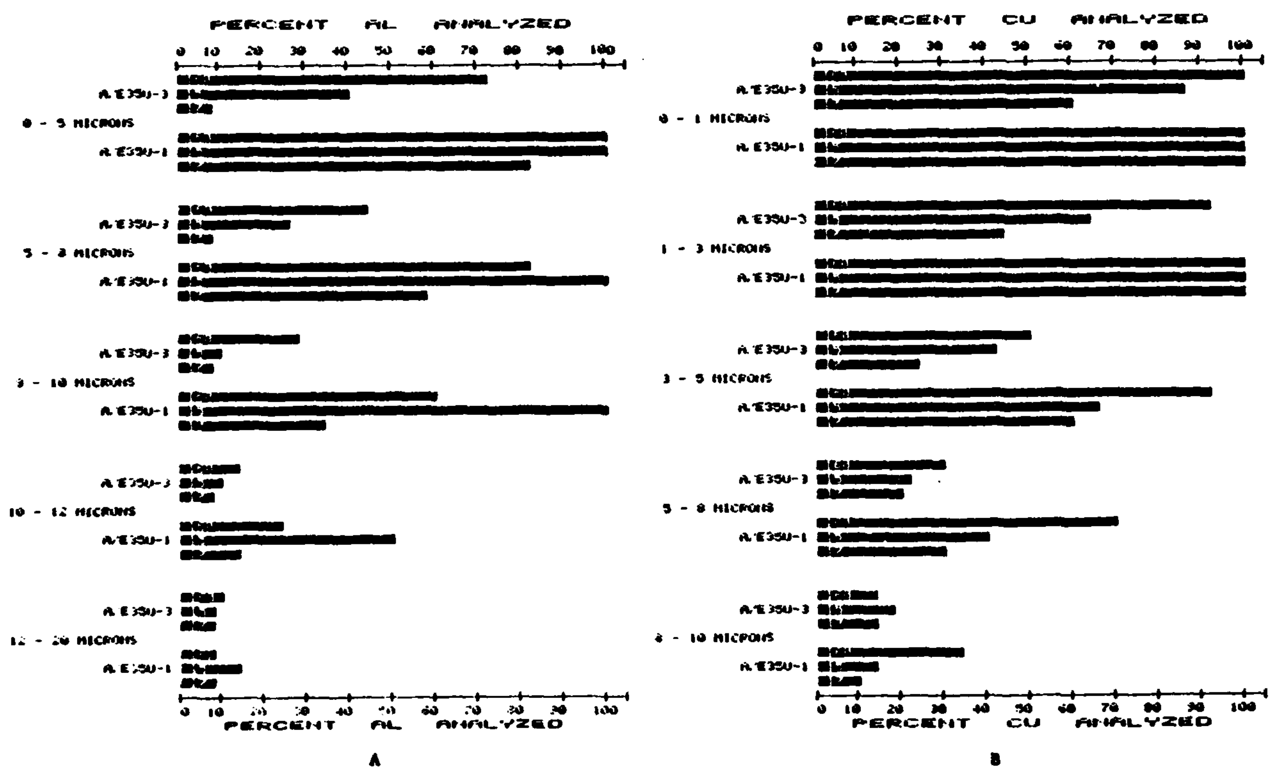

Figure 39. Effect of Electrode Configuration on the Emission Readout of the A/E35U-3 and A/E35U-1 for Al (A), Cu (B), Fe (C) and Mg (D) Powders Suspended in Conostan 245.

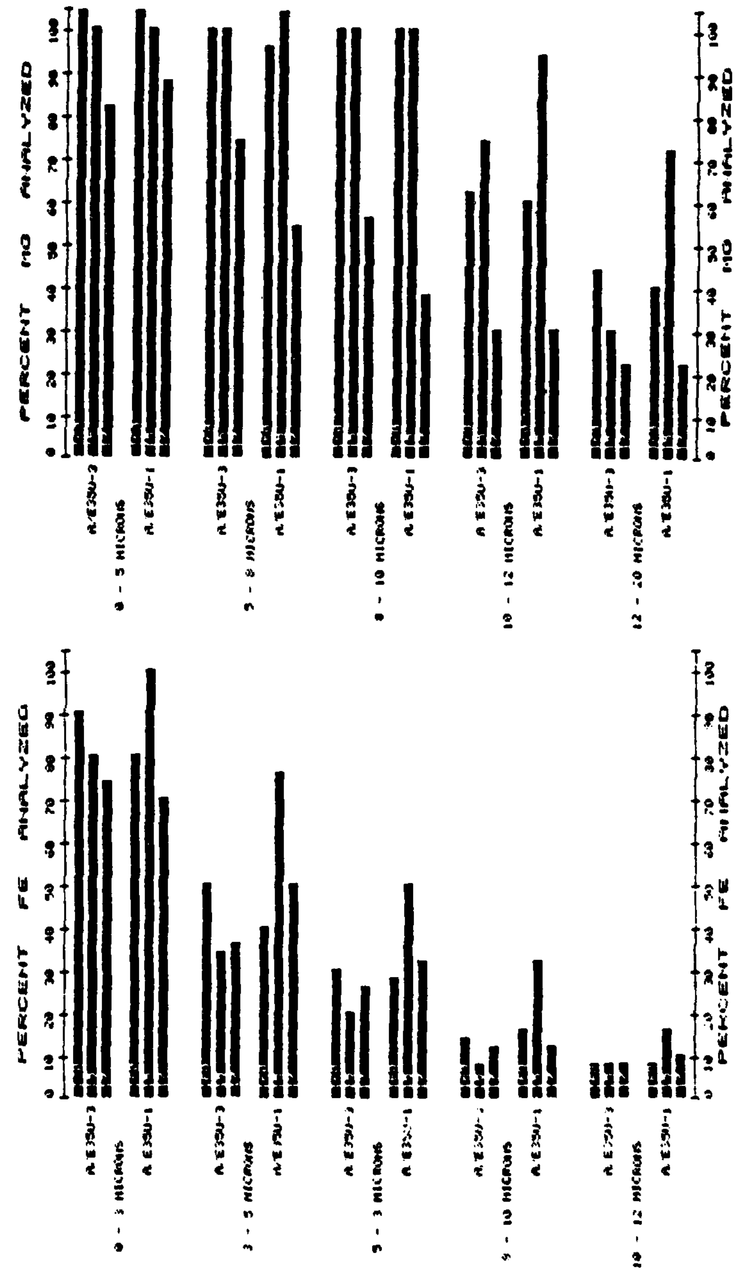

Figure 39. Concluded.

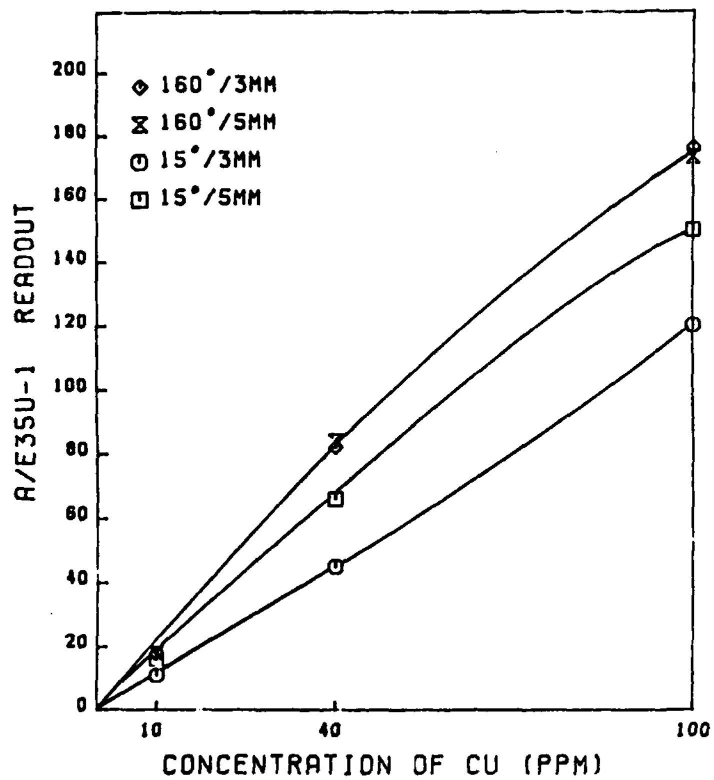

A

Figure 40. **Effect of Disk Electrode Configuration on the Emission Readout of the A/E35U-1 for Cu Conostan Standards Prepared in Exxon MIL-L-23699.**

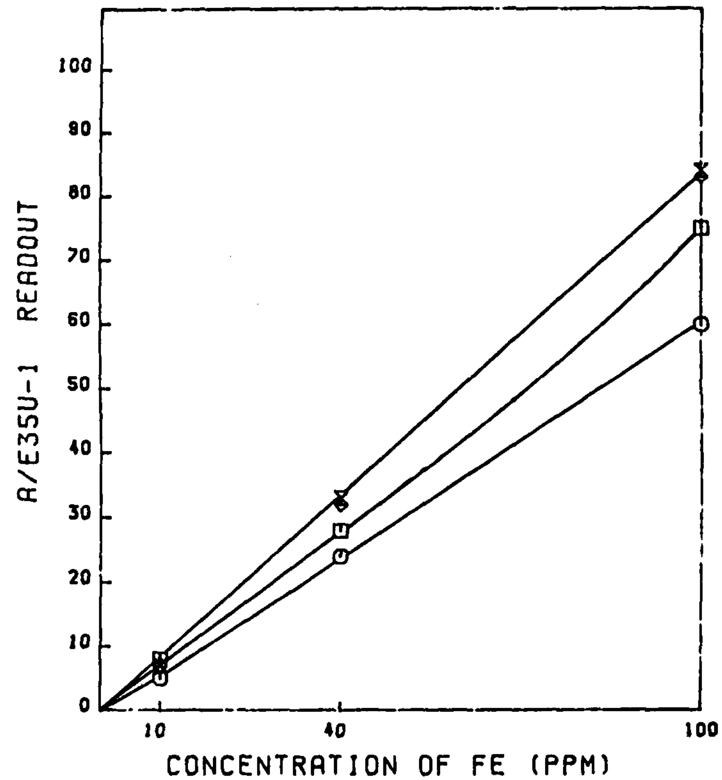

B

Figure 41. **Effect of Disk Electrode Configuration on the Emission Readout of the A/E35U-1 for Fe Conostan Standards Prepared in Conostan 245.**

AD-A127 969 SPECTROMETER SENSITIVITY INVESTIGATIONS ON THE SPECTROMETRIC OIL ANALYSIS PROGRAM(U) DAYTON UNIV OH RESEARCH INST W E RHINE ET AL. 22 APR 83 NAEC-92-169 2/2

UNCLASSIFIED N68335-81-C-4587 F/G 1/3 NL

END
DATE
FILMED
DTIC

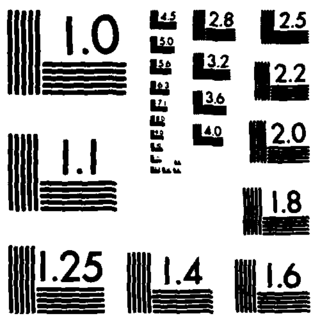

MICROCOPY RESOLUTION TEST CHART
NATIONAL BUREAU OF STANDARDS-1963-A

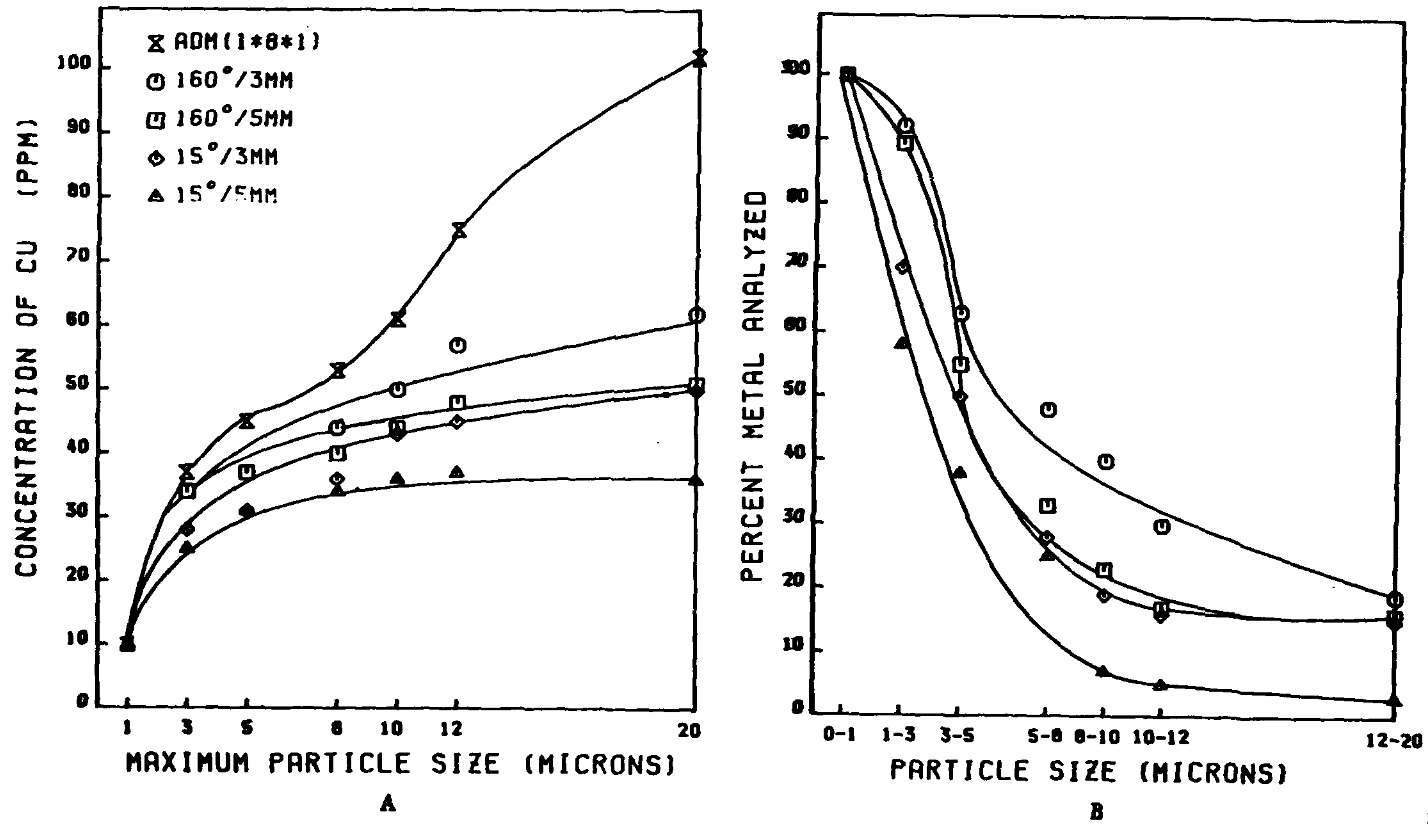

Figure 42. Effect of Disk Electrode Configuration on the Spectrometric Analysis (A) and Percent Metal Analyzed (B) by the A/E35U-1 for Cu Powder Suspended in Exxon MIL-L-23699.

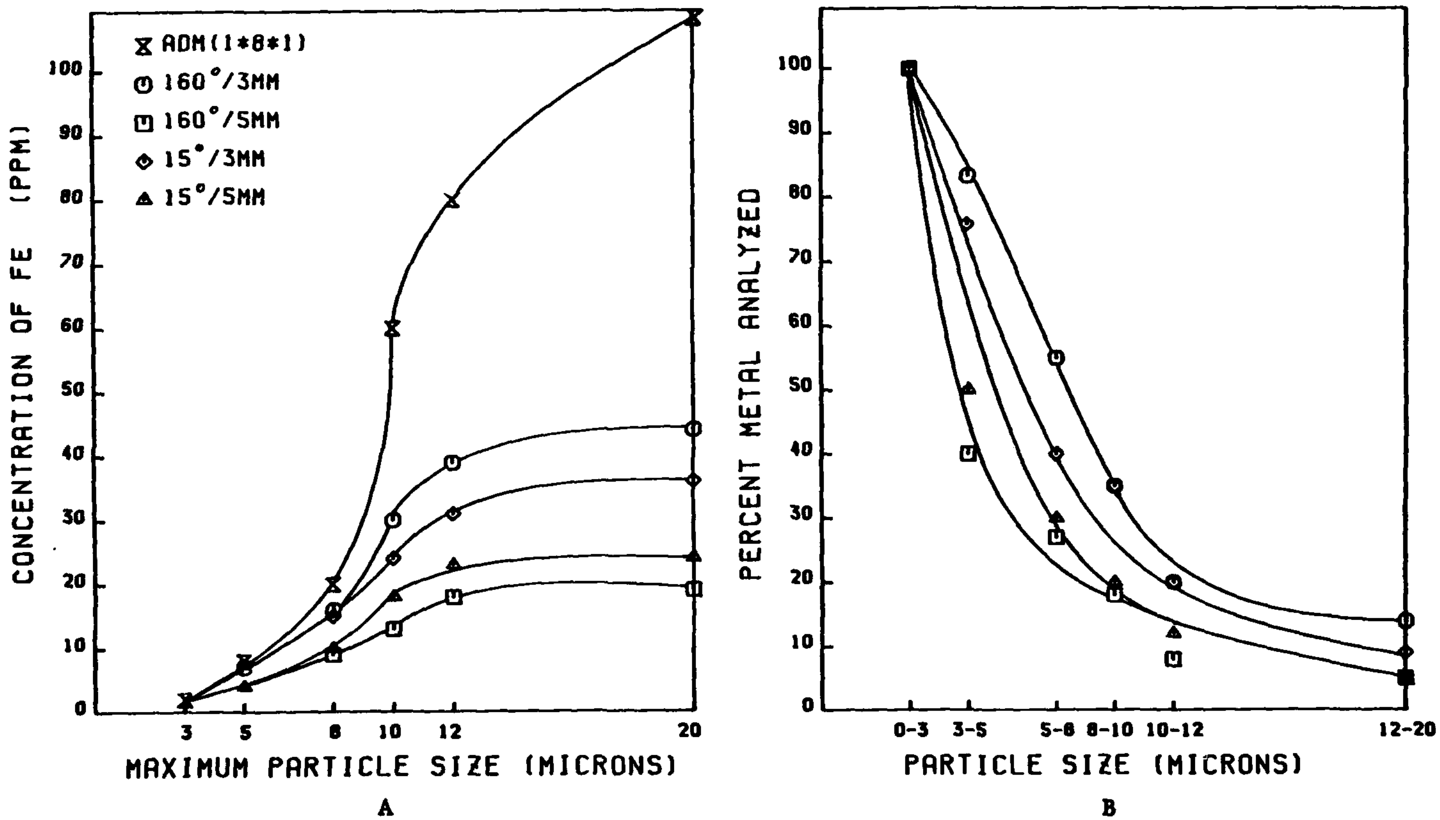

Figure 43. Effect of Disk Electrode Configuration on the Spectrometric Analysis (A) and Percent Metal Analyzed (B) by the A/E35U-1 for Fe Powder Suspended in Conostan 245.

2. ACID DISSOLUTION METHOD.

a. The acid dissolution method (Paragraph IIK) allows the quantitative analysis of wear metal particles in used oil samples without modifying the spectrometer. The particles are dissolved in situ by adding an acid/surfactant mixture to the oil. The acid dissolves any particles present and eliminates most problems associated with analyzing particles. The surfactant is added to provide a homogeneous sample suitable for analysis by the A/E35U-1 spectrometer.

b. The above method can be used to quantitatively analyze for Al, Cu, Fe, Mg, Ni and Sn wear metal particles (Table 18). However, the acidic mixture produced by this method is very corrosive (pH - 0.6) and would not be acceptable for routine operations without further modifications in the procedure. Therefore, the corrosiveness of the mixture was reduced by neutralizing the solution with a base such as an amine. Several amines were used, with the best results being obtained with triethylenetetramine (Table 19). However, matching the matrices of the standards and the samples was rather difficult. The emission signals were very dependent on the pH of the oil: acid:amine mixture (Table 20). This dependence on the matrix had the overall effect of making the analyses unreliable.

3. EFFECT OF BURN TIME. Since particle settling rates were shown to limit the particle detection capability of the A/E35U-1 and A/E35U-3 spectrometers, a shorter burn time should improve particle detection. Copper and iron powder suspensions prepared in MIL-L-23699 were analyzed on the A/E35U-1 with burn cycle times of 18 seconds and 41 seconds. The results depicted in Figure 44 show that the shorter burn times improved the capability of the A/E35U-1 to analyze particles. Shorter burn times would increase the number of samples analyzed in an average work day but may have the disadvantage of increasing the standard deviation associated with wear metal concentrations. The magnitude of improvement is not significant, and decreasing the burn time is probably not a viable solution to the problems inherent in the rotating disk emission spectrometers.

4. DIRECT SAMPLE INTRODUCTION.

a. The particle transport problems associated with the rotating disk may be eliminated by directly depositing the sample onto the disk. One approach is to precisely pump the sample directly onto the disk using a peristaltic pump. The sample can be deposited onto the disk at the two possible positions shown in Figure 45. If the sample is deposited on the disk just before the spark, it is immediately transferred to the arc. If the oil is deposited on the disk just after the spark, the heat generated by the spark may vaporize the oil and leave the wear metals on the disk surface ready to be analyzed.

TABLE 18. COMPARISON OF ACID METHOD ON THE A/E35U-1 WITH DIRECT ANALYSIS ON THE A/E35U-3

Sample	Method	Ag	Al	Cr	Cu	Fe	Mg	Ni	Sn
M-12[a]	Direct[b]	0	3.1	11.2	8.3	5.3	25	11.2	8.9
	Acid[c]	10	100	40	100	106	110	100	102
	ADM[d]	78	101	91	100	101	95	98	93
H-49[e]	Direct	1.0	-	5.3	5.7	17.1	-	-	-
	Acid	2	-	6	19	27	-	-	-
	ADM	3	-	6	20	28	-	-	-

[a]Twelve element metal-powder suspension (< 74 μm) prepared in Mobil MIL-L-7808

[b]A/E35U-3

[c]A/E35U-1

[d]AA

[e]Authentic Used Oil Sample (H = OAP Hit), MIL-L-7808

TABLE 19. EFFECTS OF DIFFERENT AMINES ON THE ACID DISSOLUTION METHOD FOR THE A/E35U-1

Amine	Acid/Amine (g/g)	Observations
Triethanol Amine	0.2/0.4	Insoluble - two phases
Tributyl Amine	0.2/0.3	Amine odor - caught fire during analysis
2-Ethylhexyl Amine	0.2/0.2	Amine odor - boils during analysis
Dioctyl Phenyl Amine	0.2/0.6	Insoluble in acid solution
Phenyl Naphthal Amine	0.2/0.6	Insoluble in acid solution
Triethylenetetramine	0.2/0.1	Separates into two phases after 48 hours

TABLE 20. EFFECT OF pH ON THE A/E35U-1 DETERMINATION OF METALS IN THE MULTIELEMENT STANDARD

Sample	pH[a]	Ag	Al	Cr	Cu	Fe	Mg	Ni	Sn
Standard[a]	7.4	109	120	76	50	120	22	80	144
	6.8	59	70	38	38	99	11	48	100

[a]Multielement standard in MIL-L-7808 neutralized with 0.10-0.11g triethylenetetramine.

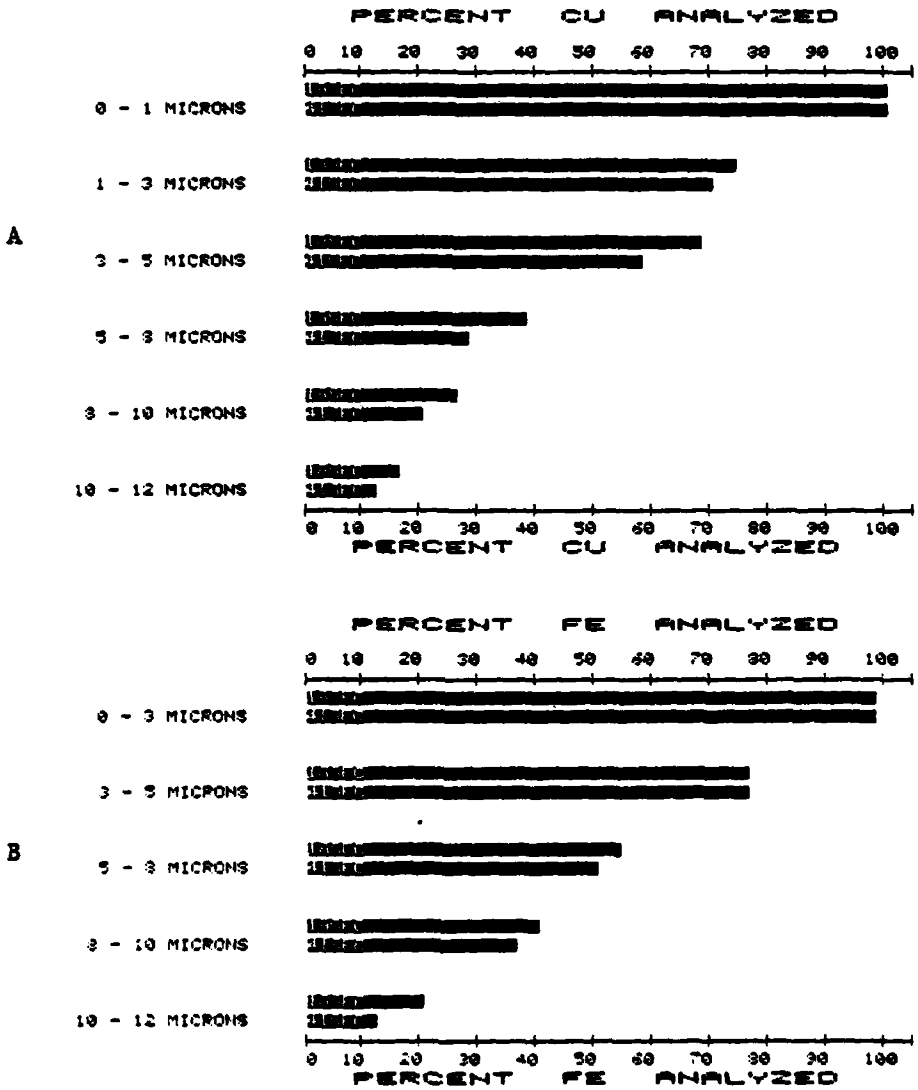

Figure 44. Effect of Burn Time on the Percent Metal Analyzed by the A/E35U-1 for Cu (A) and Fe (B) Powders Suspended in Exxon MIL-L-23699.

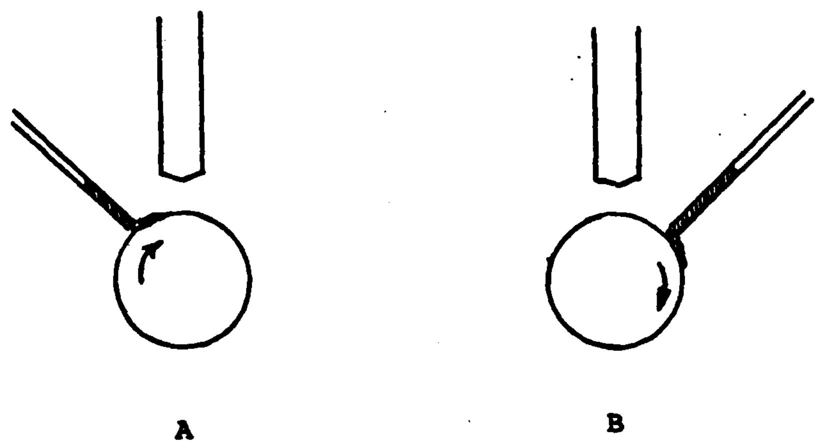

Figure 45. Direct Sample Deposition onto the Rotating Disk.

b. The preliminary results of pumping the sample onto the rotating disk were too erratic to compare the two possible deposition modes. However, direct sample deposition did improve the particle detection capability of the A/E35U-1.

c. In another approach, a fixed volume (10-40 µl) of sample was directly deposited onto the disk using a microliter pipette. Different volumes of sample were used to determine the effect of sample size on the particle detection capability and on the reproducibility of the results for the A/E35U-1. The results of analyzing the Fe 170 ppm suspension and a 10 ppm Conostan standard prepared in Mobil MIL-L-7808 are shown in Table 21. Although the emission readouts of the 10 ppm standard were independent of sample size, the particle detection capability of A/E35U-1 increased with decreasing sample size. In the case of the 10 and 20 µl samples, the oil on the surface of the electrode appeared to have been ashed or vaporized by the end of the burn cycle. The elimination of the matrix may explain the observed increases in the recovery of Fe particles determined for the 10 and 20 µl samples (Table 21).

TABLE 21. COMPARISON OF DIRECT SAMPLE DEPOSITION WITH DIRECT ANALYSIS AND WITH ASHING

DIRECT SAMPLE DEPOSITION

	Pipette				Peristaltic	Direct	
Sample[b]	10μl	20μl	30μl	40μl	Pump	Analysis	Ashing[c]
170 ppm Fe Suspension	42±3	43±3	32±1	20±4	50±5	25±1	140±30
2nd Burn[a]	20±2	24±1	34±1	29±3			
10 ppm Standard	8±1	8±1	7±1	8±1	10±5	7±2	10±3
2nd Burn	4	5	9	10±1			

[a]2nd Burn = The same disk was reburned to see if any sample remained.

[b]Mobil MIL-L-7808.

[c]Ashing done via Paragraph IVE5a(1), page 101.

d. When the disks with original sample depositions of 30 and 40 µl were reanalyzed, the readout increased for both the standard and suspensions, and no oil remained on the disk by the end of the second burn. In either case the particle detection capabilities of the direct deposition method were not quantitative and were much lower than the results obtained by ashing the sample deposited on a rotating disk electrode before analysis (Table 21).

e. The reproducibility of the analyses using a microliter pipette was better than that obtained using the peristaltic pump. Therefore, the reproducibility of the direct deposition method appears to be dependent upon the precision of the method used to deposit the sample. If the oil is ashed or vaporized by the heat of the source and the method of deposition is precise, the direct deposition method should produce analyses with low standard deviations and improved particle detection capabilities.

5. ASHING TECHNIQUES.

a. Rotating Disk Electrode.

(1) The oil sample (20 µl) was deposited on the rim of the rotating electrode. The electrode was heated to 500°C in a muffle furnace to ash or vaporize the oil. The disks were then analyzed in the usual way on the A/E35U-1. The A/E35U-1 spectrometer was used without the hood to reduce the burn time. The burn time with the disks prepared in this manner was 36 seconds.

(2) The results for the analysis of Fe powder suspensions and Conostan Fe standards prepared in Condor 105, Conostan 245 and MIL-L-7808 oils are given in Table 22. The Fe standards prepared in the various oils gave identical emission readouts, indicating that matrix effects have been eliminated.

(3) The particles in the Fe suspension were quantitatively analyzed using this technique. Therefore, this method, or a modification of it, has great promise for improving the particle detection capabilities of the rotating disk instruments.

b. Crater Tip Electrode.

(1) Twenty µl samples were deposited into the crater (hole) formed in the rim of a rotating disk electrode. The disks were placed in a muffle furnace to ash the oil and then placed on the stationary spindle of the A/E35U-1 for analysis. The burn time with the ashed disk and the hood removed was 36 seconds (Paragraph II0, page 34).

(2) The results for the analyses of Fe powder in Mobil MIL-L-7808 and Phillips Condor 105 oils are listed in Table 23. The particle detection capability of the A/E35U-1 was not improved by the ashing technique when the

TABLE 22. COMPARISON OF ASHING VS DIRECT ANALYSIS ON THE A/E35U-1 FOR FE

< 20 µm PARTICLES

OIL	DIRECT (ppm)	ASHING (ppm)	ADM(AA) (ppm)
Conostan 245	29 ± 1	110 ± 18	116 ± 2
Phillips Condor 105	29 ± 1	130 ± 25	140 ± 3
Mobil MIL-L-7808	25 ± 1	159 ± 28	170 ± 5

< 12 µm PARTICLES

	DIRECT (ppm)	ASHING (ppm)	ADM(AA) (ppm)
Conostan 245	28 ± 1	70 ± 15	80 ± 3
Phillips Condor 105	25 ± 2	108 ± 15	106 ± 1
Mobil MIL-L-7808	23 ± 1	89 ± 12	94 ± 3

A/E35U-1 READOUTS FOR 100 PPM STANDARDS

	DIRECT	ASHING
Conostan 245	43 ± 4	70 ± 15
Phillips Condor 105	60 ± 2	70 ± 10
Mobil MIL-L-7808	64 ± 2	70 ± 10

TABLE 23. ANALYSIS FOR FE BY ASHING TECHNIQUE EMPLOYING CRATER ELECTRODE

	FE CONCENTRATION (PPM)		
OIL	ADM	CRATER ELECTRODE	RDE
Mobil MIL-L-7808	170	28 ± 10	25 ± 1
Phillips Condor 105	140	23 ± 7	29 ± 1

crater electrode is employed. Therefore, the crater electrode investigation was discontinued.

c. Rotating Platform Electrode.

(1) Baer and Hodge [reference (j)] and Hodge [reference (k)] have evaluated a rotating platform electrode (RPE) as a possible alternative to the rotating disk electrode on the emission spectrometer. They reported that the rotating platform electrode appeared to be more sensitive than the rotating disk electrode and other techniques tested and was effective for the analysis of suspended matter. Based on these literature references, the rotating platform electrode was evaluated as a possible solution/alternative to the A/E35U-3's particle detection limitations.

(2) Twenty μl of sample was deposited onto the surface of the rotating platform electrode. The electrode was ashed at 500°C in a muffle furnace and placed on the rotating platform turntable for A/E35U-1 analysis. The burn time using the ashed electrode was 36 seconds.

(3) A suspension containing Al, Cu, Fe and Mg particles and a corresponding four element Conostan standard prepared in Mobil MIL-L-7808 oil were ashed and analyzed on the rotating platform electrode. The results are shown in Table 24. The particle detection capability of the A/E35U-1 is greatly improved for Cu, Fe and Mg as compared to direct analysis.

(4) To study the effect of porosity on the results of the rotating platform electrode, a rotating disk electrode (RDE) was laid flat and was employed in the same manner as the rotating platform electrode (RPE). The 20 μl of deposited sample was absorbed by the porous RDE but remained on the surface of the less porous RPE. As seen in Table 24, the porosity of the electrode has little effect on the particle detection capability of the A/E35U-1. High porosity allows more sample to be deposited onto the electrode, which increases the sensitivity of the ashing technique while reducing sampling errors. Forty μl of samples could be safely deposited onto the flat surface of the porous RDE, while 20 μl was the limit for the RPE.

Ref: (j) Baer, W. and Hodge, E. "The Spectrochemical Analysis of Solutions, A Comparison of Five Techniques". J. Appl. Spectry., V. 14, P. 141, 1960

(k) Hodge, E. "Spectrographic Tricks". J. Appl. Spectry., V. 15, P. 21, 1961.

TABLE 24. SUMMARY OF METHODS USED TO ANALYZE PARTICLES ON THE A/E35U-1[a]

METHOD	Concentration (ppm) AL	CU	FE	MG
RDE - Direct	50	30	25	66
Crater - Ashing	-	-	20	-
Rotating Platform - Ashing (nonporous electrode)	30	80	59	80
Rotating Platform - Ashing (porous electrode)	35	75	63	75
Rotating Disk - Ashing	-	99	110	101
ADM	100	109	108	108

[a]Mobil MIL-L-7808.

d. <u>Ashing Technique Keeping Disk Electrode Stationary During Preburn Cycle</u>.

(1) The preburn cycle of the A/E35U-1 lasts about 12 seconds, during which time the rotating disk and rotating platform electrodes make 6 and 2 revolutions, respectively. Therefore, most of the metal on the surface may have vaporized prior to the emission integration cycle. In an effort to increase the emission readout for the rotating disk and platform electrodes, the electrical system of the A/E35U-1 was modified so that the electrodes only rotated during the integration cycle and remained stationary during the preburn cycle. Otherwise, the ashing techniques were performed as previously described (Paragraph IVE5a(1), Page 101). The results for a 12 element metal powder suspension and corresponding multielement standard are listed in Table 25. By keeping the ashed electrode stationary during the preburn cycle, the emission from Conostan multielement standards is enhanced 1 to 4 fold for the RPE and 1 to 2 fold for the RDE when compared to the results from the previously described ashing techniques. The particle detection capabilities of the ashing technique were also improved by keeping the rotating electrode stationary during the preburn cycle (Table 25).

TABLE 25. COMPARISON OF RESULTS[a] FROM THE RPE AND THE RDE

	RPE: CONOSTAN STANDARD		RPE: M-12		RDE: CONOSTAN STANDARD		RDE: M-12	
	Stationary[b]	Rotating	Stationary[b]	Rotating	Stationary[b]	Rotating	Stationary[b]	Rotating
Al	85 ± 20[a]	71 ± 15	0	0	30 ± 8	21 ± 1	0	0
Fe	161 ± 23	93 ± 7	67 ± 23	35 ± 4	73 ± 10	47 ± 2	68 ± 6	48 ± 3
Cr	140 ± 4	120 ± 7	4 ± 1	4 ± 1	33 ± 4	22 ± 1	22 ± 2	5 ± 1
Ag	185 ± 19	90 ± 5	6 ± 6	3 ± 3	69 ± 6	30 ± 1	6 ± 6	2 ± 1
Cu	102 ± 18	31 ± 3	44 ± 22	22 ± 5	56 ± 2	35 ± 1	69 ± 10	37 ± 4
Sn	305 ± 26	250 ± 5	82 ± 57	26 ± 3	95 ± 13	81 ± 3	133 ± 8	74 ± 5
Mg	46 ± 4	37 ± 2	13 ± 6	3 ± 1	21 ± 3	12 ± 1	15 ± 1	7 ± 1
Ni	112 ± 23	48 ± 1	8 ± 9	2 ± 1	30 ± 4	24 ± 1	32 ± 6	1 ± 1
Si	54 ± 8	30 ± 2	4 ± 6	1 ± 1	32 ± 1	25 ± 2	0	2 ± 1

[a] A/E35U-1 Spectrometer Readout.

[b] Electrode stationary during preburn cycle.

(2) However, the particle detection capabilities of the rotating platform electrode remain lower than those attained with the rotating disk electrode. The RDE produced excellent recoveries for Cu, Fe, Mg, Ni and Sn metal particles (Table 25).

(3) Table 25 compares the analytical results obtained with the RPE and the RDE for the analysis of Conostan Standards and the M-12 suspension. The RPE and RDE were used without any modification in their geometrics; however, they were not allowed to rotate during the preburn cycle. The analyses clearly show that the analytical results obtained for the Conostan standards are 1.5 to 4 fold higher for the RPE. However, the metal powder suspension yielded different results. The RPE and RDE gave comparable results for Ag, Al, Fe and Mg suspensions but differed in the remaining metals. The RDE gave higher results for Cr, Cu, Ni and Sn, while the RPE gave higher results for Si.

(4) The reason the RPE yields much higher instrument readouts for the Conostan standards than does the RDE could be explained by comparing the porosity of the electrodes. The rotating disk electrodes are more porous than the rotating platform electrodes. Thus it is easier for the dissolved standard to penetrate the rotating disk electrode. The greater porosity results in reduced sensitivity. However, for the RPE, the majority of the deposited standard remains on the surface due to the less permeable electrode, resulting in improved readout as illustrated in Table 25.

(5) When suspensions of metal powders are analyzed instead of Conostan standards, the metal particles do not penetrate either the rotating disk electrode or the rotating platform electrode, regardless of the porosity of the electrodes. Therefore, differences in spectrometer readouts are much less for the particles and are comparable for most metals. Since these results are preliminary, we cannot make a conclusion as to which is the best technique. However, the conclusion can be made that the ashing technique has the potential of being the best technique for enhancing the A/E35U-3's particle detection capabilities.

V. CONCLUSIONS

A. COMPARISON OF AE AND AA ANALYSES.

1. Historically, the wear metal concentrations obtained from A/E35U-3 spectrometers have always been higher than those obtained from atomic absorption spectrometers. To date, very little research has been done to determine the reasons for the observed differences, and separate wear metal guidelines were established for each instrument. In order to accurately assess the A/E35U-3's particle detection capabilities, it was considered essential that the analytical results from the AA and AE spectrometers agree, since the actual metal concentration in each filtrate was determined by an AA spectrometer (Paragraph IVA1b).

2. In the initial stages of this work, we concluded that the analytical results from the A/E35U-3 were superficially high due to matrix and concomitant element effects (Paragraph IVA1b). These effects were eliminated during the particle detection capability study by analyzing single element standards in the various oils. The spectrometer readout for each single element standard was plotted versus its corresponding concentration to prepare working curves. The concentration of metal detected in the metal powder suspensions was determined from the appropriate working curve. When this procedure is followed, the analytical results from the AE instruments are in full agreement with the AA analytical results (Paragraph IVA3c).

3. Since the matrix affects the analytical results from the RDE spectrometers, we compared the analytical results obtained from Conostan standards dissolved in Mobil MIL-L-7808 and di-2-ethylhexyl azelate. For the four elements studied, we concluded that the additives in Mobil MIL-L-7808 enhance the Fe emission signal, but depress the emission from Al, Cu and Mg (Paragraph IVA4).

B. COMPARISON OF 14 AND 20 ELEMENT STANDARDS.

1. Since the JOAP-TSC is planning to replace the 20-element standards with 14-element standards, we analyzed 14- and 20-element standards dissolved in 1100 and 245 base oils. In both 1100 and 245 base oils, emission from Ti in the 14-element standard was enhanced by 9-10 ppm. The enhanced Ti emission is significant and would affect the Ti calibration for the A/E35U-3 spectrometer (Paragraph IVB3).

2. The base oil affected the emission from Na, and the Na emission was higher in 245 base oil. Since all the other metals gave similar results in both hydrocarbon oils, we concluded that slight variations in the hydrocarbon base oil will not adversely affect the calibration standards (Paragraph IVB4).

C. PARTICLE DETECTION CAPABILITIES.

1. Initially, we analyzed suspensions of metal particles and confirmed that the analyses performed on the A/E35U-3 and the A/E35U-1 are particle size dependent (Paragraph IVC1). From these initial investigations, we concluded that Al, Cr, Fe and Mg particles are analyzed better by the A/E35U-1, while Ag, Cu and Ni particles are analyzed better by the A/E35U-3. These results suggested that there may be a dependence on the element's density, since the lighter elements are analyzed better on the A/E35U-1 and the denser elements are analyzed better on the A/E35U-3.

2. Data was also collected on suspensions of Arizona Road Dust (ARD), TiC and Si_3N_4 particles. We concluded that neither the A/E35U-3 nor the A/E35U-1 is capable of quantitatively detecting Si in ARD or Si_3N_4 particles which have been filtered through a 1 μm filter (Paragraphs IVC6 and IVC7).

D. FACTORS WHICH AFFECT THE PARTICLE DETECTION CAPABILITIES.

1. EFFICIENCY OF PARTICLE TRANSPORT.

a. The data collected on the metal powder suspensions shows that the RDE spectrometers cannot analyze metal particles effectively. To determine the reasons for the low particle detection capabilities, we examined the factors which might be responsible. The first factor examined was the rotating disk's capability for transporting particles to the source. The results indicated that the rotating disk is not efficiently transporting particles to the source and limits the capabilities of the RDE spectrometers (Paragraph IVD2c(2)).

b. The transport efficiency was observed to be inversely proportional to particle size (Paragraph IVD2a), but the efficiencies were slightly different for the A/E35U-1 and the A/E35U-3. The only difference between the two instruments is the length of the preburn cycle which is 12 seconds on the A/E35U-1 but only 6 seconds on the A/E35U-3. The shorter preburn time on the A/E35U-3 results in higher particle transport efficiencies (Paragraph IVD2b(4)).

c. The differences in particle transport efficiencies for the A/E35U-1 and the A/E35U-3 increase with particle density. For example, the transport efficiencies for Mg particles (1.74 g/ml) are similar for both instruments, but the differences in the particle transport efficiencies are larger for Ag (10.5 g/ml), and Ag is transported better on the A/E35U-3 (Paragraph IVD2b(7)).

d. In light of the low transport efficiencies, we concluded that there must be a factor which limits the particle transport efficiency of the rotating disk (Paragraph IVD2d(1)). The factor most likely responsible was the particle settling rates which we subsequently investigated. The particle transport efficiency decreased with time and temperature, confirming that particle settling rates limit the capabilities of the rotating disk (Paragraph IVD2d(3)).

e. The particle transport efficiency is not dependent on the concentration of particles in suspension (Paragraph IVD2f), but it does depend on the viscosity of the matrix (Paragraph IVD2g(2)). The oil's viscosity affects both the amount of oil and the size of the particles transported to the source. The efficiency of particle transport is 100% for Al, Fe and Mg particles less than 20 µm suspended in Conostan 245.

f. The effect of particle morphology was investigated by analyzing suspensions of five different metal powders. The spherical Ventron Fe particles were more difficult to analyze than the ball-milled Fe powder. We concluded that particle morphology does have an effect on particle detection (Paragraph IVD2h(3)).

2. <u>EFFICIENCY OF THE SOURCE</u>.

a. Since the A/E35U-3 transports particles to its source more efficiently than the A/E35U-1, the particle detection capabilities of the A/E35U-3 were expected to be higher than those for the A/E35U-1. However, when the Al, Cr, Fe and Mg powders suspended in MIL-L-7808 were analyzed on both instruments, higher concentrations were obtained with the A/E35U-1 (Paragraph IVC1).

b. To determine the efficiencies of the sources used on the AE spectrometers, the suspensions of Al, Cu, Fe and Mg in Conostan 245 were used. Since the particle transport efficiency for Al, Fe and Mg particles less than 20 µm and Cu particles less than 8 µm in size is 100% in Conostan 245 for both instruments, the percent metal analyzed by the spectrometers is equal to their respective source efficiencies. Since the Al, Cu, Fe and Mg particles were analyzed better by the A/E35U-1, we conclude that the source on the A/E35U-1 is more efficient than the source on the A/E35U-3 (Paragraph IVD3a(2)).

c. Although the transport efficiency is 100% for Al, Fe and Mg particles in Conostan 245, the percent metal analyzed (%A) was much lower than expected. Less than 50% of the Fe and Al particles greater than 5 µm in size were detected by the A/E35U-3. Although the particle transport improves with an increase in the matrix's viscosity, the percent metal analyzed by the A/E35U-3 does not increase to the same extent, and even decreases for Cu, Mo and Ti particles (Paragraph IVD3b(2)(c)). We conclude that the increased quantity of oil transported for the more viscous oils decreases the particle detection capabilities of the A/E35U-3 (Paragraph IVD3b(2)(d)). On the other hand, the quantity of oil transported by the disk has very little effect on the particle detection capabilities of the A/E35U-1 (Paragraph IVD3b(2)(e)). Again we conclude that the source on the A/E35U-1 is more effective for wear metal analyses.

d. To determine if the chemical composition of the matrix affects the source efficiencies of the AE spectrometers, particle suspensions prepared in hydrocarbon oil (Phillips Condor 105) and an ester oil (Mobil MIL-L-7808) were used. The efficiency of particle transport is similar in these two oils, and any observed differences are attributed to the matrix. On the A/E35U-3 the optimum detection of Cu particles was obtained in the hydrocarbon oil, while the optimum detection of Al and Fe particles was obtained in the ester oil. On the A/E35U-1 the optimum detection of Cu and Al particles was obtained in the hydrocarbon oil. Therefore, we conclude that the matrix composition affects the particle detection capabilities of both the A/E35U-1 and the A/E35U-3 (Paragraph IVD3b(3)(c)).

e. The effect of particle composition was also investigated. For particles (< 5 µm) of Mg, Al and ARD suspended in MIL-L-23699, the percent metal analyzed was 100%, 50% and 10% respectively (Paragraph IVD3c). We conclude that the composition of the particles also affects the particle detection capabilities of the A/E35U-3, but the concentration of particles in suspension was observed to have no effect on the A/E35U-3's detection capabilities (Paragraph IVD3d(3)).

f. The effect of particle morphology was investigated by analyzing five different metal powders. The particles in the Ventron Fe powder were more difficult to analyze than the particles in the ball-milled Fe powder. We concluded that the difference in particle shape was responsible (Paragraph IVD3e(3)).

g. The effect of electrode configuration was investigated, because the A/E35U-1 and the A/E35U-3 employ different upper electrodes. We observed that the electrode recommended for each instrument gave the highest recoveries of particles, i.e., the 15° taper electrode gives optimum results on the A/E35U-1 and the 160° tip angle electrode gives optimum results on the A/E35U-3 (Paragraph IVD3f(4)). However, when the same electrode was used in each instrument, the results from the A/E35U-1 were always higher, indicating the source electronics are responsible for the higher efficiency of the A/E35U-1 (Paragraph IVD3f(4)).

h. The effect of the rotating electrode was investigated by using 3-and 5-mm disk electrodes. The narrower disk electrode did not affect metal particle analyses on the A/E35U-3, but it improved metal particle analyses on the A/E35U-1. Of the various electrode configurations tested, the best particle analyses were obtained on the A/E35U-1 using the 3 mm disk and the 160° tip angle electrode (Paragraph IVD3f(8)).

E. METHODS STUDIED TO IMPROVE PARTICLE DETECTION CAPABILITIES.

1. The results presented in Section IVE show that the particle size detection capability of the AE spectrometers can be improved. Since the particle transport efficiencies of the disk are limited by particle settling rates, a shorter burn time was expected and was verified to improve

the particle recoveries of the A/E35U-1. However, the improvements were small and did not improve the efficiency of the source (Paragraph IVE3).

2. An acid dissolution method which dissolves the metal particles and produces a homogeneous solution for analysis was developed which quantitatively analyzes Al, Cu, Fe, Mg, Ni and Sn particles. The acid method increased the analysis time by only 3 minutes, but produced a corrosive solution which could not be neutralized without affecting the reliability of the analytical results (Paragraph IVE2b).

3. To eliminate the particle transport limitations of the disk, the sample was deposited directly onto the disk electrode. The method of the direct deposition is potentially quantitative, but it is presently limited by the low reproducibility of the deposition process (Paragraph IVE4e).

4. To eliminate inefficiencies of both the source and the rotating disk electrode, the oil sample was deposited directly onto a lower electrode and placed in a muffle furnace to vaporize (ash) the oil. The crater electrode produced results which were lower or equal to those obtained by direct analysis (Paragraph IVE5b(2)). However, both the ashed RDE and the RPE gave improved particle detection, with the RDE giving higher recoveries than the RPE (Paragraphs IVE5a(3) and (IVE5c(2)). Further increases in instrument readout were obtained by keeping the electrodes stationary during the preburn cycle (Paragraph IVE5d(1)). At this point, we conclude that both (RPE and RDE) ashing techniques improved particle detection, and the RDE produced quantitative recoveries for Cu, Fe, Mg, Ni and Sn particles, while the RPE gave nonquantitative results for all the metal powders (Paragraph IVE5d(3)).

5. The main difference between the RPE and the RDE ashing methods are the orientation of the electrodes in the instrument. One reason the results differ for the two methods is that the spark excites particles differently from the flat surface of the RPE than it does from the curved surface of the RDE. Since these results are preliminary, we cannot make a conclusion as to which is the best technique. However, the conclusion can be made that the ashing techniques have the most potential for improving the A/E35U-3's particle detection capabilities (Paragraph IVE5d(5)).

VI. RECOMMENDATIONS

A. Our research indicates that the emission spectrometers are limited by the low particle transport efficiency of the rotating disk and the energy of the source. The source has insufficient energy to vaporize both the oil and the wear metal particles.

B. To improve the particle detection capabilities of the rotating disk emission spectrometer, we recommend that more research be conducted to develop methods which will provide efficient transport of particles to the source. Preliminary investigations suggest that particles can be quantitatively transported to the source by directly depositing the sample onto the rotating disk.

C. Since the source has insufficient energy to vaporize both the oil and the wear metal particles, vaporizing the oil prior to analysis would reduce the limitations of the source. Therefore, successful analyses of wear metal particles should be possible by depositing the oil on the disk and removing the oil prior to analysis. The oil can be vaporized (ashed) by placing the disk in a muffle furnace. After the oil has vaporized, the disk is placed in the instrument and analyzed in the usual manner. We refer to these analysis methods as ashing techniques. Preliminary results suggest that the particle detection capabilities of the emission spectrometers can be improved using these methods. Ashing techniques have the additional advantage of minimizing the matrix effects, since the matrix has been removed (ashed).

D. Additional research on ashing methods is needed, since all the wear metals were not detected equally well using the ashing techniques. We observed that Al particles were particularly difficult to detect. Also, ashing techniques need to be developed which can easily be incorporated into the A/E35U-3 spectrometer.

E. Another approach we recommend would involve investigating the energetics of the source. By increasing the energy of the source so that enough energy is present to vaporize both the particles and the oil, the particle detection capabilities of the emission spectrometers should improve. We believe that this approach should be investigated after the particle transport problems have been solved.

VII. REFERENCES

(a) Beerbower, A. "Spectrometry and other Analysis Tools for Failure Prognosis". J. American Soc. of Lub. Engineers, V. 32, No. 6, P. 285-293, 1975.

(b) Seifert, W.W. and Westcott, V.C. "Investigation of Iron Content of Lubricating Oils Using a Ferrograph and an Emission Spectrometer". Wear, V. 23, No. 2, P. 239, 1973.

(c) Naval Aviation Integrated Logistic Support Center Report No. 03-41 of 27 May 1976: An Investigation of the Navy Oil Analysis Program (NOAP).

(d) Lee, R., Technical Support Center, Naval Air Station, Pensacola, FL. Private Communication, 1979.

(e) AFWAL Report No. TR-82-4017 of February 1982: Evaluation of Plasma Source Spectrometers for the Air Force Oil Analysis Program.

(f) Naval Air Systems Command Report No. NA17-15-50 of 1 May 1977: Joint Oil Analysis Program Laboratory Manual.

(g) Baird Atomic Corp. Report No. FSN6650-937-4401 of 15 May 1972: "Spectrometer, Engine Oil Analysis, A/E35U-1 Technical Manual".

(h) Baird-Atomic Corp. Report No. FSN6650-251-0712 of 1 February 1973: "Operation Instructions, Maintenance Instructions, Fluid Analysis Spectrometer (FAS-2)".

(i) Perkin-Elmer Corp. Report No. PC-1 of March 1973: Analytical Methods for Atomic Absorption Spectrophotometry.

(j) Baer, W. and Hodge, E. "The Spectrochemical Analysis of Solutions, A Comparison of Five Techniques". J. Appl. Spectry., V. 14, P. 141, 1960.

(k) Hodge, E. "Spectrographic Tricks". J. Appl. Spectry., V. 15. P. 21, 1961.

VIII. BIBLIOGRAPHY

1. Bartels, T.; Slater, M. "Comparison of the Effectiveness of Emission Spectrographic and Atomic Absorption Techniques for Measuring Iron Particles in Lubricating Oils". Atomic Absorption Newsletter, V. 9, P. 75, 1970.

2. Baudin, G. "Influences Mutuelles en Spectrographic sur Solution des Elements Fe, Ni, Cr, Ti Pris Trois a Trois". Compt. Rend., V. 250, P. 1818,1960.

3. Bear, W.; Hodge, E. "The Spectrochemical Analysis of Solutions, A Comparison of Five Techniques". Appl. Spectry., V. 14, P. 141, 1960.

4. Bibl, W.; Brenneke, H.; Marold, M. "Der Einfluss der Olmatrix bei der Emissionsspektreoskopischen Bestimmung von Metallischen Abrieb in Schmierolen von Triebwerken". Mikrochim. Acta, V. 8, P. 501, 1978.

5. Eichhoff, H.; Picard, K. "Eine Kapillarelektrode aus Metal zur direkten, spectrochemischen Untersuchung von Losungen". Spectrochim. Acta, V. 7, P. 396, 1956.

6. Errera, J. "Colloidal Supports for Obtaining the Emission Spectra of Solutions". Compt. Rend., V. 176, P. 1874, 1923.

7. Feldman C. "Direct Spectrochemical Analysis of Solutions Using Spark Excitation and the Porous Cup Electrode". Anal. Chem., V. 21, P. 1041, 1949.

8. Flickinger, L.; Polley, E.; Galleta, F. "Direct Reading Analysis of Steel Solutions Using a Reservoir-Cupped Center Post Electrode". Anal. Chem., V. 30, P. 502, 1958.

9. Fred, M.; Nachtriels, N.; Tomkins, F. "Spectrochemical Analysis by the Copper Spark Method". J. Opt. Soc. Am., V. 37, P. 279, 1947.

10. Fry, O. "The Spectrographic Analysis of Lubricating Oils". Appl. Spectrosc., V. 10, P. 65, 1956.

11. Gassman, A.; O'Neill, W. "The Use of a Porous-Cup Electrode in the Spectrographic Analyses of Lubricating Oils". Proceed., Amer. Petrol. Inst., V. 29M, P. 79, 1949.

12. Gramont, A. "Apparatus for the Production of Spark Spectra of Solutions". Compt. Rend., V. 145, P. 1170, 1907.

13. Grampurohit, S.; Rao, P. "Spectrographic Analysis of Wear Metals in Lubricating Oils I and II". Indian J. Pure Appl. Phys., V. 15, P. 424, 1977.

14. Guttman, W. "Losungsspektralanalyse mit zwei rotierenden Electroden". Naturwissenschaften, V. 47, P. 128, 1960.

15. Hodge, E. "Spectrographic Tricks". Appl. Spectry., V. 15, P. 21, 1961.

16. Hultgren, R. "The Spark-in-Flame Method of Spectrographic Analysis and a Study of the Mutual Effects of Elements on One Another's Emission". J. Amer. Chem. Soc., V. 54, P. 2320, 1932.

17. Jackson, D. "Comparison of Atomic Absorption and Emission Spectroscopy in the Evaluation of Lubrication in Normally-Operating Diesel Engines". Lubrication Engineering, V. 28, P. 76, 1972.

18. Jantzen, E. "The Spectroscopical Analysis of Metal Wear Based on Oil Investigations of Aircraft Turbine Engines". Deutsche Luft-und Raumfahrt, V. 73, No. 6, AD .907240, 1973.

19. Jolibois, P.; Bossuet, R. "Sur la structure de l'etincelle eclantant a la surface d'une solution". Comp. Rend., V. 202, P. 400, 1936.

20. Kiers, R.; Englis, D. "Solution Method for Spectrographic Analysis Utilizing a Dripping Electrode". Ind. Eng. Chem., Anal. Ed., V. 12, P. 275, 1940.

21. Kyuregyan, S.; Marenova, M. "A Direct Spectral Method for Determining Wear Product in Lubricating Oils". Chemistry and Technology Fuels and Oils, U.S.S.R, V. 12, P. 527, 1967.

22. Lamb, F. "Determination of Blood Magnesium Quantitative Spectrochemical Method". Ind. Eng. Chem., Anal. Ed., V. 13, P. 185, 1941.

23. Lukas, M.; Giering, L. "The Effects of Metal Particle Size in the Analysis for Wear Metals Using the Rotating Disc Atomic Emission Technique". Bundesakademie Fur Wehrverwaltung und Wehrtechnik, 95a.01, 1978.

24. Lundegardgm H, "The Quantitative Emission Spectral Analysis of Inorganic Elements in Solutions". Metallwirshaft, V. 17, P. 122, 1938.

25. MacGowan, R. "Spectrochemical Analysis of Oils Using (Vacuum Cup) Electrode". Appl. Spectrosc., V. 15, P. 179, 1961.

26. Meloche, V.; Shapiro, R. "Determination of Calcium and Magnesium in Lake Waters by Means of a Rotating Silver Disc Electrode". Anal. Chem., V. 26, P. 347, 1954.

27. Mitchell G.; Orne, G.; Farrel, F. "Simple Cup Electrode for Spectrographic Analysis of Solutions". Spectrochim Acta., V. 15, P. 272, 1959.

28. Navy Oil Program, "TSC Technical Reports, 1973 Series" Reports TR 1-73 to TR 12-73 reviewed.

29. Nitchie, C. "Quantitative Analysis with the Spectrograph". Ind. Eng. Chem., Anal. Ed., V. 1, P. 1, 1929.

30. Pagliasotti, J. "Spectrochemical Analysis with the Rotating Electrode". Appl. Spectrosc., V. 9, P. 153, 1955.

31. Philcox, H. "The Design and Use of an Improved Rotating Disk Electrode for Spectrographic Analysis of Solutions". Spectrochim. Acta, V. 16, P. 384, 1960.

32. Russel, R. "Emission Spectroscopy in an Oil Laboratory". Anal. Chem., V. 20, P. 296, 1948.

33. Scheibe, G.; Rivas, A. "Eine neue Methode der Quantitative Emissionsspektralanalyse, verwendbar auch als Mikromethode". Agnew. Chem., 1936, 49, 443. V. 49, P. 443, 1936.

34. Schroeder, W.; Strasheim, A.; van Niekark, J. "A High Repetition Rate High Voltage Spark Source and Its Application to the Analysis of wear Metal in Oils". Develop. Appl. Spectr., V. 10, P. 269, 1972.

35. Straub, W.; Bauer, S.; Cooke, W. "Spark in Flame Spectroscopy". Spectrochim Acta, V. 12, P. 377, 1958.

36. Talka, R. "Excitation Apparatus for Emission Spectroscopy of Solutions". Gov. Patent 1,798,323, 5 Nov 1970.

37. U.S. Air Force Report No. AFWAL Report No. TR-82-4017 of February 1982: Evaluation of Plasma Source Spectrometers for the Air Force Oil Analysis Program.

38. U.S. Atomic Energy Comm. Report No. ORNL-2774 of 1960.

39. Uzumasa, Y; Okuna, H.; "Spectrographic Analysis II. A New Method of Spectrum Analysis of Solutions". J. Chem. Soc. Japan, V. 54, P. 631, 1933.

40. Zink, T. "A Vacuum Cup Electrode for the Spectrochemical Analysis of Solutions". Appl. Spectry., V. 13, P. 94, 1959.

APPENDIX A

ANALYTICAL RESULTS OF THE A/E35U-1 AND A/E35U-3 SPECTROMETERS FOR CONOSTAN STANDARDS AND METAL POWDER SUSPENSIONS

LIST OF ILLUSTRATIONS

LIST OF ILLUSTRATIONS (CONT'D)

LIST OF ILLUSTRATIONS (CONT'D)

LIST OF ILLUSTRATIONS (CONT'D)

LIST OF ILLUSTRATIONS (CONCLUDED)

A. Single element Conostan standards were analyzed on the A/E35U-1 and A/E35U-3 spectrometers. Presented herein are the working curves produced by plotting the instrument readout for each standard vs the standard's concentration (Figures A1-A7).

B. To determine the particle size detection capabilities of the A/E35U-1 and A/E35U-3 spectrometers, metal powder suspensions with known maximum particle sizes were analyzed on the A/E35U-1 and A/E35U-3. The plots of the metal concentrations plus the disk transport efficiency vs maximum particle size and the plots of the percent metal analyzed vs particle size for each metal powder suspension are also presented herein (Figures A8-A52).

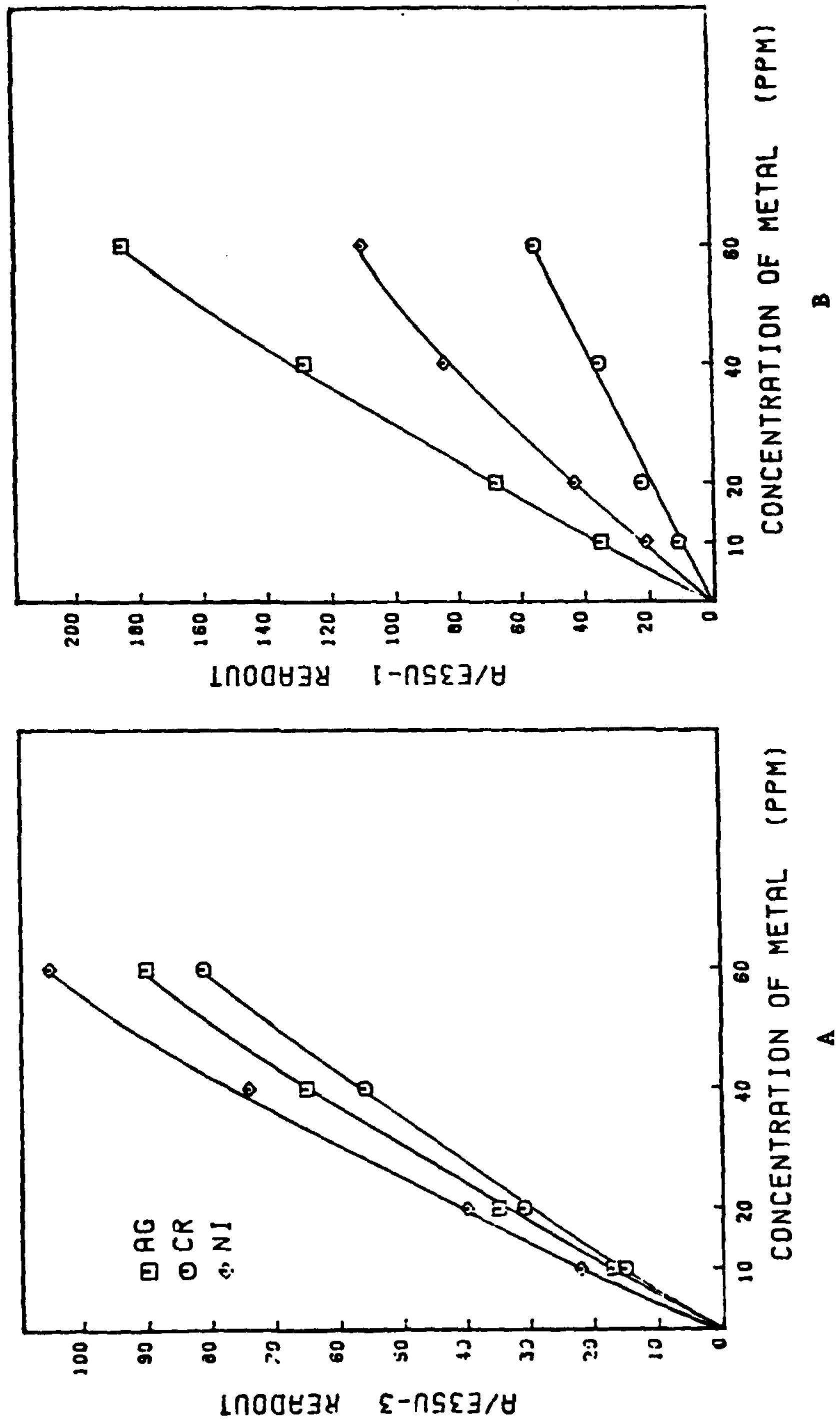

Figure A1. Working Curves for the Determinations of Ag, Cr and Ni in Mobil MIL-L-7808 on the A/E35U-3 (A) and on the A/E35U-1 (B).

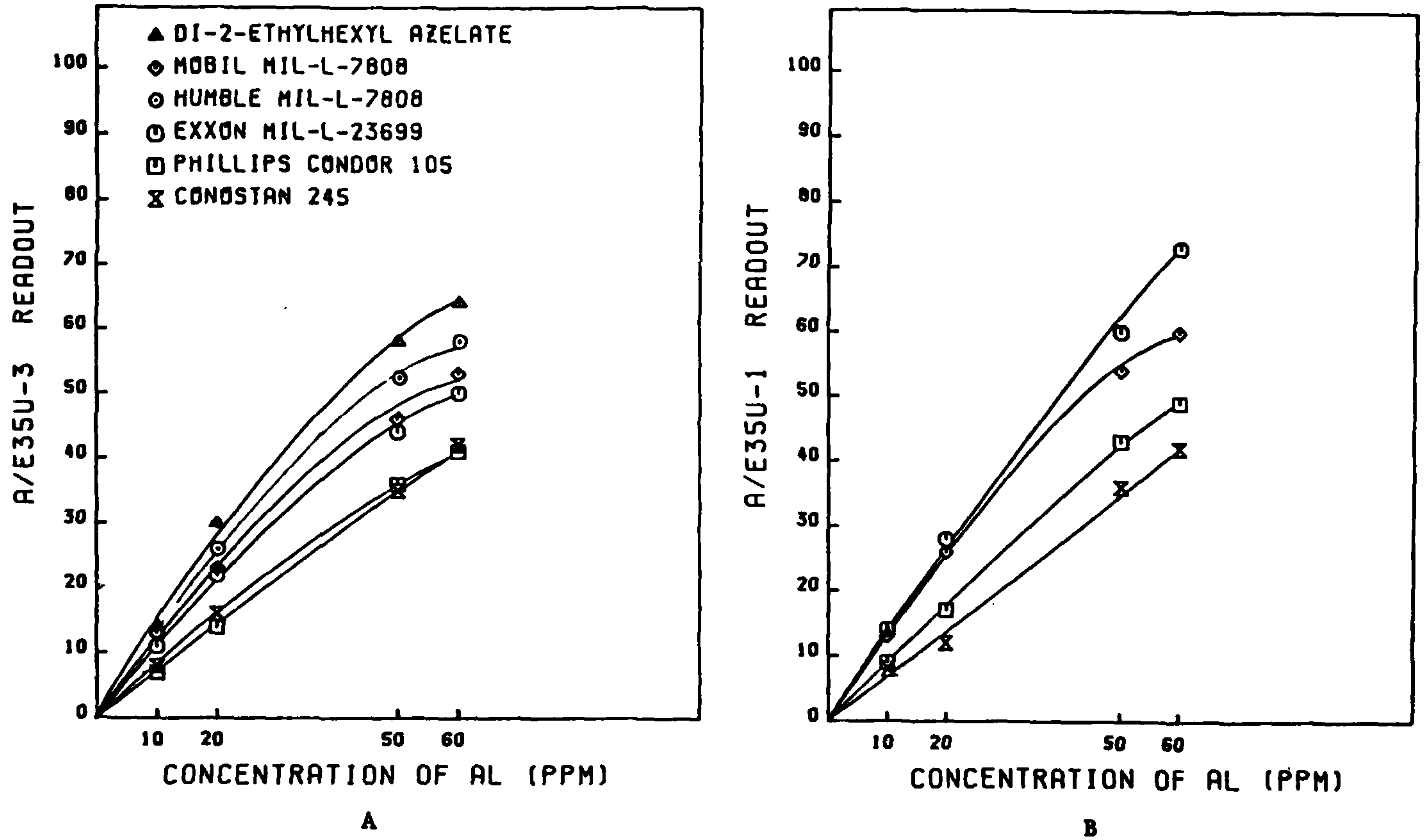

Figure A2. Working Curves for the Determination of Al on the A/E35U-3 (A) and on the A/E35U-1 (B).

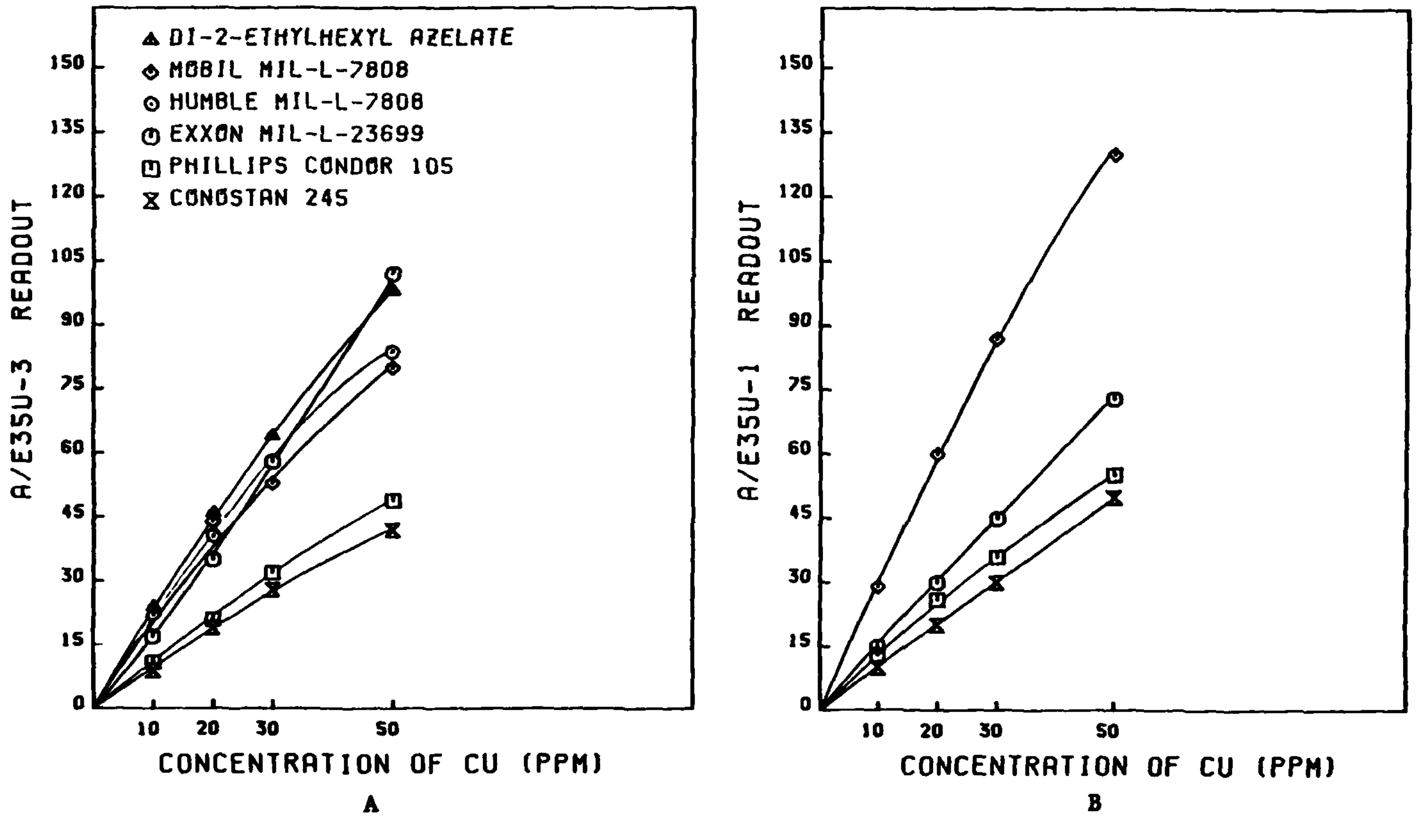

Figure A3. Working Curves for the Determination of Cu on the A/E35U-3 (A) and on the A/E35U-1 (B).

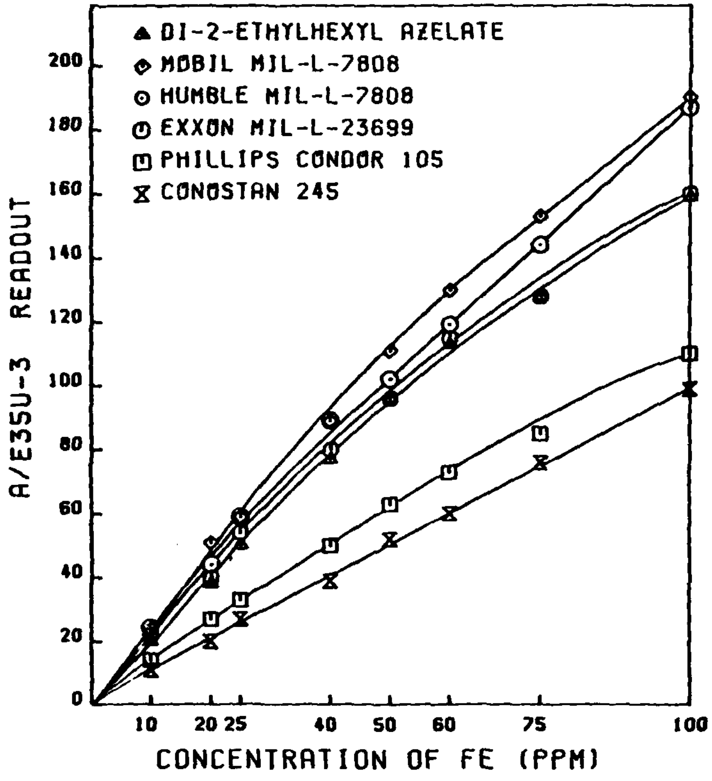

A

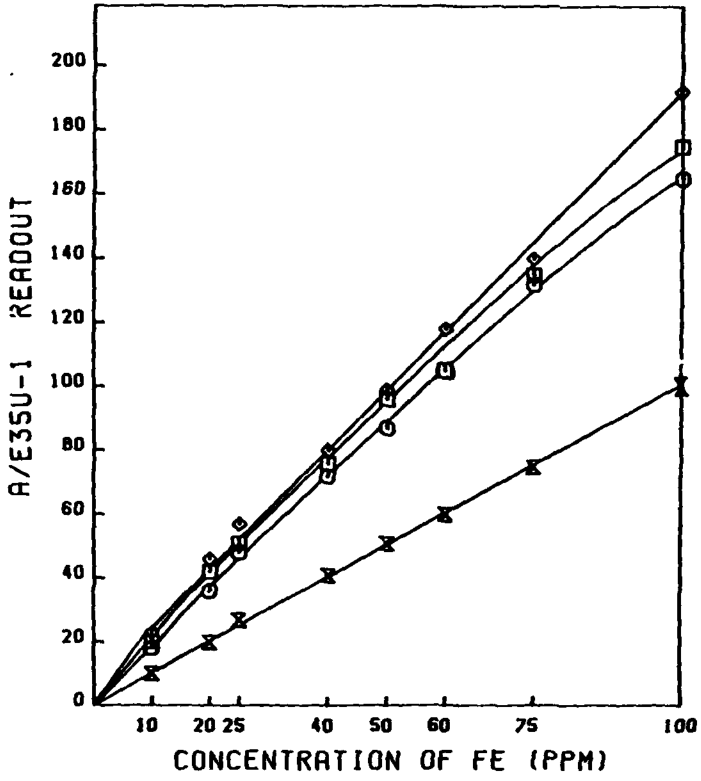

B

Figure A4. Working Curve for the Determination of Fe-AEE on the A/E35U-3 (A) and on the A/E35U-1 (B).

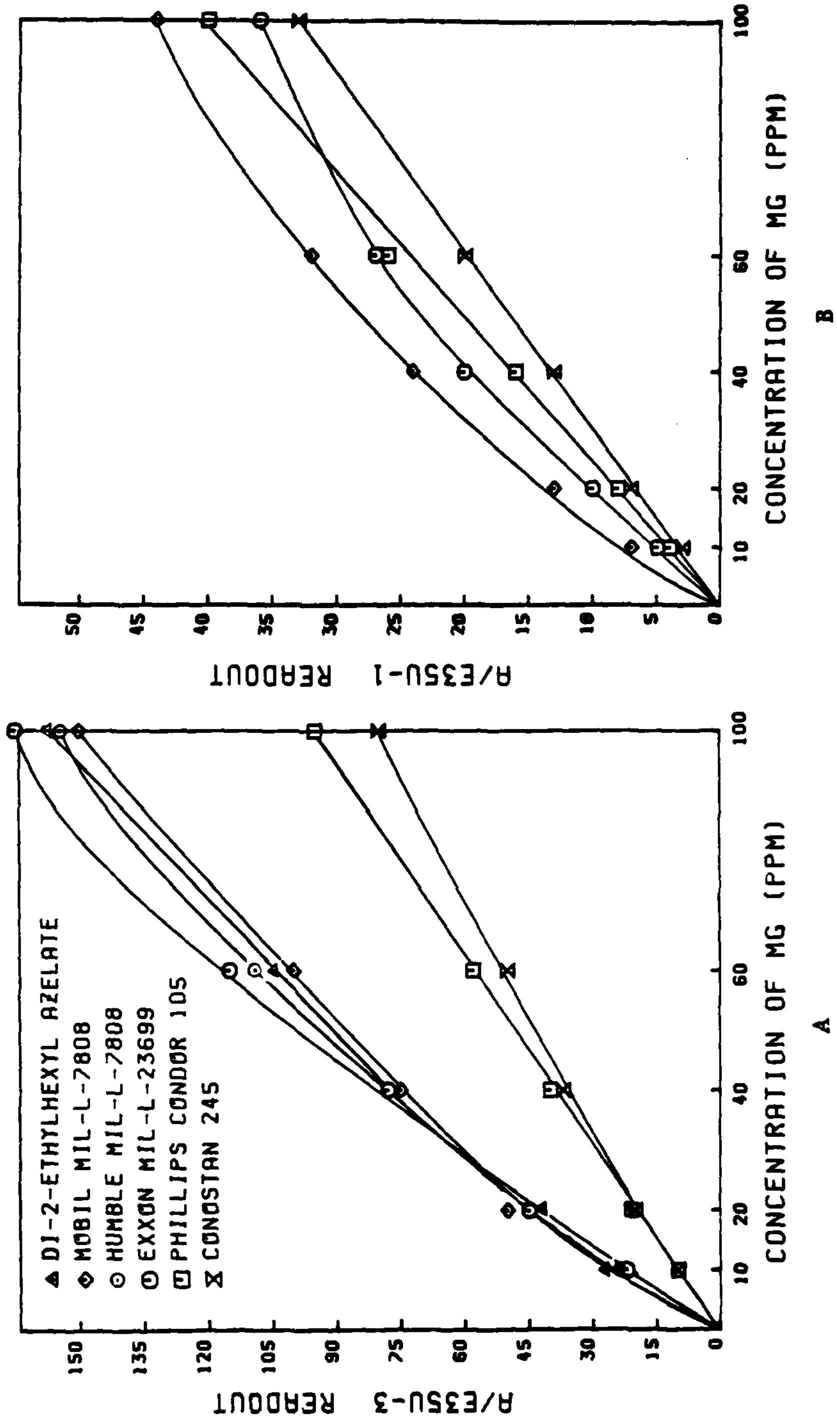

Figure A5. Working Curves for the Determination of Mg on the A/E35U-3 (A) and on the A/E35U-1 (B).

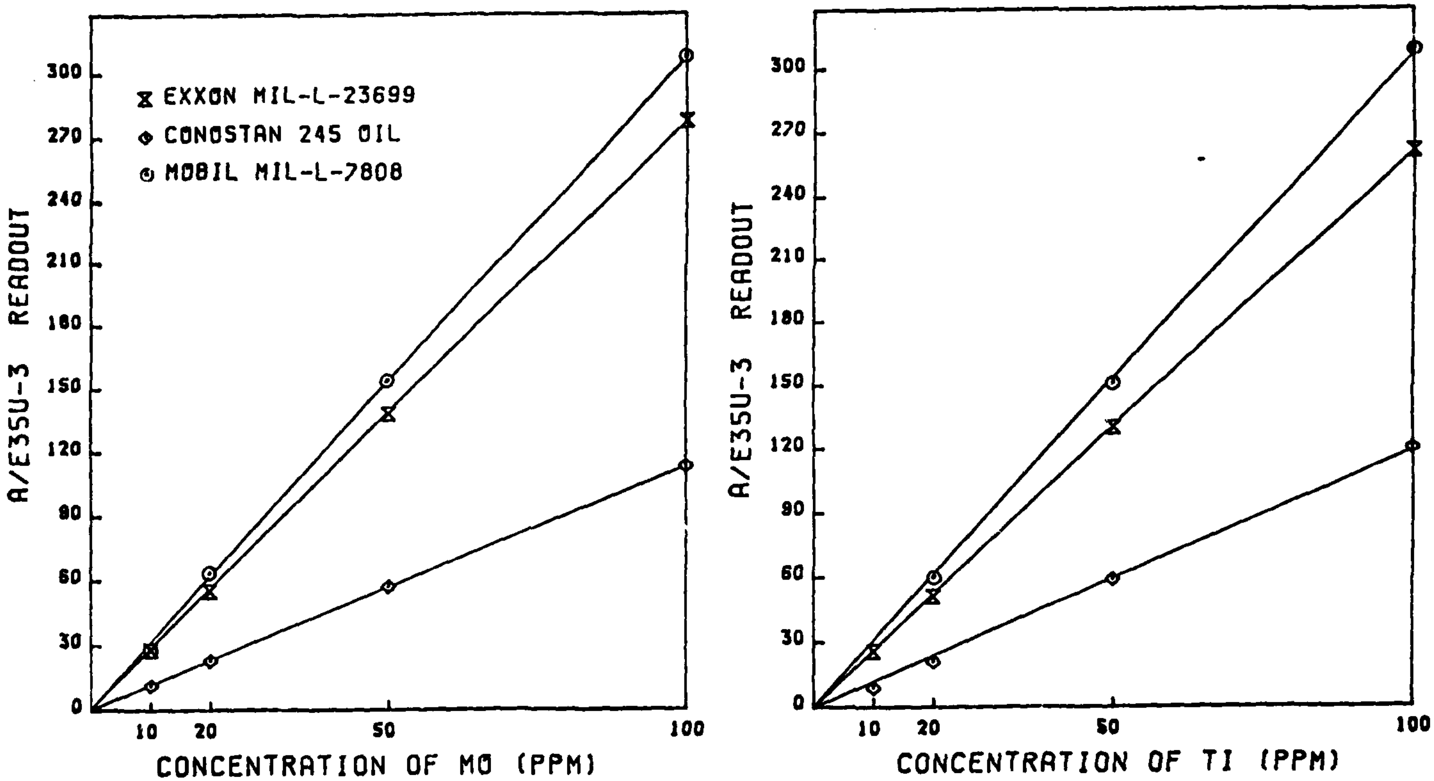

A

B

Figure A6. Working Curves for the Determination of Mo (A) and of Ti (B) on the A/E35U-3.

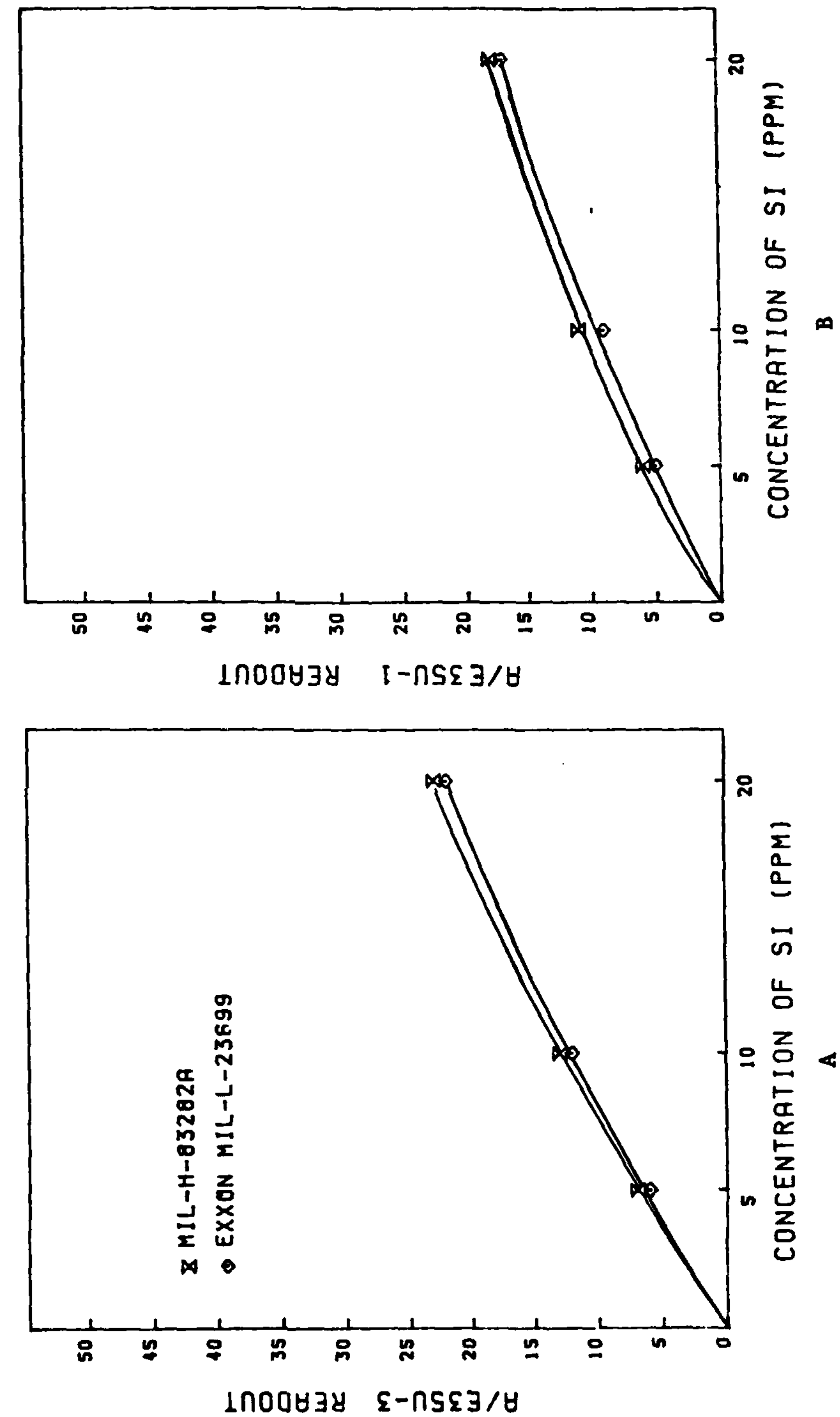

Figure A7. Working Curves for the Determination of Si on the A/E35U-3 (A) and on the A/E35U-1 (B).

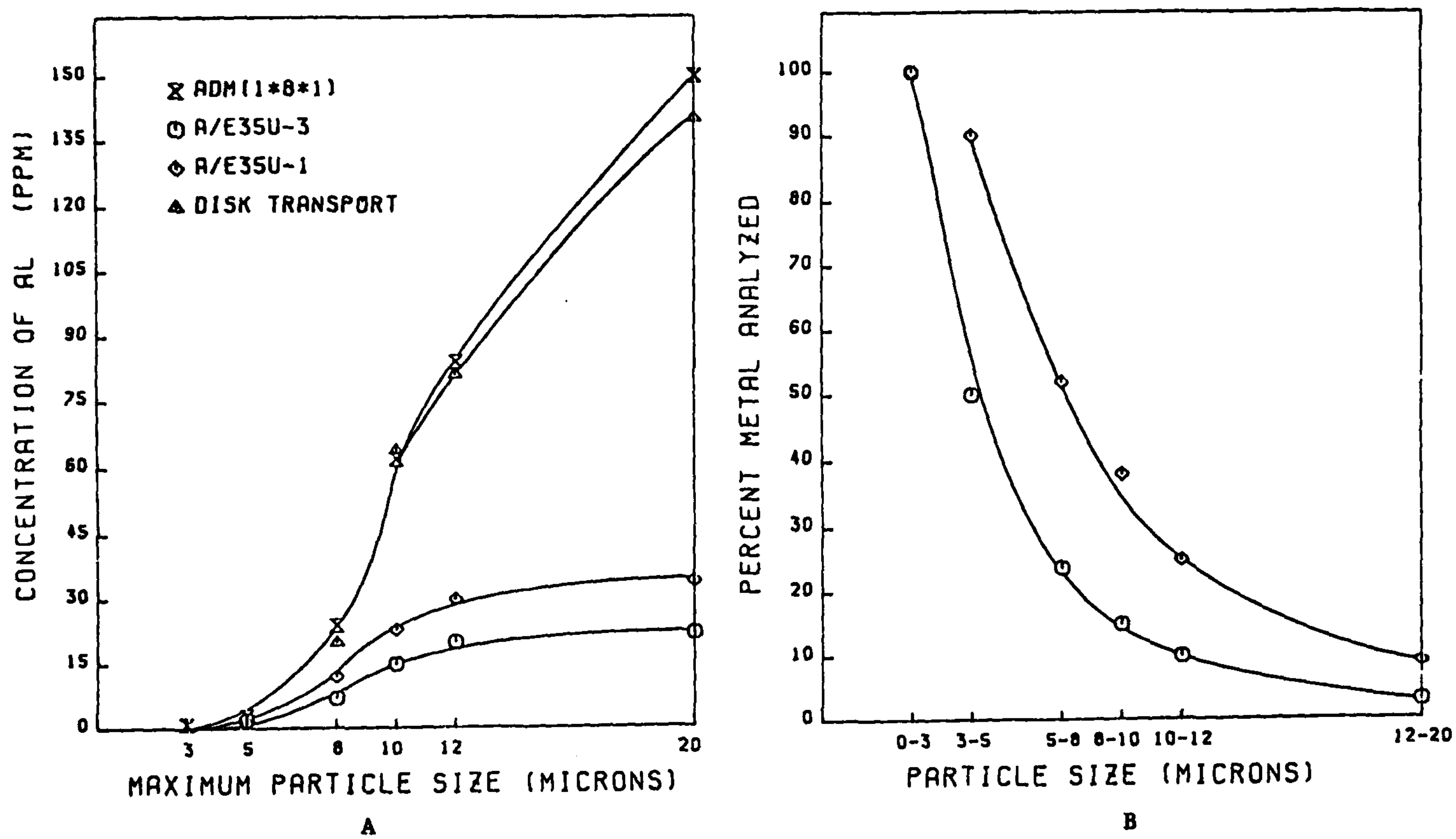

Figure A8. Spectrometric Analysis (A) and Percent Metal Analyzed (B) for Al Powder Suspended in Exxon MIL-L-23699.

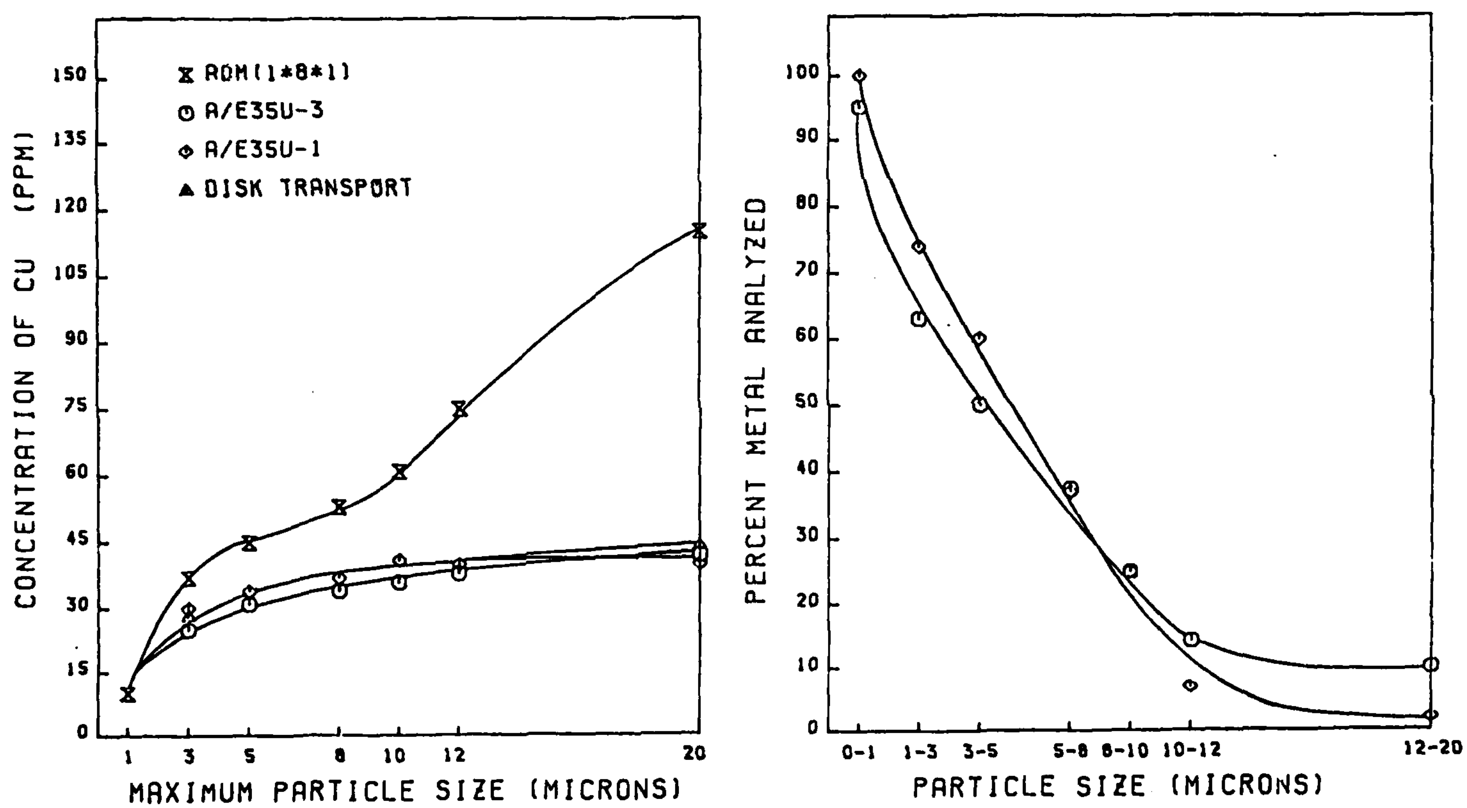

A

B

Figure A9. Spectrometric Analysis (A) and Percent Metal Analyzed (B) for Cu Powder Suspended in Exxon MIL-L-23699.

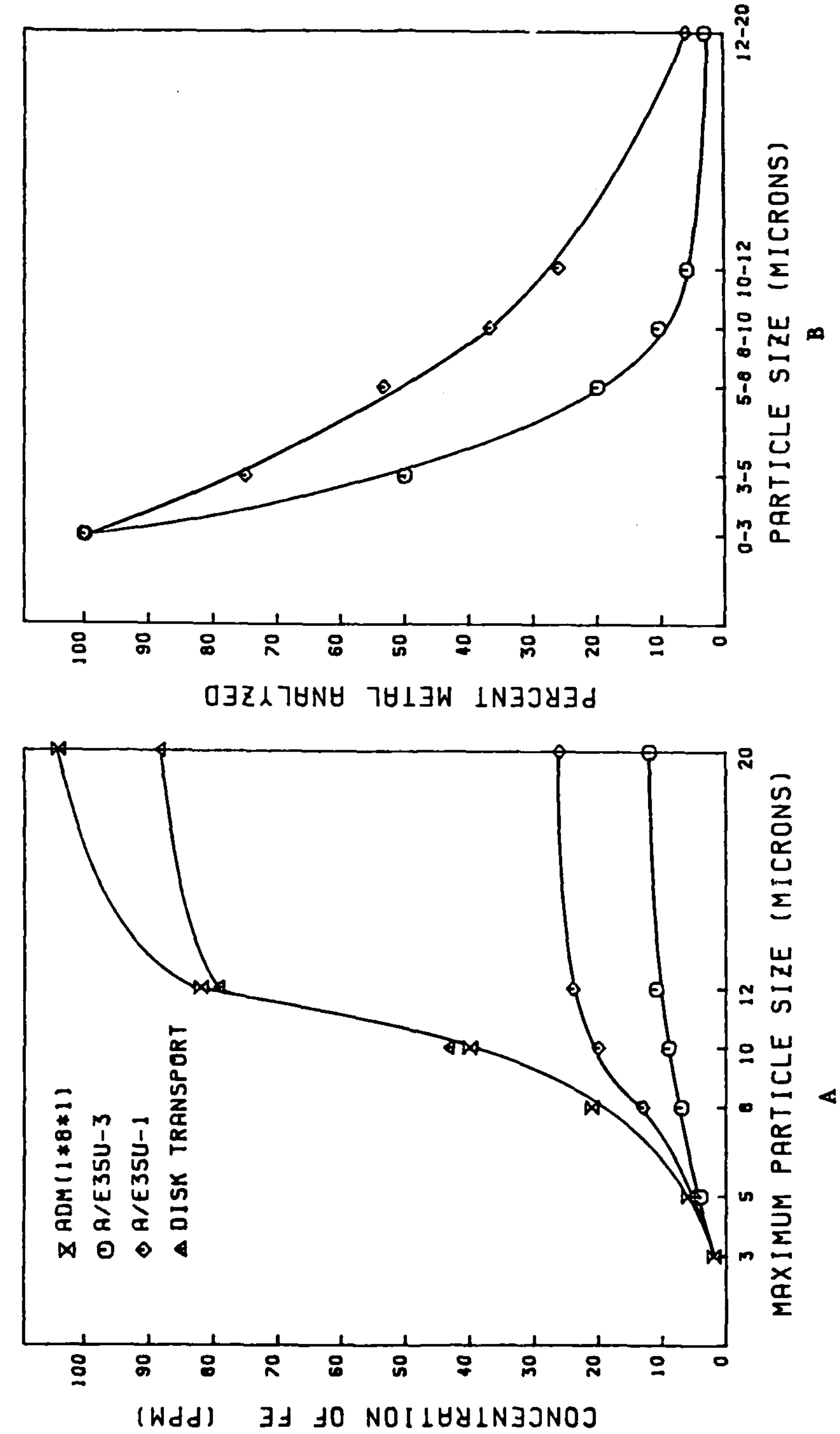

Figure A10. Spectrometric Analysis (A) and Percent Metal Analyzed (B) for Fe-AEE Powder Suspended in Exxon MIL-L-23699.

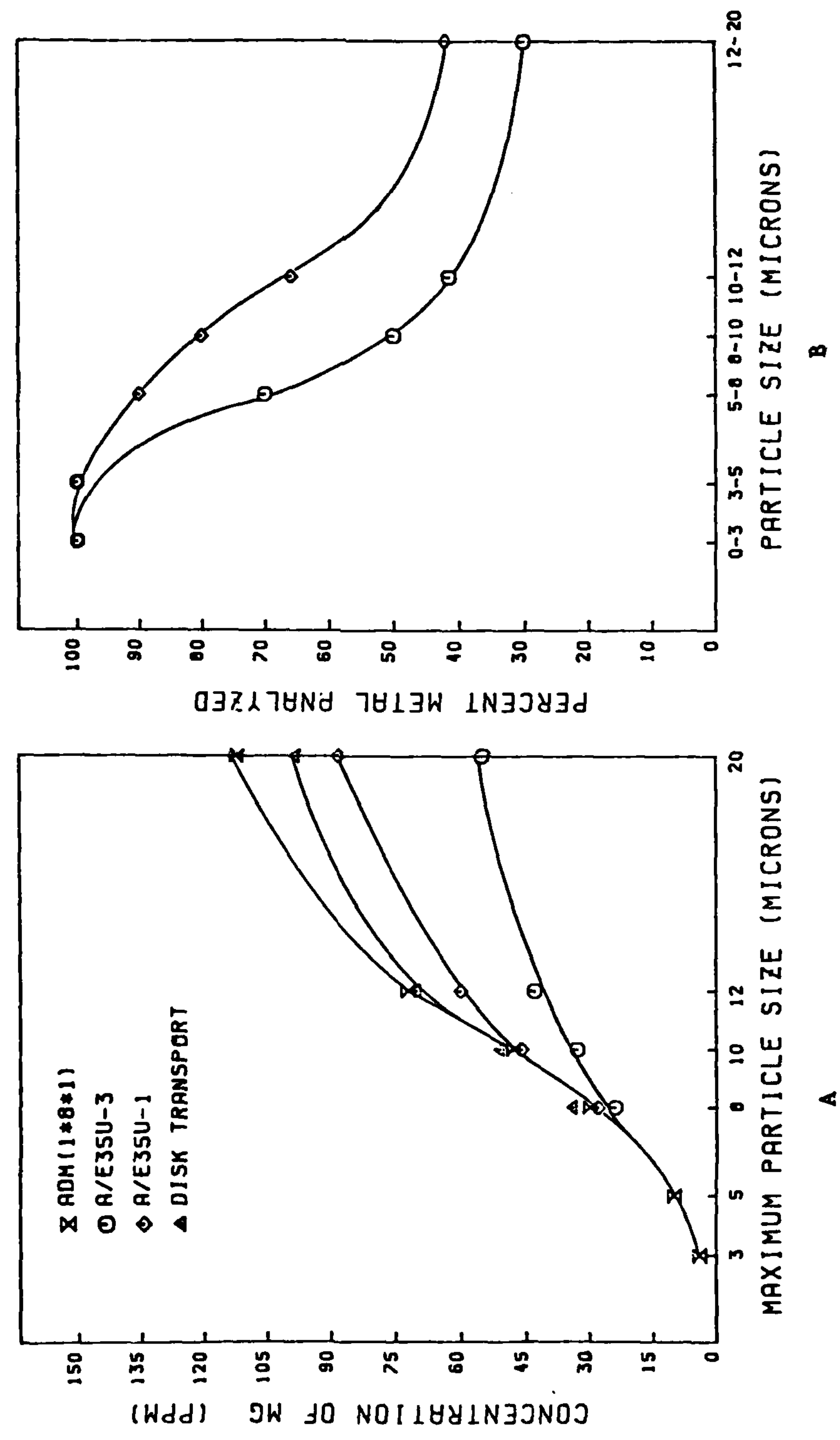

Figure A11. Spectrometric Analysis (A) and Percent Metal Analyzed (B) for Mg Powder Suspended in Exxon MIL-L-23699.

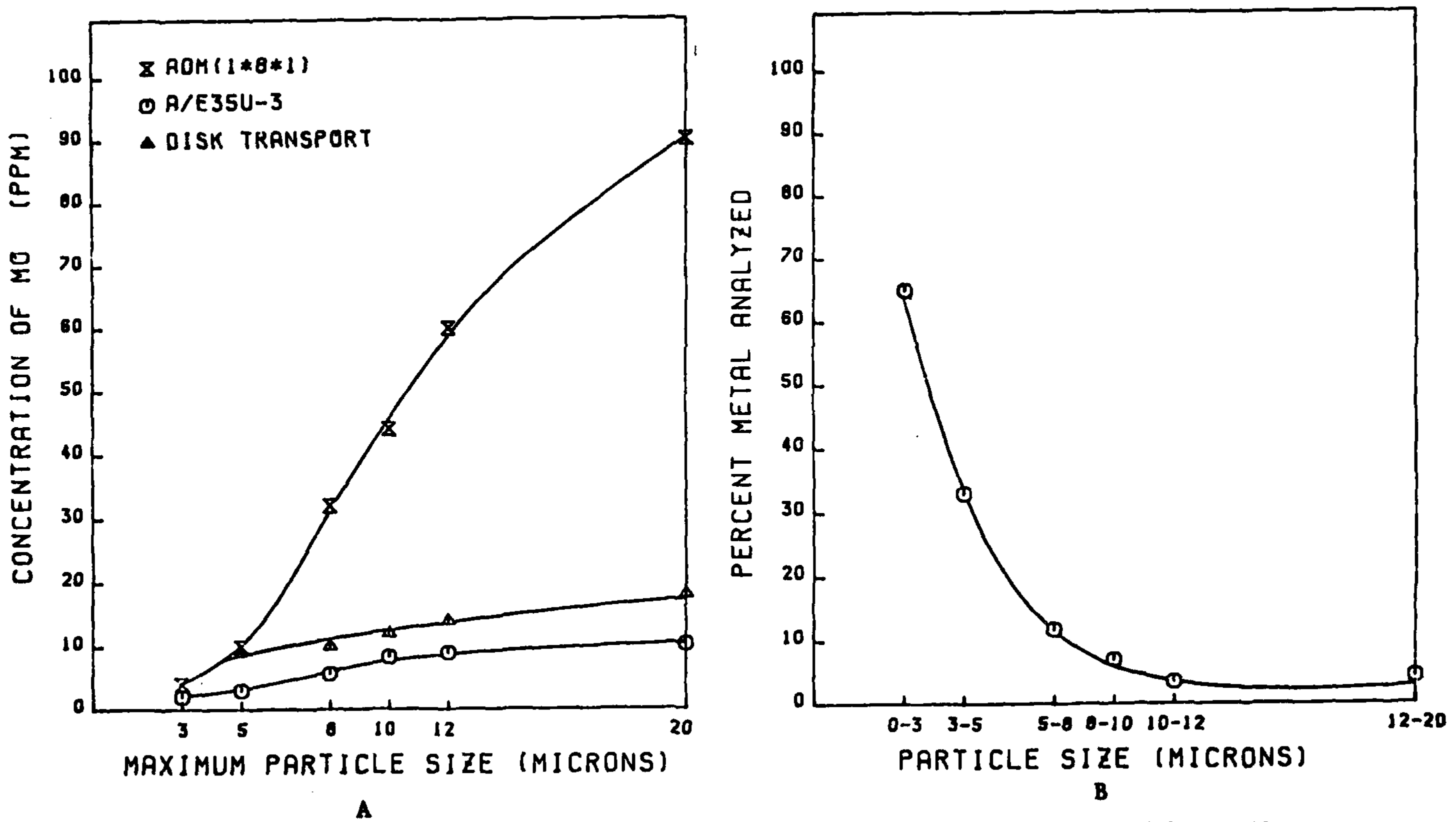

Figure A12. Spectrometric Analysis (A) and Percent Metal Analyzed (B) for Mo Powder Suspended in Exxon MIL-L-23699.

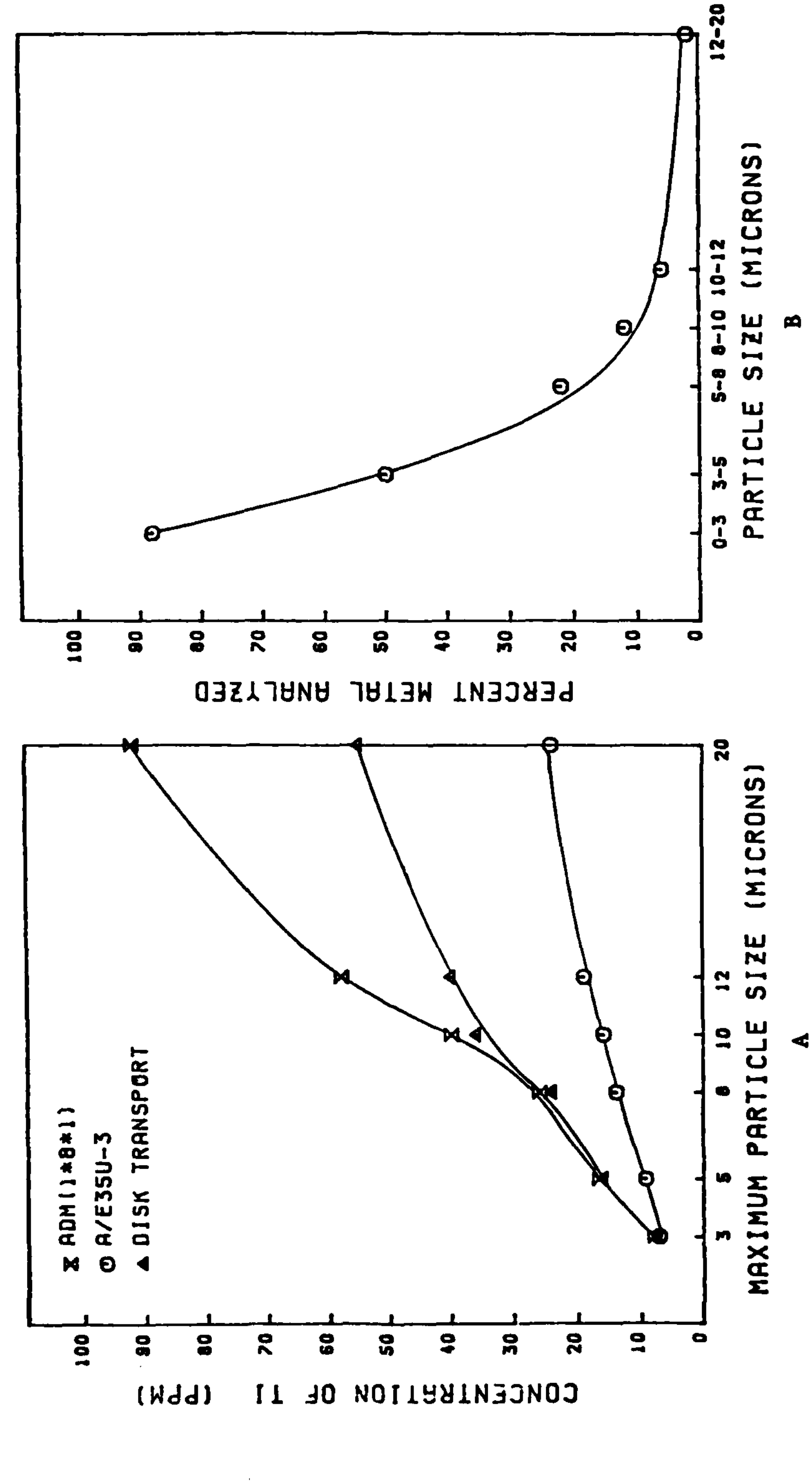

Figure A13. Spectrometric Analysis (A) and Percent Metal Analyzed (B) for Ti Powder Suspended in Exxon MIL-L-23699.

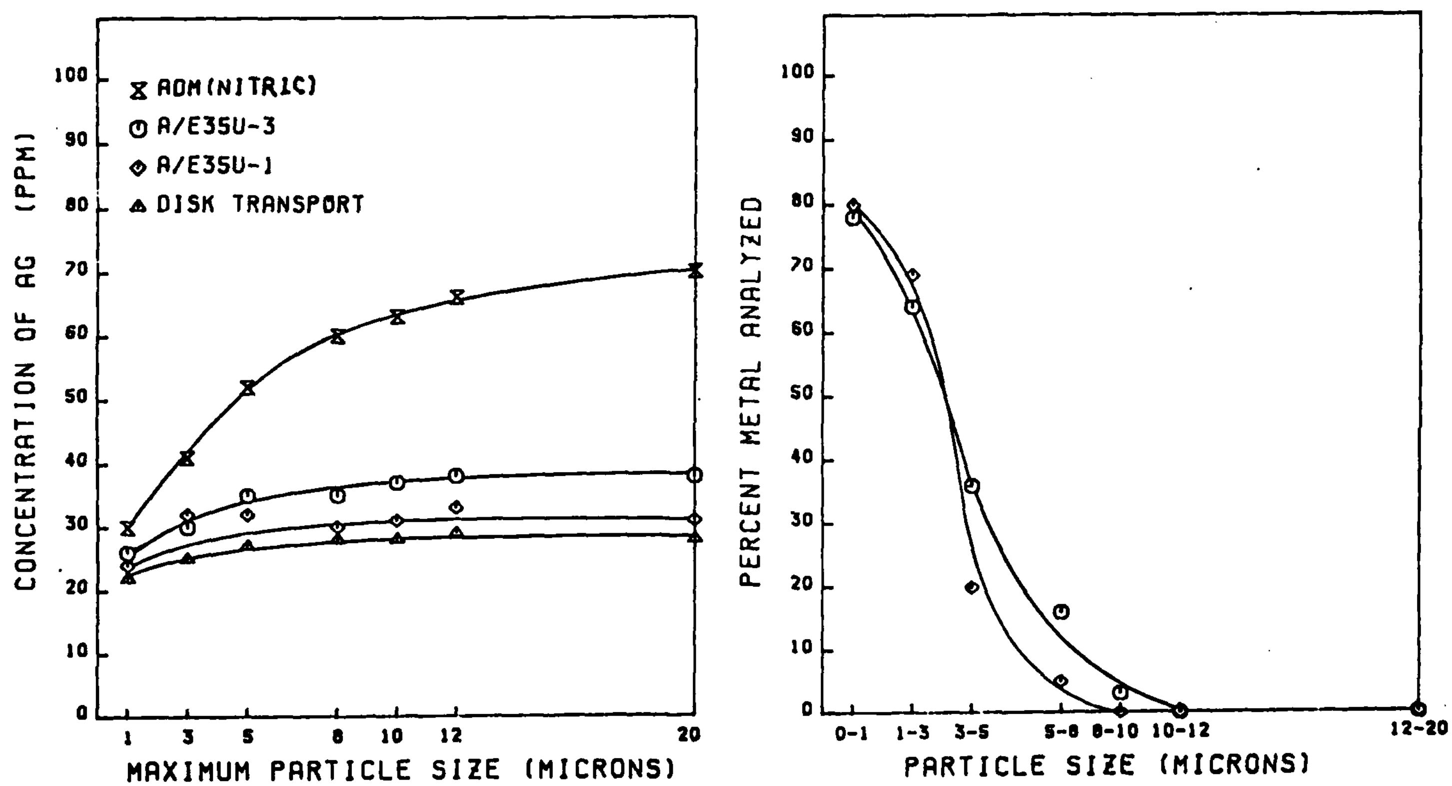

A   B

Figure A14. Spectrometric Analysis (A) and Percent Metal Analyzed (B) for Ag Powder Suspended in Mobil MIL-L-7808.

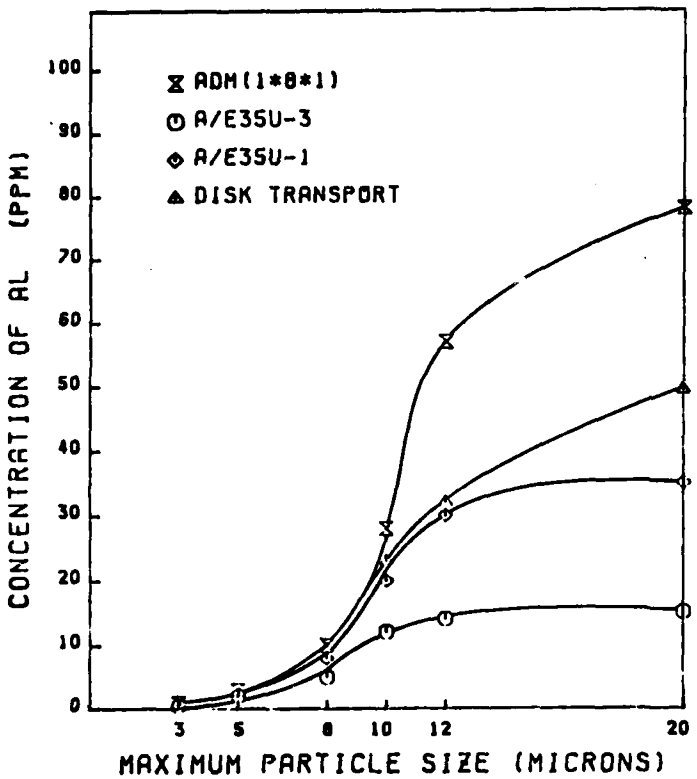

A

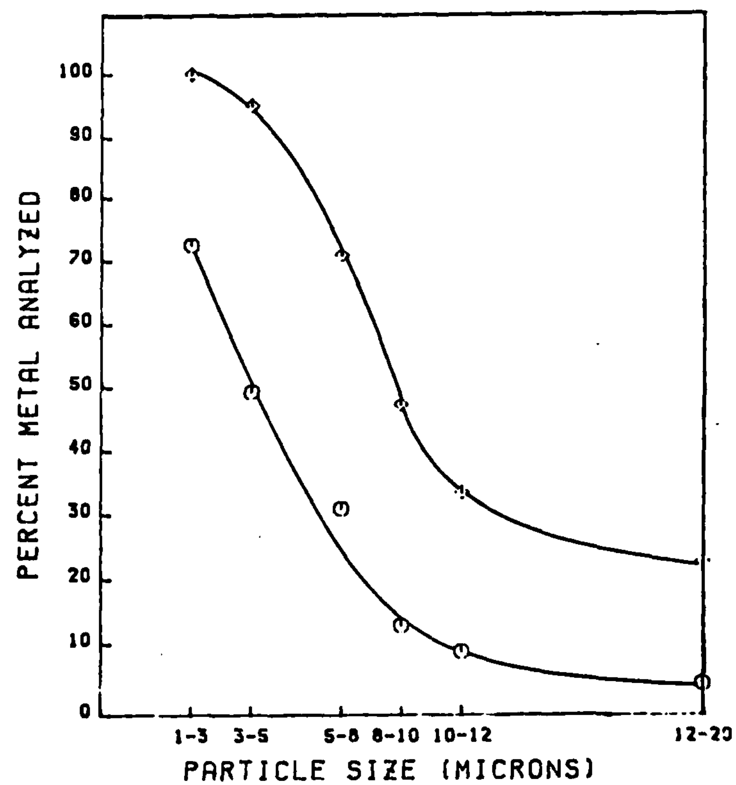

B

Figure A15. Spectrometric Analysis (A) and Percent Metal Analyzed (B) for Al Powder Suspended in Mobil MIL-L-7808.

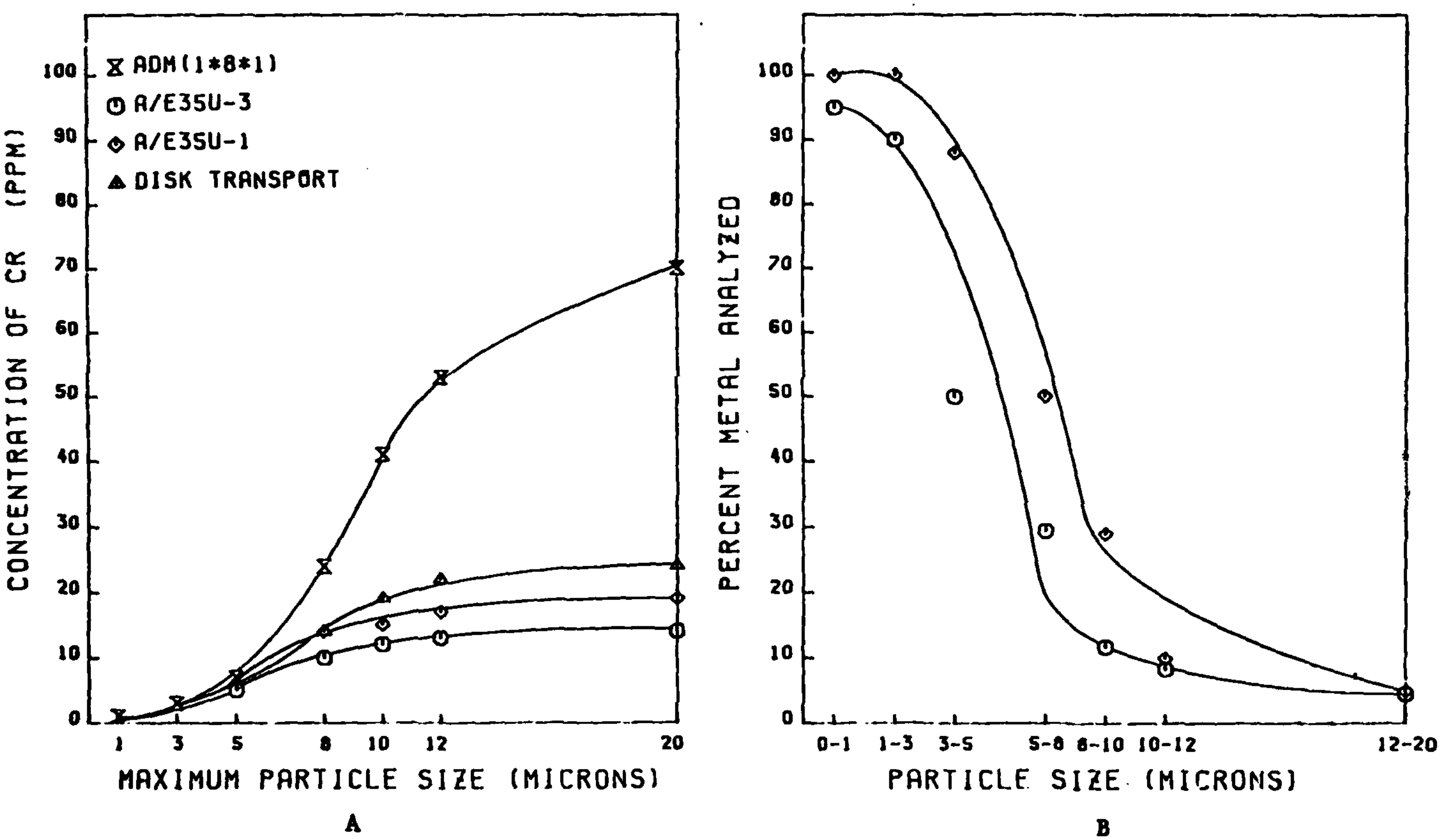

Figure A16. Spectrometric Analysis (A) and Percent Metal Analyzed (B) for Cr Powder Suspended in Mobil MIL-L-7808.

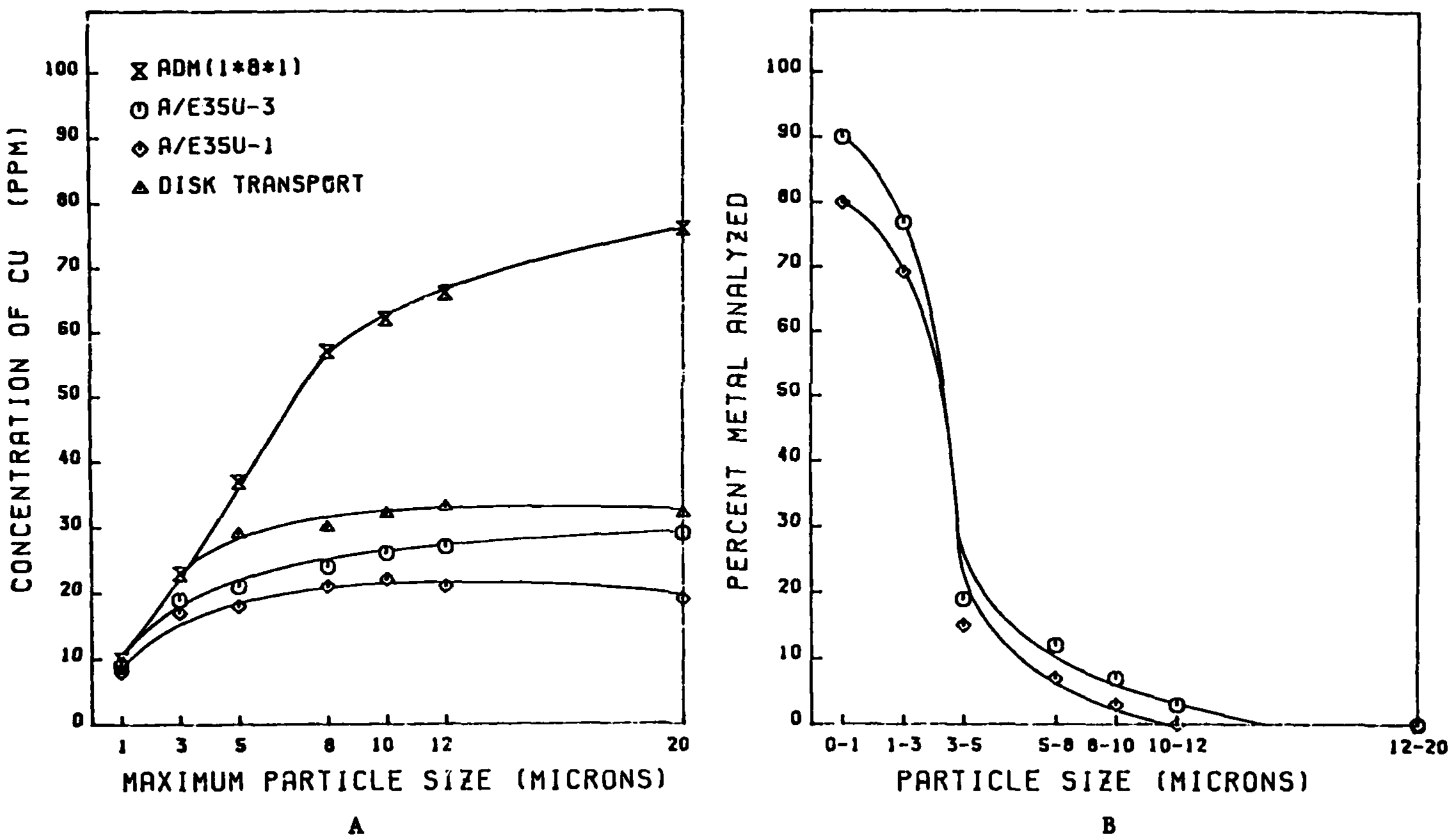

Figure A17. Spectrometric Analysis (A) and Percent Metal Analyzed (B) for Cu Powder Suspended in Mobil MIL-L-7808.

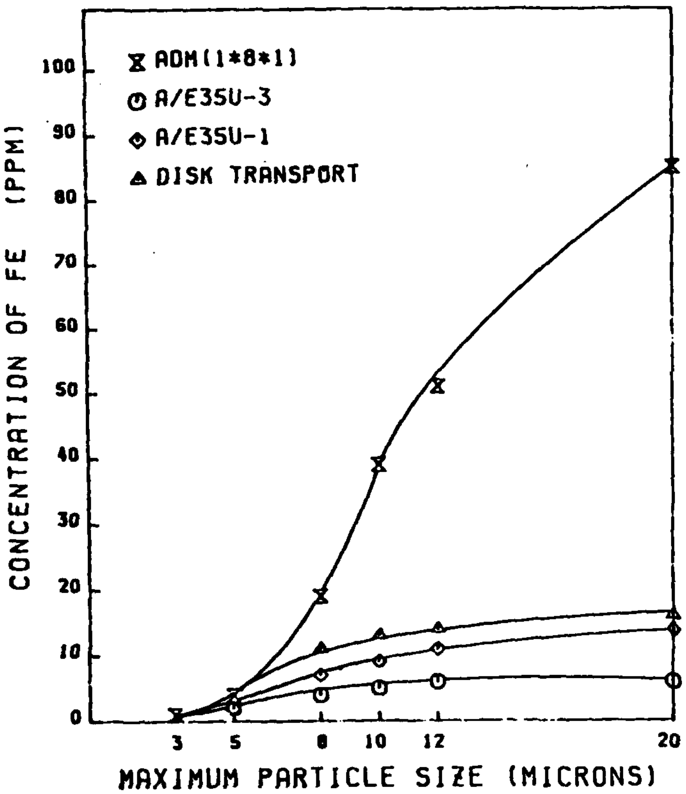

A

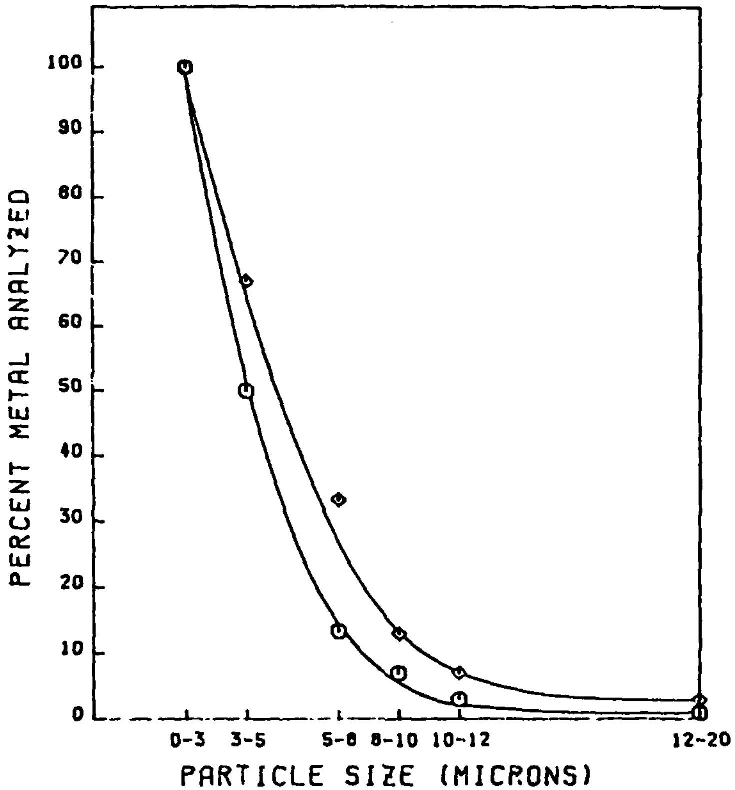

B

Figure A18. Spectrometric Analysis (A) and Percent Metal Analyzed (B) for Fe-AEE Powder Suspended in Mobil MIL-L-7808.

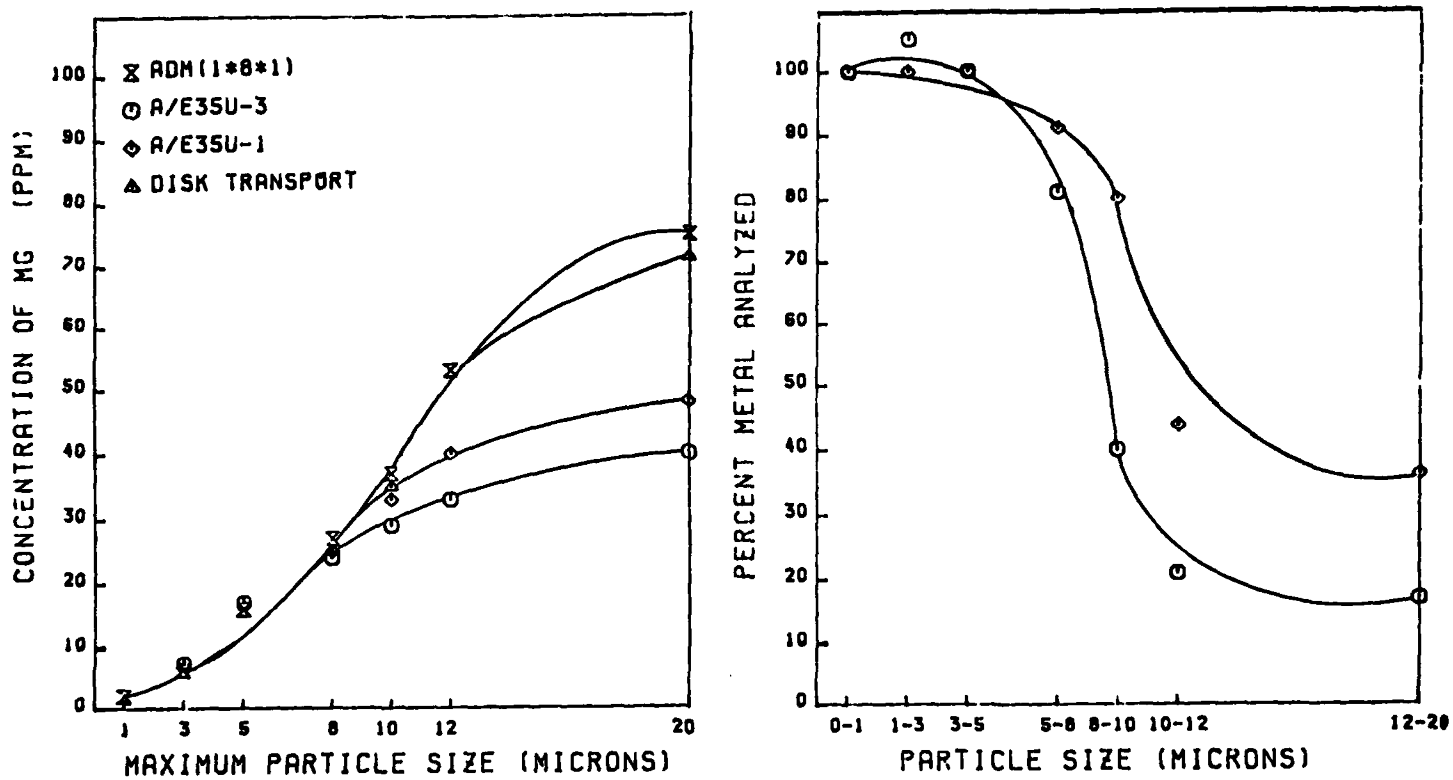

A

B

Figure A19. Spectrometric Analysis (A) and Percent Metal Analyzed (B) for Mg Powder Suspended in Mobil MIL-L-7808.

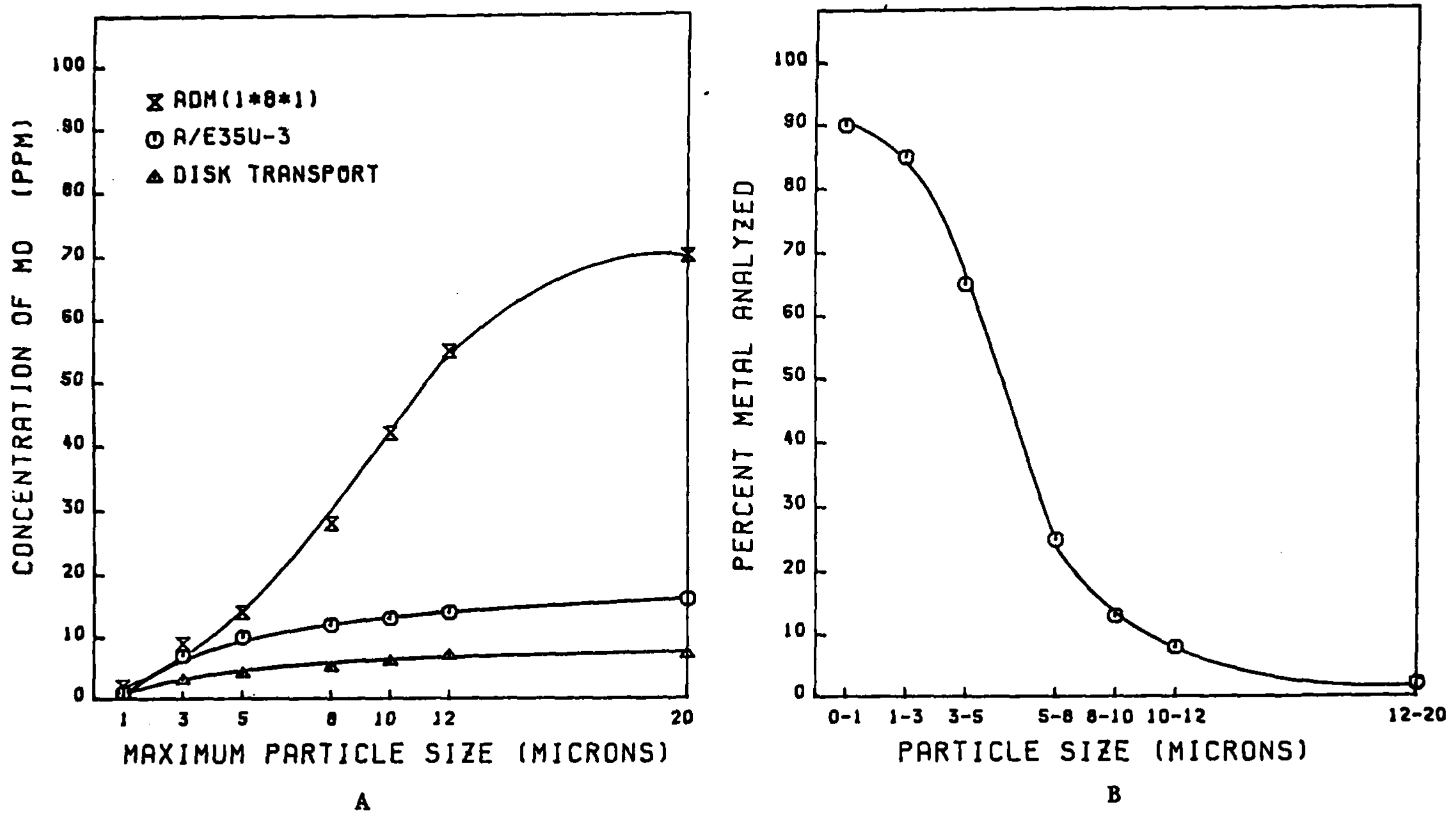

Figure A20. Spectrometric Analysis (A) and Percent Metal Analyzed (B) for Mo Powder Suspended in Mobil MIL-L-7808.

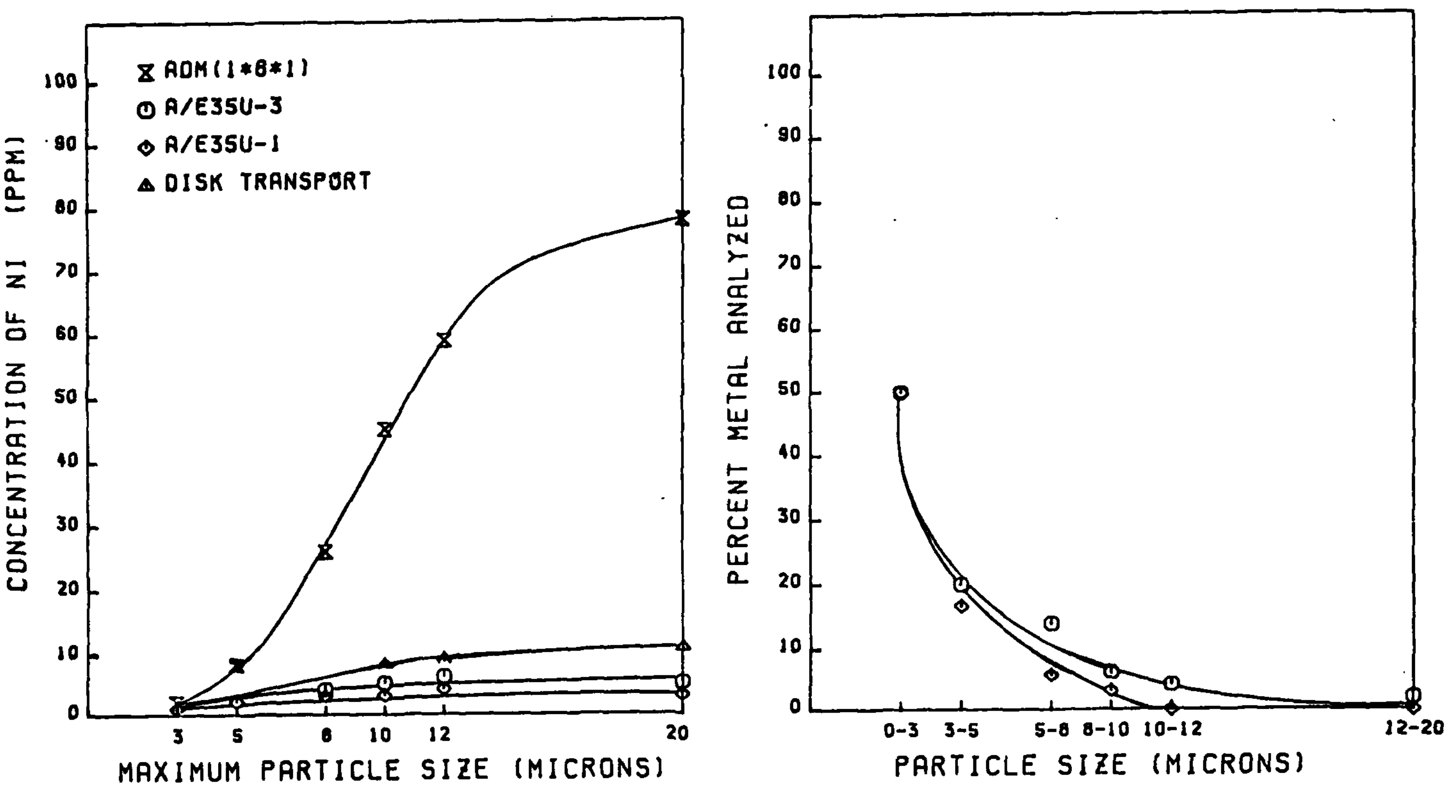

A B

Figure A21. Spectrometric Analysis (A) and Percent Metal Analyzed (B) for Ni Powder Suspended in Mobil MIL-L-7808.

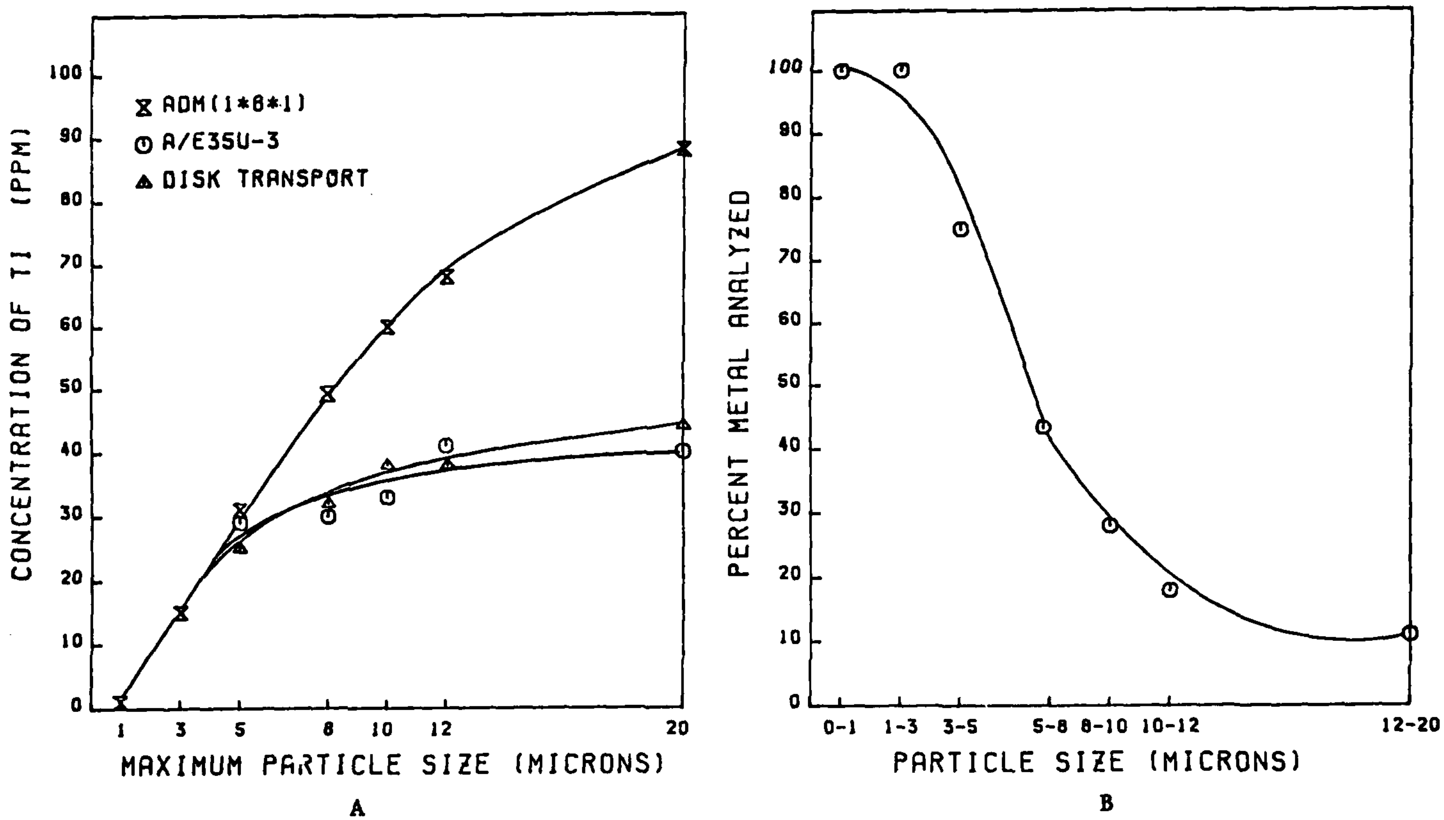

Figure A22. Spectrometric Analysis (A) and Percent Metal Analyzed (B) for Ti Powder Suspended in Mobil MIL-L-7808.

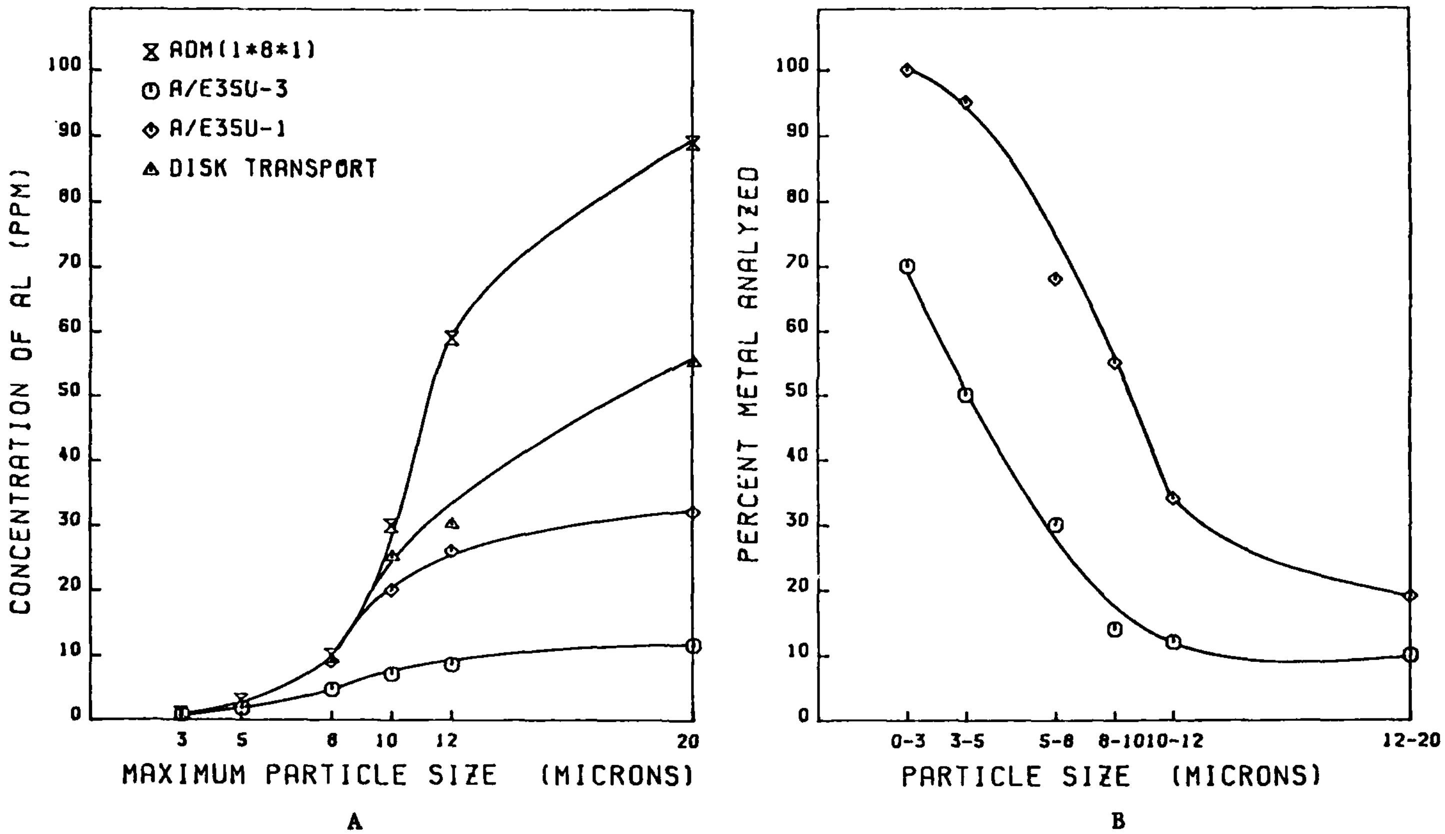

Figure A23. Spectrometric Analysis (A) and Percent Metal Analyzed (B) for Al Powder Suspended in Humble MIL-L-7808.

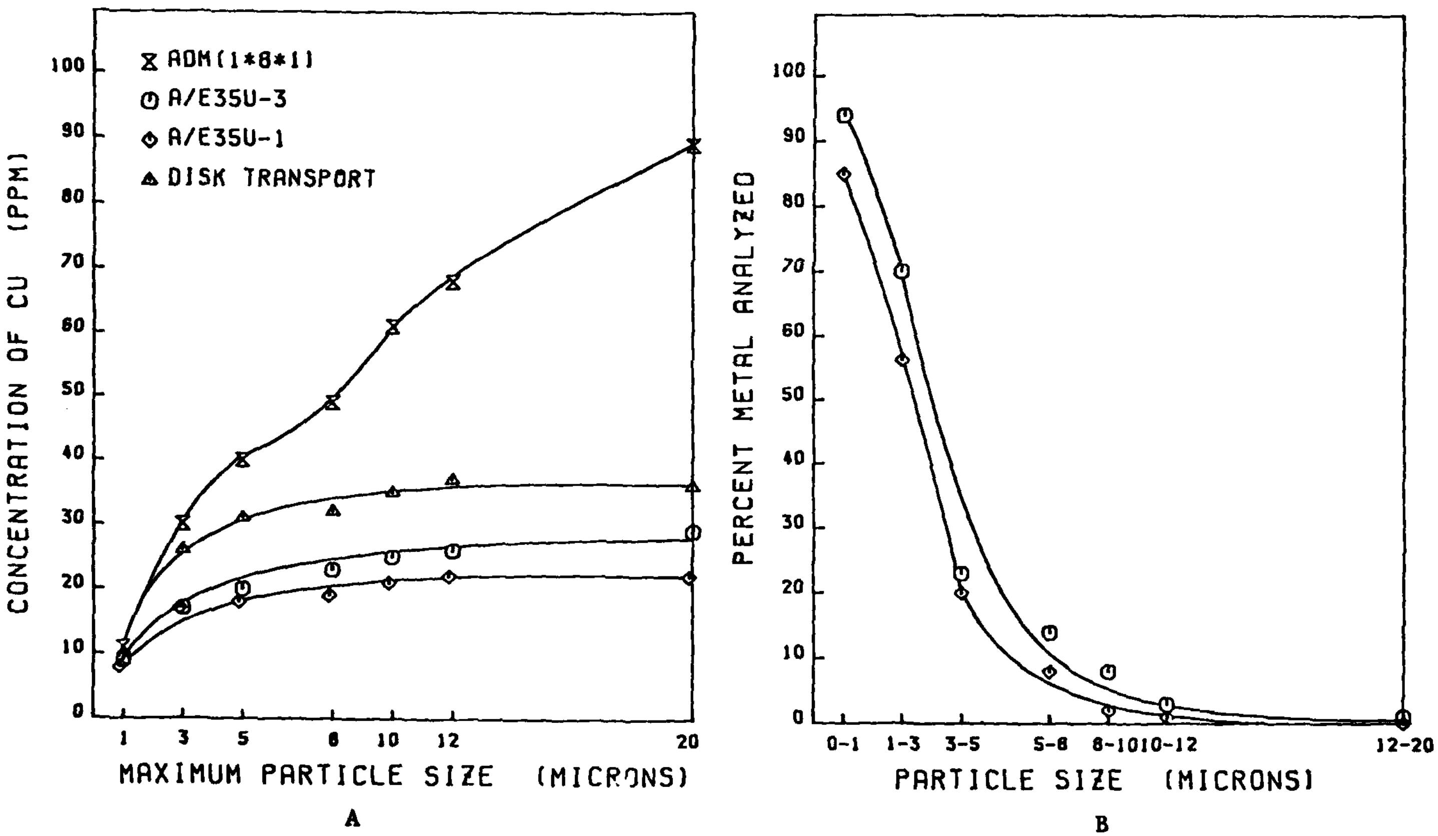

Figure A24. Spectrometric Analysis (A) and Percent Metal Analyzed (B) for Cu Powder Suspended in Humble MIL-L-7808.

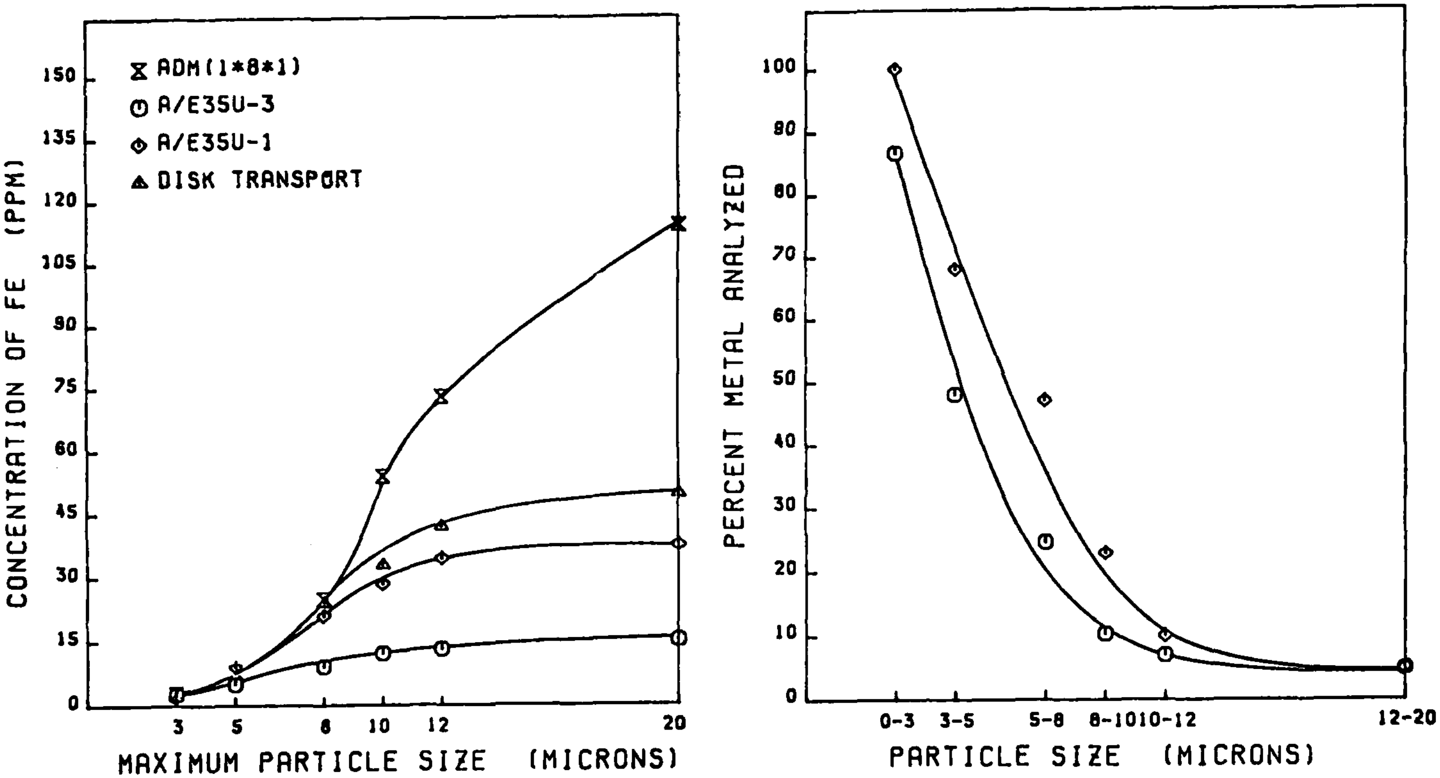

A

B

Figure A25. Spectrometric Analysis (A) and Percent Metal Analyzed (B) for Fe AEE Powder Suspended in Humble MIL-L-7808.

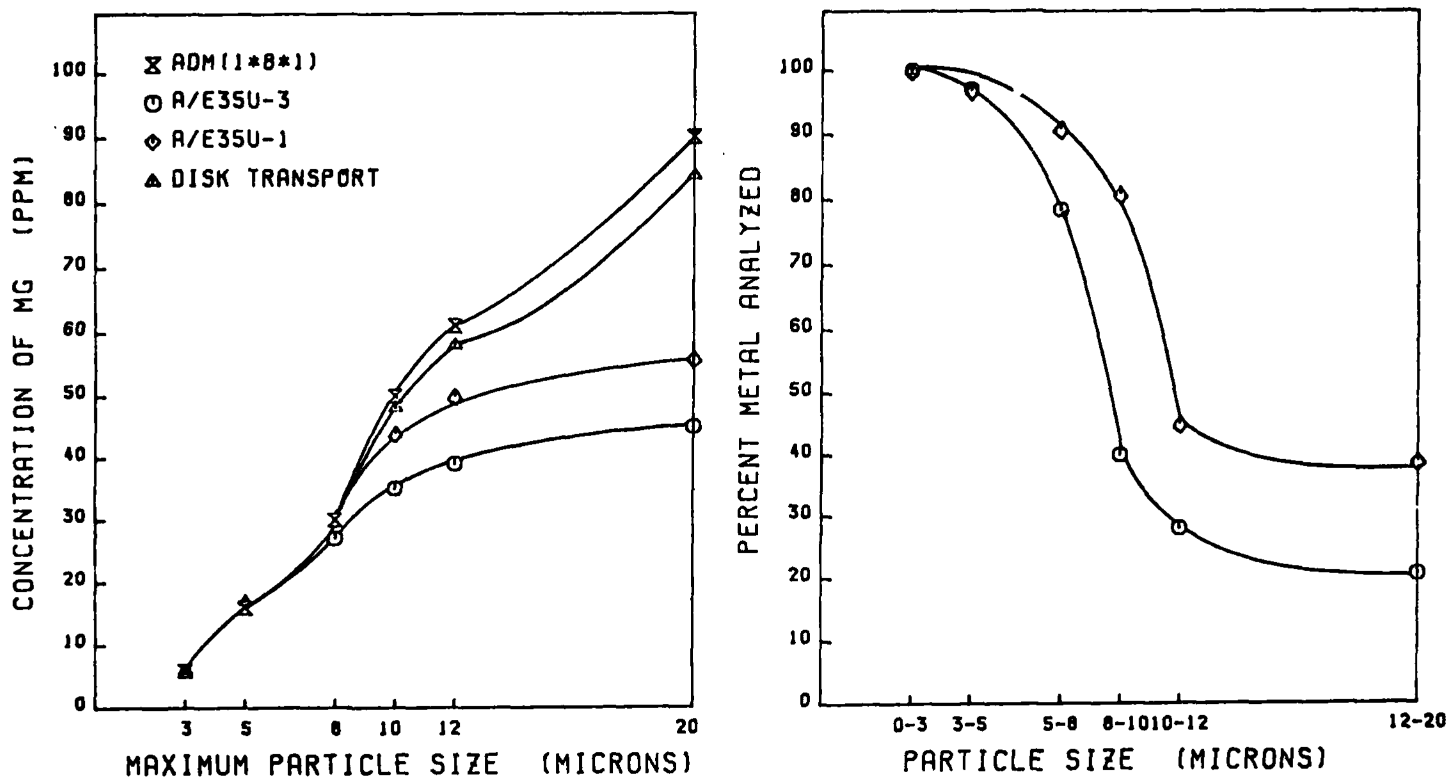

A

B

Figure A26. Spectrometric Analysis (A) and Percent Metal Analyzed (B) for Mg Powder Suspended in Humble MIL-L-7808.

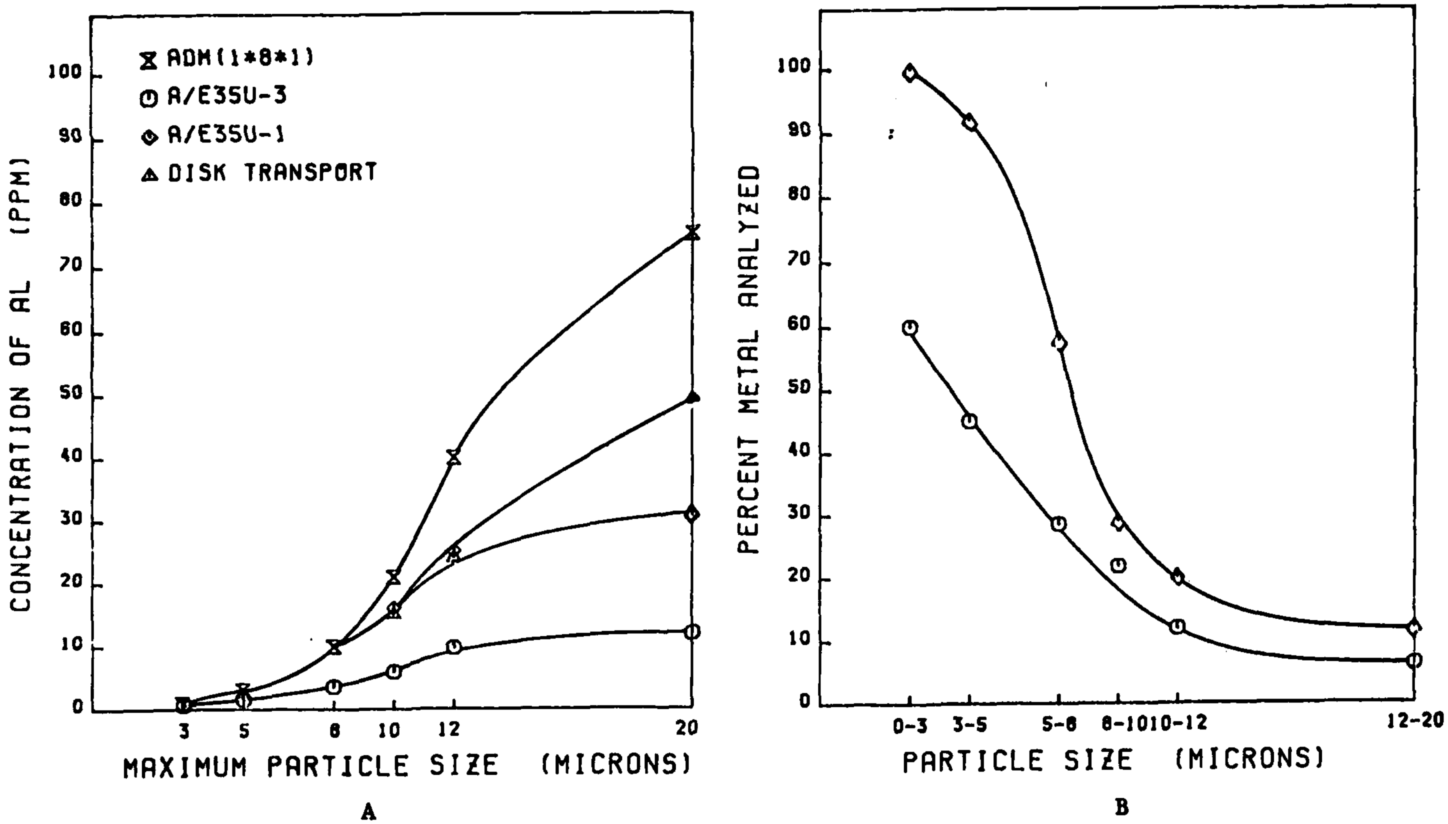

Figure A27. Spectrometric Analysis (A) and Percent Metal Analyzed (B) for Al Powder Suspended in Di-2-Ethylhexyl Azelate.

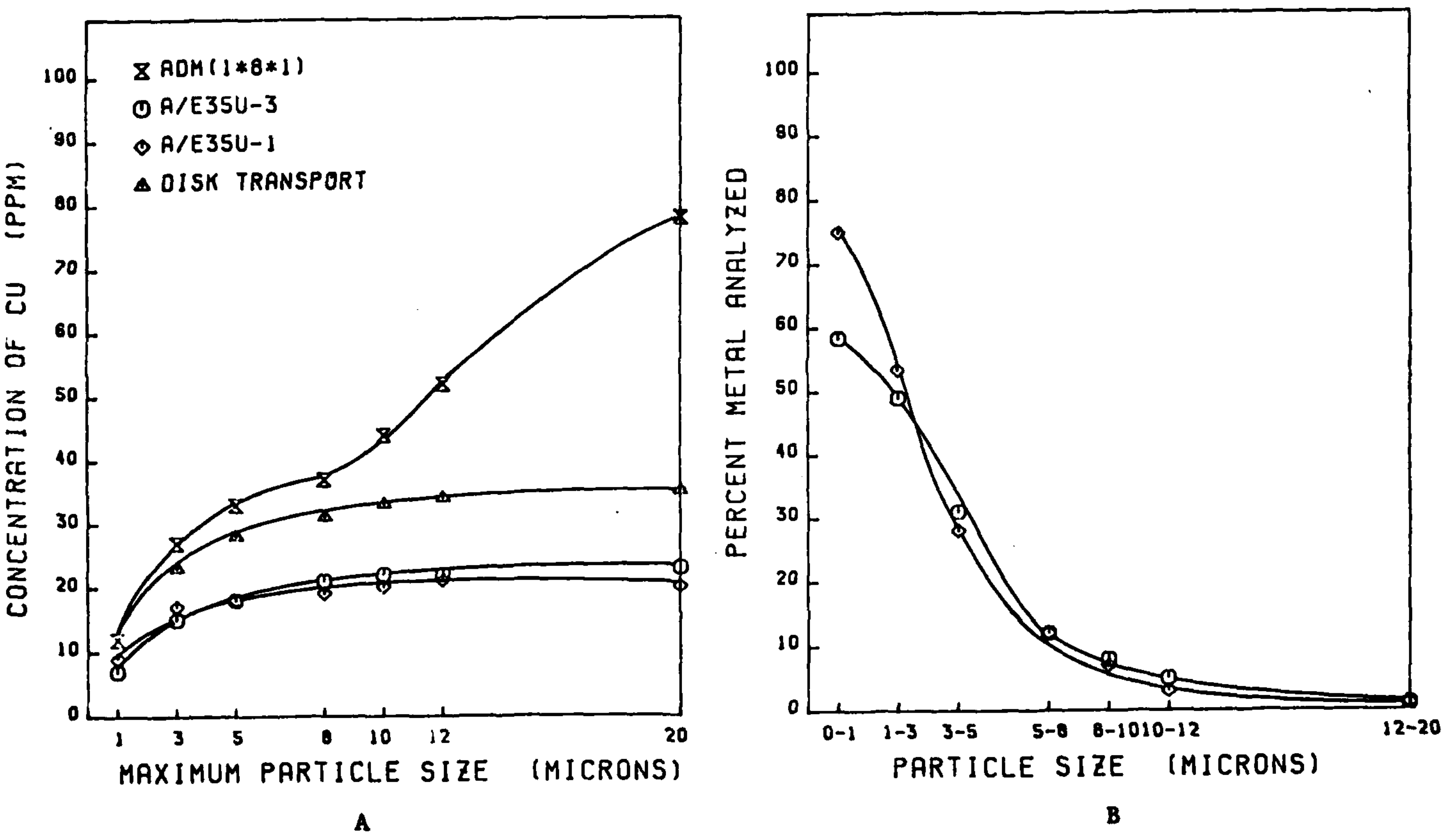

Figure A28. Spectrometric Analysis (A) and Percent Metal Analyzed (B) for Cu Powder Suspended in Di-2-Ethylhexyl Azelate.

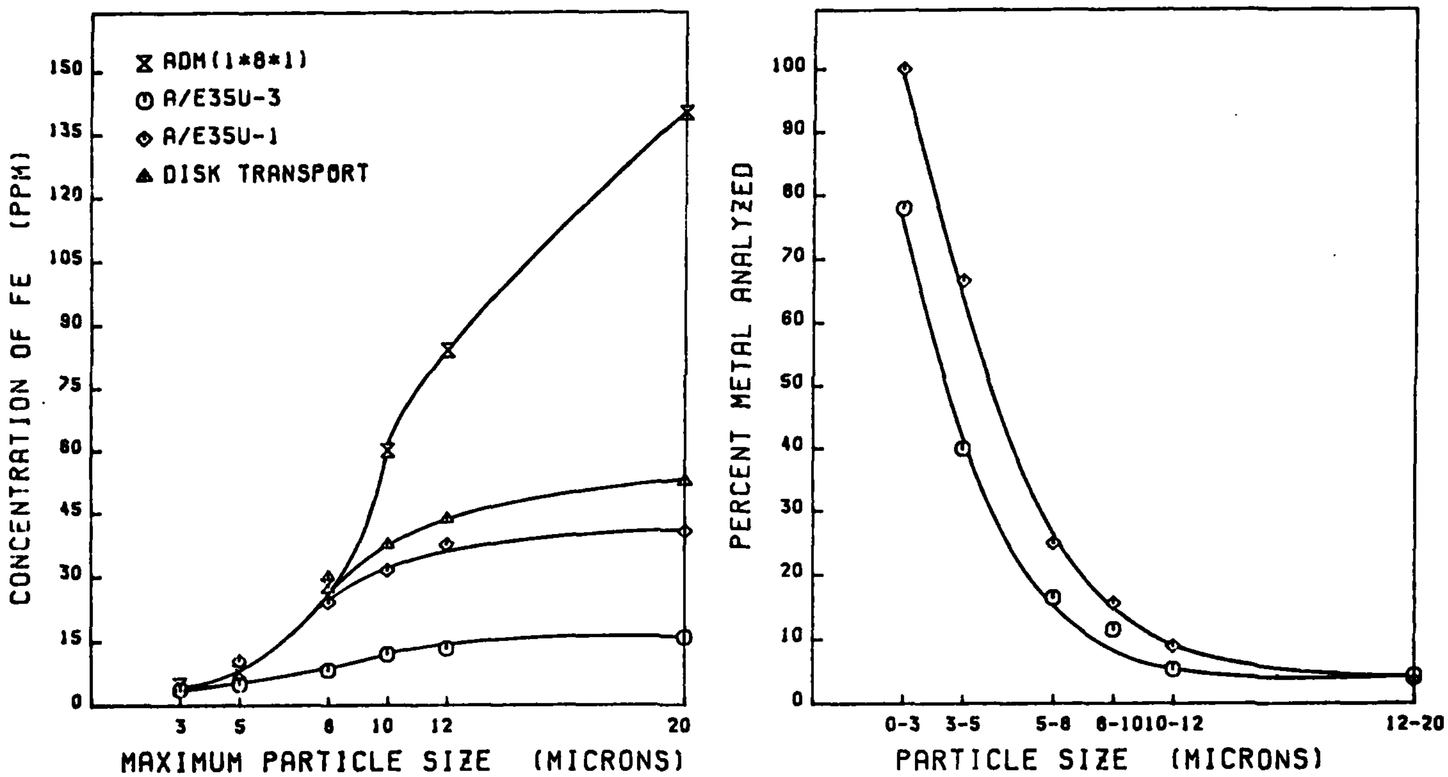

A

B

Figure A29. Spectrometric Analysis (A) and Percent Metal Analyzed (B) for Fe-AEE Powder Suspended in Di-2-Ethylhexyl Azelate.

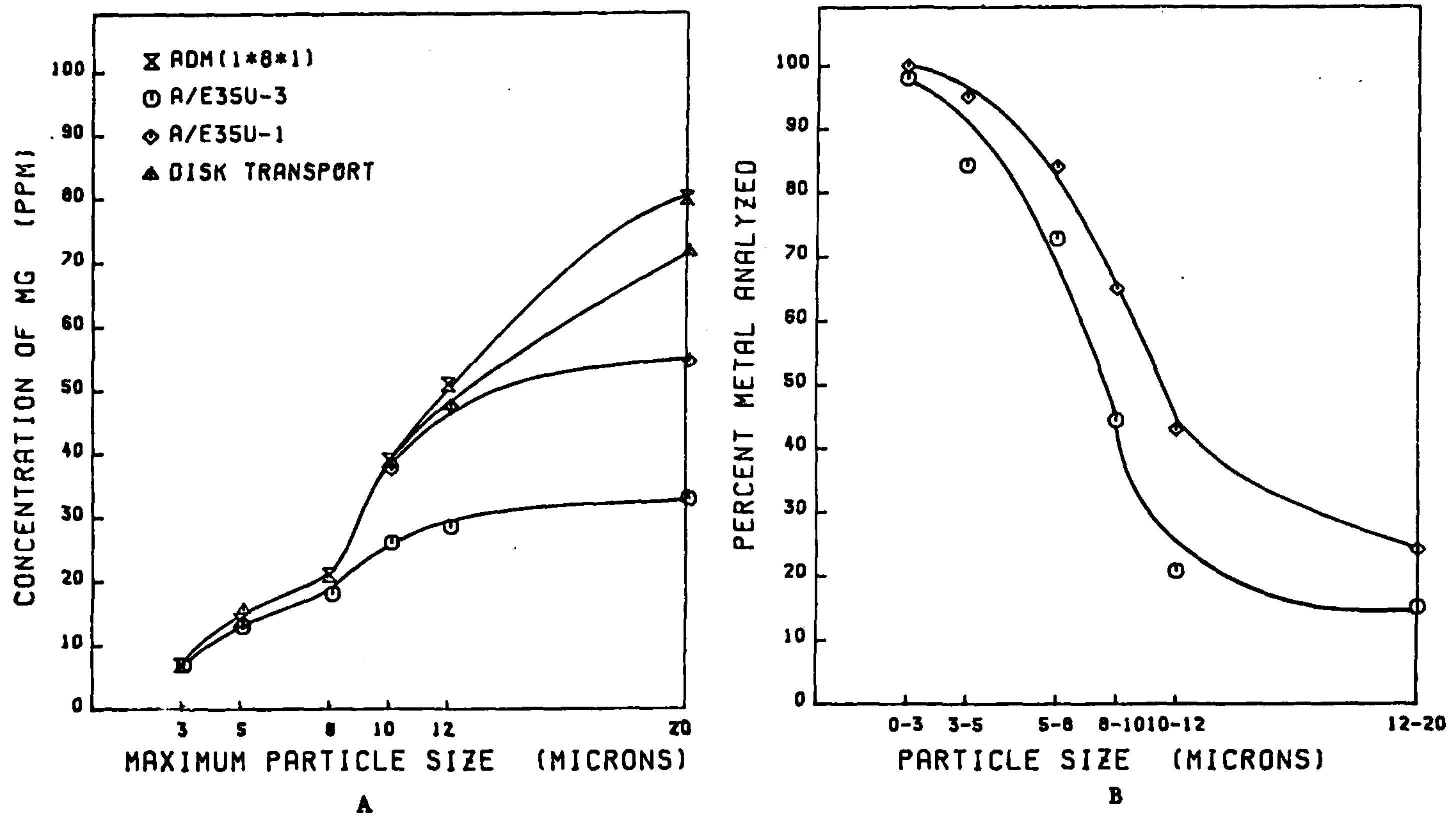

Figure A30. Spectrometric Analysis (A) and Percent Metal Analyzed (B) for Mg Powder Suspended in Di-2-Ethylhexyl Azelate.

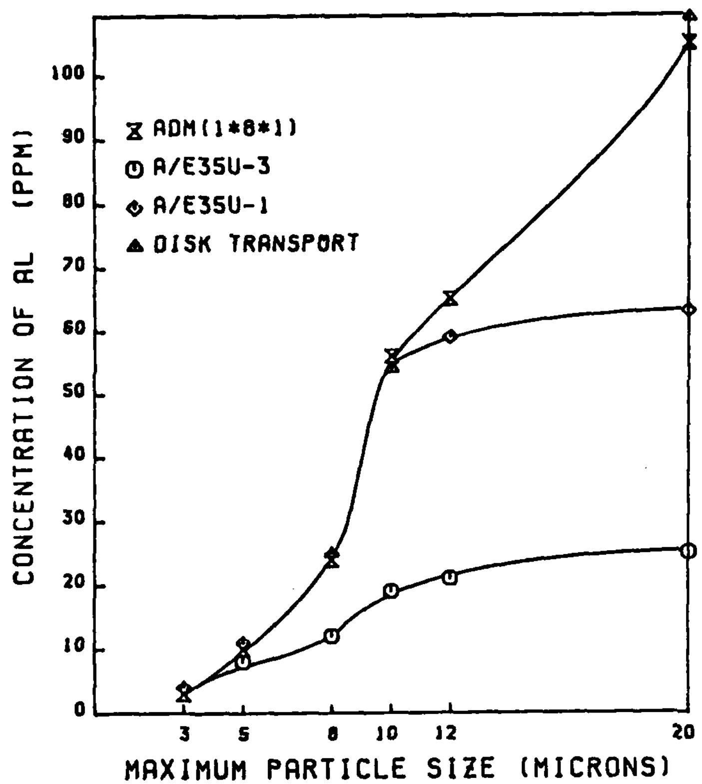

A

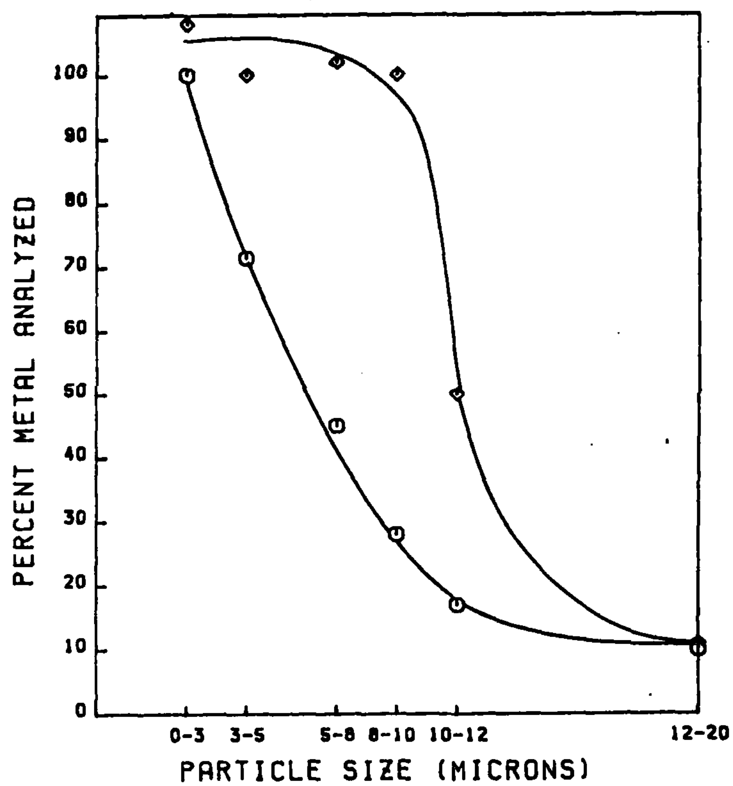

B

Figure A31. Spectrometric Analysis (A) and Percent Metal Analyzed (B) for Al Powder Suspended in Conostan 245.

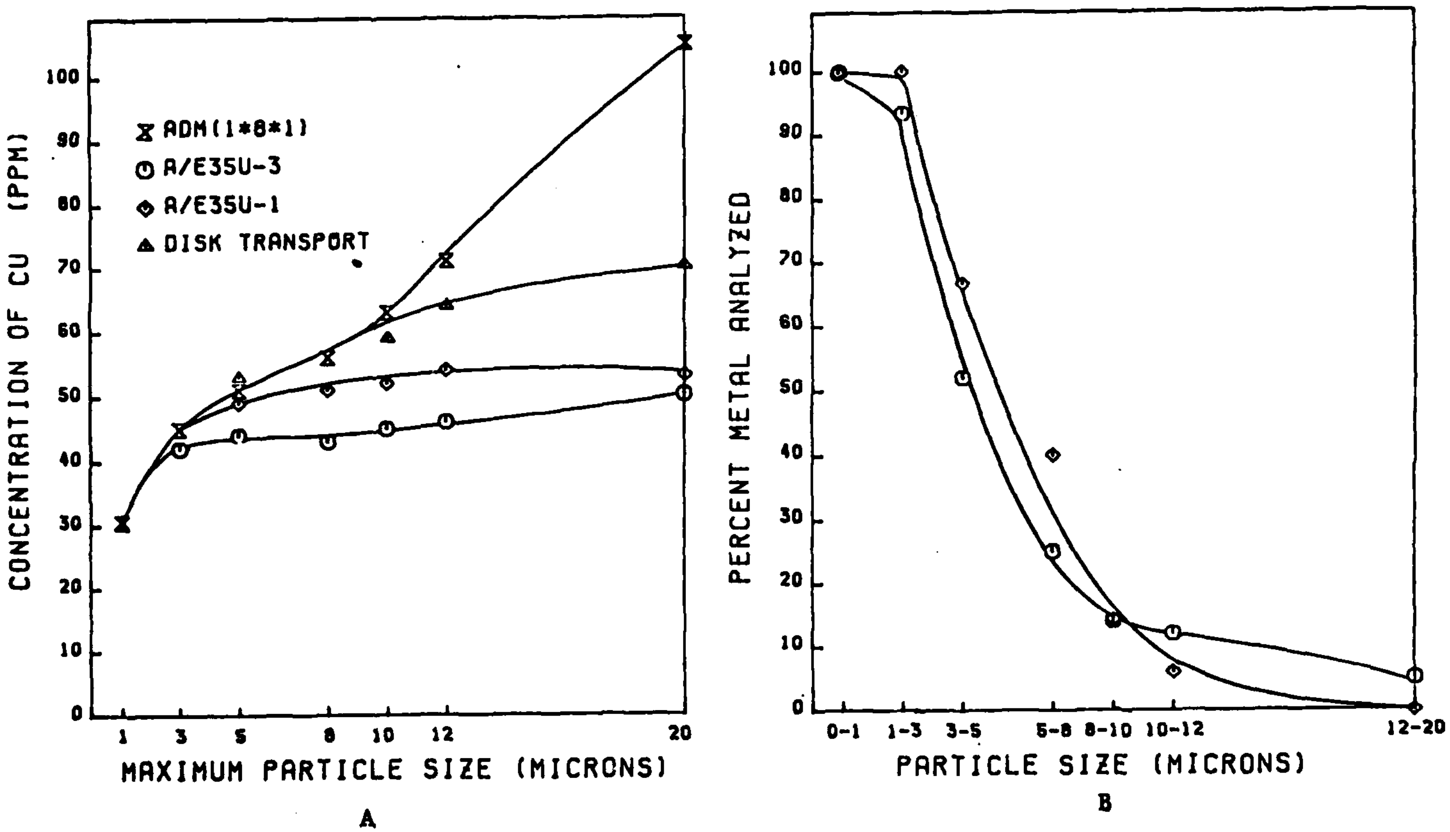

Figure A32. Spe trometric Analysis (A) and Percent Metal Analyzed (B) for Cu Powder Suspended in Conostan 245.

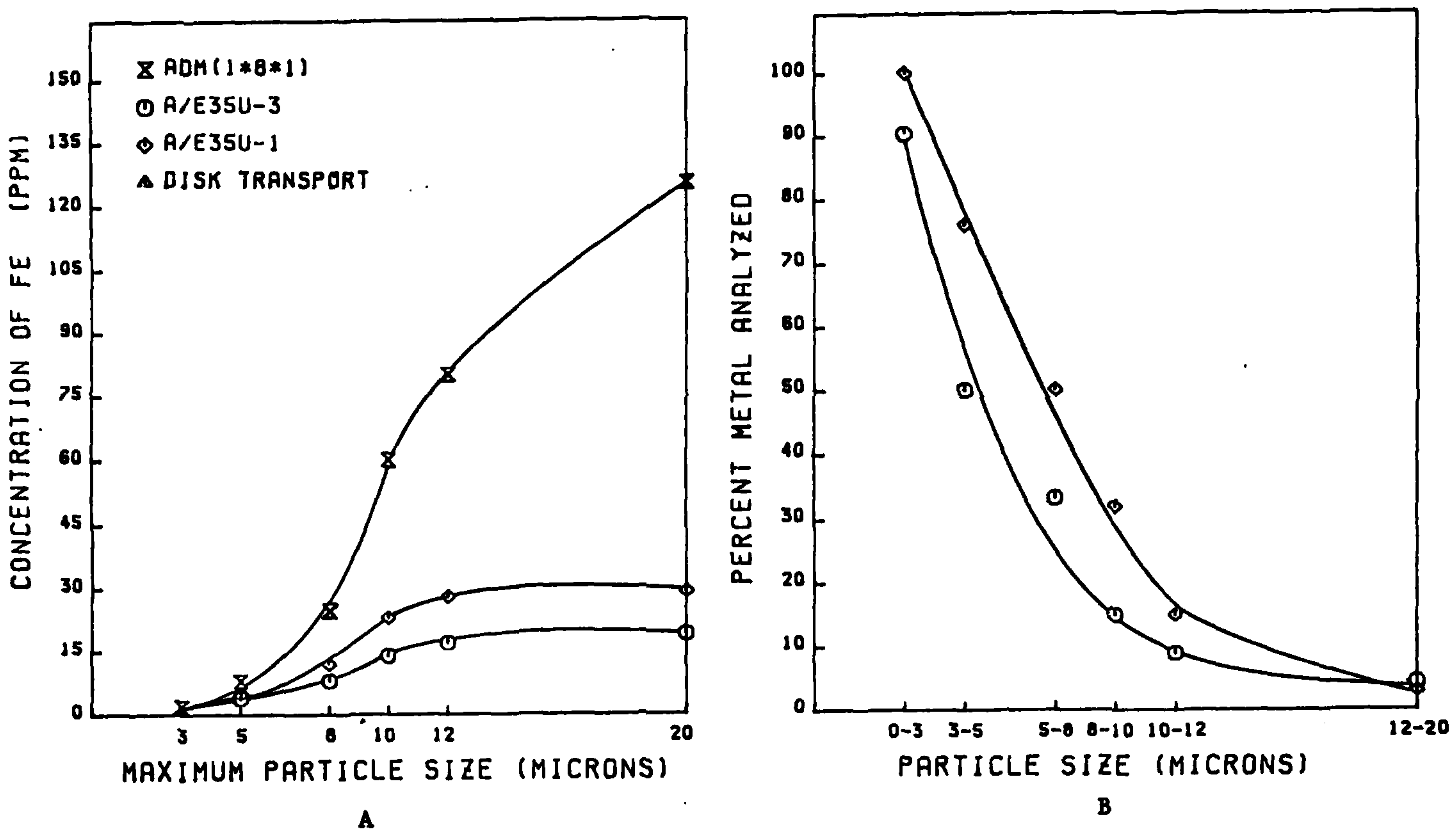

Figure A33. Spectrometric Analysis (A) and Percent Metal Analyzed (B) for Fe-AEE Powder Suspended in Conostan 245.

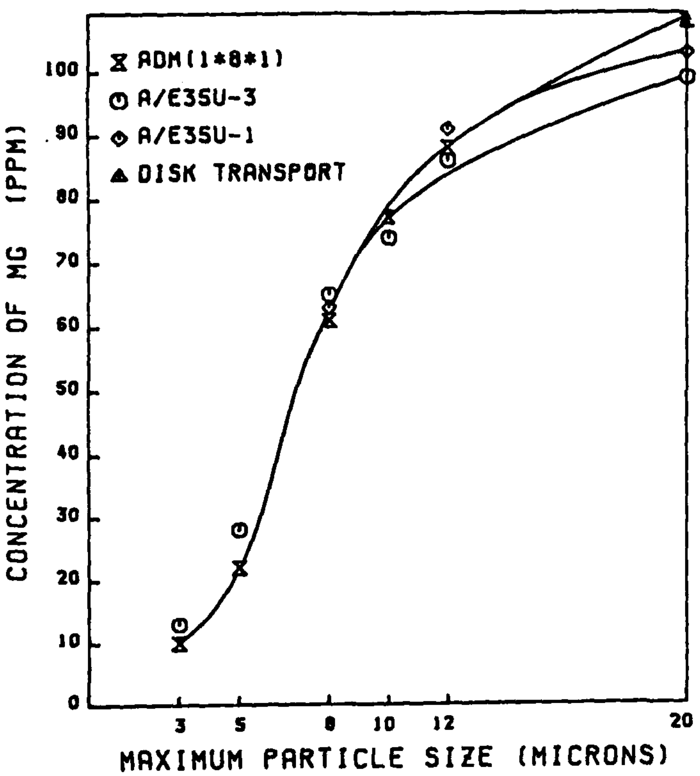

A

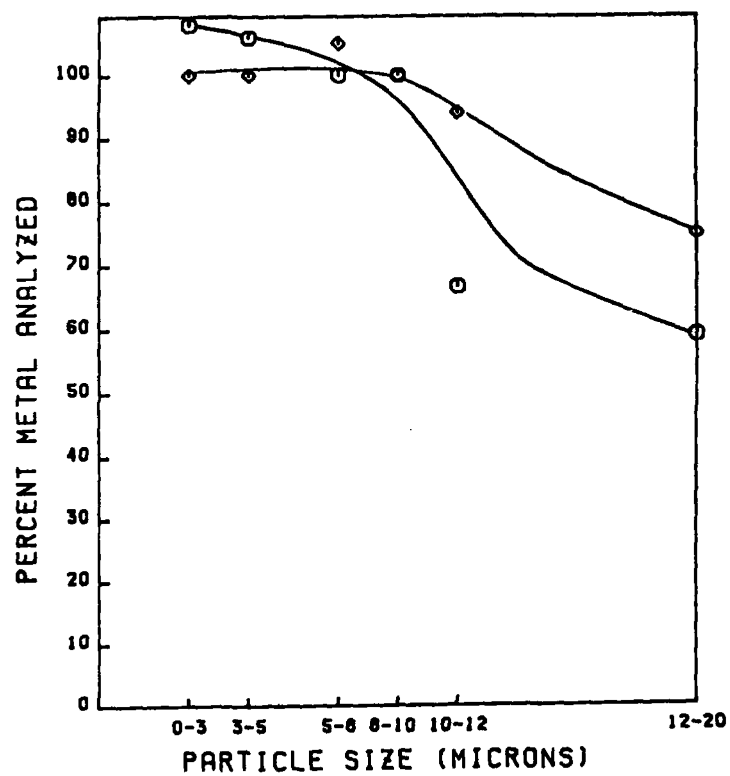

B

Figure A34. Spectrometric Analysis (A) and Percent Metal Analyzed (B) for Mg Powder Suspended in Conostan 245.

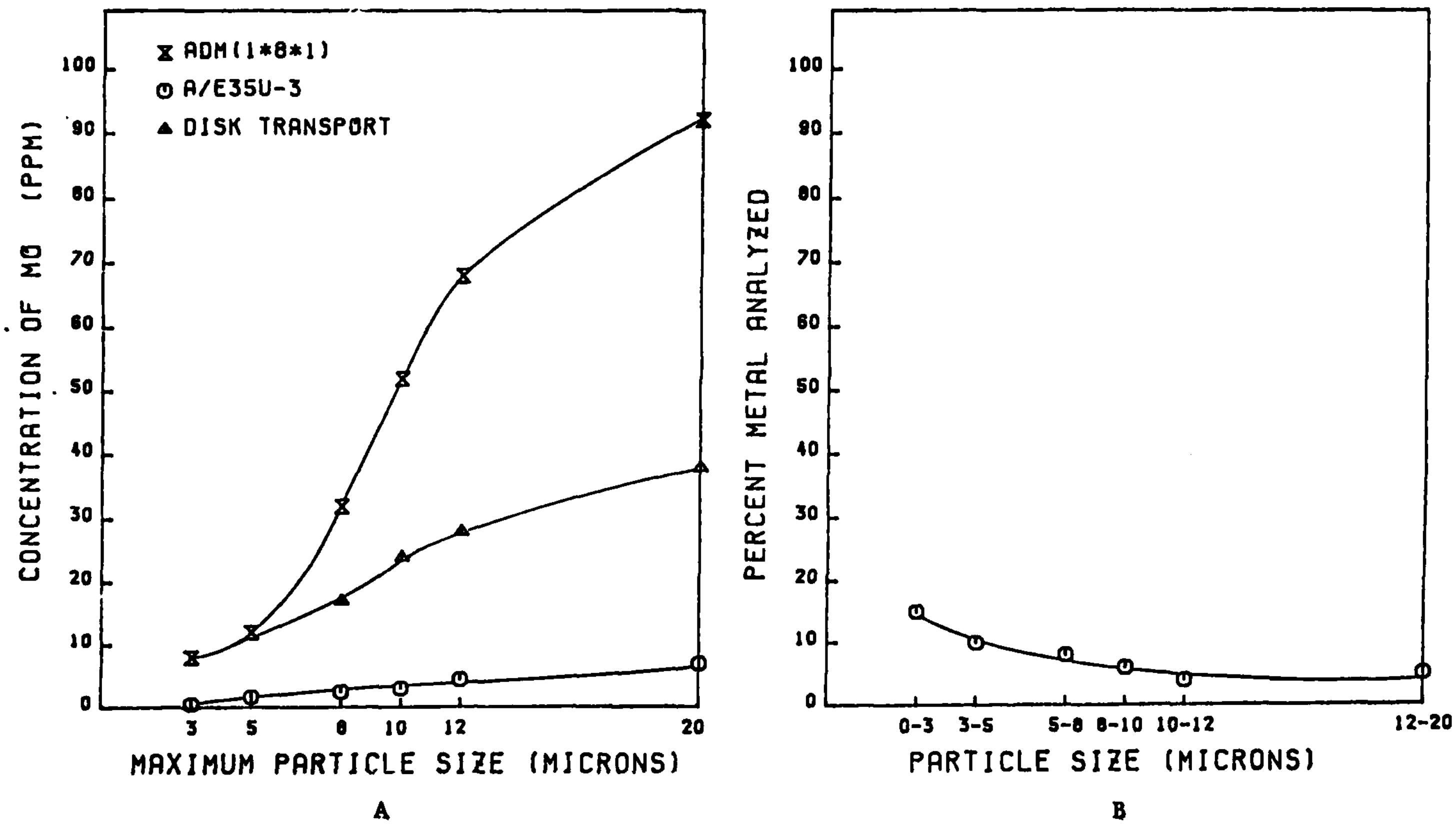

Figure A35. Spectrometric Analysis (A) and Percent Metal Analyzed (B) for Mo Powder Suspended in Conostan 245.

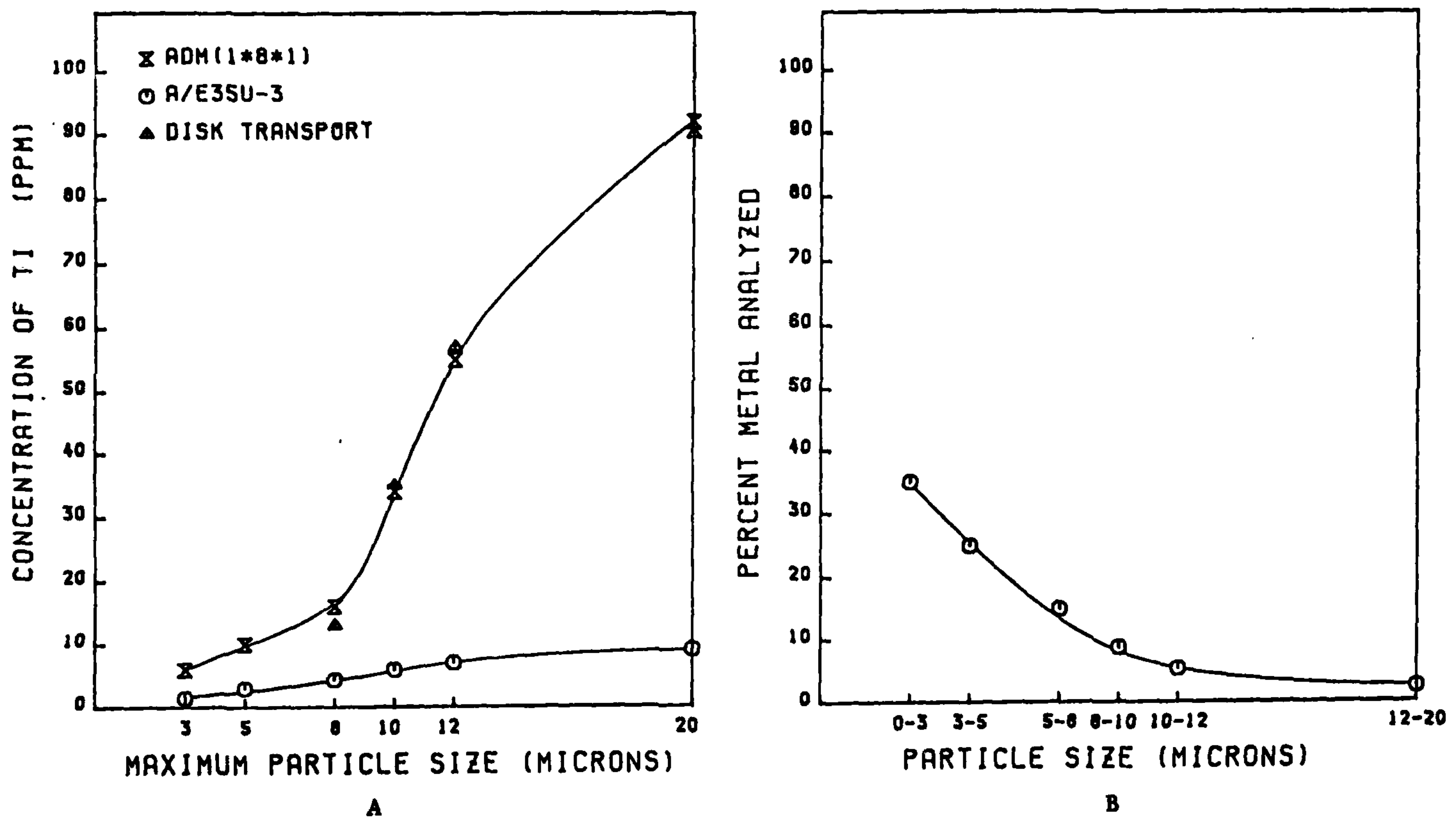

Figure A36. Spectrometric Analysis (A) and Percent Metal Analyzed (B) for Ti Powder Suspended in Conostan 245.

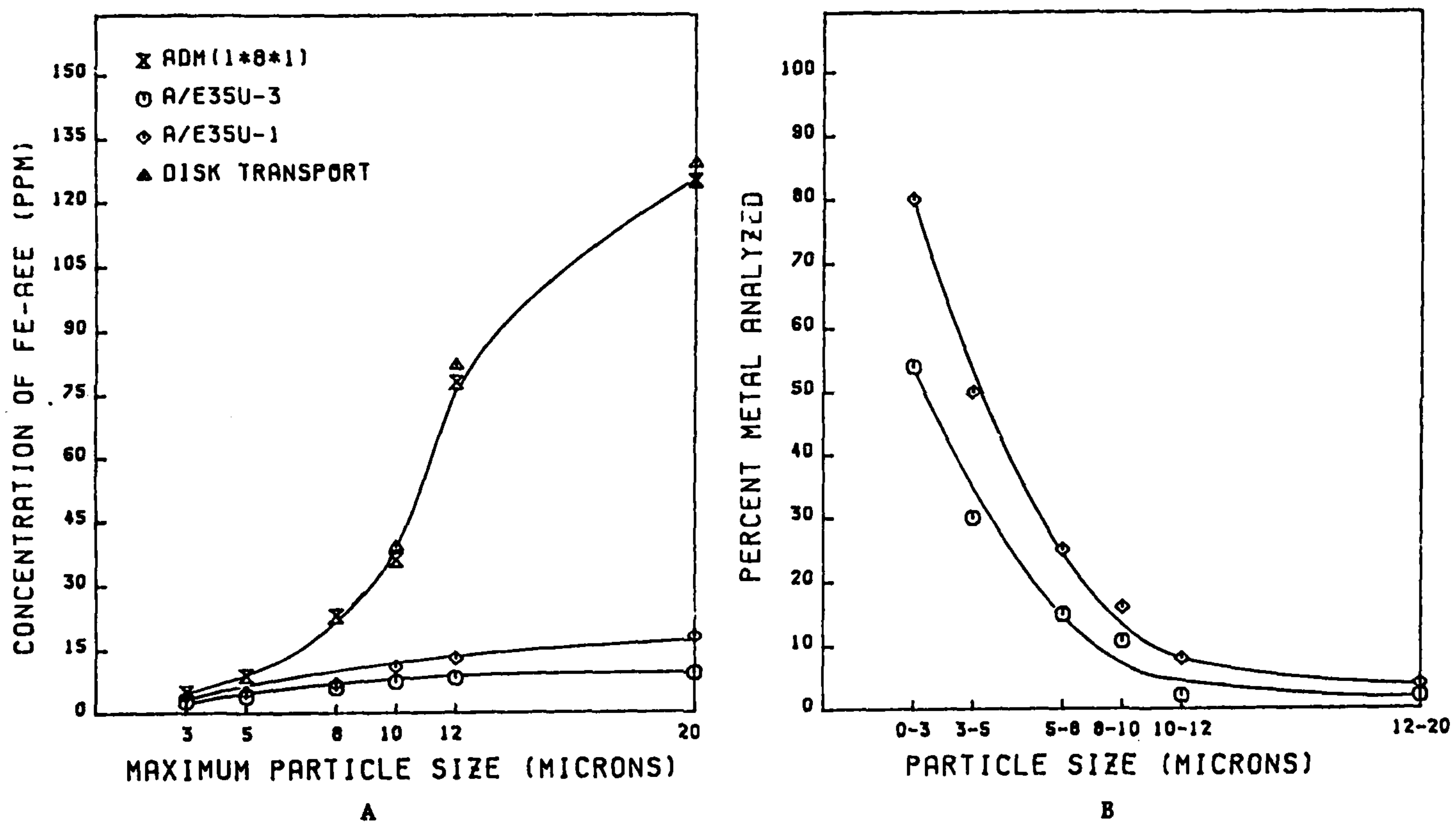

Figure A37. Spectrometric Analysis (A) and Percent Metal Analyzed (B) for Fe-AEE Powder Suspended in Conostan 245.

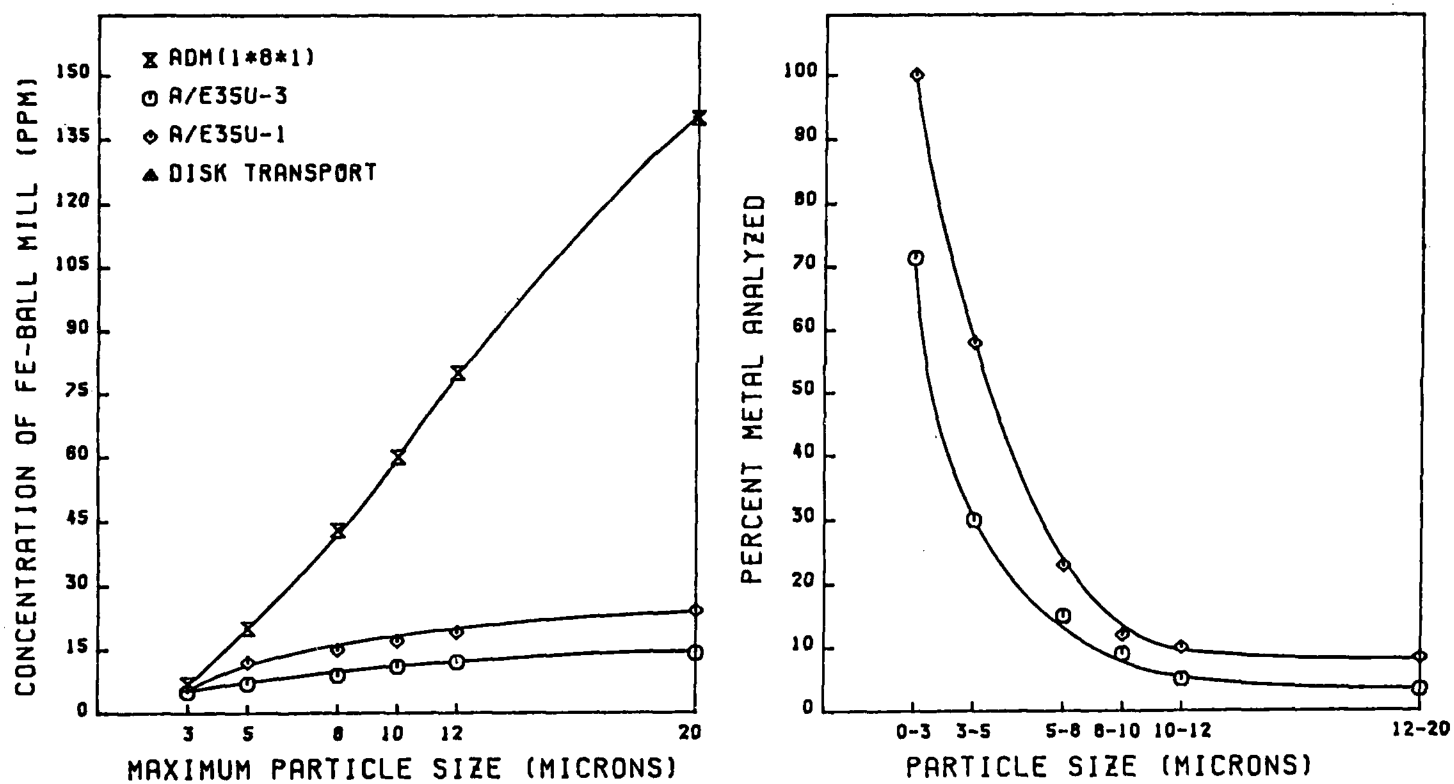

A B

Figure A38. Spectrometric Analysis (A) and Percent Metal Analyzed (B) for Fe-Ball Milled Powder Suspended in Conostan 245.

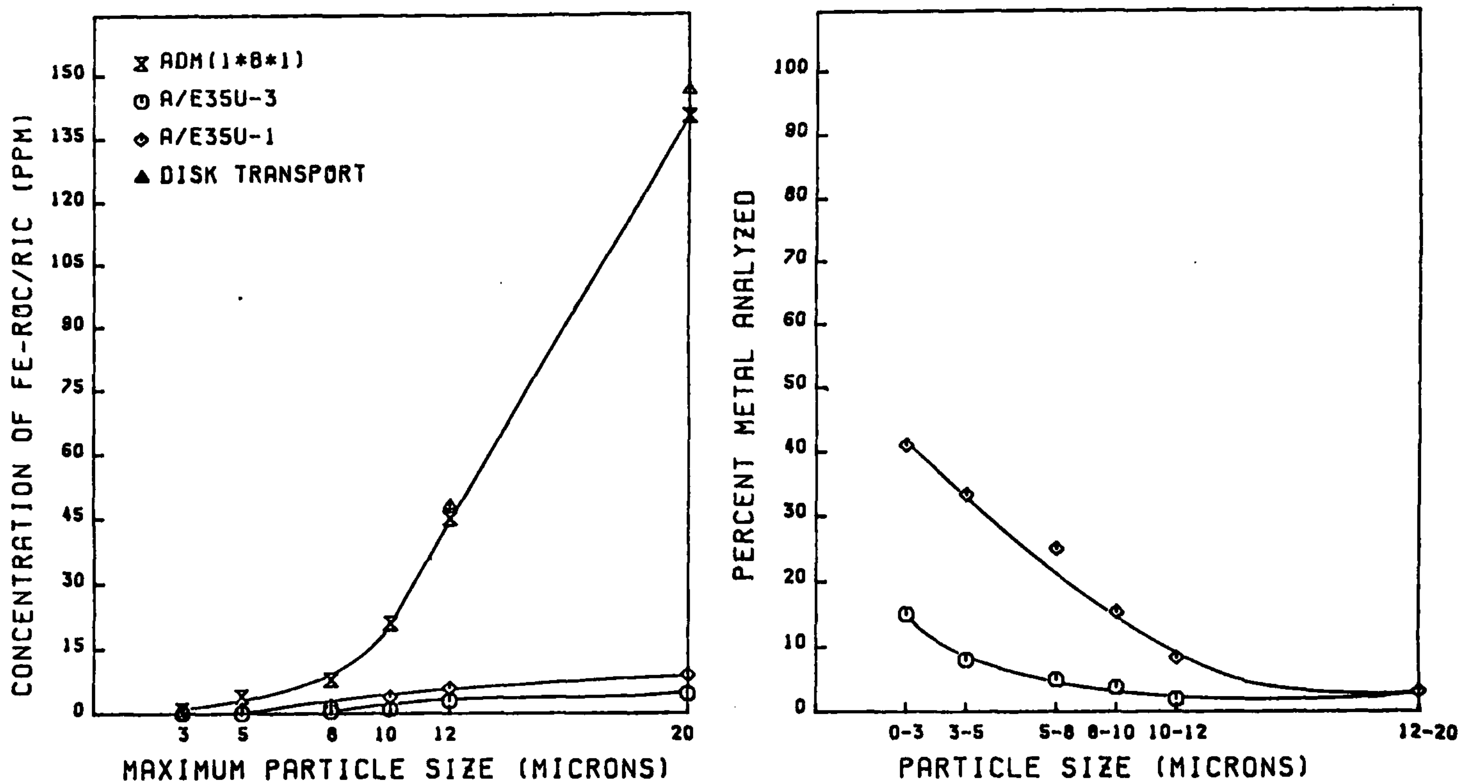

A

B

Figure A39. Spectrometric Analysis (A) and Percent Metal Analyzed (B) for Fe-ROC/RIC Powder Suspended in Conostan 245.

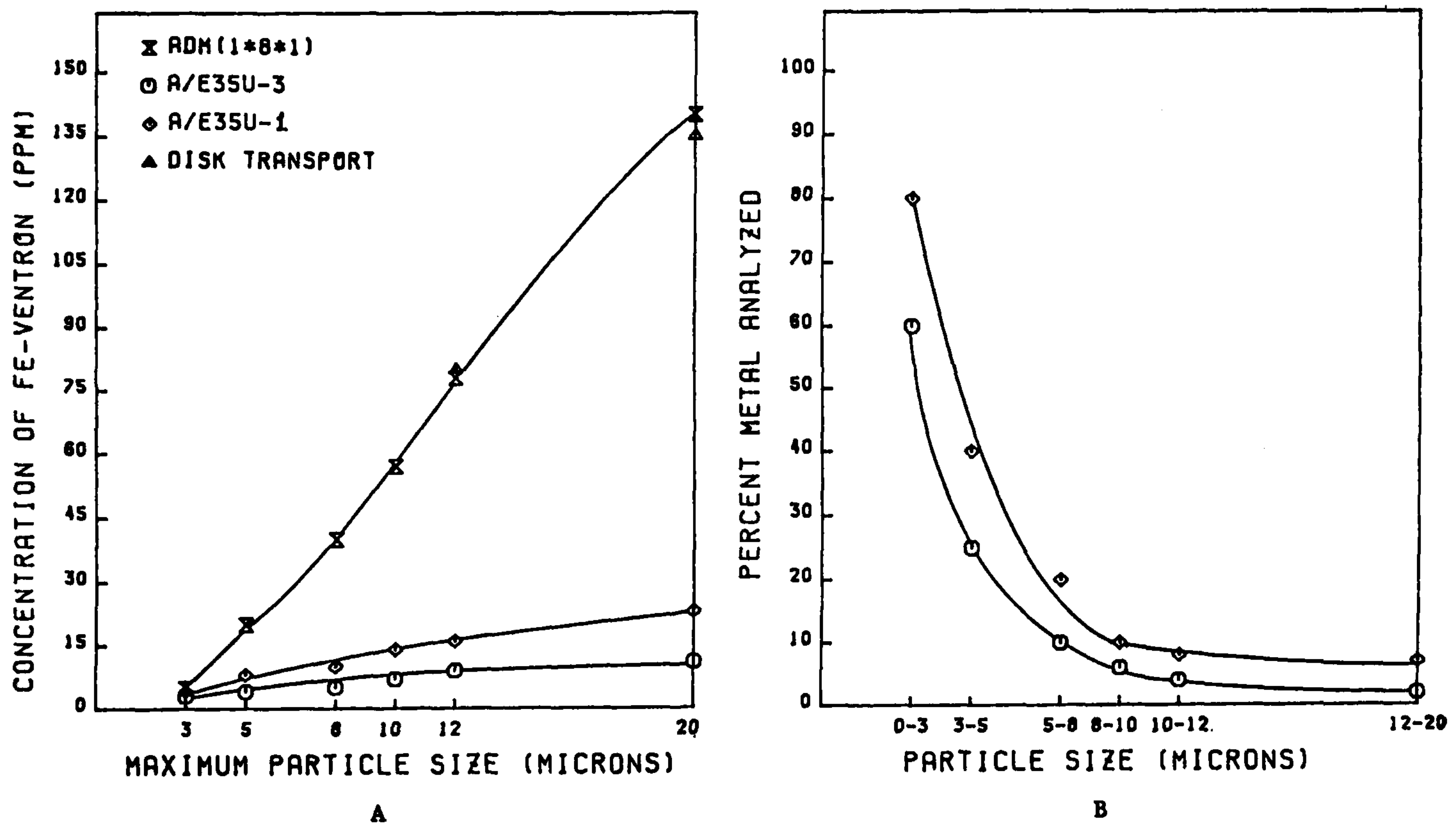

Figure A40. Spectrometric Analysis (A) and Percent Metal Analyzed (B) for Fe-Ventron Powder Suspended in Conostan 245.

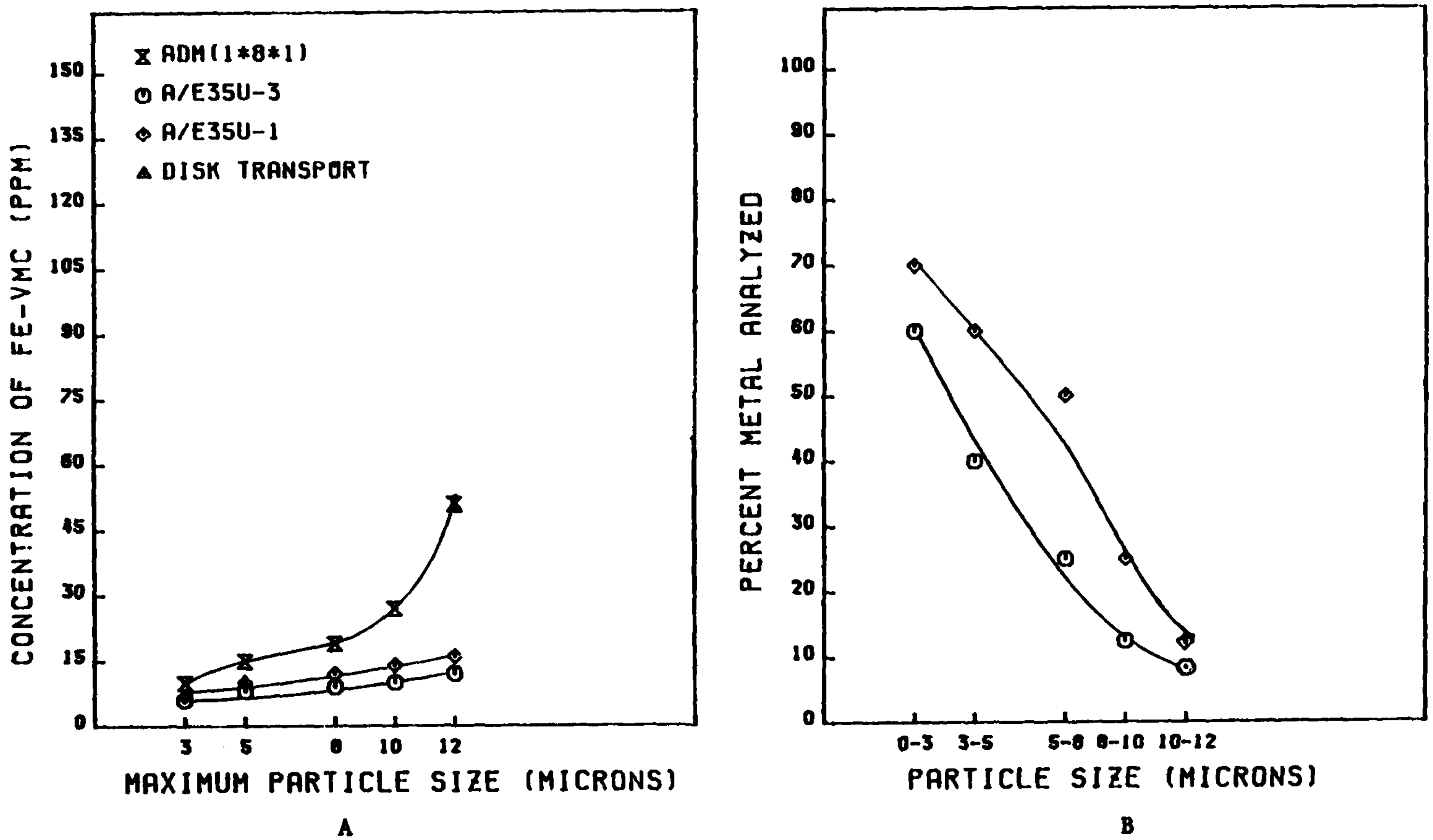

Figure A41. Spectrometric Analysis (A) and Percent Metal Analyzed (B) for Fe-VMC Powder Suspended in Conostan 245.

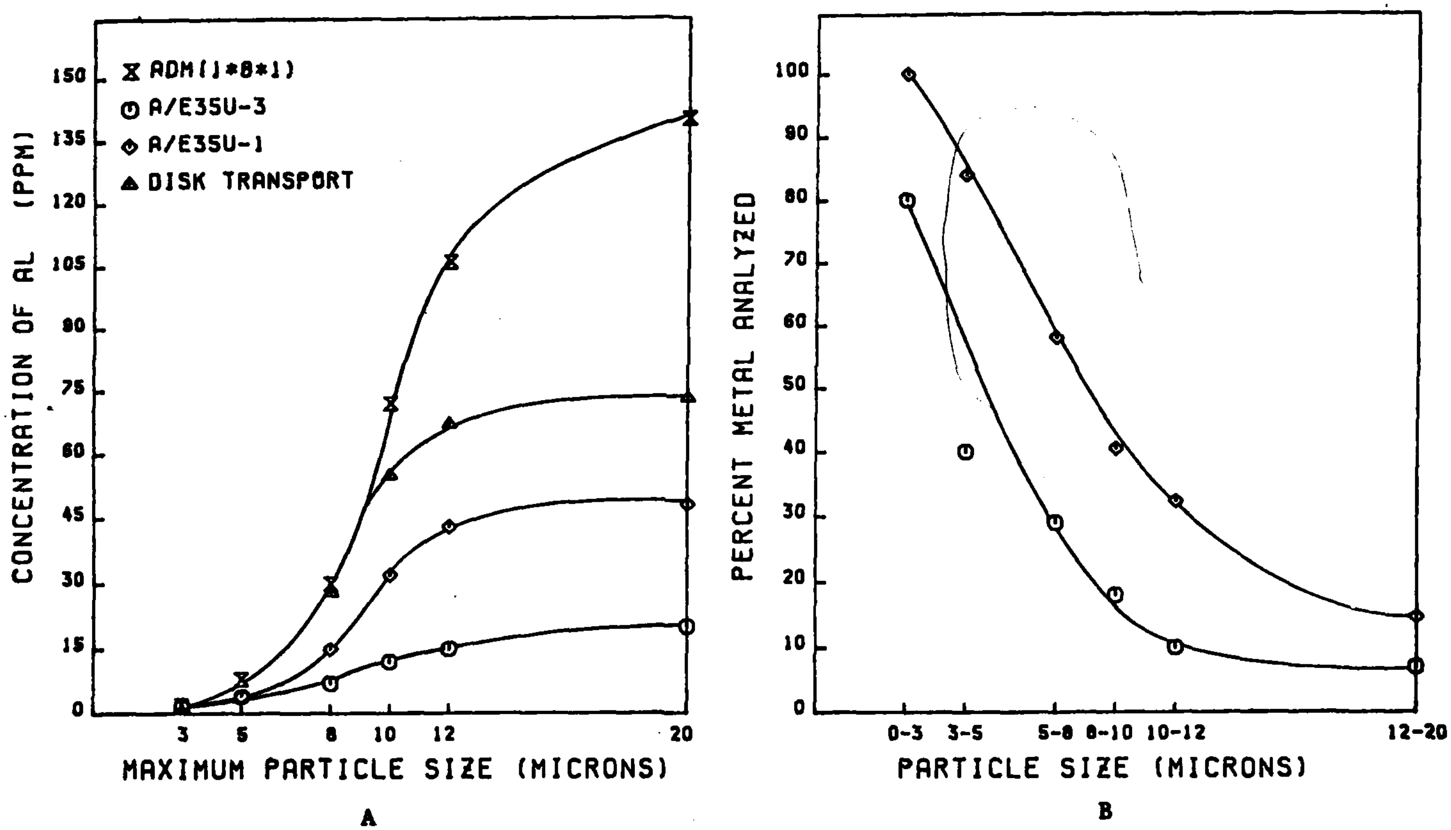

Figure A42. Spectrometric Analysis (A) and Percent Metal Analyzed (B) for Al Powder Suspended in Phillips Condor 105.

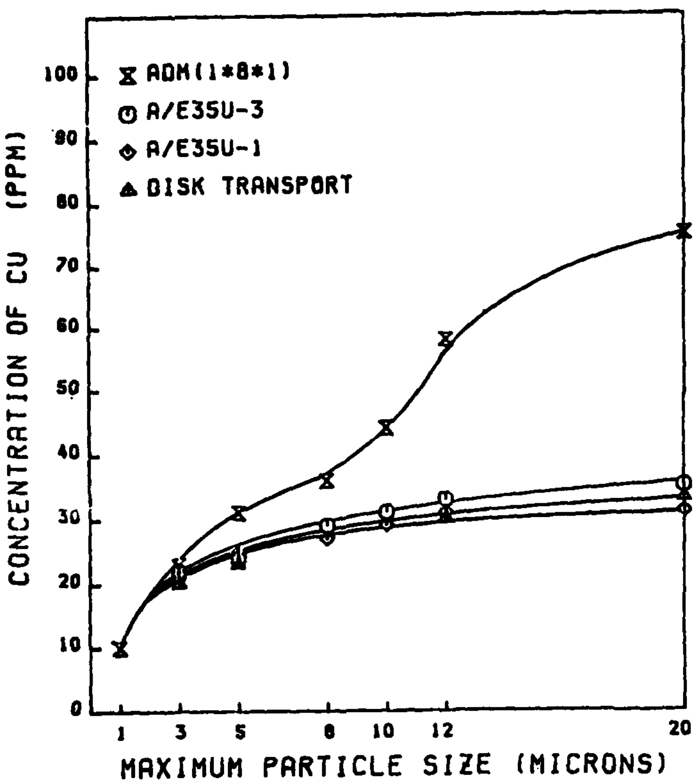

A

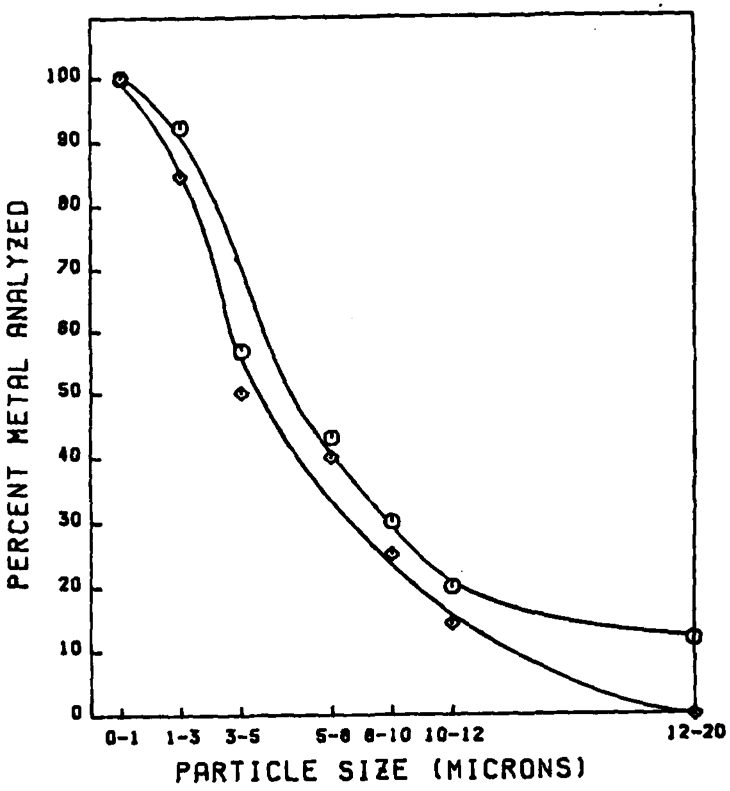

B

Figure A43. Spectrometric Analysis (A) and Percent Metal Analyzed (B) for Cu Powder Suspended in Phillips Condor 105.

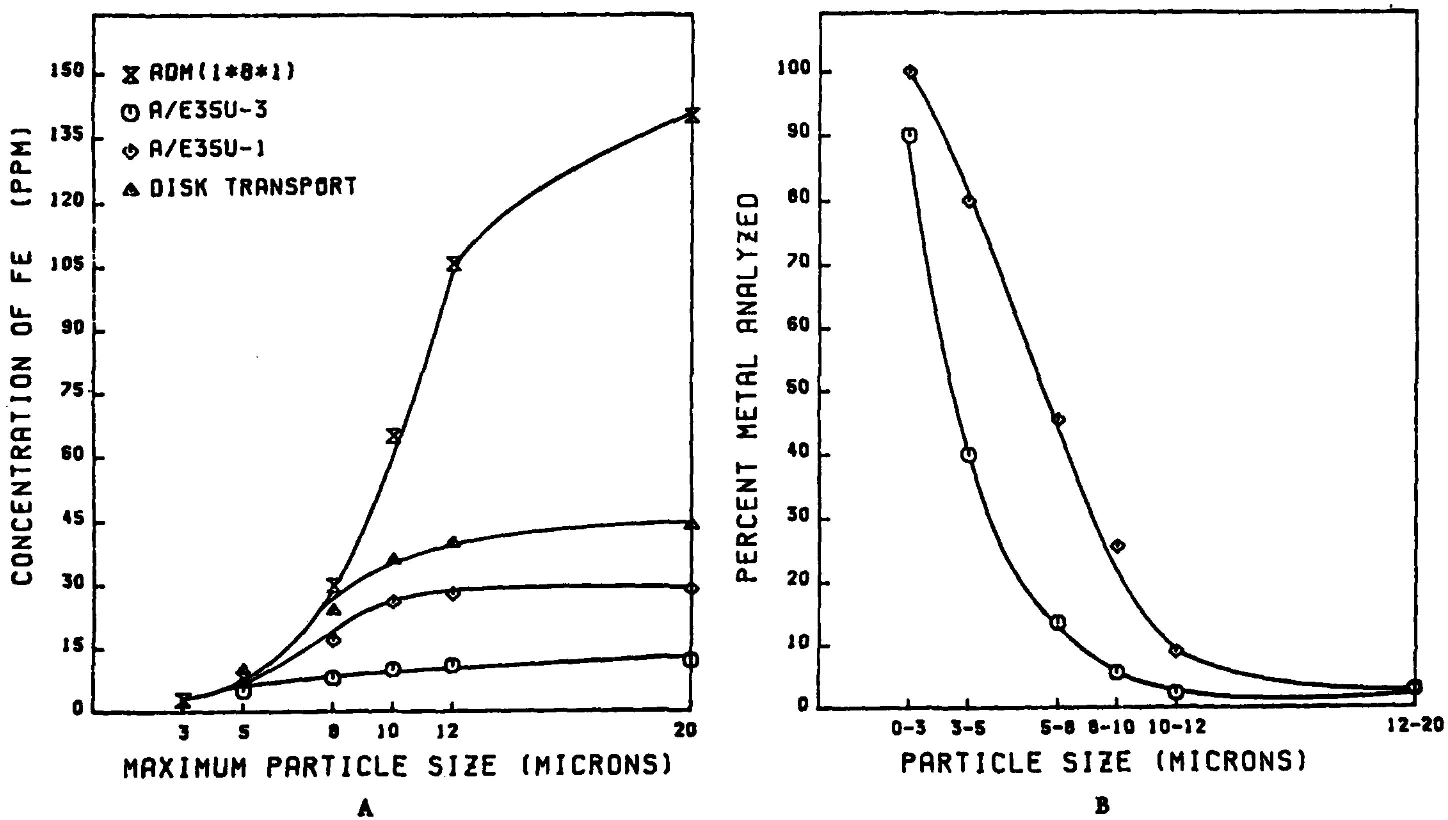

Figure A44. Spectrometric Analysis (A) and Percent Metal Analyzed (B) for Fe-AEE Powder Suspended in Phillps Condor 105.

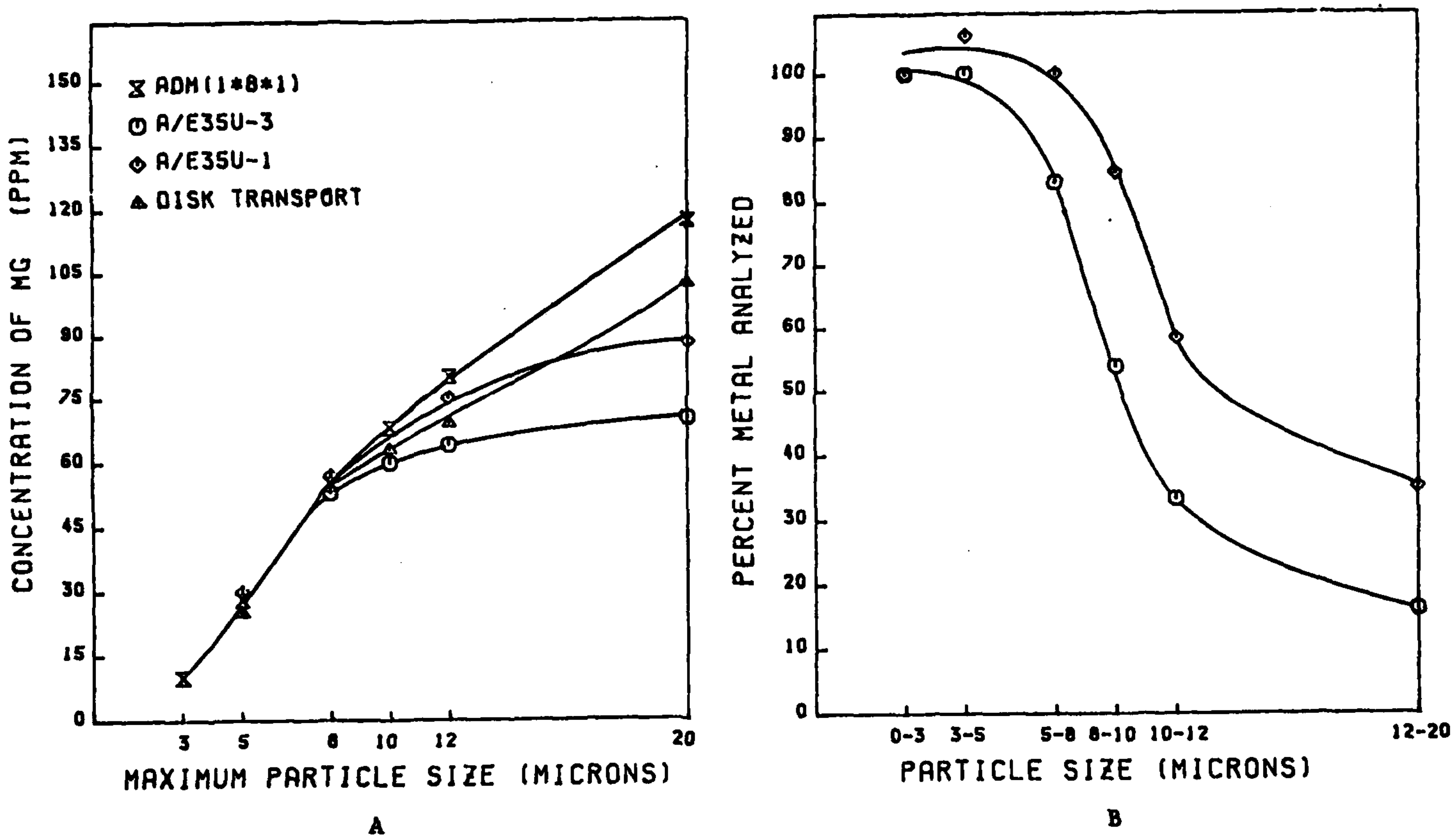

Figure A45. Spectrometric Analysis (A) and Percent Metal Analyzed (B) for Mg Powder Suspended in Phillips Condor 105.

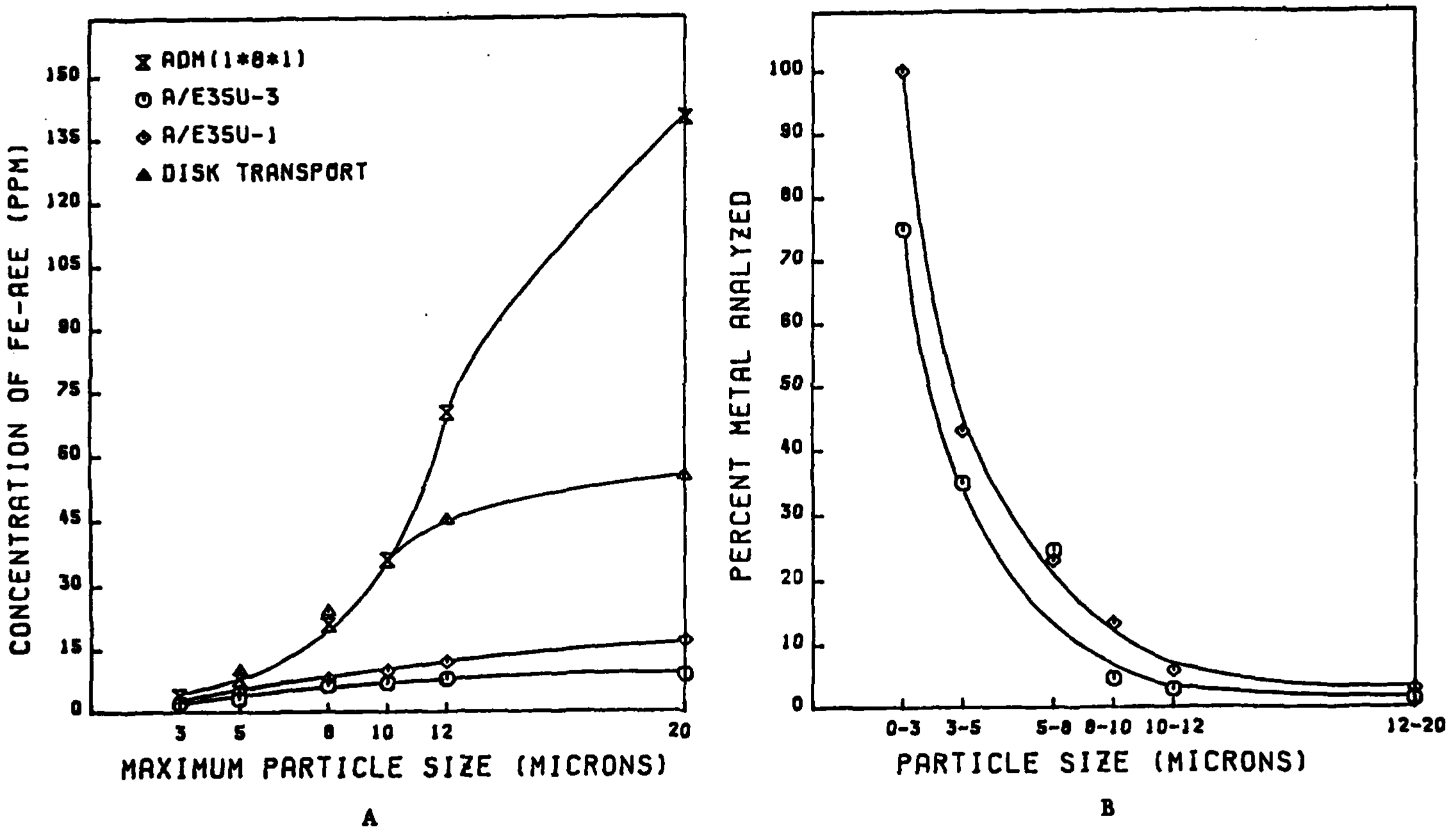

Figure A46. Spectrometric Analysis (A) and Percent Metal Analyzed (B) for Fe-AEE Powder Suspended in Light Mineral Oil.

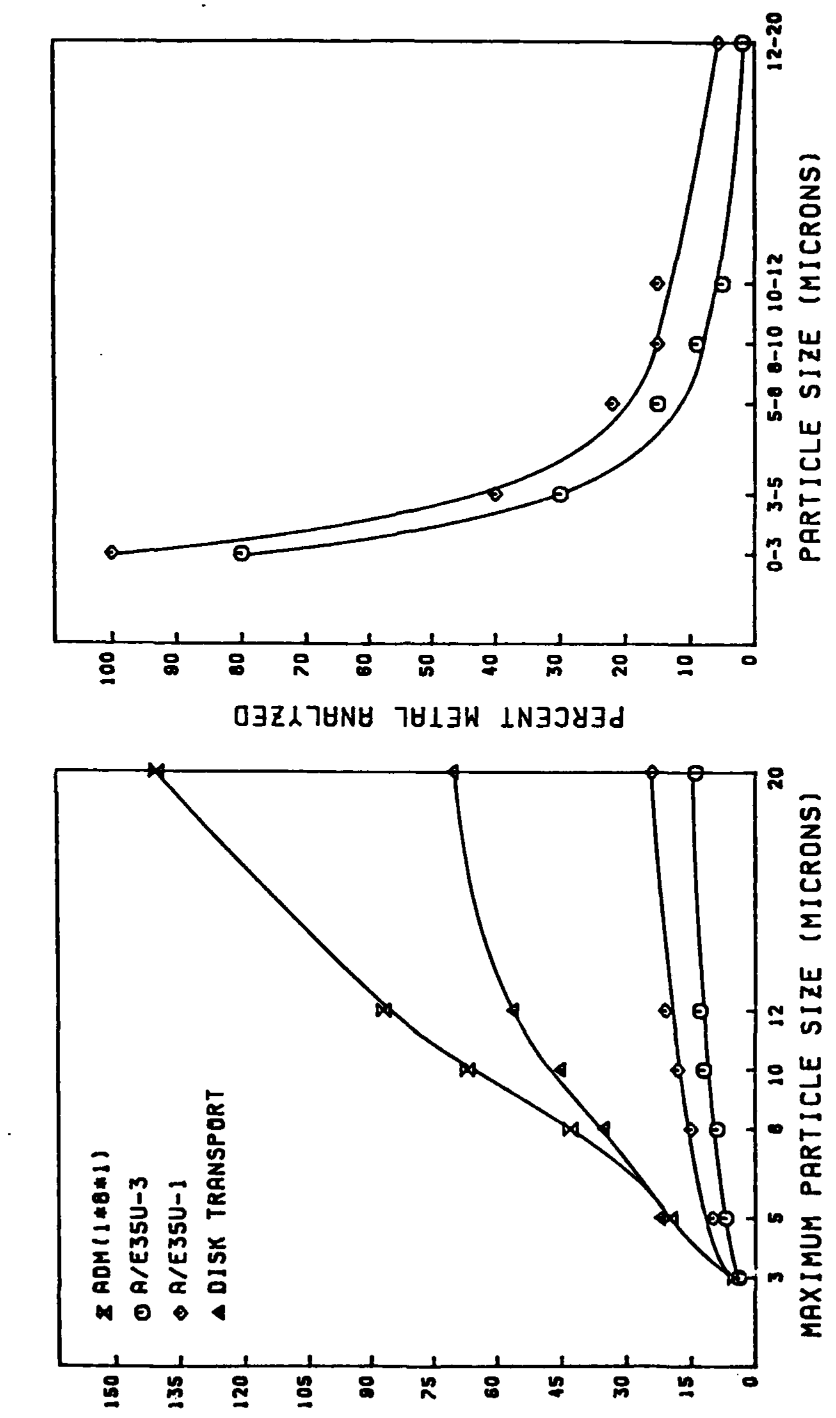

Figure A47. Spectrometric Analysis (A) and Percent Metal Analyzed (B) for Fe-Ball Milled Powder Suspended in Light Mineral Oil.

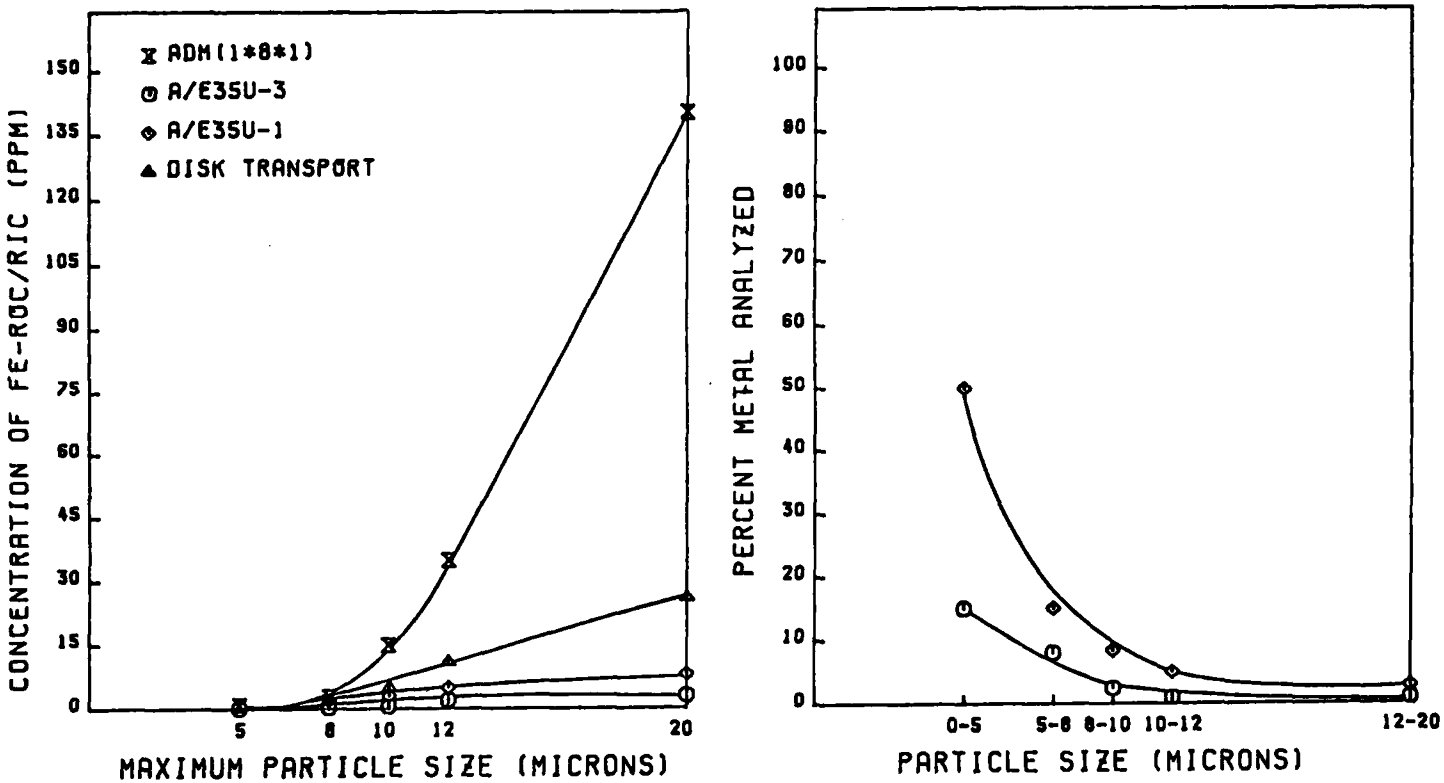

A

B

Figure A48. Spectrometric Analysis (A) and Percent Metal Analyzed (B) for Fe-ROC/RIC Powder Suspended in Light Mineral Oil.

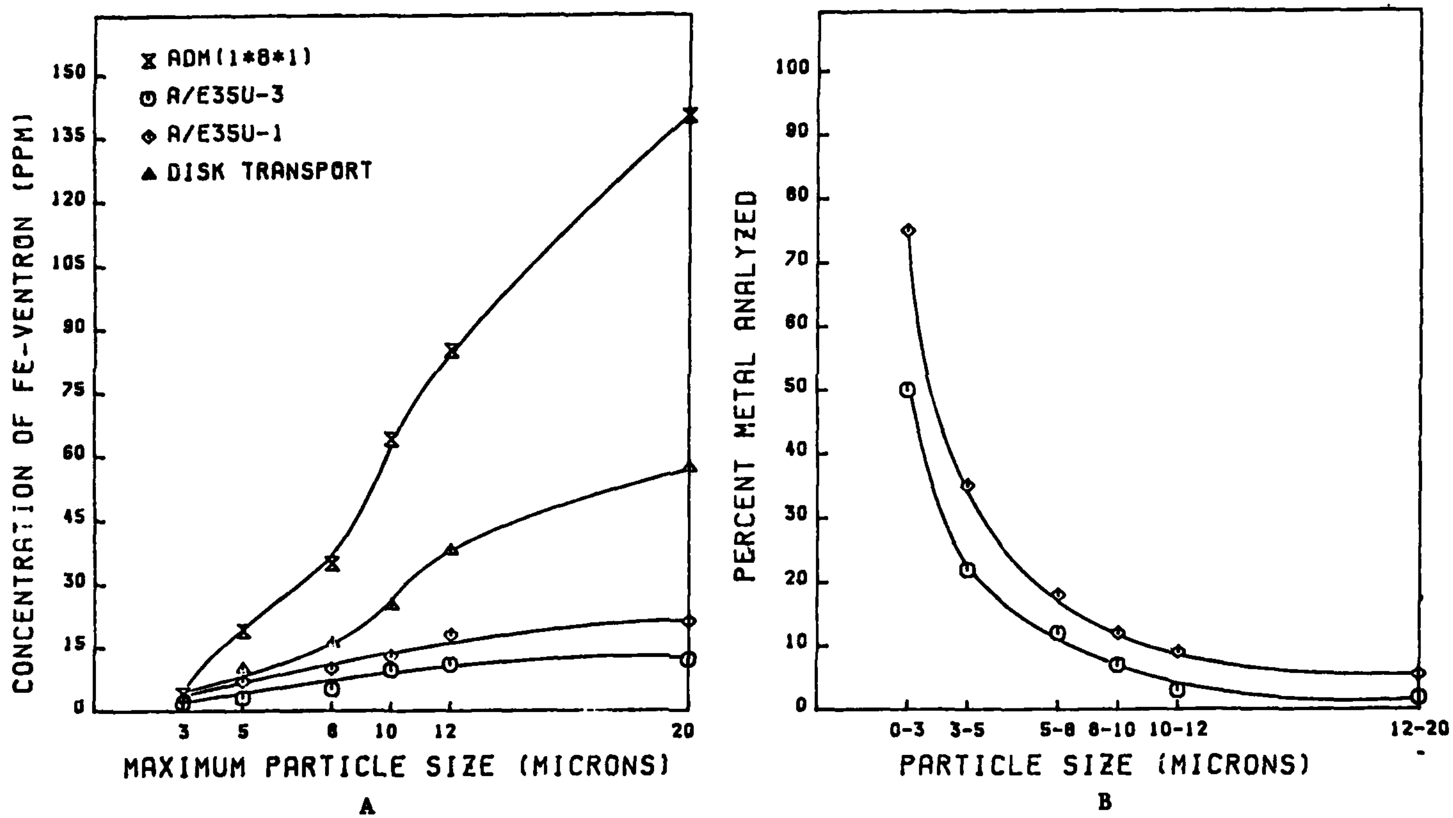

Figure A49. Spectrometric Analysis (A) and Percent Metal Analyzed (B) for Fe-Ventron Powder Suspended in Light Mineral Oil.

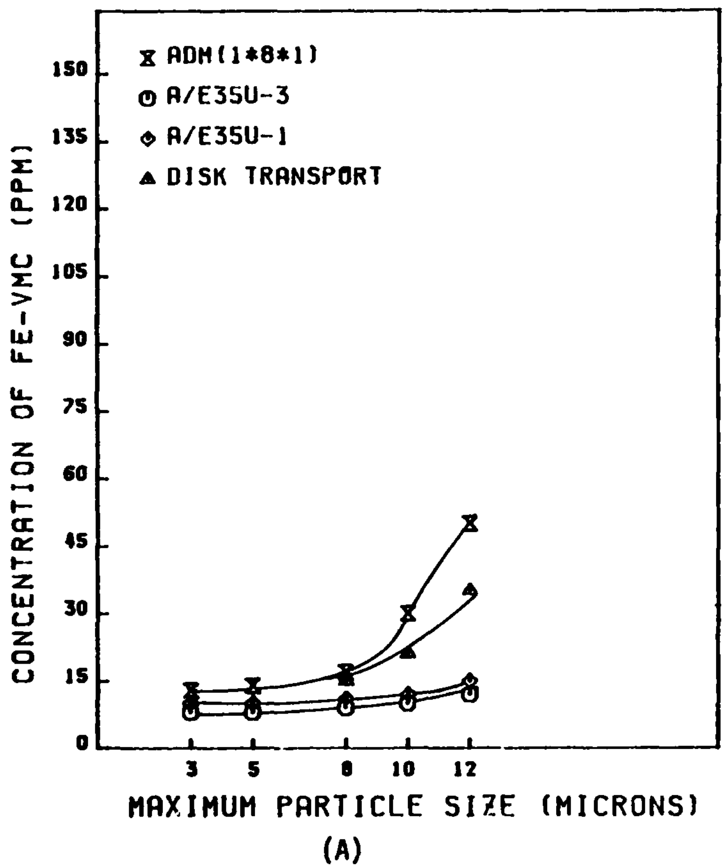

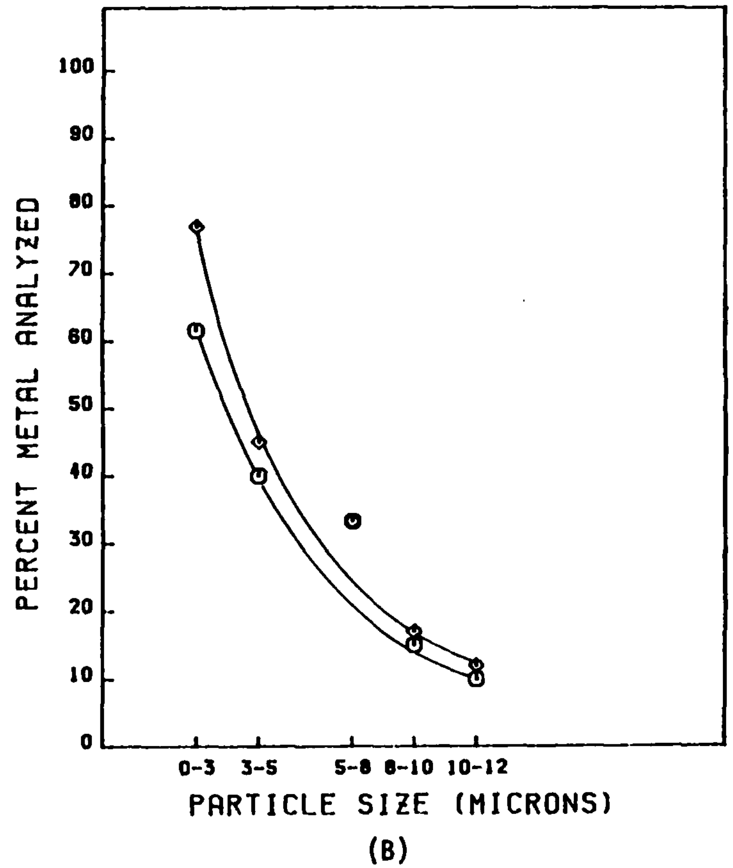

Figure A50. Spectrometric Analysis (A) and Percent Metal Analyzed (B) for Fe-VMC Powder Suspended in Light Mineral Oil.

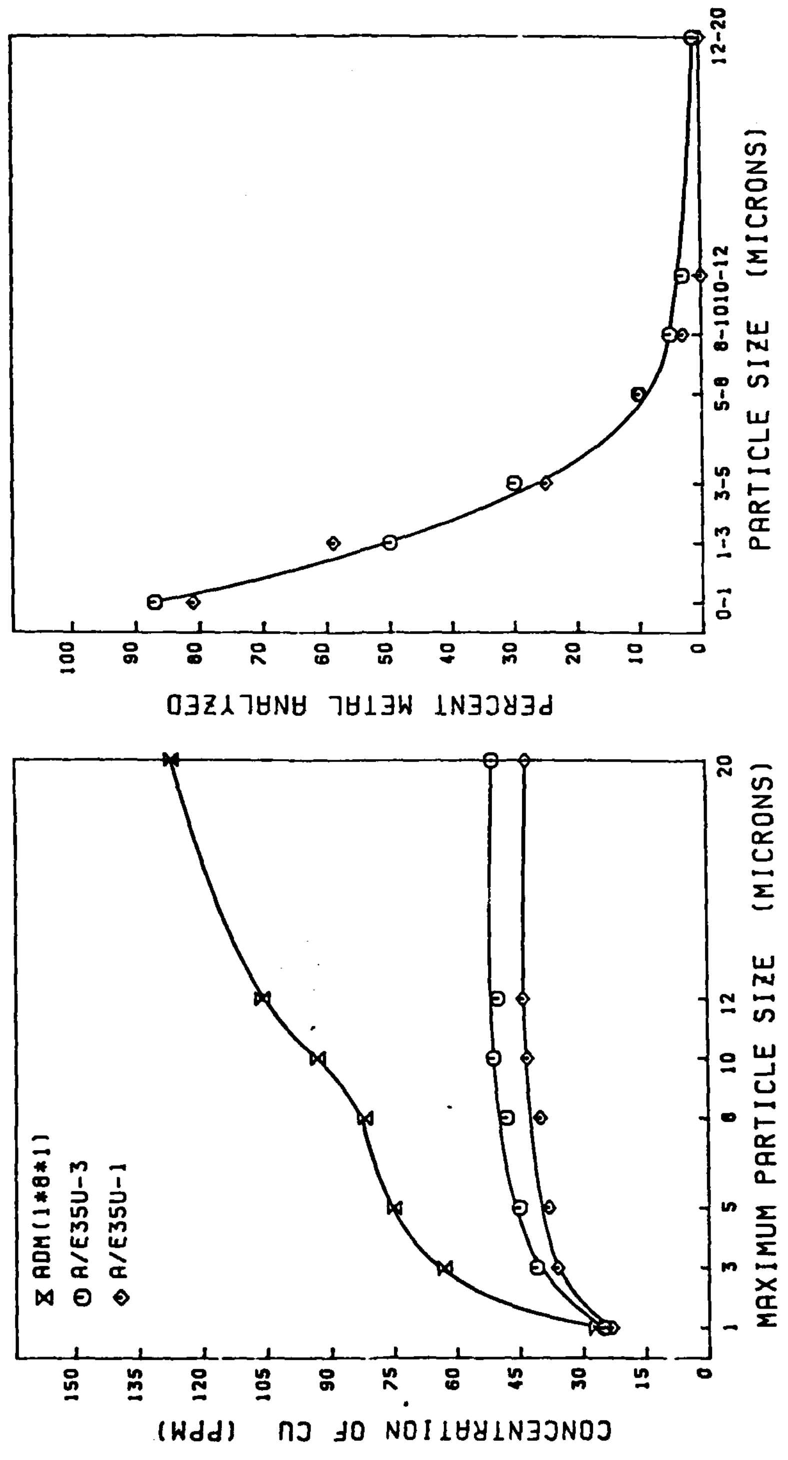

Figure A51. Spectrometric Analysis (A) and Percent Metal Analyzed (B) for Cu Powder Suspended in MIL-H-83282A.

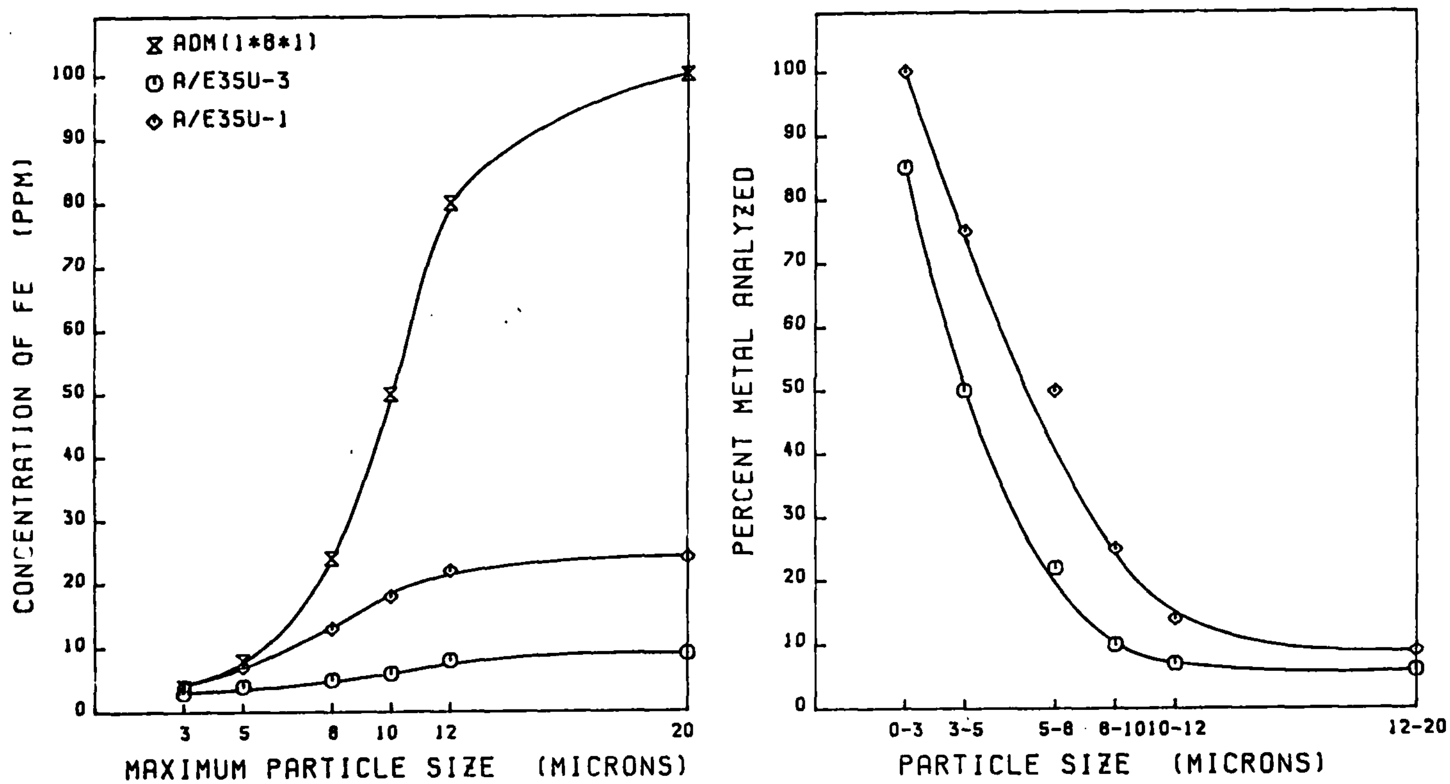

A B

Figure A52. **Spectrometric Analysis (A) and Percent Metal Analyzed (B) for Fe-AEE Powder Suspended in MIL-H-83282A.**

[illegible]

[illegible]

[illegible]

[illegible]

[illegible]

[illegible]C

[illegible] (85)

92719

[illegible]

[illegible] Director
Building 780
Naval Air Station
Pensacola, FL 32508

Commanding Officer
Naval Air Rework Facility (440)
Naval Air Station
Pensacola, FL 32508
Attn: Navy Program Manager/AP

[illegible]

REVISION LIST

REVISION	PAGES AFFECTED

END

DATE
FILMED

6-83

DTIC